



Laporan Akhir Projek Penyelidikan Jangka Pendek

**Study On Simultaneous Phase Inversion
And Nanoparticle-Membrane Matrix
Binding Process : Dispersity And Its
Effect On Foulant Degradation**

by

**Dr. Ooi Boon Seng
Prof. Abdul Latif Ahmad
Dr. Lim Jit Kang**

2013

E. **ABSTRACT OF RESEARCH**

(An abstract of between 100 and 200 words must be prepared in Bahasa Malaysia and in English. This abstract will be included in the Annual Report of the Research and Innovation Section at a later date as a means of presenting the project findings of the researcher/s to the University and the community at large)

In this project, different types of titanium dioxide (TiO₂) nanoparticles (NPs) (PC-20, P25 and X500) in various particle sizes were incorporated as nanofiller into polyvinylidene fluoride (PVDF) UF membrane matrix via the novel in-situ colloidal precipitation method. Through this novel method, stabilized TiO₂ NPs suspension was uniformly embedded into the polymer matrix during the simultaneous phase inversion process. The presence of TiO₂ NPs on membrane surface do not provide any significant changes on the membrane physical structure, suggesting that in-situ colloidal precipitation is an ideal method to prepare mixed-matrix membrane. The performance of the mixed-matrix membrane (MMM) were evaluated by measuring membrane permeate flux and humic acid (HA) rejection. Experiment results demonstrated that flux of the membranes had improved due to the increased membrane hydrophilicity. Mixed-matrix membrane using DMAc as polymer solvent with 0.01 g/L X500 in the coagulation bath exhibited extraordinary permeability (58.81 L/m² h ± 1.96), with superior retention properties (98.76% ± 0.05) of HA. The membrane with well dispersed X500 TiO₂ exhibited both superior anti-fouling and defouling properties due to its smoother surface and its highly reactive surface layer. Hydroxyl-functionalized polymer matrix containing well-dispersed P25 also has superior relative flux ratio, flux recovery ratio and irreversible flux recovery ratio (UV) compared to the pristine membrane.

Abstrak Penyelidikan

(Perlu disediakan di antara 100 - 200 perkataan di dalam Bahasa Malaysia dan juga Bahasa Inggeris.

Abstrak ini akan dimuatkan dalam Laporan Tahunan Bahagian Penyelidikan & Inovasi sebagai satu cara untuk menyampaikan dapatan projek tuan/puan kepada pihak Universiti & masyarakat luar).

Dalam projek ini, pelbagai jenis titanium dioksida (TiO₂) zarah nano (ZN) (PC-20, P25 dan X500) berlainan saiz telah ditambah sebagai pengisi nano ke dalam matriks membran UF polivinilidene fluorida (PVDF) melalui kaedah baru mendakan berkoloid. Melalui kaedah baru ini, TiO₂ ZN yang seragam boleh ditambah ke dalam matriks polimer semasa fasa proses penyongsangan serentak. Kehadiran TiO₂ ZN pada permukaan membran didapati tidak memberikan apa-apa perubahan ketara ke atas struktur fizikal membran, menunjukkan bahawa kaedah mendakan berkoloid adalah kaedah yang sesuai untuk menyediakan membran matriks bercampur. Prestasi membran bercampur matriks (MMM) telah dinilai dengan mengukur kadar fluks membran dan penolakan asid humik (HA). Hasil kajian menunjukkan bahawa fluks membran telah bertambah baik kerana sifat hidrofilik membran telah meningkat. Membran bercampur matriks menggunakan DMAc sebagai pelarut polimer berserta 0.01 g/L X500 dalam takungan pengentalan mempamerkan kebolehtelapan yang luar biasa (58.81 L/m² h ± 1.96), dengan ciri- penolakan yang lebih baik (98.76% ± 0.05) HA. Membran dengan sebaran X500 TiO₂ yang halus mempamerkan kedua-dua sifat anti-kotoran dan penyahkotoran dengan baik. Kelebihan ini adalah kerana permukaan membran yang lebih licin dan lapisan permukaan yang sangat reaktif. Matriks polimer difungsikan melalui hidrosil dan mengandungi P25 didapati mempunyai peningkatan dalam nisbah unggul relatif fluks, nisbah pemulihan fluks dan nisbah pemulihan fluks tidak berubah (UV) berbanding dengan membran asli.

F. SUMMARY OF RESEARCH FINDINGS

Ringkasan dapatan Projek Penyelidikan

As a summary, this project devised a novel method of preparing MMM via in situ colloidal precipitation method. Conditions have been optimized to develop fine and uniformly distributed TiO₂ NPs into the membrane matrix to improve the hydrophilicity and functionality of the membrane. Colloidal stable TiO₂ NPs in coagulation bath was first prepared combining the ultrasonic and pH peplization method. The stable TiO₂ colloid was then embedded into the membrane matrix during phase inversion process to avoid the TiO₂ agglomeration problem due to the viscous effect. Using the novel in-situ colloidal precipitation method, the pore formation and particles embedment were carried out simultaneously so that the changes of physical structure of PVDF/TiO₂ MMMs was minimized.

It was found that the membrane prepared using NMP and DMAc as solvent has better particle size distribution compared to DMF. Membrane with NMP as solvent gave bigger pore size but smaller and irregular particle size, whereas membrane prepared with DMAc has narrow particle size distribution pattern. Additionally, the particle size increased with the increasing of TiO₂ concentration in the coagulation bath. It was found that PVDF/TiO₂ MMM system that was prepared using DMAc as solvent and immersed in coagulation bath with X500 TiO₂ NPs has a comparatively well distributed, regular and smaller TiO₂ NPs on membrane surface. The particle size distributions is mainly contributed by the smaller and stable TiO₂ NPs in the suspension bath. System with greater R_g/R_p ratio which has better thermodynamic stability is therefore required for favorable particle distribution. Smaller X500 particle size on the membrane (under the same concentration) unexpected give higher contact angle compared to the neat PVDF membrane. However, surface energy analysis showed that X500 MMMs with better dispersion has better affinity towards water which indicating the enhanced membrane hydrophilicity.

Filtration tests with HA solution proved that permeability of the MMMs is significantly improved due to its increasing porosity attribute to the nanogap between the particles and the polymer matrix (defect) as well as enhanced hydrophilicity. The optimum membrane prepared with 0.01 g/L X500 showed significant flux improvement (58.81 ± 1.96 L/m² h) and HA rejection (98.76 ± 0.05 %) which could be attributed to the better particle distribution, smaller particle size as well as increasing hydrophilicity. The synergistic effect of TiO₂ NPs on membrane water flux and rejection could be realized only if the NPs were well dispersed. The fine and well TiO₂ dispersions on membrane polymeric matrix was found to have significant effects on the membrane anti-fouling and defouling properties. It is attributed to their reduced surface roughness as well as increasing surface energy. This finding is manifested through the improved RFR and FRR values of X500 series PVDF/TiO₂ MMMs.

The ultimate advantage of incorporating photocatalytic TiO₂ NPs into the membrane matrix and their self-cleaning properties was evaluated by degrading the HA adsorbed on the membrane surface under mild UV light irradiation. It was found that photocatalytic oxidation could be an effective process for degrading permanent fouled HA by breaking the hydrophobic and electrostatic interactions between HA and membrane. It was proven that P25 TiO₂ with mixed 25% rutile and 75% anatase crystallinity, produced superior UV-cleaning properties with the highest membrane IFRR(UV) value. A considerably high IFRR(UV) was also obtained for uniformly dispersed X500 on the membrane surface, which has more active surface sites due to the improved dispersions. However, the photocatalytic properties of P25 MMMs are compensated by its rough surface. This problem can be solved by hydroxylate the polymer matrix to improve the dispersion. Hydroxyl-functionalized P25 MMM containing a well-dispersed photocatalyst with large surface-to-volume ratio is considered to be an attractive membrane which promises highly amalgamation application of anti-fouling, defouling and UV-cleaning (self-cleaning) capacity.

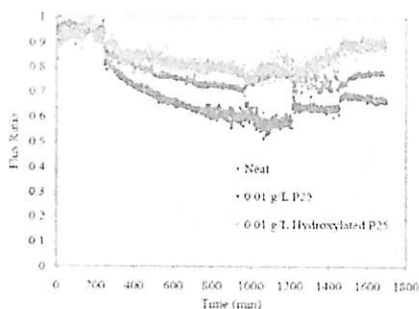


Fig. 1: Permeation test of the mixed mamatrix membrane

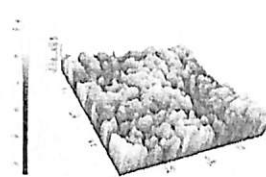


Fig. 2: AFM images of mixed matrix membrane

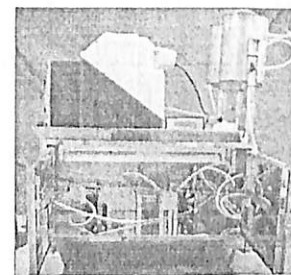


Fig. 3: Rig set up for permeation test

G. COMPREHENSIVE TECHNICAL REPORT

Laporan Teknikal Lengkap

Applicants are required to prepare a comprehensive technical report explaining the project.
(This report must be attached separately)

Sila sediakan laporan teknikal lengkap yang menerangkan keseluruhan projek ini.
[Laporan ini mesti dikepilkan]

Please refer to Attachment A

List the key words that reflect our research:

Senaraikan kata kunci yang mencerminkan penyelidikan anda:

English	Bahasa Malaysia
Mixed matrix Membrane	Membran matriks bercampur
antifouling	anti-kotoran
photocatalytic	pemangkinan foto

H. a) Results/Benefits of this research
Hasil Penyelidikan

No. Bil:	Category/Number: Kategori/ Bilangan:	Promised	Achieved
1.	Research Publications (Specify target journals) <i>Penerbitan Penyelidikan (Nyatakan sasaran jurnal)</i>	3	Journal (7) Symposium (4)
2.	Human Capital Development		
	a. Ph. D Students	1	1
	b. Masters Students	1	1
	c. Undergraduates (Final Year Project)	0	1
	d. Research Officers	1	0
	e. Research Assistants	1	5
	f. Other: Please specify		
3.	Patents <i>Paten</i>	1	0
4.	Specific / Potential Applications <i>Spesifik/Potensi aplikasin</i>	1	0
5.	Networking & Linkages <i>Jaringan & Jalinan</i>	2	2
6.	Possible External Research Grants to be Acquired <i>Jangkaan Geran Penyelidikan Luar Diperoleh</i>	1	2

- Kindly provide copies/evidence for Category 1 to 6.

b) Equipment used for this research.
Peralatan yang telah digunakan dalam penyelidikan ini.

Items Perkara	Approved Equipment	Approved Requested Equipment	Location
Specialized Equipment Peralatan khusus		1) Dell Precision M4700 Mobile Workstation 2) Prosesan Data –Ipad – 64GB	Room 2.06
	1) High Pressure peristaltic pump 2) Dead End stirred cell <i>(Change to high pressure stirred cell)</i>	1) High Pressure Stirred Cell	Lab 2.04
Facility Kemudahan			
Infrastructure Infrastruktur			

- Please attach appendix if necessary.

I. BUDGET / SAJET

Total Approved Budget : RM 192,071.00
Total Additional Budget : RM 0.00
Grand Total of Approved Budget : RM 192,071.00

Yearly Budget Distributed

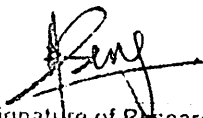
Year 1 : RM 82,251.00
Year 2 : RM 59,890.00
Year 3 : RM 49,890.00

Additional Budget Approved

Year 1 : RM 0.00
Year 2 : RM 0.00
Year 3 : RM 0.00

Total Expenditure : RM 191,792.00
Balance : RM 278.82

- Please attach final account statement from Treasury


Signature of Researcher
Tandatangan Penyelidik

6/2/2014
Date
Tarikh

COMMENTS OF PTJ'S RESEARCH COMMITTEE
KOMEN JAWATANKUASA PENYELIDIKAN PERINGKAT PTJ

H.

General Comments:
Ulasan Umum

high output from this project.



Signature and Stamp of Chairperson of PTJ's Evaluation Committee
Tandatangan dan Cop Pengerusi Jawatankuasa Penilaian PTJ

Date : 6/2/14
Tarikh

Signature and Stamp of Dean/ Director of PTJ
Tandatangan dan Cop Dekan/ Pengerah PTJ



Date : 6/2/14
Tarikh

PROFESOR DR. JAWA HILLY JAMALUDIN
School of Oriental Languages
University of Sains Malaysia, Jeli Pengangsan
14300 Kubang Keroh, Negeri Sembilan
Penang, MALAYSIA

Technical Report for RUI Grant (1001/PJKIMIA/811172)

Title

Preparation and characterization of a simultaneous pore forming and titanium binding nanocomposite membrane for fouling mitigation

Objectives

In this work, three different types of TiO₂ nanoparticles (NPs) (PC-20, P25 and X500) were incorporated into PVDF membrane to produce a mixed-matrix membrane via in situ colloidal precipitation method. The corresponding membranes were prepared by dissolving the PVDF into different organic solvent (N-methyl-2-pyrrolidone (NMP), N,N-dimethyl formamide (DMF) or N-N-dimethylacetamide (DMAc)) which underwent phase inversion and colloidal precipitation in TiO₂ suspension bath. In order to avoid agglomeration and to maintain the stability of TiO₂ NPs in the coagulation bath, TiO₂ NPs were dispersed in the bath via ultrasonication and peptization. The membranes performance in term of permeation flux and rejection were then evaluated using cross-flow filtration system. The ultimate advantage of incorporating photocatalytic TiO₂ NPs into the membrane matrix could be tested based on the long hour study of membranes with HA model solution which provides the information on its anti-fouling and self-cleaning functionality. The efficiency of the surface photocatalysis are evaluated based on the flux recovery. In overall, the objectives of the project are:

- i. To study the formation of nanocomposite polymeric membrane with well dispersed TiO₂ in the membrane matrix
- ii. To study the interaction between nanoparticle and polymeric material
- iii. To study the cleaning mechanism of nanocomposite membrane under radiation of UVC and sunlight

Introduction

Polyvinylidene fluoride (PVDF) is one of the most extensively applied membrane materials in the industry. However, hydrophobic nature is the most critical limitation of current PVDF membrane in its dignified application as a valuable means of HA separation as they exhibit susceptibility toward inherent problem of membrane fouling.

Irreversible deposition and adsorption of HA particles (solute) on membrane surface or into the membrane pores will consequence in membrane deterioration. HA has been demonstrated to be the major constituent causing membrane fouling during the drinking water treatment process by a number of previous studies. This phenomenon demands considerable attention as it can greatly reduce the membrane permeation, affect the quality of the water produced and increasing transmembrane pressure (TMP) which leads to a higher operational cost, and shorten the membrane lifespan. Therefore, membrane fouling always a major obstacle for widespreading of UF membrane implementation.

To increase the membrane performance, membranes is then being cleaned physically, biologically or chemically. Physical cleaning of membrane could effectively solve the reversible fouling phenomenon but for irreversible fouling or scaling problem, intense chemical cleaning is required. However, high chemical usage in chemical cleaning will impose another additional environmental pollution. Therefore, a greener membrane cleaning method such as self-cleaning (surface photocatalytic) is required.

Since hydrophobic adsorption of HA particles on membrane surface is the key role in membrane fouling, the surface property of membrane is the most important factor affecting membrane fouling. Therefore, hydrophilic modification is a potential method to enhance the functionality of PVDF membrane against the fouling.

The unique large surface-to-volume ratio and strong reactivity properties of titanium dioxide (TiO₂) nanoparticles (NPs) with photocatalytic properties make it an ideal candidate to be incorporated into polymeric matrix as hydrophilic filler. Beneficial effects of TiO₂-based membranes

in improving the membrane permeability, fouling-resistance and self-cleaning properties have been reported recently. However, high surface energy of TiO₂ NPs often results in agglomeration; leading to low functional surface area, which is a conspicuous drawback for application. Therefore, for feasible application, it is crucial to obtain fine and stable nanodispersions for production of thin mixed-matrix membrane films with low surface roughness and high surface area of TiO₂ NPs.

Research Methodology

The overall experiment procedures used in this study can be categorized into three segments. TiO₂ colloid suspension stability was first studied at the beginning of the project. Second segment converse on the neat PVDF membrane and PVDF/TiO₂ mixed-matrix membrane development under different membrane synthesis parameters. It was followed by membrane performance evaluation in terms of membrane filtration flux and HA rejection as well as the membrane fouling studies. These characterization method include X-ray Diffraction (XRD), Transmission Electron Microscope (TEM), Fourier Transform Infrared (FTIR) spectroscopy, Dynamic Light Scattering (DLS), Energy Dispersive X-ray (EDX), streaming potential, Field Emission Scanning Electron Microscopy (FESEM), particle size distribution on membrane surface, Atomic Force Microscope (AFM), contact angle, pore size distribution and Thermal Gravimetric Analysis (TGA). The flowchart of the overall experimental works is summarized in Figure 1.

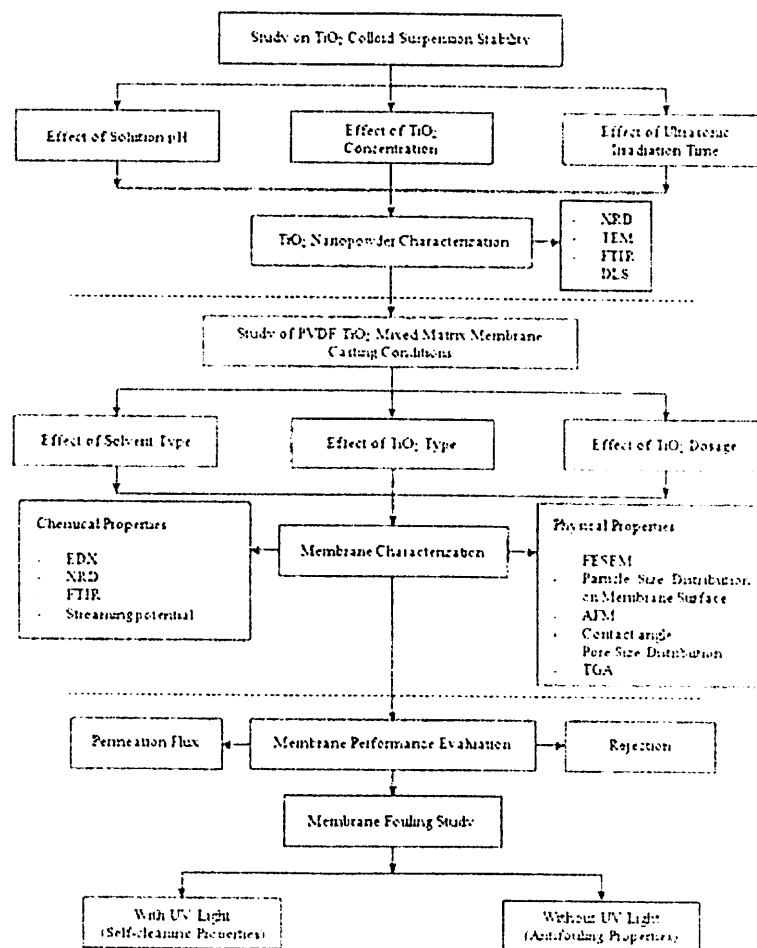


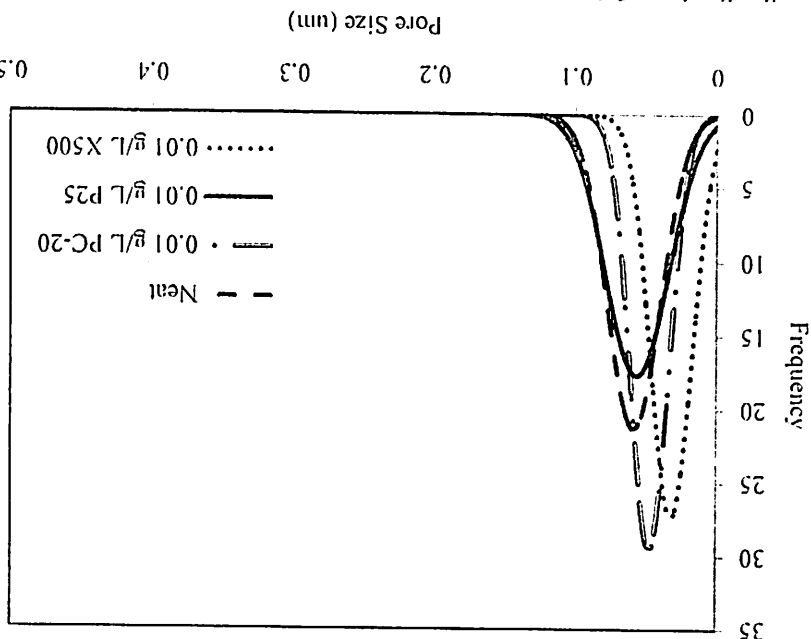
Figure 1: Flowchart of overall experimental works

As seen in Fig. 2(a), the SEM top surface images of PVDF/TiO₂ mixed-matrix membranes prepared using DMAc as a solvent and immersed in 0.01 g/L colloidal suspensions of different types of commercial TiO₂. The connected pores were observed on the surface of all PVDF membranes. The experimental results indicated that the choice of commercial TiO₂ nanopowder does not contribute to any significant structural change of membrane morphology.

The presence and dispersion of TiO₂ in the membrane structure was further confirmed by energy-dispersive X-ray spectrometer (EDX) mapping. The distribution of TiO₂ NPs throughout the PVDF/TiO₂ mixed-matrix membrane structure was observed and is presented in Fig. 2(b). Different types and sizes of commercial TiO₂ nanopowder have different particle size distribution patterns on the membrane surface. It could be clearly seen that X500 (which has the smallest size of TiO₂) was better dispersed into the membrane compared to the systems using PC-20 and P25. The lesser degree of TiO₂ clustering in the membrane prepared using X500 is attributed to its higher thermodynamic stability (high ratio of radius of gyration to particle size) during phase separation.

The Membrane performance or flux data are presented in terms of normalized flux (J/J_0), which is the instantaneous flux over the initial flux. The effect of TiO₂ type (PC-20, P25, X500) on the performance of mixed-matrix membranes was studied at a TiO₂ concentration of 0.01 g/L, while the CaCl₂ concentration and pH were adjusted to 1 mM and pH 7.0, respectively.

Fig. 1. Pore size distribution of the PVDF/TiO₂ mixed-matrix membranes and neat PVDF membrane as a function of TiO₂ type



Pore size distributions of the neat PVDF membrane and PVDF/TiO₂ mixed-matrix membrane are shown in Fig. 1. As can be seen in Fig. 1, all of the membranes prepared had very close mean pore sizes. The mean pore diameter, d_{pore} for the neat PVDF membrane was approximately 0.060 μ m. Overall, changes in membrane pore size were not significant, P25 has the closest morphology to the neat membrane. This observation indicated that in situ colloidal precipitation with a colloidal stable TiO₂ suspension is an ideal method to prepare membranes with minimum changes to their physical properties.

Research Findings

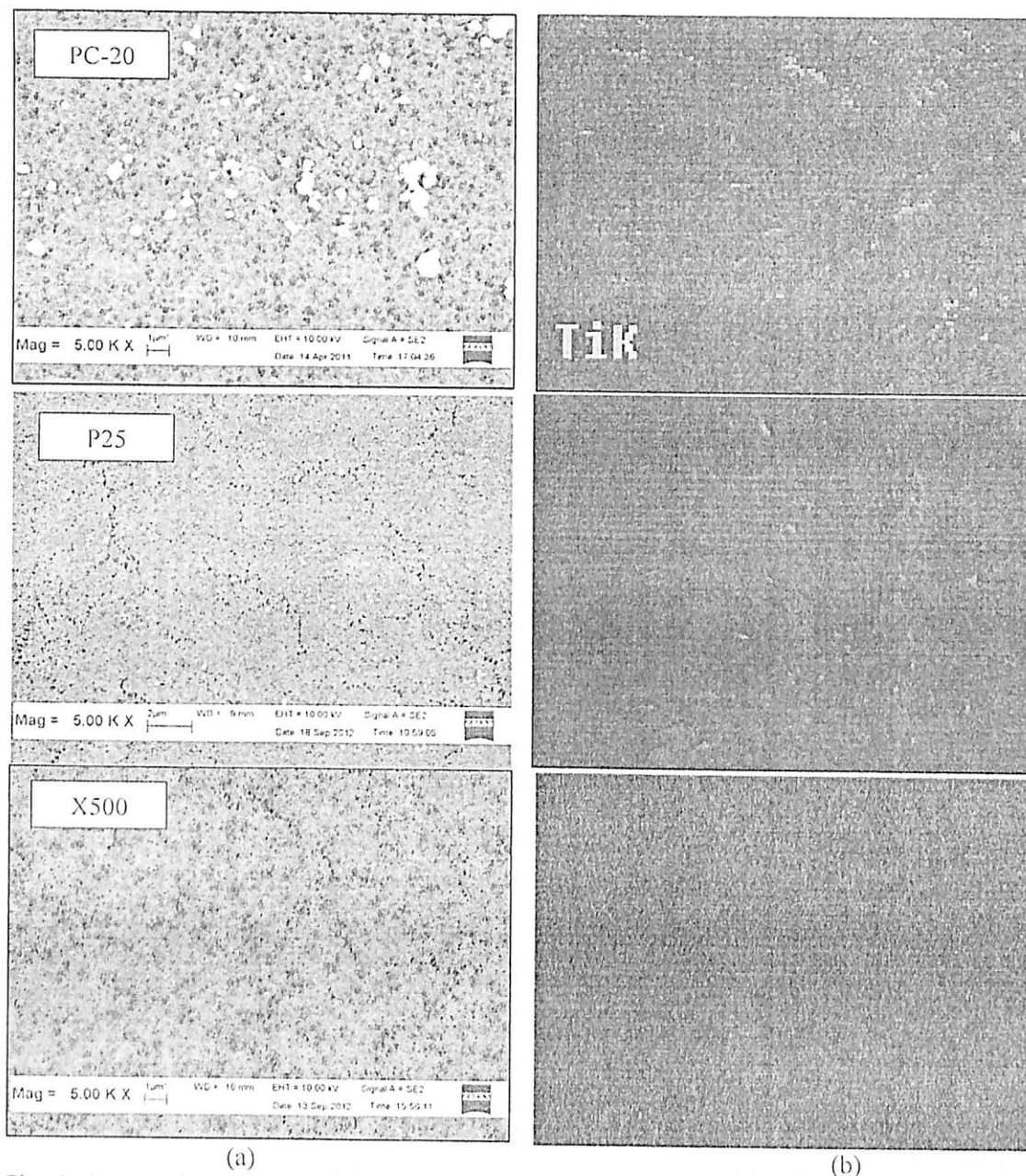


Fig. 2. Top surface (a) FESEM micrographs and (b) EDX mapping of PVDF/TiO₂ mixed-matrix membranes with different types of TiO₂ in a coagulation bath at a concentration of 0.01 g/L

As depicted in Table 1, the membranes gave initial water fluxes of 34.97 ± 2.25 L/m² h, 43.21 ± 4.31 L/m² h, 37.67 ± 1.11 L/m² h and 58.81 ± 1.96 L/m² h for the neat membrane and membranes prepared with PC-20, P25 and X500 as hydrophilic filler, respectively. The permeate fluxes show that the mixed-matrix membranes are relatively more permeable with the addition of TiO₂. The flux increased upon integration of TiO₂ NPs was due to several reasons. Upon adding TiO₂, the increased hydroxyl groups on the TiO₂ surface could enhance the permeate water flux. Another plausible reason for the flux enhancement as shown by the PC-20 mixed-matrix membrane, which denotes a slightly more hydrophobic surface, might be due to increase porosity attributed to the nanogaps between the particles and the polymer matrix.

Table 1: Water flux recovery and cleaning properties of neat PVDF membrane and PVDF/TiO₂ mixed-matrix membranes

Membrane	Initial Water Flux (L/m ² h)	RFR (%)	FRR (%)	IFRR(UV) (%)
M	34.97 ± 2.25	24.24	82.03	0.10
M1	43.21 ± 4.31	23.48	78.58	5.74
M2	37.67 ± 1.11	36.07	61.89	16.56
M3	58.81 ± 1.96	14.69	78.24	15.30

PVDF/TiO₂ mixed-matrix membranes with homogeneously distributed X500 particles have the best membrane permeability, suggesting that X500 (fully anatase) is more hydrophilic and therefore promises a better HA fouling mitigation effect. It is also proposed that the homogeneous particle dispersion of X500 particles offers a larger NP surface area, which increases the number of adsorption sites for water molecules on the membrane surface. Water molecules were attracted into the membrane matrix in the nonporous regions, thus enhancing the permeability of X500 membranes. On the other hand, the high aggregation tendency of PC-20 and P25 might block the membrane pores during immersion precipitation and reduce the membrane flux.

The flux data resulting from successive filtration are illustrated in Fig. 3. The HA fouling tendency was clearly revealed by RFR values of 24.24%, 23.48%, 36.07% and 14.69% for the neat PVDF membrane and the PVDF/TiO₂ mixed-matrix membranes embedded with PC-20, P25 and X500, respectively, after 12 hours of HA filtration (the end of HA fouling). Although the membrane pore size for PC-20, P25 and X500 membranes used in this study were much smaller than the equivalent size of HA aggregates, the RFR results are in accordance with the pore size distribution. Membranes X500 and PC-20, which have smaller pore sizes compared to the neat membrane, were found to have more fouling resistance compared to the neat and P25 membrane. However, the subsequent accumulation on the membrane surface resulted in a diminishing effective membrane pore size, thus leading to further physical retention and causing an increase in hydraulic resistance.

Although the hydrophilicity has been improved by incorporating TiO₂, membrane P25 shows pore plugging and high surface roughness problems, which compensate for the hydrophilicity of the P25 mixed-matrix membrane and eventually led to poorer fouling properties compared to the neat PVDF membrane. Coarser membranes can much more easily absorb impurities from water and reduce the surface energy compared to smoother membrane surfaces, with lower roughness and surface energy.

In the case of X500, in which the particle distribution was enhanced, the HA fouling propensity of the membrane was greatly reduced, as shown by the lowered RFR compared to the neat PVDF membrane. This result proves the advantage of using fine and uniformly distributed NPs in preventing membrane fouling. The improvement of the membranes' anti-fouling potential primarily resulted from i) the smoother surface layer and ii) the presence of well-distributed TiO₂ NPs on the membrane, which attracted water molecules and formed a thin shielding water layer to prevent hydrophobic adsorption between HA macromolecules and the membrane. Therefore, it is suggested that the advantages of NP embedment can only be realized when the particles are uniformly distributed within the polymeric matrix.

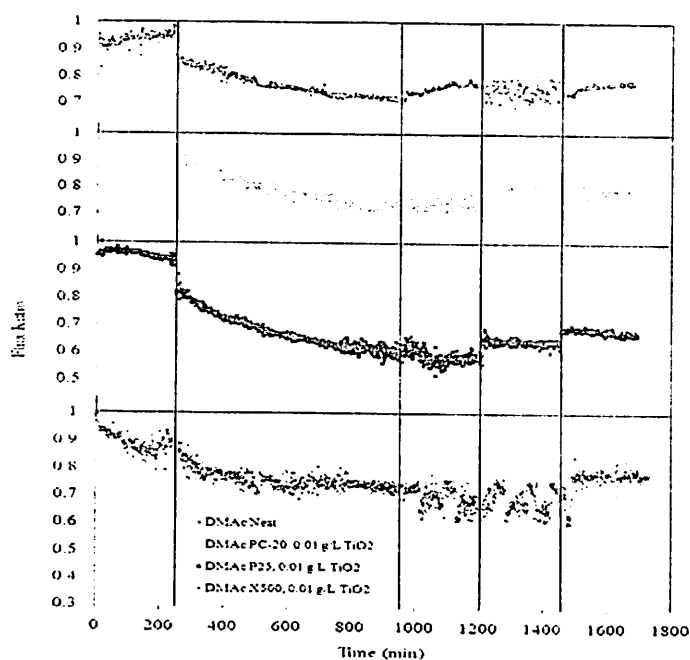


Fig. 3. Effect of TiO_2 type on PVDF/ TiO_2 mixed-matrix membrane anti-fouling potential during five stages: pure water flux for 4 h, HA solution filtration for 12 h, hydraulic cleaning pure water flux for 4 h, water flux for 4 h after 3 h of UV irradiation and water flux for 4 h after a 2nd round of 3 h UV irradiation. Operation conditions during the experiment: $[\text{HA}] = 2 \text{ mg/L}$; $[\text{Ca}^{2+}] = 1 \text{ mM}$ (as CaCl_2); pH 7.0; temperature = $25 \pm 1 \text{ }^\circ\text{C}$; cross-flow velocity = 4.0 L/hr, operating pressure = 0.5 bar; light intensity = 1.53 mW/cm^2 .

Membrane fouling can be reversible or irreversible; reversible fouling in this study resulted from reversible HA deposition, which could be removed by simple hydraulic cleaning. By contrast, irreversible fouling was caused by the strong adsorption of HA molecules onto the surface or the entrapment of HA molecules in pores; irreversible fouling is very difficult to remove by hydraulic cleaning. In this case, membrane cleaning was studied by scouring the membrane surface with pure distilled water. Cleaning was performed by recirculating pure water at 0.04 L/min for 4 hours. As shown in Fig. 3, flux increased when the membrane was washed with pure distilled water. The water flux can be recovered by up to 82.03%, 78.58%, 61.89% and 78.24% for the neat membrane and the membranes prepared with PC-20, P25 and X500, respectively. This observation indicates that flux decline due to pore blocking or surface reversible deposition can be significantly improved using hydraulic force.

Photocatalytic degradation of the adsorbed HA was performed after physical cleaning by irradiating the membrane surfaces twice with a UV lamp at a light intensity of 1.53 mW/cm^2 for 3 hours each. After irradiating with UV light, the fouled membrane, which was initially dark brown in color gradually changed to light brown and almost yellow when photocatalytic oxidation was employed, while the color of the fouled neat PVDF membrane remained the same. As seen in Fig. 6, the filtration flux of the mixed-matrix membrane was effectively enhanced after irradiating with UV. This result proves that the effect of photocatalysis on mixed-matrix membranes provides additional cleaning properties. During photocatalytic degradation, TiO_2 particles on the mixed-matrix membrane surface interact with UV light to generate electrons (e^-) and holes (h^+). The photogenerated holes trap H_2O or O_2 to yield H^+ and highly active $\text{HO}\cdot$ radicals, which are an effective oxidation agent in destroying HAs. Generally, $\text{HO}\cdot$ attacks the HA molecule through hydroxyl addition or hydrogen extraction. Meanwhile, dissolved oxygen (DO) in water can capture electrons and produce O_2^- , which reacts with HA or HA intermediates. DO can further form $\cdot\text{OH}$ by protonation, which results in the degradation of HA. Additionally, UV light illumination will hydrolyze water molecules on the surface of TiO_2 NPs and produce extra $\cdot\text{OH}$ groups. Therefore, the TiO_2 -embedded mixed-matrix membranes are more hydrophilic compared to the neat PVDF membrane due to their higher affinity with water.

The high water affinity of the membranes diminishes hydrophobic adsorption between HA molecules and the mixed-matrix membrane surfaces. Therefore, it is expected that UV irradiation can reduce irreversible HA fouling on mixed-matrix membranes.

IFRR(UV) values of 0.10, 5.74, 16.56 and 15.30 were recorded for the neat membrane and the membranes prepared with PC20, P25 and X500, respectively. It is obvious that the IFRR(UV) of the TiO₂-blended membranes is higher than that of the neat PVDF membrane, indicating that no significant degradation occurred in the absence of TiO₂, as the UV light alone failed to degrade HA deposited on the membrane surface. A considerable improvement in terms of IFRR(UV) was obtained for the P25 mixed-matrix membrane. The high photocatalytic activity of the P25 mixed-matrix membrane is attributed to its crystalline properties of P25 which consists of 75% anatase. Particle size is another important parameter for photocatalysis because it directly affects the specific surface area of a catalyst. The X500 membrane, which has a smaller particle size (12 times smaller) compared to PC-20 has more active surface sites and a higher surface charge carrier transfer rate in photocatalysis. Therefore, it is reasonable that the X500 mixed-matrix membrane also showed excellent photocatalytic activity.

High surface tension between the NPs and the polymer matrix were overcome by partially hydroxylizing the PVDF polymer via the Fenton reaction. The Fenton reaction was followed by the embedment of TiO₂ particles via simultaneous solvent exchange and phase inversion in a colloidal stable suspension bath. The resulting OH functional group on the PVDF-OH polymer matrix was expected to promote stronger interactions with the fine NPs and PVDF-OH to improve the distribution, lower surface roughness (low fouling) and promote a higher reactive surface area (better UV-cleaning).

To prove that the PVDF-OH polymer with more hydroxyl groups has better anti-fouling properties, a QCM-D adsorption study of 20 mg/L HA solution on the neat PVDF membrane and PVDF-OH membrane was carried out. Fig. 4 clearly reveals that the frequency change (Δf) of the PVDF-OH membrane related primarily to the change in mass adsorbed (Δm) was lower than the frequency change of the neat PVDF membrane. In other words, the rate and extent of membrane fouling of the PVDF membrane are higher than the rate and extent of membrane fouling of the PVDF-OH membrane. The thickness of the fouled PVDF-OH membrane is more readily reduced compared to the PVDF membrane.

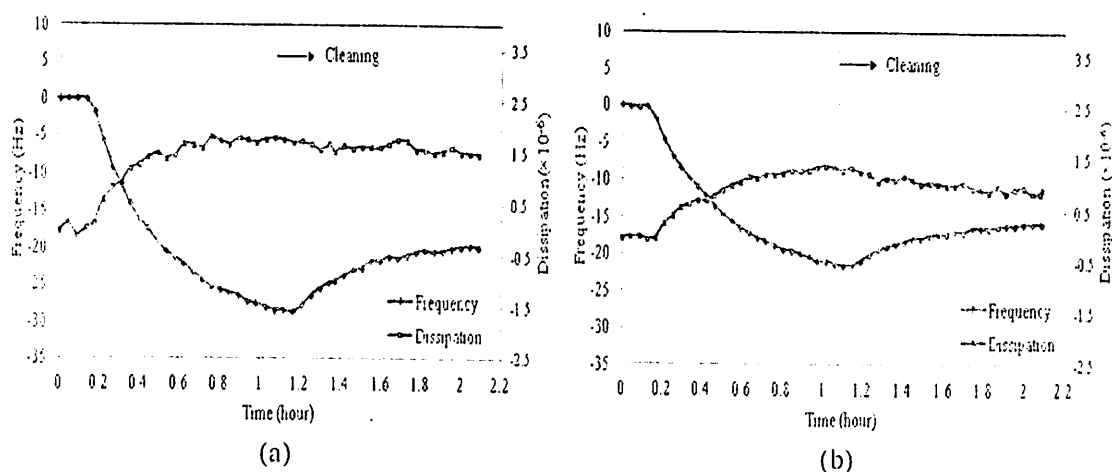


Fig. 4. Dissipation change (ΔD) and frequency change (Δf) of (a) neat PVDF membrane and (b) neat PVDF-OH membrane during three cycles of cross-flow process: deionized water flow for 5 minutes, HA solution flow for 1 hour, deionized water flow of hydraulic cleaning for 1 hour. Casting solution composition: PVDF/DMAc = 5: 95. Operation conditions during the experiment: [HA] = 20 mg/L; [Ca²⁺] = 1 mM (as CaCl₂); pH 7.0; temperature = 25 ± 1°C; constant cross-flow rate = 50.0 μL/min

The HA fouling tendency was revealed clearly by the considerable flux decline in Fig. 5 with RFR values of 24.24%, 36.07% and 15.24% for the neat PVDF membrane, PVDF/TiO₂ MMM and PVDF-OH/TiO₂ MMM, respectively, after 12 hours of HA filtration (the end of HA fouling). Visual observation revealed that the membrane surface was covered with a thin dark brown deposit layer (gel

formation) at the end of the filtration, confirming the existence of the fouling layer. In the PVDF-OH/TiO₂ MMM system, in which the particle distribution was enhanced, the HA fouling propensity of the membrane was greatly reduced, as shown by the lower RFR value compared to the neat PVDF membrane and unmodified PVDF/TiO₂ MMM. This finding shows that the fine and uniformly distributed NP membrane with lower surface roughness and higher surface energy was responsible for its anti-fouling properties.

A significant increment in flux was found after the membrane was washed with pure distilled water. The permeation flux recovery was expressed in terms of the FRR. The water flux can be recovered up to 82.03%, 61.89% and 87.32% for the neat PVDF membrane, PVDF/TiO₂ MMM and PVDF-OH/TiO₂ MMM, respectively. This observation indicated that the flux decline caused by HA was mostly reversible, most likely due to the surface reversible deposition that could be improved significantly using hydraulic force.

Again, the recovery of the PVDF/TiO₂ MMM flux appeared to have a lower FRR than the neat PVDF membrane. This observation further supports the suggestion that irregular surface roughness promoted the adsorption of HA molecules that are difficult to remove due to the zero shear near the surface. The PVDF-OH/TiO₂ MMM was likely to show an extraordinary advantage for membrane defouling properties. This quality was further enhanced by the uniform roughness of the membrane surface due to the trapping of air in the cavities between the drop and the hierarchical nodular structure of the membrane surface (wetting resistance), which could easily repel the water by rolling off the water with anchoring HA.

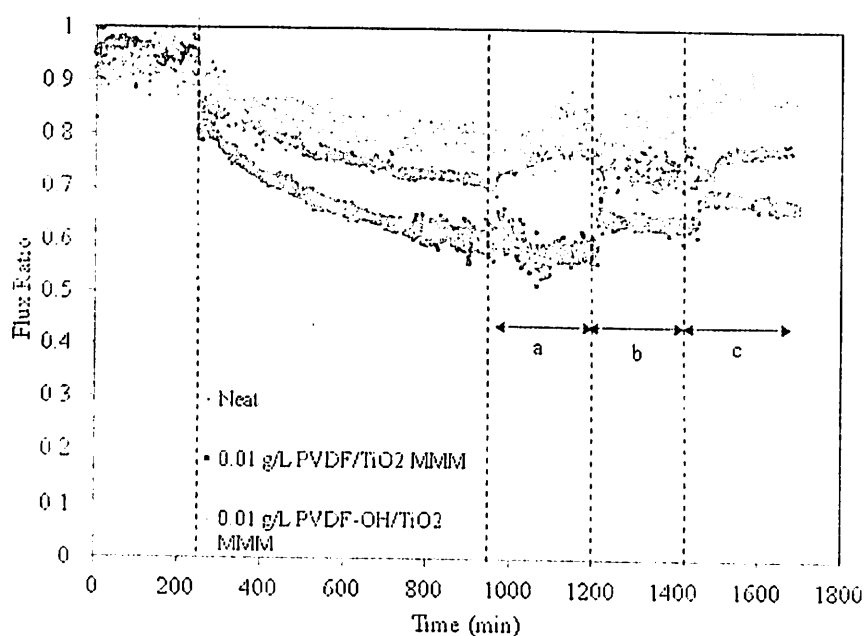


Fig. 5. Effect of the hydroxyl-functionalized P25 MMM on anti-fouling potential during five cycles of the cross-flow filtration process: PWF for 4 hours, HA solution filtration for 12 hours, hydraulic cleaning PWF for 4 hours, water flux for 4 hours after 3 hours of UV irradiation and water flux for 4 hours after a 2nd round of 3 hours UV irradiation. Operation conditions during the experiment: [HA] = 2 mg/L; [Ca²⁺] = 1 mM (as CaCl₂); pH 7.0; temperature = 25 ± 1 °C; cross-flow velocity = 4.0 L/h, operating pressure = 0.5 bar; light intensity = 1.53 mW/cm². [a] hydraulic cleaning, [b] hydraulic cleaning after 3 hours of UV irradiation, [c] hydraulic cleaning after another subsequent 3 hours of UV irradiation.

The filtration flux of the MMM was effectively enhanced after UV irradiation. These results prove that the effect of photocatalysis on the MMMs did provide additional cleaning properties. IFRR(UV) values of 0.10, 16.56 and 11.15 were recorded for the neat PVDF membrane, PVDF/TiO₂ MMM and PVDF-OH/TiO₂ MMM respectively. The IFRR(UV) obviously had an insignificant effect on the neat membrane, as the UV light alone failed to degrade HA deposited on the membrane

surface. Because photocatalytic activity of the MMM is contributed by the embedded TiO₂ NPs, it is reasonable to find that the PVDF-OH/TiO₂ MMM also showed enhanced photocatalytic activity. The amalgamation of superior anti-fouling, defouling and UV-cleaning ability of the PVDF-OH/TiO₂ MMM prepared using the in-situ colloidal precipitation method was therefore attractive for longer operational lifetimes that could reduce its operating costs.

Summary

As a summary, this project devised a novel method of preparing MMM via in situ colloidal precipitation method. Conditions have been optimized to develop fine and uniformly distributed TiO₂ NPs into the membrane matrix to improve the hydrophilicity and functionality of the membrane. Colloidal stable TiO₂ NPs in coagulation bath was first prepared combining the ultrasonic and pH peptization method. The stable TiO₂ colloid was then embedded into the membrane matrix during phase inversion process to avoid the TiO₂ agglomeration problem due to the viscous effect. Using the novel in-situ colloidal precipitation method, the pore formation and particles embedment were carried out simultaneously so that the changes of physical structure of PVDF/TiO₂ MMMs was minimized.

It was found that the membrane prepared using NMP and DMAc as solvent has better particle size distribution compared to DMF. Membrane with NMP as solvent gave bigger pore size but smaller and irregular particle size, whereas membrane prepared with DMAc has narrow particle size distribution pattern. Additionally, the particle size increased with the increasing of TiO₂ concentration in the coagulation bath. It was found that PVDF/TiO₂ MMM system that was prepared using DMAc as solvent and immersed in coagulation bath with X500 TiO₂ NPs has a comparatively well distributed, regular and smaller TiO₂ NPs on membrane surface. The particle size distributions is mainly contributed by the smaller and stable TiO₂ NPs in the suspension bath. System with greater *Rg/Rp* ratio which has better thermodynamic stability is therefore required for favorable particle distribution. Smaller X500 particle size on the membrane (under the same concentration) unexpected give higher contact angle compared to the neat PVDF membrane. However, surface energy analysis showed that X500 MMMs with better dispersion has better affinity towards water which indicating the enhanced membrane hydrophilicity.

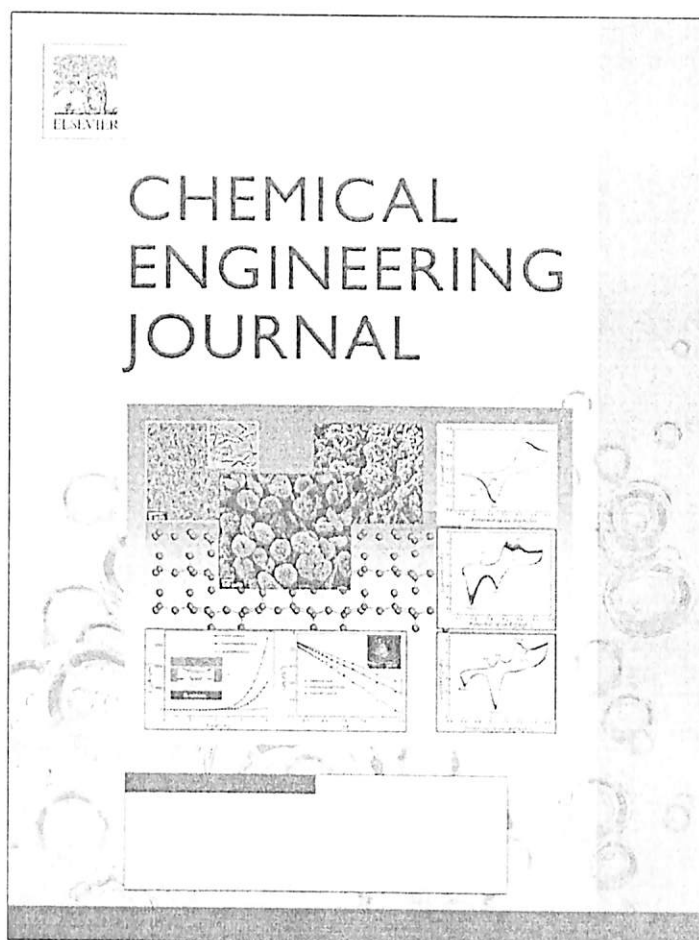
Filtration tests with HA solution proved that permeability of the MMMs is significantly improved due to its increasing porosity attribute to the nanogap between the particles and the polymer matrix (defect) as well as enhanced hydrophilicity. The optimum membrane prepared with 0.01 g/L X500 showed significant flux improvement (58.81 ± 1.96 L/m² h) and HA rejection (98.76 ± 0.05 %) which could be attributed to the better particle distribution, smaller particle size as well as increasing hydrophilicity. The synergistic effect of TiO₂ NPs on membrane water flux and rejection could be realized only if the NPs were well dispersed. The fine and well TiO₂ dispersions on membrane polymeric matrix was found to have significant effects on the membrane anti-fouling and defouling properties. It is attributed to their reduced surface roughness as well as increasing surface energy. This finding is manifested through the improved RFR and FRR values of X500 series PVDF/TiO₂ MMMs.

The ultimate advantage of incorporating photocatalytic TiO₂ NPs into the membrane matrix and their self-cleaning properties was evaluated by degrading the HA adsorbed on the membrane surface under mild UV light irradiation. It was found that photocatalytic oxidation could be an effective process for degrading permanent fouled HA by breaking the hydrophobic and electrostatic interactions between HA and membrane. It was proven that P25 TiO₂ with mixed 25% rutile and 75% anatase crystallinity, produced superior UV-cleaning properties with the highest membrane IFRR(UV) value. A considerably high IFRR(UV) was also obtained for uniformly dispersed X500 on the membrane surface, which has more active surface sites due to the improved dispersions. However, the photocatalytic properties of P25 MMMs are compensated by its rough surface. This problem can be solved by hydroxylate the polymer matrix to improve the dispersion. Hydroxyl-functionalized P25 MMM containing a well-dispersed photocatalyst with large surface-to-volume ratio is considered to be an attractive membrane which promises highly amalgamation application of anti-fouling, defouling and UV-cleaning (self-cleaning) capacity.

Project
Outputs

Research
Publications

Provided for non-commercial research and education use.
Not for reproduction, distribution or commercial use.



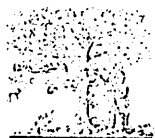
(This is a sample cover image for this issue. The actual cover is not yet available at this time.)

This article appeared in a journal published by Elsevier. The attached copy is furnished to the author for internal non-commercial research and education use, including for instruction at the authors institution and sharing with colleagues.

Other uses, including reproduction and distribution, or selling or licensing copies, or posting to personal, institutional or third party websites are prohibited.

In most cases authors are permitted to post their version of the article (e.g. in Word or Tex form) to their personal website or institutional repository. Authors requiring further information regarding Elsevier's archiving and manuscript policies are encouraged to visit:

<http://www.elsevier.com/copyright>



ELSEVIER

Contents lists available at SciVerse ScienceDirect

Chemical Engineering Journal

journal homepage: www.elsevier.com/locate/cejChemical
Engineering
Journal

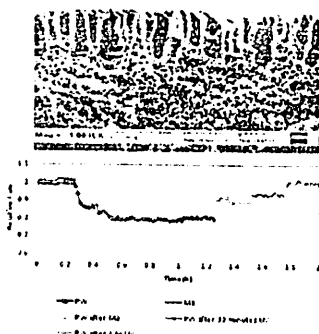
Preparation of PVDF–TiO₂ mixed-matrix membrane and its evaluation on dye adsorption and UV-cleaning properties

H.P. Ngang^a, B.S. Ooi^{a,*}, A.L. Ahmad^a, S.O. Lai^b^aSchool of Chemical Engineering, Engineering Campus, Universiti Sains Malaysia, Seri Ampangan, 14300 Nibong Tebal, Penang, Malaysia^bFaculty of Engineering & Science, Setapak Campus, Universiti Tunku Abdul Rahman, Jalan Genting Kelang, Setapak 53300, Kuala Lumpur, Malaysia

HIGHLIGHTS

- ▶ The hydrophilicity of the mixed-matrix membrane was greatly enhanced.
- ▶ Both standard blocking and cake filtration mechanisms took part in the filtration.
- ▶ The mixed-matrix membrane has significant UV-cleaning properties.
- ▶ The mixed-matrix membrane could provide 100% flux recovery ratios.

GRAPHICAL ABSTRACT



ARTICLE INFO

Article history:

Received 7 February 2012
 Received in revised form 14 May 2012
 Accepted 15 May 2012
 Available online 23 May 2012

Keywords:

PVDF
 TiO₂
 Mixed-matrix membrane
 UV-cleaning
 Permeability
 Methylene blue

ABSTRACT

In this study, the polyvinylidene fluoride (PVDF)–Titanium dioxide (TiO₂) mixed-matrix membranes were prepared via phase inversion technique. The properties of PVDF–TiO₂ mixed-matrix membranes were characterized based on pore size distribution, membrane porosity, field emission scanning electron microscope (FESEM) and photocatalytic behavior. The hydrophilicity of the mixed-matrix membrane was enhanced and resulted in the improved pure water permeability (392.81 ± 10.93 l/m² h bar) compared to that 76.99 ± 4.87 l/m² h bar of the neat membrane. The neat and mixed-matrix membranes were further investigated in terms of filtration, adsorption and UV-cleaning properties based on methylene blue (MB) solution. Mixed-matrix membranes showed excellent removal efficiency (~99%) when sodium dodecyl sulfate (SDS) was introduced into the MB feed solution. The produced mixed-matrix membrane shows some slight photocatalytic properties improvement as FTIR results reviewed that the cleavage of –C=N bonding due to MB adsorption reduced more significantly with the presence of TiO₂ NPs and ultraviolet (UV) light irradiation. The UV-cleaning properties of the mixed-matrix membrane were further proved by the 100% flux recovery ratios (FRRs) for mixed-matrix membrane, suggesting that the embedded TiO₂ NPs was photocatalytically active and able to degrade the adsorbed MB in the membrane.

© 2012 Elsevier B.V. All rights reserved.

1. Introduction

Membrane technology has emerged as an advanced separation technology in various industrial applications over the past few decades. In recent year, ultrafiltration (UF) is considered as a promising method which can be operated with minimal chemical

additives, very low energy usage, easy automation, and optimal quality of treated water [1].

Micellar enhanced ultrafiltration (MEUF) is one of the energy efficient membrane separation process useful in wastewater treatment. The process involves the addition of sodium dodecyl sulfate (SDS) surfactant at a concentration higher than its critical micelle concentration (CMC) to form the large amphiphilic aggregate micelles. The micelles are formed through ionic binding between the solutes with the oppositely charged micelle surface which

* Corresponding author. Tel.: +60 4 5996418.

E-mail address: chobs@eng.usm.my (B.S. Ooi).

facilitated the removal of metal ions and trace organic pollutants using lower pressure method [2]. Micelles containing solubilized organic compounds (having larger size than the membrane pore) are retained by the membrane and a permeate stream passing through the membrane is nearly free from impurities [1,3].

However, one of the main barriers to extensive use of such UF process is membrane fouling. Decline in permeate flux due to adsorption of organic compounds on the membrane surface causes serious issues related to membrane fouling [4–8]. Besides, MB also caused serious irreversible fouling on membrane matrix which attract great attention on membrane fouling analysis.

The semi crystalline polyvinylidene fluoride (PVDF) is one of the most attractive polymer materials in microporous membrane industry because of its thermal stabilization and high mechanical strength [9,10]. However, the PVDF UF membrane exhibits hydrophobic nature, leading to severe membrane fouling and decline in membrane permeability, which have become a barrier for wastewater treatment due to its high surface energy between water and membrane surface [11].

Various methods have been applied to improve the hydrophilicity and performance of PVDF membrane. Membrane fouling can be reduced by addition of hydrophilicity materials to the membrane casting solution [12–14]. The preparation of novel organic-inorganic composite membranes with control properties has been widely used recently. Titanium dioxide nanoparticles (TiO₂ NPs) have received most attention over other NPs due to its stability, commercial availability, excellent photocatalytic, antibacterial and UV-cleaning properties [12,14–16].

Recent studies indicate that photocatalytic oxidation is an emerging alternative technology for wastewater treatment involving reactive dyes such as methylene blue (MB). It has been demonstrated that organic contaminants can be oxidized to carbon dioxide, water and simple mineral acids at low temperatures on TiO₂ photocatalysts in the presence of UV or near-UV illumination [17]. Lakshmi et al. [18], Tayade et al. [19], as well as Yu and Chuang [20] studied the photocatalytic oxidation of MB in aqueous TiO₂ suspension. The use of TiO₂ in suspension is a promising method for MB photodegradation due to its large surface area of TiO₂ available for the reaction. However, the TiO₂ NPs must be removed in the post-treatment process which requires a solid-liquid separation stage, leading to higher overall operating cost in the process. Alternatively, TiO₂ NPs incorporation onto PVDF membrane matrix was carried out in this study to eliminate the need of post-treatment.

Many research works had been carried out on the passive anti-fouling properties of mixed-matrix membrane by determining its fouling rate based on protein adsorption. However, in the present work, not only we observed the adsorption and sieving phenomenon of dye or micellar enhanced dye of the mixed-matrix membrane but for the first time, we provide a direct investigation on the membrane UV-cleaning properties based on the photodegradation of dye adsorbed on the membrane surface. The performance of mixed-matrix membranes was compared with that of neat membranes under similar operating conditions in order to evaluate its flux recovery ratio (FRR) under ultraviolet (UV) light irradiation.

2. Materials and methods

2.1. Materials

Polyvinylidene fluoride (Solef® PVDF) was supplied by Solvay Solexis, France. N,N-dimethylacetamide (DMAc), sodium dodecyl sulfate (SDS) and methylene blue (MB) were purchased from Merck, Germany. Anatase TiO₂ NPs, PC-20 (20 nm) was purchased from TitanPE Technologies, Inc., Shanghai. PVDF and TiO₂ NPs were

dried in an oven at 70 °C for overnight prior to use, while other organic chemicals were obtained in reagent grade purities and used as received. Distilled water was used for all the experiments.

2.2. Membrane preparation

TiO₂ NPs (1.5 wt.%) was dispersed in the DMAc solvent under sonication for 15 min. The PVDF powder was then dissolved into the TiO₂ solution and stirred at 60–70 °C for 4 h to ensure a complete dissolution. The solution was left to stir overnight at 40 °C to form a homogenous solution. The final solution was then subjected to further sonication for 30 min and allowed to cool down to room temperature. Solvent loss by evaporation was negligible due to the high boiling points of DMAc (164–166 °C). The details of the membrane synthesis parameters on MEUF process are summarized in Table 1.

The solution was then cast on the tightly woven polyester sheet using automatic film applicator (Elcometer 4340, EU). Subsequently, it was immediately immersed into the water bath of distilled water to allow the phase inversion to occur for 24 h to remove the residual solvent. The PVDF membrane was kept in the distilled water prior to use.

2.3. Membrane characterization

2.3.1. Pore size distribution

The pore size distribution of the membrane was determined using the Capillary Flow Porometer, Porolux 1000 (Benelux Scientific, Belgium). The membrane samples with diameter of 20 mm were immersed in perfluoroethers (wetting liquid) prior to test and characterized using a liquid extrusion technique in which the differential gas pressure and flow rates through wet and dry samples were measured. The pore size distributions were then analyzed using the LabView software.

2.3.2. Membrane porosity

The asymmetric porous membrane porosity, A_k , was defined as the volume of the pores divided by the total volume of the membrane. To prepare the wet and dry membranes, three pieces of square flat sheet membranes with the size of 2.5 cm × 2.5 cm were dried in an oven at 60 °C until constant weight was observed and the weight of dry membrane was recorded. The membrane samples were then immersed into 2-butanol (Merck, Germany), and degassed for 30 s to avoid air trap in the membrane pores, and left at room temperature for 2 h. Lastly, the membrane surface was dried using filter paper and weighted immediately to avoid evaporation of 2-butanol from membranes pores. The membrane porosity was calculated using the following equation:

$$A_k = \frac{(w_1 - w_2) \rho_b}{(w_1 - w_2) \rho_p + w_2 \rho_b} \times 100\% \quad (1)$$

where A_k is the porosity of the membrane (%), w_1 and w_2 are the weights of the wet and dry membrane (g), respectively, ρ_p and ρ_b are the specific gravities of the PVDF polymer (1.78 g/cm³) and 2-butanol (0.81 g/cm³) (assuming that all materials kept their specific gravity constant in the wetted condition, and there was no air trap in the membrane pores), respectively. 2-Butanol a non-solvent for

Table 1
The detail of the membrane synthesis parameter on MEUF process.

Membrane	PVDF (wt%)	DMAc (wt%)	TiO ₂ (wt%)
Neat membrane	18	82	0
Mixed-matrix membrane	18	80.5	1.5

PVDF [21] was chosen as a wetting liquid because it did not swell the PVDF membrane and wetted well the hydrophobic PVDF membrane to ensure complete pores filling by capillarity [22].

2.3.3. Field emission scanning electron microscope

The cross-sectional morphologies of the neat and mixed-matrix membranes were observed under field emission scanning electron microscope (FESEM CARI ZEISS SUPRA 35VP, Germany). The membranes were initially dried with a filter paper to remove the remaining distilled water on the membrane surface, and air dried for FESEM observation. The membranes were immersed in liquid nitrogen and fractured carefully to have a clean brittle fracture for FESEM images. Membrane surface was coated with a thin layer of gold under vacuum before being tested using K 550 sputter coater to provide electrical conductivity. The samples were examined under the FESEM at potentials of 10.0 kV at 1000× image magnifications.

2.3.4. Adsorption study

The adsorption studies were carried out using a dead-end stirred cell (Amicon 8200, Millipore Co., USA) with a capacity of 200 ml, where the disc membrane has a diameter of 6 cm with a geometric area of 28.27 cm² (excluding the area covered by the O-ring). The synthesized flat sheet membrane was cut into the disc shape and laid on top of the membrane holder in a circular stirred cell unit, thus covered and tightened with a rubber O-ring. The stirring speed was maintained at 200 rpm using the controllable magnetic hot plate stirrer and the operating temperature was 27 ± 2 °C.

The adsorption efficiency was monitored continuous for 24 h by collecting 2 ml of samples at every predetermined time. The desired concentration of MB–SDS in the feed solution and MB–SDS samples concentration analysis were measured using a UV spectrophotometer (UV Mini-1240, Shimadzu) on the basis of measurement of color intensity at the maximum absorbance of 662 nm.

2.3.5. Photodegradation experiment

The neat and mixed-matrix membrane after MB UF process were cut into several small square coupons and mounted onto glass slides using double-sided tape to ensure a flat membrane surface. The glass slides were immersed in a petri dish which was filled with ~50 ml of distilled water to ensure the same water level throughout the whole photodegradation experiment. The photodegradation ability of neat and mixed-matrix membrane were carried out using Ultra Violet A (UVA) light chamber with Tubular low-pressure mercury vapor fluorescent lamps, UVA lamp (Actinic

BL TL-K 40W/10-R1SL, Philip) at light intensity of 2.5 ± 0.2 mW/m² measured using sensor monitor (Model 5.0 classic version, sglux).

The acquired fourier transform infrared spectroscopy (FTIR) spectra were obtained from the neat and mixed-matrix membrane surfaces using an FTIR spectroscopy (Thermo Scientific, Nicolet iS10, USA) to determine the extent of MB degradation. The FTIR spectroscopy was equipped with an OMNI-Sample Attenuated Total Reflection (ATR) smart accessory with diamond crystal operated at 45°. The membranes were scans at a resolution of 4 cm⁻¹ within wave number of 4000–525 cm⁻¹. The changes of absorbance over different reaction time were determined based on the wave number of 1599 cm⁻¹ which indicated the C=N bonding. To minimize experimental error, the FTIR spectra measurements were repeated 10 times for each sample at different point locations of membrane and the results were then averaged.

2.4. Dead-end UF experiment

The UF experiments were performed in a dead-end stirred cell (Amicon 8200, Millipore Co., USA) with a capacity of 200 ml, where the disc membrane had a diameter of 60 mm with a geometric area of 28.27 cm² (excluding the area covered by the O-ring). The applied pressure of the UF system was controlled by N₂ gas and the operating temperature was 27 ± 2 °C. The stirring speed was maintained at 200 rpm using a controllable magnetic hot plate stirrer (Heidoph MR Hei-Standard, Germany). The desired MB concentration in the feed solution was achieved by diluting the appropriate volume from a stock MB solution of 100 mg/l to a final volume of 1000 ml. The predetermined amount of SDS was added as binding agent to the feed solution before UF process. In each experimental run, the feed solution was stirred at 300 rpm for 30 min and introduced to the feed tank of the dead-end UF unit. The permeate flux and filtration efficiency were measured for every 10 ml of permeate collected. The permeate flux (*J*) was calculated by the following equation:

$$J = \frac{V}{A\Delta t} \quad (2)$$

where *V* (m³) is the volume of permeated water, *A* (m²) is the membrane area, and Δt (h) is the UF operating time. The concentrations of MB with and without SDS surfactant in the feed and permeate were measured using a UV spectrophotometer (UV Mini-1240, Shimadzu) on the basis of measurement of color intensity at the maximum absorbance of 662 and 665 nm. Two calibration curves using different standard solutions containing different concentrations of

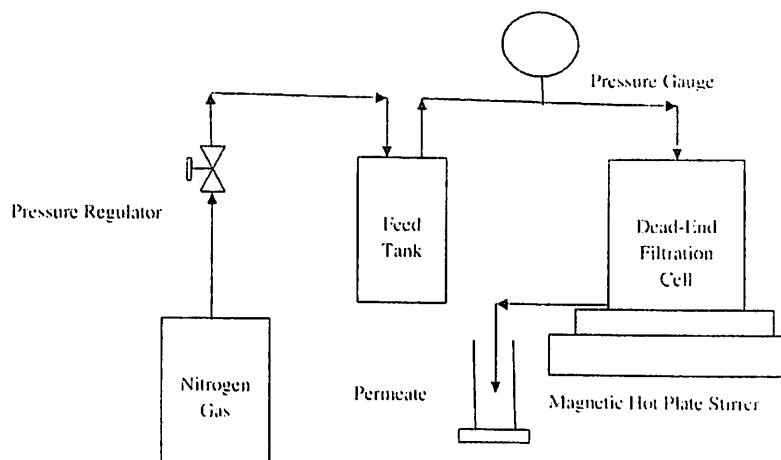


Fig. 1. Schematic diagram of dead-end UF unit.

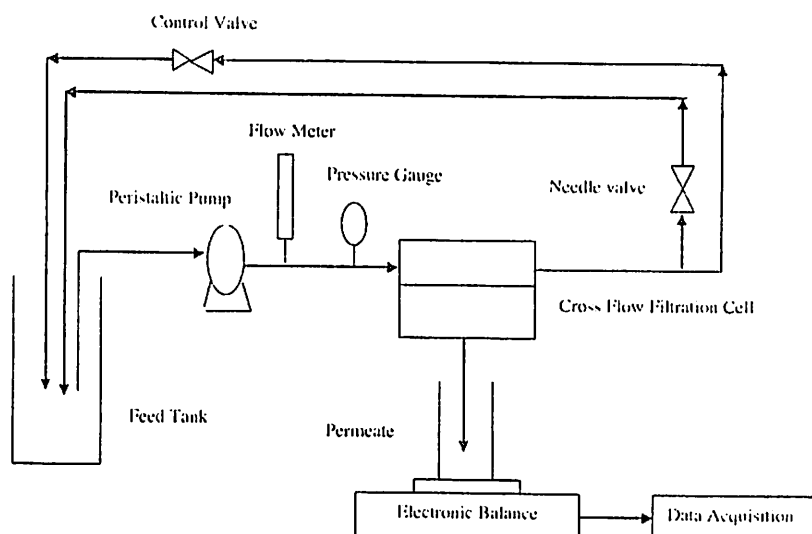


Fig. 2. Schematic diagram of cross-flow UF unit.

MB and MB with SDS were determined. The UF efficiency of the dye removal from the feed solution was calculated using the following equation:

$$R(\%) = \left[1 - \frac{C_p}{C_0} \right] \times 100\% \quad (3)$$

where C_p is the dye concentration in the permeate and C_0 is the initial concentration of the dye in the feed.

The schematic diagram of dead-end UF unit is shown in Fig. 1.

2.5. Cross-flow UF experiment

The UV-cleaning experiments were carried out in a cross-flow UF unit, where the disc membrane had a diameter of 4 cm with a geometric area of 12.57 cm² (excluding the area covered by the O-ring). The applied pressure of the filtration system was controlled by a needle valve to a constant pressure of 0.5 bar. The operating temperature was 27 ± 2 °C.

The desired MB concentration in the feed solution was achieved by diluting the appropriate volume from a stock solution of 100 mg/l MB to a final volume of 1000 ml of 10 mg/l MB and introduced to the feed tank of the cross-flow UF unit. Feed pressure was continually monitored to ensure that constant pressure was applied throughout the experiments. The pure water and MB solution were charged into a 2-l. feed tank and re-circulated at a constant flow rate of 60 ml/min using a peristaltic pump (Materflex L/S Digital Economy Drive, Model: 77800-60, Cole Parmer Instrument Company). Permeate flow rate were continually recorded using an electronic balance which was connected to a data acquisition system (AND Super Hybrid Sensor, Model: Fx-3000i, A&D Company, Limited). The permeate flux (J) was calculated using Eq. (2). All the results presented were average data obtained from three membrane samples. The schematic diagram of cross-flow UF unit is shown in Fig. 2.

3. Results and discussion

3.1. Effect of operating pressure on membrane flux and rejection

The feed solutions consist of MB and SDS was subjected to the UF process at the operating pressures of 0.2, 0.4, 0.6, 0.8 and 1.0 bar. The effects of operating pressure on neat and mixed-matrix

membrane are presented in Fig. 3. It is evident that both the water and MB-SDS permeate flux increased linearly with operating pressure. Operating pressure is the effective driving force for UF process, suggesting that increasing the operation pressure will increase the effective driving force for the solvent transport and resulting in high permeate flux [23–25].

Mixed-matrix membrane showed higher permeability as compared to neat membrane in both pure water and MB-SDS UF processes. The pure water permeabilities were 392.81 ± 10.93 and 76.99 ± 4.87 l/m² h bar, whereas the MB-SDS permeabilities were 138.43 ± 4.25 and 31.72 ± 3.12 l/m² h bar for mixed-matrix and neat membranes, respectively. The higher pure water permeabilities of mixed-matrix membrane over the neat membrane permeabilities could be attributed to the changes of membrane pore size. Fig. 4 shows that mixed-matrix membrane had larger maximum pore radius (45 nm) compared to the neat membrane (25 nm). It could be further proved from the FESEM cross-sectional images (Fig. 5) which revealed that larger inner pore size for mixed-matrix membrane was observed as compared to that for neat membrane. The membranes have the physical properties as listed in Table 2.

According to Hagen Poiseuille Equation, membrane flux could be predicted using the following equation:

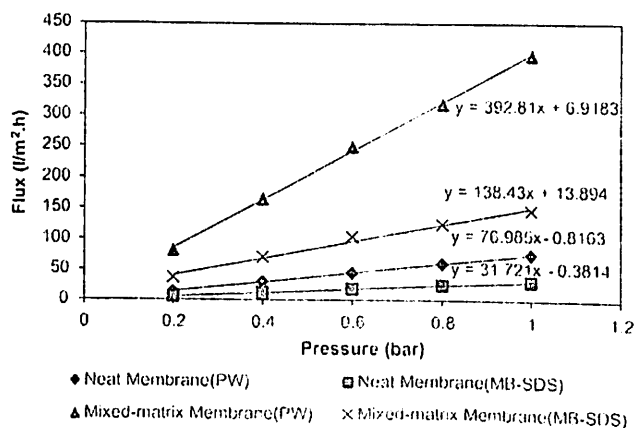


Fig. 3. Effect of the operating pressure on membrane permeability for neat and mixed-matrix membranes for MB and SDS concentrations at 10 and 20 mM, respectively under room temperature.

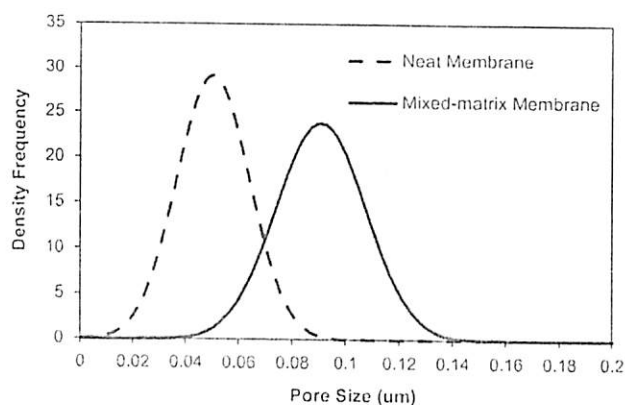


Fig. 4. Pore size distributions of neat and mixed-matrix membranes.

$$Q_p = \frac{\Delta P \pi d_p^4}{128 \mu \Delta x} \quad (4)$$

where Q_p is the volumetric flow rate of single pore (L/h), ΔP is the operating pressure (bars), d_p is the pore diameter (nm), Δx is the membrane thickness (μm) and μ is the solution viscosity (Pa s).

By considering the pore size distribution, the total flux could be expressed as

$$J = \frac{\sum N_i Q_p}{\sum N_i \pi d_p^2 / 4} \quad (5)$$

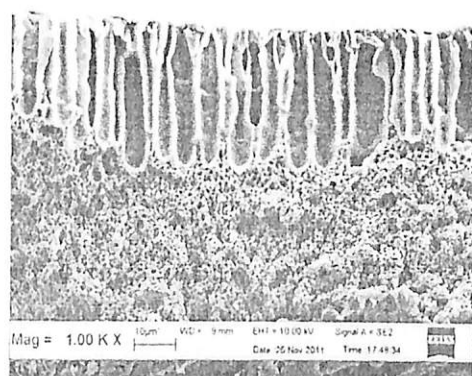
$$J = \frac{\sum N_i \Delta P \pi d_p^4 / (128 \mu \Delta x)}{\sum N_i \pi d_p^2 / 4} = \frac{A_k \Delta P}{32 \mu \Delta x} \frac{\sum N_i d_p^4}{\sum N_i d_p^2} \quad (6)$$

$$J = \frac{A_k \Delta P}{32 \mu \Delta x} \frac{\sum N_i d_p^4}{\sum N_i d_p^2} = \frac{A_k \Delta P}{32 \mu \Delta x} \frac{\sum f_i N d_p^4}{\sum f_i N d_p^2} = \frac{A_k \Delta P}{32 \mu \Delta x} \frac{\sum f_i d_p^4}{\sum f_i d_p^2} \quad (7)$$

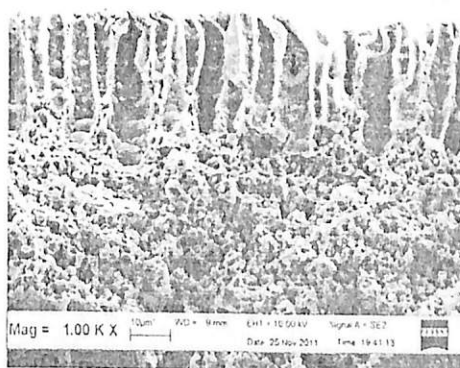
where J is the volumetric flux (L/h m^2), A_k is the membrane porosity, N_i is the number of pores having diameter of $d_{p,i}$, f_i is the fraction of the number of pores with diameter $d_{p,i}$ and N is the total number of pores.

The theoretical flux ratio between mixed matrix membrane and neat membrane could be expressed as

$$\frac{J_{MM}}{J_{NE}} = \frac{(A_k)_{MM} (\Delta x)_{NE} (\sum f_i d_p^4)_{MM} (\sum f_i d_p^2)_{NE}}{(A_k)_{NE} (\Delta x)_{MM} (\sum f_i d_p^4)_{NE} (\sum f_i d_p^2)_{MM}} \quad (8)$$



(a)



(b)

Fig. 5. Cross-section of: (a) neat, (b) mixed-matrix UF membranes.

Table 2
Physical properties of the neat and mixed-matrix membranes.

Membrane characteristics	Neat membrane	Mixed-matrix membrane
Maximum pore radius (r_p), nm	25	45
Pure water permeability ($J_w/\Delta P$), $\text{l/m}^2 \text{ h bar}$	76.99 ± 4.87	392.81 ± 10.93
Porosity (A_k), %	64.53 ± 0.07	65.13 ± 0.05
Thickness (Δx), μm	117 ± 0.85	110 ± 0.33

The subscript MM represents mixed-matrix membrane whereas the subscript NE represents neat membrane.

The theoretical flux ratio ($J_{w,MM}/J_{w,NE}$) calculated based on the membrane properties was 3.0, whereas the experimental value of the flux ratio was 5.1, indicating that the flux enhancement of mixed-matrix membrane was not solely caused by the changes of physical properties, but to certain extent by the pore hydrophilization due to the incorporation of TiO_2 NPs. TiO_2 NPs could form surface hydroxyl group that attracted water molecules to pass through the membrane, leading to the permeate flux increment. Bae and Tak [26] observed similar phenomenon that TiO_2 composite membrane could be more hydrophilic than neat polymeric membrane due to the higher affinity of TiO_2 towards water.

Fig. 6 shows the effect of operating pressure on the MB-SDS rejection for neat and mixed-matrix membranes. It can be seen that neat membrane had better rejection performance at higher operating pressure compared to the mixed-matrix membrane.

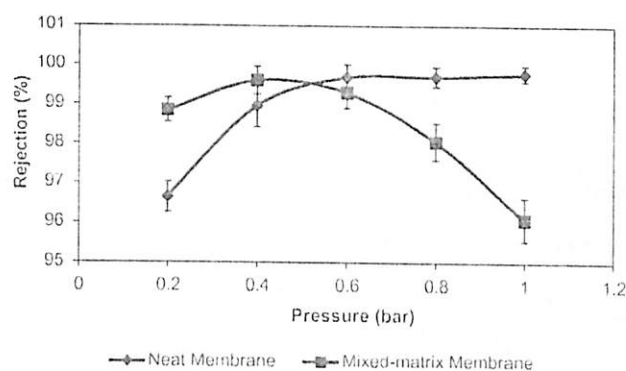


Fig. 6. Effect of the operating pressure on the MB-SDS rejection for neat and mixed-matrix membranes.

For mixed-matrix membrane, MB–SDS rejection decreased slightly with the increase of operating pressure, ranging from 99.71% at 0.2 bar to 96.09% at 1.0 bar, respectively. These data provided us the important information regarding the maximum operating pressure that can be used for such systems. It can also be observed in Fig. 6 that the optimum operating pressure for such systems was found to be 0.5 bar and the corresponding rejections for neat and mixed-matrix membrane exceeded 99%.

It is not surprising that the rejection capability of mixed-matrix membrane decreased compared to that of the neat membrane at higher pressure as mixed matrix-membrane had larger pore size. At higher operating pressure, the higher pore to solute ratio of mixed-matrix membrane allowed the convective transport of solutes through the membrane [27]. Moreover, higher operating pressure also resulted in micelles compaction that enabled the micelle to squeeze through the membrane pores [6]. Ahmad and Puasa [23] also observed the same phenomenon as the operating pressure increased, the micellar enhanced dye rejection would decrease accordingly. Besides, a compacted micelle would reduce the dye solubility which led to less amount of dye removed.

3.2. Effect of SDS concentration on MB flux and rejection

In this experiment, the MB concentration in the feed solution was fixed at 10 mg/l and an operating pressure of 0.5 bar was applied, while the feed SDS concentrations were adjusted to 0, 0.25, 0.5, 1.0 and 2.5 CMC where CMC is critical micelle concentration (1 CMC = 8 mM of SDS) [28].

Fig. 7 shows the effect of SDS concentration on the flux of neat and mixed-matrix membrane. It was found that the permeate fluxes for both neat and mixed-matrix membrane decreased as the SDS concentration increased. Zaghbani et al. [29] reported the phenomenon of flux reduction at higher SDS concentration is generally attributed to the effects of membrane fouling and concentration polarization. Concentration polarization which was caused by deposition of SDS micelles on the membrane surface led to the increased solution mass transfer resistance. Beyond the solubility limit, the micelles deposited on membrane surface would build up gel type layer and caused pores blockage. Besides, higher SDS concentration formed small and compact micelles as reported by Fang et al. whereby the small and compact micelles might plug the membrane pores easily as compared to large and incompact micelles which only deposited on membrane surface [30].

Fig. 7 shows that permeate fluxes decreased as much as 53.72% and 56.94% with the increasing SDS concentration in the feed solution from 0 to 2.5 CMC, for neat and mixed-matrix membranes,

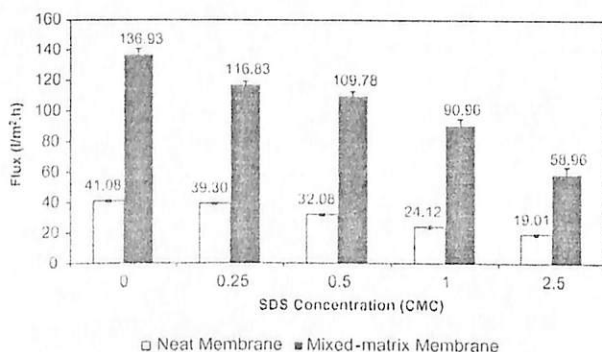


Fig. 7. Effect of the SDS concentration on MB–SDS flux for neat membrane and mixed-matrix membranes. MB concentration and operating pressure were 10 mg/l and 0.5 bar, respectively at room temperature.

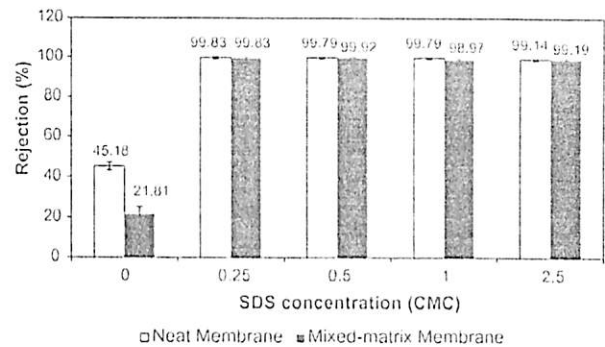


Fig. 8. Effect of the SDS concentration on MB–SDS rejection for neat and mixed-matrix membranes. The MB concentration and operating pressure were 10 mg/l and 0.5 bar, respectively at room temperature.

respectively. Beyond 1.0 CMC (8 mM), a higher reduction in flux was observed for mixed-matrix membrane, indicating that micelles formation greatly provided higher resistance to permeate flow through cake layer formation. However, its effect on the neat membrane was slightly lesser due to the larger micelle to pore ratio (0.04) compared to that (0.02) for the mixed matrix membrane.

Fig. 8 shows the effect of SDS concentration in the feed solution, on membrane rejection. Without the SDS, there were about 45% and 22% of MB rejections for neat membrane and mixed-matrix membrane, respectively. Under neat SDS free condition, it was unlikely that the better pore size of neat membrane could be attributed to its smaller pore size as both had relatively very small solute to pore size ratio. Adsorption is the most possible mechanism for dye removal as it could be noticed from the rapid presence of blue stain on the membrane surface which was difficult to be cleaned. In order to prove that, dye adsorption study was carried out using the same stirred cell without applying pressure. The adsorption profile of MB–SDS in similar conditions (membranes with 0.06 m diameter immersed in 200 ml of MB–SDS solution of 10 mg/l MB and 20 mM SDS at room temperature) were measured for both neat and mixed-matrix membrane. Fig. 9 shows that complete adsorption could be achieved within 30 h for both membranes. Mixed-matrix membranes had higher rate of adsorption compared to the neat membrane, mainly due to the highly connected pore

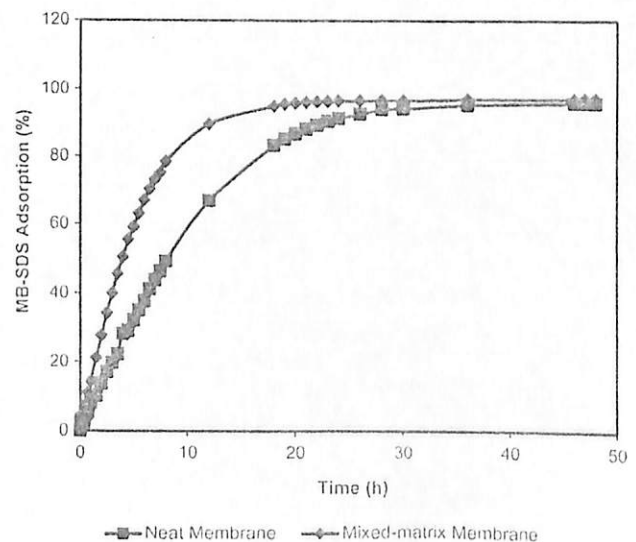


Fig. 9. Rate of adsorption of MB–SDS for neat and mixed-matrix membranes.

structure which make the PVDF sites more accessible to the dye adsorption through diffusion.

Fig. 8 reviews that the rejections for both membranes were sharply increased to nearly 100% when SDS was added into the feed solution, a phenomenon also observed by Huang et al. [8] and Zaghbani et al. [29]. The reasons of this phenomenon might be due to (i) concentration polarization effect and cake layer formation, (ii) precipitation of MB with small amount of SDS surfactant, and (iii) direct adsorption of MB on membrane surface and pores as discussed earlier. Theoretically, there was almost negligible micelle formed at the SDS concentration below 1.0 CMC, however, as concentration polarization occurred on the membrane surface, the concentration of SDS might exceed 1 CMC and resulted in micelle formation. For reason (ii), as reported by Misra et al. [31], for MB feed solution with SDS below 1.0 CMC, MB could be rejected by precipitation with a small amount of SDS molecules. Lastly, the direct adsorption of MB onto the TiO_2 surface could be enhanced as SDS could reduce the surface tension between the solution and constricted pore size which created more accessible adsorption sites. As a result, the rejections of both membranes were improved drastically.

3.3. Effect of methylene blue concentration

The SDS concentration in the feed solution was fixed at 20 mM [29] and an operating pressure of 0.5 bar was applied to observe the effect of MB concentration on the permeate flux and rejection. The experiments were carried out by varying the MB concentration at 10, 50 and 100 mg/l. Fig. 10 shows the effect of MB concentration on permeate fluxes of neat and mixed-matrix membranes. The permeate fluxes decreased as the MB concentration increased, where increasing 10 times in MB concentration had reduced the flux as much as 20.3% and 7.5% for neat and mixed-matrix membranes, respectively. However, compared to the effect of SDS, membrane fouling contributed by the amphiphilic SDS concentration is more significant. The reduction in permeate flux was at higher MB concentration is due to the buildup of free MB adsorption onto the membrane surface which formed the deposit layer near the membrane surface, and eventually building up additional resistance for permeate to pass through the membrane. Huang et al. [8] also found that the permeate flux decreased as the feed MB concentration increased. The higher fouling rate of neat membrane compared to that of the mixed-matrix membrane was mainly caused by the previously postulated reason in which MB is more favorable to adsorb on the PVDF matrix than TiO_2 .

Fig. 11 shows the effect of MB concentration in the feed solution on MB–SDS rejection. The rejection decreased for both neat and mixed-matrix membranes when the MB concentrations increased.

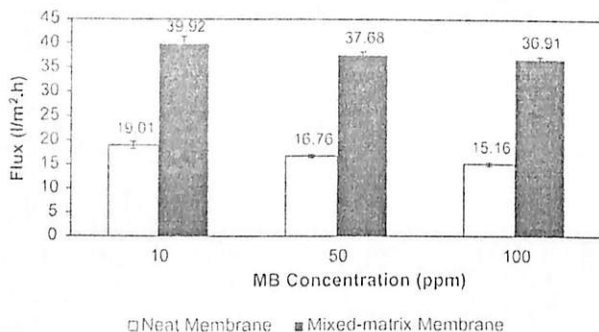


Fig. 10. Effect of the MB concentration on the MB–SDS flux for neat and mixed-matrix membranes. The SDS concentration and operating pressure were 20 mM and 0.5 bar, respectively at room temperature.

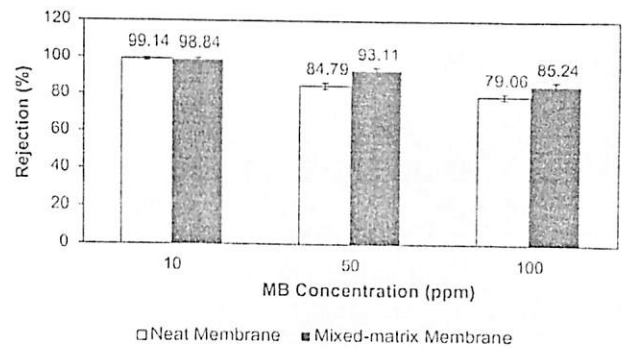


Fig. 11. Effect of the MB concentration on the MB–SDS rejection for neat and mixed-matrix membranes. The SDS concentration and operating pressure were 20 mM and 0.5 bar at room temperature.

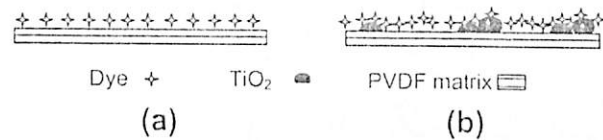


Fig. 12. Schematic diagram of dye adsorption on (a) neat membrane and (b) mixed-matrix membrane.

This result could be due to the complete coverage of adsorption site onto membrane surface at higher MB concentrations, leading to the decreasing of MB–SDS rejection. The rejection for neat and mixed-matrix membranes were reduced as much as 20% and 13.6%, respectively when the MB concentrations were increased from 10 to 100 mg/l. At high MB concentrations, mixed-matrix membrane showed better rejection compared to neat membrane, suggesting that mixed-matrix membrane provided more accessible adsorption sites compared to the neat membrane as illustrated in Fig. 12.

3.4. UV-cleaning properties of neat and mixed-matrix membranes

The UV-cleaning properties of neat and mixed-matrix membranes were studied using cross-flow UF process containing 10 mg/l MB solution without SDS. Its performance was based on the flux recovery of pure water performed over a period of time. Figs. 13 and 14 show the time-dependent permeate flux of the neat and mixed-matrix membranes, respectively. The pure water flux recoveries were observed for three consecutive ultraviolet (UV) light irradiation cycles. In order to study the UV-cleaning

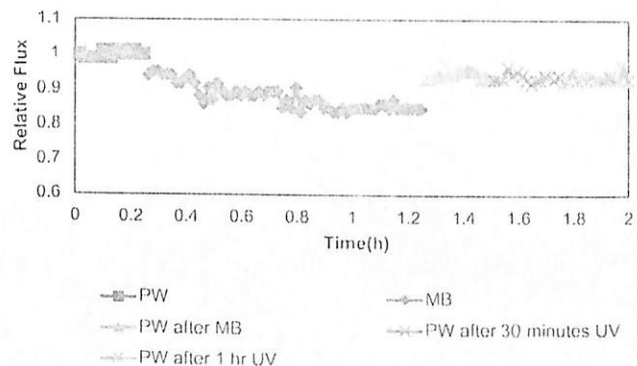


Fig. 13. The time-dependent permeation flux of the neat membrane during five cycles of cross-flow UF process.

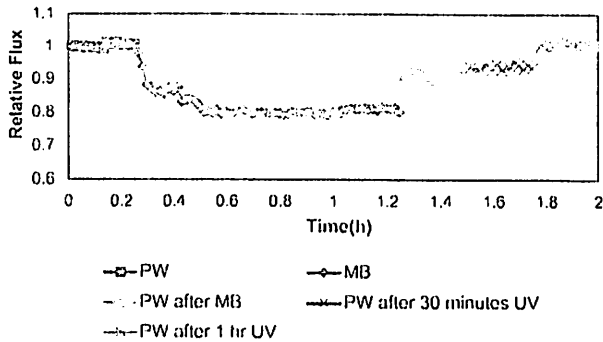


Fig. 14. The time-dependent permeation flux of the mixed-matrix membrane during five cycles of cross-flow UF process.

properties, both membranes were subjected to pure MB fouling through cross-flow filtration. It was observed that the rate of permeation flux decline for MB filtration was higher during the initial 20 min and then became slower and approached plateau after 1 h. Fouling normally occurred at different stages as discussed earlier. Initially, the MB started to be adsorbed and accumulate on membrane pores and surface, leading to the reduction of membrane permeability due to the pore constriction. It was then forming a definite thickness of cake layer after certain period of filtration time which gradually decelerated the permeation flux and reached a constant flux.

After the flux reaching the constant, the membranes were rinsed by circulating pure water to remove loosely bound MB with and without UV light irradiation. The flux profiles were recorded and presented in Figs. 13 and 14. The flux recovery ratios (FRRs) were determined based on the following equation:

$$FRR = \frac{J_{w,t}}{J_{w,i}} \times 100\% \quad (9)$$

where $J_{w,t}$ is the pure water flux at any predetermined time and cleaning condition, $J_{w,i}$ is the initial pure water flux.

It was observed that the flux could be recovered through surface scoring by recirculating the pure water across the surface at 60 ml/min. The FRR value for neat membrane (94.19%) was slightly higher than that for mixed-matrix membrane (91.35%), indicating that the pore constriction is more serious for the bigger pores. The photoresponse of the membranes was further tested under UV light irradiation. After subsequent cleaning by rinsing with pure water and UV light irradiation, further flux increment was observed for mixed-matrix membrane but not for the neat membrane. As shown in Figs. 13 and 14, the FRRs for neat membrane was maintained at 94.19% but for mixed-matrix membrane, a cascading increased of FRR to about 100% was achieved within 1 h of irradiation. This observation indicates that the embedded TiO_2 was photocatalytically active and able to degrade the adsorbed MB more effectively in the membrane.

In order to prove the better photodegradation ability of the mixed-matrix membrane, the time-dependent MB degradation by UV light irradiation on neat and mixed-matrix membranes were carried out through FTIR bonding cleavage observation. As illustrated in Fig. 15, it could be clearly seen that the (C=N) bonding (1599 cm^{-1}) on membrane could be scissor from aromatic ring in the MB structure by UV light irradiation. The disappearance of the C=N bonds in the MB adsorbed on the membrane as shown in Fig. 16 was used as an indicator for the degree of degradation. Fig. 17 shows the relative C=N absorbance value for the MB adsorbed on the membrane. It could be observed that rapid bonding cleavage occurred within 1 h of UV light irradiation with the higher

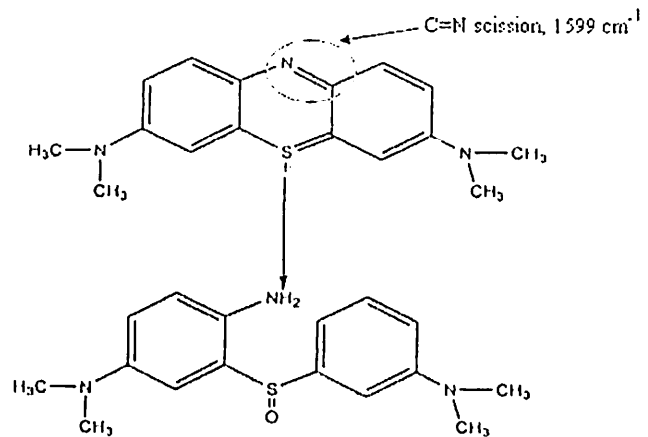


Fig. 15. Photocatalytic degradation pathway of the MB [34].

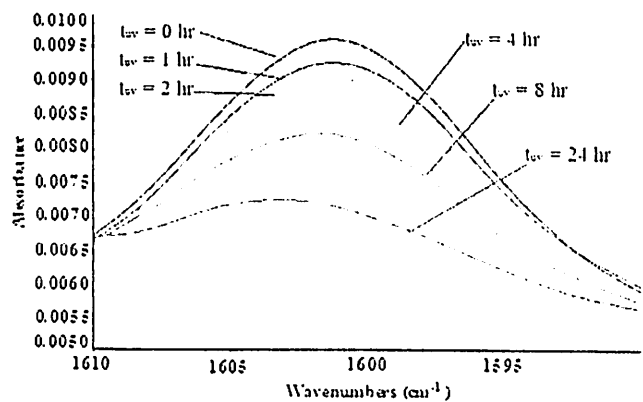


Fig. 16. Effect of UV light irradiation time interval during C=N bond scission for MB molecules degradation.

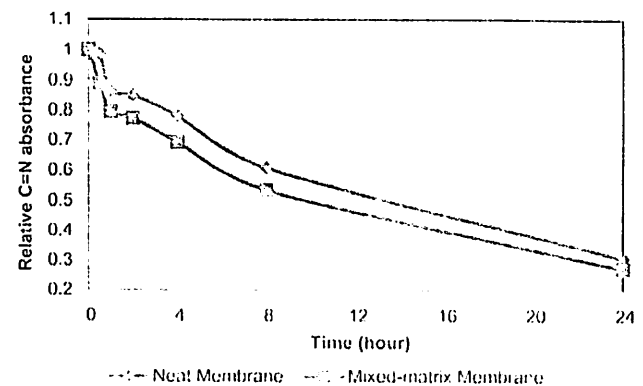


Fig. 17. The time-dependent MB degradation by UV light treatment for neat and mixed-matrix membranes.

rate of degradation for mixed-matrix membrane compared to that for the neat membrane. Being the primary oxidizing species in the photocatalytic oxidation process, a group of active oxidant reagents such as hydroxyl radical (OH^\cdot) and superoxide radical anion ($\text{O}_2^{\cdot-}$) from TiO_2 NPs photocatalysed degradation process appeared on the surface of mixed-matrix membrane after UV light irradiation. The electron in the conduction band could be absorbed by the dye molecules, leading to the formation of a dye radical anion

[32]. The subsequent reaction of the radical anion could lead to degradation and removal of the membrane foulant effectively as compared to neat membrane. On the other hand, the photocatalytic behavior of neat membrane was not a surprising phenomenon as the MB was light sensitive which also photosensitizer [33].

4. Conclusions

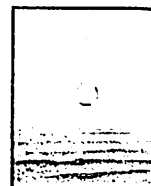
PVDF-TiO₂ mixed-matrix UF membrane was prepared via phase inversion by dispersing TiO₂ NPs into the PVDF matrix. Although the mixed-matrix membrane had some physical properties changes, the membranes hydrophilicity and subsequently permeation flux were greatly improved. The addition of TiO₂ NPs also improved the permeability of membrane. The pure water permeabilities were 392.81 ± 10.93 and 76.99 ± 4.87 l/m² h bar, whereas the MB-SDS permeabilities were 138.43 ± 4.25 and 31.72 ± 3.12 l/m² h bar for mixed-matrix and neat membrane, respectively. The produced mixed-matrix membrane with its adsorptive properties could be operated under pressure as low as 0.5 bar with the corresponding rejection exceeded 99% with the presence of SDS even below its CMC value. Performance of mixed-matrix membrane surpassed the neat membrane at higher MB concentration as NPs could provide extra adsorption sites for the MB. It was proven that the mixed matrix membrane is photocatalytically active as it shows better MB degradation compared to the neat membrane with ~100% pure water flux recovery under 1 h of UV light irradiation.

Acknowledgments

The authors wish to thank the financial supports from Universiti Sains Malaysia (RU Grant) (1001/PJKIMIA/811172), Malaysia Toray Science Foundation (MITSF) Science and Technology Research Grant (304/PJKIMIA/6050179/M126), MOSTI eSciencefund (305/PJKIMIA/6013604), USM Membrane Cluster and Ministry of Higher Education (MyMaster).

References

- [1] B. Sarkar, S. DasGupta, S. De, Application of external electric field to enhance the permeate flux during micellar enhanced ultrafiltration, *Sep. Purif. Technol.* 66 (2009) 263–272.
- [2] I. Xiarchos, A. Jaworska, G. Zakrzewska-Trznadel, Response surface methodology for the modelling of copper removal from aqueous solutions using micellar-enhanced ultrafiltration, *J. Membr. Sci.* 321 (2008) 222–231.
- [3] M. Bielska, J. Szymanowski, Micellar enhanced ultrafiltration of nitrobenzene and 4-nitrophenol, *J. Membr. Sci.* 243 (2004) 271–283.
- [4] I. Koyuncu, D. Topacik, E. Yuksel, Reuse of reactive dyehouse wastewater by nanofiltration, process water quality and economical implications, *Sep. Purif. Technol.* 36 (2004) 77–85.
- [5] A. Aouni, C. Fersi, B. Cuartas-Urbe, A. Bes-Pla, M.J. Alcaina-Miranda, M. Dhabbi, Study of membrane fouling using synthetic model solutions in UF and NF processes, *Chem. Eng. J.* 175 (2011) 192–200.
- [6] A.L. Ahmad, S.W. Puasa, M.M.D. Zulkali, Micellar-enhanced ultrafiltration for removal of reactive dyes from an aqueous solution, *Desalination* 191 (2006) 153–161.
- [7] L. Zheng, Y. Su, L. Wang, Z. Jiang, Adsorption and recovery of methylene blue from aqueous solution through ultrafiltration technique, *Sep. Purif. Technol.* 68 (2009) 244–249.
- [8] J.-H. Huang, C.-F. Zhou, G.-M. Zeng, X. Li, J. Niu, H.-J. Huang, L.-J. Shi, S.-B. He, Micellar-enhanced ultrafiltration of methylene blue from dye wastewater via a polysulfone hollow fiber membrane, *J. Membr. Sci.* 365 (2010) 138–144.
- [9] L. Sauguet, C. Boyer, B. Ameduri, B. Boutevin, Synthesis and characterization of poly(vinylidene fluoride)-g-poly(styrene) graft polymers obtained by atom transfer radical polymerization of styrene, *Macromolecules* 39 (2006) 9087–9101.
- [10] F. Liu, N.A. Hashim, Y. Liu, M.R.M. Abed, K. Li, Progress in the production and modification of PVDF membranes, *J. Membr. Sci.* 375 (2011) 1–27.
- [11] W.-Z. Lang, Z.-L. Xu, H. Yang, W. Tong, Preparation and characterization of PVDF-PFSA blend hollow fiber UF membrane, *J. Membr. Sci.* 288 (2007) 123–131.
- [12] J.-H. Li, Y.-Y. Xu, L.-P. Zhu, J.-H. Wang, C.-H. Du, Fabrication and characterization of a novel TiO₂ nanoparticle self-assembly membrane with improved fouling resistance, *J. Membr. Sci.* 326 (2009) 659–666.
- [13] A. Kazmjou, J. Mansouri, V. Chen, The effects of mechanical and chemical modification of TiO₂ nanoparticles on the surface chemistry, structure and fouling performance of PES ultrafiltration membranes, *J. Membr. Sci.* 378 (2011) 73–84.
- [14] A. Rahimpour, M. Jahanshahi, B. Rajaeian, M. Rahimnejad, TiO₂ entrapped nano-composite PVDF/SPEs membranes: preparation, characterization, antifouling and antibacterial properties, *Desalination* 278 (2011) 343–353.
- [15] S.S. Madaeni, N. Chaemi, Characterization of self-cleaning RO membranes coated with TiO₂ particles under UV irradiation, *J. Membr. Sci.* 303 (2007) 221–233.
- [16] R.A. Damodar, S.-J. You, H.-H. Chou, Study the self cleaning, antibacterial and photocatalytic properties of TiO₂ entrapped PVDF membranes, *J. Hazard. Mater.* 172 (2009) 1321–1328.
- [17] M. Hussain, N. Russo, G. Saracco, Photocatalytic abatement of VOCs by novel optimized TiO₂ nanoparticles, *Chem. Eng. J.* 166 (2011) 138–149.
- [18] S. Lakshmi, R. Renganathan, S. Fujita, Study on TiO₂-mediated photocatalytic degradation of methylene blue, *J. Photochem. Photobiol. A* 88 (1995) 163–167.
- [19] R.J. Tayade, P.K. Surofia, R.G. Kulkarni, R.V. Jasra, Photocatalytic degradation of dyes and organic contaminants in water using nanocrystalline anatase and rutile TiO₂, *Sci. Technol. Adv. Mater.* 8 (2007) 455–462.
- [20] Z. Yu, S.S.C. Chuang, The effect of Pt on the photocatalytic degradation pathway of methylene blue over TiO₂ under ambient conditions, *Appl. Catal. B* 83 (2008) 277–285.
- [21] J. Bandrup, E.H. Immergut, H.A. Grulke, E.H. Immergut, E.A. Grulke, *Polymer Handbook*, Wiley-Interscience, United States of America, 1999.
- [22] A.L. Ahmad, N. Ideris, B.S. Ooi, S.C. Low, A. Ismail, Morphology and polymorph study of a polyvinylidene fluoride (PVDF) membrane for protein binding: effect of the dissolving temperature, *Desalination* 278 (2011) 318–324.
- [23] A.L. Ahmad, S.W. Puasa, Reactive dyes decolorization from an aqueous solution by combined coagulation/micellar-enhanced ultrafiltration process, *Chem. Eng. J.* 132 (2007) 257–265.
- [24] G.-M. Zeng, K. Xu, J.-H. Huang, X. Li, Y.-Y. Fang, Y.-H. Qu, Micellar enhanced ultrafiltration of phenol in synthetic wastewater using polysulfone spiral membrane, *J. Membr. Sci.* 310 (2008) 149–160.
- [25] R.-S. Juang, S.-H. Lin, L.-C. Peng, Flux decline analysis in micellar-enhanced ultrafiltration of synthetic waste solutions for metal removal, *Chem. Eng. J.* 161 (2010) 19–26.
- [26] T.-H. Bae, T.-M. Tak, Effect of TiO₂ nanoparticles on fouling mitigation of ultrafiltration membranes for activated sludge filtration, *J. Membr. Sci.* 249 (2005) 1–8.
- [27] G.-M. Zeng, X. Li, J.-H. Huang, C. Zhang, C.-F. Zhou, J. Niu, L.-J. Shi, S.-B. He, F. Li, Micellar-enhanced ultrafiltration of cadmium and methylene blue in synthetic wastewater using SDS, *J. Hazard. Mater.* 185 (2011) 1304–1310.
- [28] M.J. Rosen, *Surfactants and Interfacial Phenomenon*, third ed., Wiley-Interscience, New York, 2004.
- [29] N. Zaghbani, A. Hafiane, M. Dhabbi, Separation of methylene blue from aqueous solution by micellar enhanced ultrafiltration, *Sep. Purif. Technol.* 55 (2007) 117–124.
- [30] Y.-Y. Fang, G.-M. Zeng, J.-H. Huang, J.-X. Liu, X.-M. Xu, K. Xu, Y.-H. Qu, Micellar-enhanced ultrafiltration of cadmium ions with anionic-nonionic surfactants, *J. Membr. Sci.* 320 (2008) 514–519.
- [31] S.K. Misra, A.K. Mahatele, S.C. Inpathi, A. Dakshinamoorthy, Studies on the simultaneous removal of dissolved DBP and TBP as well as uranyl ions from aqueous solutions by using micellar-enhanced ultrafiltration technique, *Hydrometallurgy* 96 (2009) 47–51.
- [32] K. Natarajan, T.S. Natarajan, H.C. Bajaj, R.J. Tayade, Photocatalytic reactor based on UV-LED/TiO₂ coated quartz tube for degradation of dyes, *Chem. Eng. J.* 178 (2011) 40–49.
- [33] S.J. Wagner, D. Robinette, J. Storry, X.Y. Chen, J. Shumaker, L. Benade, Differential sensitivities of viruses in red cell suspensions to methylene blue photosensitization, *Transfusion* 34 (1994) 521–526.
- [34] A. Houas, H. Lachheb, M. Ksibi, E. Elaloui, C. Guillard, J.-M. Herrmann, Photocatalytic degradation pathway of methylene blue in water, *Appl. Catal. B* 31 (2001) 145–157.



Preparation of mixed-matrix membranes for micellar enhanced ultrafiltration based on response surface methodology

H.P. Ngang, A.L. Ahmad, S.C. Low, B.S. Ooi^{*}

School of Chemical Engineering, Engineering Campus, Universiti Sains Malaysia, Seri Ampangan, 14300 Nibong Tebal, Penang, Malaysia

ARTICLE INFO

Article history:

Received 13 October 2011

Received in revised form 16 February 2012

Accepted 19 February 2012

Available online 13 March 2012

Keywords:

Response surface methodology

Central composite design

Optimization

Micellar-enhanced ultrafiltration

Methylene blue

ABSTRACT

The response surface methodology (RSM) was used in this work to develop an optimum membrane for micellar-enhanced ultrafiltration (MEUF). The mixed-matrix membranes were prepared by adding TiO₂ nanoparticles into polyvinylidene fluoride (PVDF) solution and cast at different thicknesses. Flat-sheet PVDF membranes were prepared via the phase inversion technique on the basis of central composite design (CCD). The objective function of the optimization is to prepare membrane with high rejection and flux for micellar enhanced methylene blue (MB-SDS) ultrafiltration. The interactive effects of the various parameters, namely polymer concentration, membrane casting thickness and TiO₂ concentration towards rejection of MB-SDS and permeation flux were evaluated. CCD was employed to obtain the mutual interaction between the various parameters. The optimum membrane could be prepared under polymer concentration of 18 wt.%, casting thickness of 400 μm and TiO₂ concentration of 1.62 wt.%. The experimental value of permeation flux and rejection was 53.28 ± 2.75 L/h.m² and $99.02 \pm 0.55\%$, respectively. These values were found to be in good agreement and very close to the optimized value predicted from CCD, which were 57.68 L/h.m² and 98.77% . The results show that process optimization using CCD was reliable to produce membrane with desired performance.

© 2012 Elsevier B.V. All rights reserved.

1. Introduction

The uncontrolled discharge of dye-containing waste stream to the environment creates a serious problem to the environment. Among the dyes, methylene blue (MB) for example has been widely used in textile finishing, as hair colorant, paper coloring, paint production and as a sensitizer in photo-oxidation of organic pollutants [1]. Various methods are available for the removal of colored dyes from wastewater such as adsorption [2], flocculation/coagulation method [3], and biodegradation [4]. Activated carbon is a commonly used material for dye adsorption, however it is relatively expensive in term of manufacturing and regeneration [2]. On the other hand, the flocculation treatment process produces a large amount of sludge which causes disposal problem, thus increasing the operation cost [3]. Dye, due to its poor biodegradability is inefficient to be treated using conventional biodegradation technique [4].

Compared to the conventional processes, membrane based separation processes have become an attractive alternative for the treatment of industrial wastewater containing dye due to their unique separation capability, easy to scale-up and low energy consumption [5]. Micellar enhanced ultrafiltration (MEUF) is one of the energy efficient membrane separation process which involve ionic surfactant at concentration equal or higher than the critical micelle concentration

(CMC) through ionic binding between the dye with the oppositely charged micelle surface [6]. Nonetheless, an associated problem with MEUF is the membrane fouling phenomenon due to the pore blocking and surface adsorption [7] which leads to the unwanted flux reduction problem.

Membrane fouling could be reduced by hydrophilic modification of the polymeric membrane surface [8] by embedding inorganic nanoparticles into the polymeric matrix. A more recent approach to improve the membrane antifouling property is by incorporating TiO₂ nanoparticles on the membrane structure and surface. Besides its hydrophilic nature, TiO₂ particles can degrade organic foulant effectively under the UV irradiation [9] which makes it more proactive in handling the fouling problem. TiO₂ had gained special attention among different metal oxides due to its good chemical stability, antibacterial property, availability, and photocatalytic effect [10,11].

The hydrophilic modification by TiO₂ particles was incorporated in poly(ether sulfone) filtration membranes to improve the membrane permeability and fouling resistance of by imparting hydrophilicity to their surface [12]. Madaeni and Ghaemi (2007) had studied the effects of coating of membrane surface with TiO₂ particles and UV radiation in creating self cleaning membrane. The flux of the coated PVDF/TiO₂ membrane after being radiated by UV light increased significantly due to the self cleaning properties created by TiO₂ particles [13]. TiO₂ entrapped composite membrane showed lower flux decline compared to neat Polysulfone (PSF), PVDF and Polyacrylonitrile (PAN) membrane. It was found that fouling mitigation effect increased with nanoparticles content, but above limiting concentration, fouling mitigation did not increase [14].

^{*} Corresponding author. Tel.: +60 4 5996418.
E-mail address: chobs@eng.usm.my (B.S. Ooi).

Table 1
Processing parameter involved in central composite design (CCD).

Variable	Symbol	Real values of coded levels					Variation interval, <i>i</i>
		$-\alpha$	-1	0	$+1$	$+\alpha$	
Polymer concentration, wt.%	A	10.5	12	15	18	19.5	3
Casting thickness, μm	B	150	200	300	400	450	100
TiO ₂ concentration, wt.‰	C	0	1	3	5	6	2

In spite of these advantages, the incorporation of TiO₂ nanoparticles could unavoidably alter the physical properties of membrane which would affect the membrane performance. The conventional approach for optimizing the process variables requires huge experimental efforts, which would be very time consuming and yet ignoring the interaction effects between the considered parameters of the process [15,16]. Such a limitation may be overcome by the statistical experimental design approach, which reduces the number of experiments as well as provides an appropriate model for process optimization, allowing for the evaluation of the influence of inter-variable interactions on the process outcome [15]. Construction of mathematical models in the field of membrane science and technology is a valuable tool for prediction and optimization of membrane separation processes [17]. For example, Ahmad et al. (2009) successfully optimized their membrane with desired lateral flow performance by using RSM with only 20 experimental runs [18] while Ismail and Lai (2004) showed in their research that defect-free asymmetric membranes for gas separation can be prepared

by optimizing dope formulations and preparation conditions using RSM [19].

In this paper, the experimental approach on preparing PVDF/TiO₂ mixed-matrix membrane for MEUF performance using RSM was carried out. Polymer concentration, membrane casting thickness and TiO₂ concentration have been identified as dominant fabrication parameter in controlling membrane fouling and separation properties of the mixed-matrix membranes. The specific objectives of the present study were to apply a three factor CCD combined with RSM to optimize the membrane fabrication parameters for maximizing the permeation flux and MB rejection under micellar enhanced condition.

2. Material and methods

2.1. Materials

Polyvinylidene fluoride (Solef® PVDF) was supplied by Solvay Solexis, France, N,N-dimethylacetamide (DMAc), sodium dodecyl sulfate (SDS) and methylene blue (MB) were purchased from Merck, Germany. Anatase TiO₂, PC-20 (20 nm) was purchased from TitanPE Technologies, Inc., Shanghai. PVDF was dried in oven at 70 °C before use, while other organic chemicals were obtained in reagent grade and used as received. Distilled water was used for all experiment.

2.2. Membrane preparation

The predetermined amount of TiO₂ was dispersed in DMAc solvent under sonication for 15 min. PVDF powder was then dissolved into

Table 2
Design layout and response of central composite design (CCD).

Run number	Factor input variables						Response	
	Polymer concentration, wt.%	Level A	Casting thickness, μm	Level B	TiO ₂ concentration, wt.‰	Level C	Flux, L·m ⁻² ·h	Rejection, %
1	15	0	300	0	3	0	87.82	91.70
2	12	-1	400	+1	5	+1	139.69	89.33
3	15	0	150	- α	3	0	42.45	72.96
4	15	0	300	0	3	0	89.23	89.54
5	19.5	+ α	300	0	3	0	55.13	95.80
6	18	+1	200	-1	5	+1	70.52	75.16
7	10.5	- α	300	0	3	0	100.27	85.93
8	15	0	300	0	0	- α	31.20	96.16
9	12	-1	200	-1	5	+1	93.29	83.29
10	15	0	300	0	3	0	79.21	92.60
11	15	0	450	+ α	3	0	108.56	92.23
12	15	0	300	0	6	+ α	114.72	84.88
13	15	0	300	0	3	0	90.67	87.37
14	18	+1	200	-1	1	-1	5.83	93.39
15	18	+1	400	+1	5	+1	103.53	87.45
16	18	+1	400	+1	1	-1	42.48	98.77
17	15	0	300	0	3	0	87.82	91.69
18	12	-1	200	-1	1	-1	31.79	85.27
19	15	0	300	0	3	0	77.38	93.59
20	12	-1	400	+1	1	-1	96.47	86.44

Table 3
Analysis of variance (ANOVA) for membrane permeation flux regression model and model terms.

Response	Model terms	Sum of squares (SS)	Degree of freedom (DF)	Mean square (MS)	F-value	Prob > F
Membrane permeate flux, L/m ² ·h						
Quadratic model		20501.23	6	3416.87	105.22	0.0001
	A	3414.35	1	3414.35	105.14	0.0001
	B	6267.74	1	6267.74	193.01	0.0001
	C	10124.08	1	10124.08	311.76	0.0001
	B ²	180.64	1	180.64	5.56	0.0347
	C ²	291.45	1	291.45	8.98	0.0103
	AB	214.45	1	214.45	6.60	0.0233
Residual		422.16	13	32.47		
	Lack of fit	265.38	8	33.17	1.06	0.4985
	Pure error	156.78	5	31.36		
Cor total		20923.39	19			

Significant

Not significant

Table 4
Summary of ANOVA and regression analysis for membrane permeation flux.

Response model	R-Squared	Adj R-Squared	Pred R-Squared	Adeq precision
Quadratic model	0.9798	0.9705	0.9550	39.972

the TiO₂ solution and stirred at 60–70 °C for 4 h to ensure a complete dissolution of the polymers. The solution was left to stir overnight at 40 °C. The final solution was then subjected to further sonication for 30 min and let to cool down to room temperature. Solvent loss by evaporation was negligible due to the high boiling points of DMAc (164–166 °C).

The solution was then cast on the tightly woven polyester sheet using an automatic film applicator (Elcometer 4340, E.U.). It was then immediately immersed into the water bath of distilled water and let the phase inversion occur for 24 h in order to remove the

residual solvent. PVDF membrane was kept in distilled water prior to use.

2.3. Polymer solution characterization

The viscosity of polymer solution was measured using a Model DV-III Programmable Rheometer (Brookfield, USA) at 27 ± 2 °C to evaluate the rheology effect of polymer solution prepared under different concentrations of TiO₂ nanoparticles. The rotation speed was fixed at 10 rpm and the viscosities were measured after shearing for 30 s. The viscosity obtained was the average of three time replicates.

2.4. Membrane characterization

2.4.1. Field emission scanning electron microscope

The top surface and cross-sectional morphologies of the fabricated PVDF membranes were observed under Field Emission Scanning

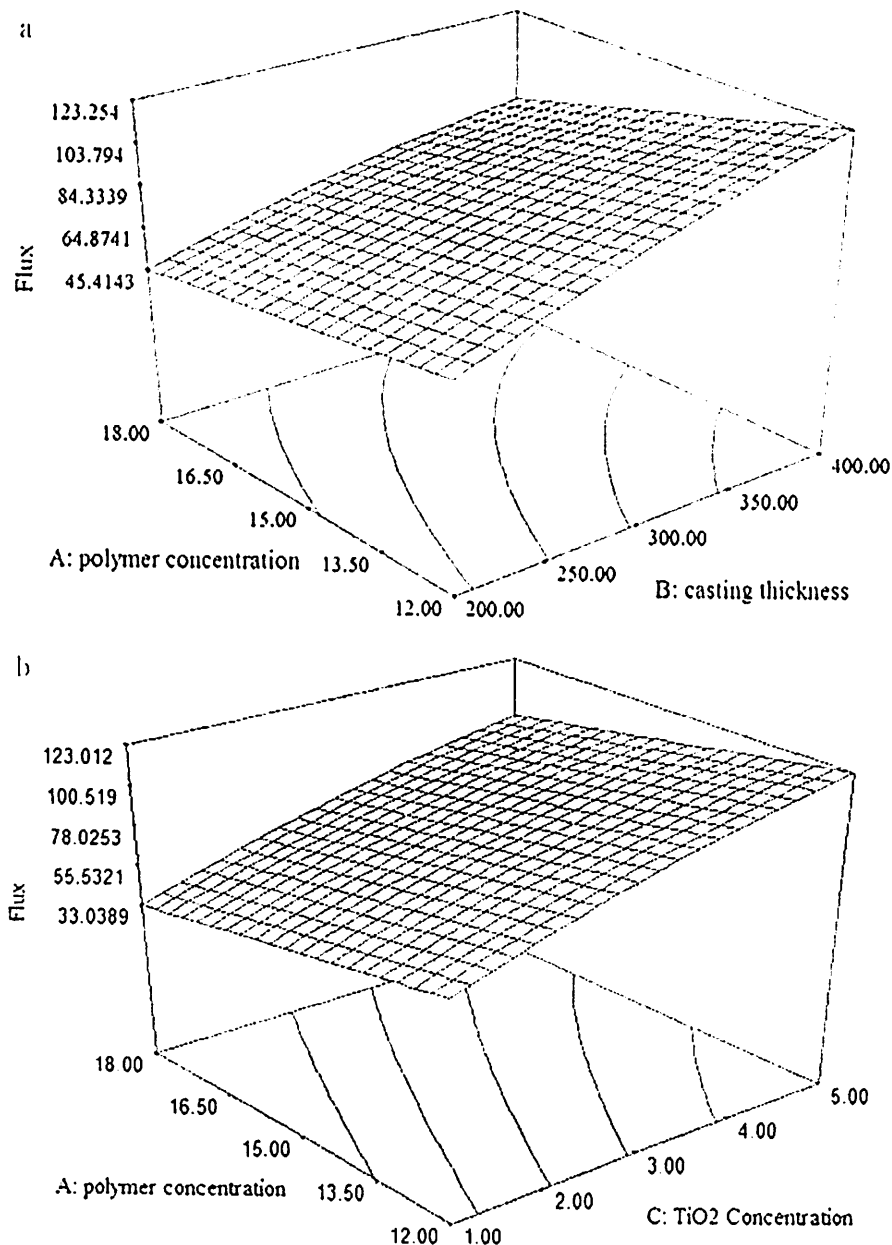


Fig. 1. Response surface plotted on (a) polymer concentration; casting thickness; (b) polymer concentration; TiO₂ concentration for membrane permeation flux.

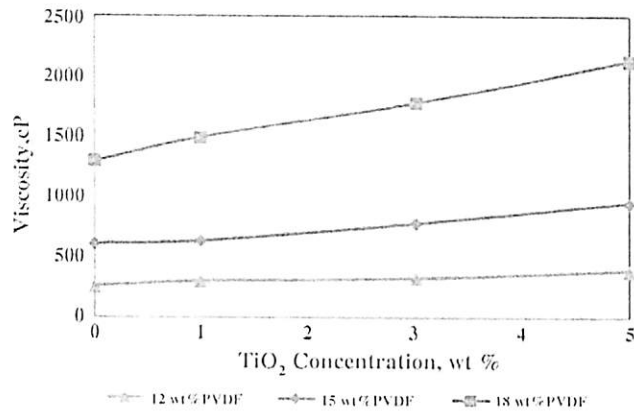


Fig. 2. Viscosity of different PVDF concentration ultrafiltration polymer solutions with different TiO₂ concentrations.

Electron Microscope (FESEM CARL ZEISS SUPRA 35VP, Germany). The membrane was immersed in liquid nitrogen and fractured carefully to have a clean brittle fracture for FESEM cross-sectional images. Membrane

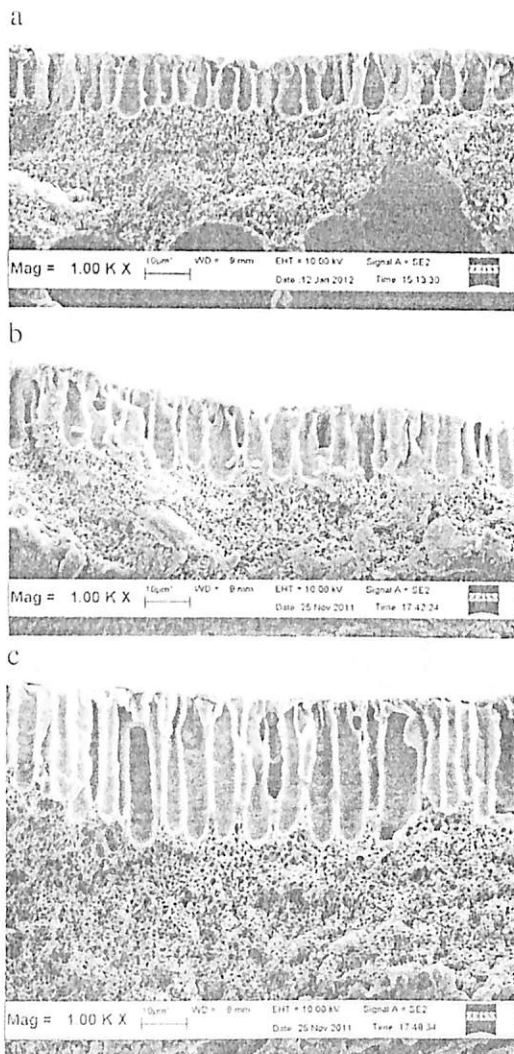


Fig. 3. FESEM images of 18 wt.% of neat PVDF ultrafiltration membrane cross-sectional for casting thickness of (a) 200 μm; (b) 300 μm; and (c) 400 μm.

samples were dried at room temperature and were coated with a thin layer of gold under vacuum using K 550 sputter coater to provide electrical conductivity. The samples were examined under the FESEM at potentials of 5 kV for top surface morphologies and 10.0 kV for cross-sectional images. Membrane final thicknesses were measured by thickness gage (Mitutoyo Corporation, Japan).

2.4.2. Pore size distribution

The pore size distributions of the membrane were determined using the Capillary Flow Porometer, Porolux 1000 (Benelux Scientific, Belgium). The membrane samples with a diameter of 20 mm were characterized by using a liquid extrusion technique in which the differential gas pressure and flow rates through wet and dry samples were measured. The pore size distributions were analyzed using the LabView software.

2.4.3. Contact angle

The membrane surface wettability was characterized using water contact angle instrument (Rame-Hart Model 300 Advanced Goniometer) based on sessile drop methods. All membrane films were cut into square coupons and mounted onto glass slides. Water drops were controlled at constant volume using the motor-driven syringe. The acquired images were analyzed using DROPimage software to obtain the measurement of contact angles. To minimize experimental error, the contact angle measurement was repeated 5 times for each sample and then averaged.

2.4.4. Atomic force microscopy

An atomic force microscope, AFM (Park Scientific, Korea, XE-100) was employed to analyze the surface morphology and roughness of the membranes. The membranes were dried at room temperature prior to surface measurement. The membranes were cut into pieces of 2 cm by 2 cm and were placed on specific sample holders and areas of 10 μm × 10 μm of each membrane were scanned by non-contact mode. The same scan size was used for all samples for comparison purpose.

2.5. Dead-end ultrafiltration experiments

The UF experiments were performed in a dead-end stirred cell (Amicon 8200, Millipore Co., USA) with a capacity of 200 ml, where the disk membrane has a diameter of 60 mm with a geometric area of 28.27 cm² (excluding the area cover by the O-ring). The applied pressure of the filtration system was controlled at 0.5 bar by N₂ gas and operating temperature was 27 ± 2 °C. The stirring speed was maintained at 200 rpm using the controllable magnetic stirrer (Heidoph MR3000D, Germany). The desired concentration of MB in the feed solution was achieved using the appropriate volume from a stock solution of MB 100 mg/L diluted to a final volume of 1000 ml of 10 mg/L MB. A final 20 mM of SDS was added as a binding agent to the feed solution before filtration. In each experimental run, the feed solution was stirred at 300 rpm using magnetic stirrer (Heidoph MR3000D, Germany) for 30 min and introduced to the feed tank of the UF Test Rig. The flux and filtration efficiency were measured for every 10 ml of permeate collected.

The pure water flux (J) was calculated by Eq. (1):

$$J = \frac{V}{A\Delta t} \quad (1)$$

where V is the volume of permeated water, A (m²) is the membrane area, and Δt (h) is ultrafiltration operation time. The concentration of MB with SDS surfactant in feed and permeate was measured with a UV spectrophotometer, model UV mini-1240 (Shimadzu) on the basis of measurement of color intensity at the maximum absorbance of 662 nm. A calibration curve using different solutions containing different concentrations of MB with SDS was determined. The

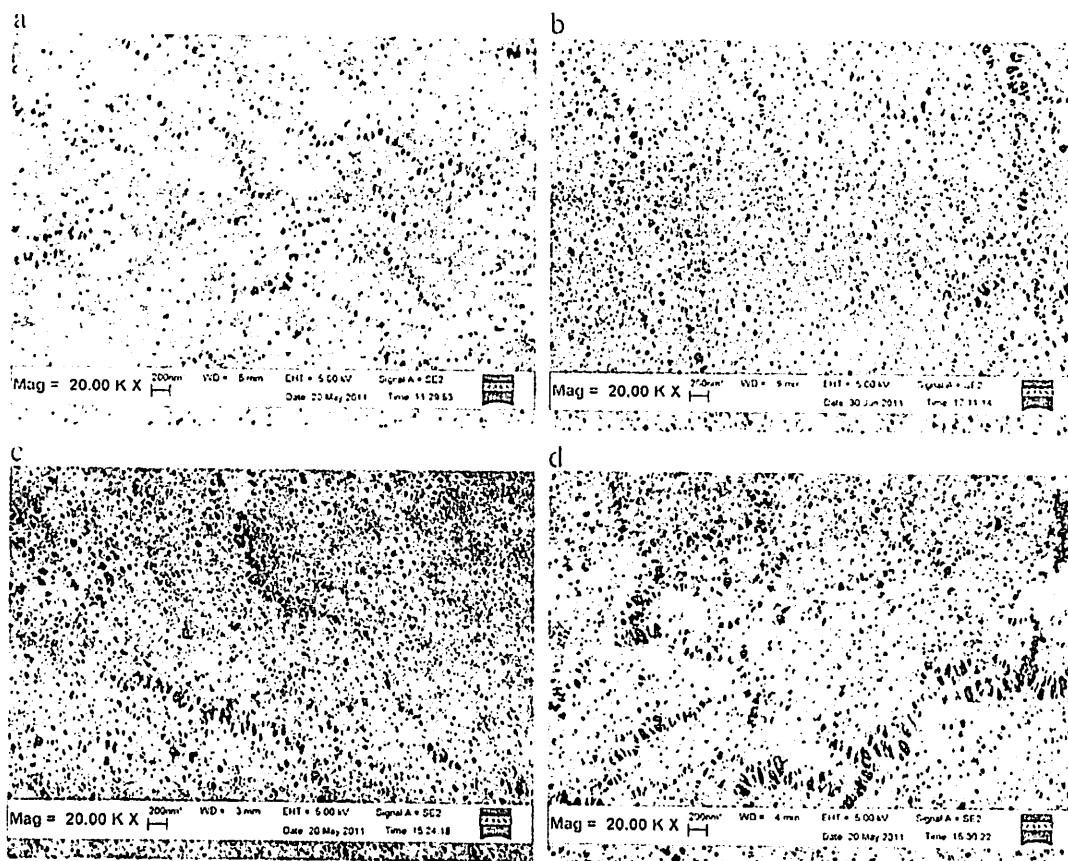


Fig. 4. SEM images of 18 wt.% of PVDF ultrafiltration membrane surface at casting thickness of 400 μm for (a) neat; (b) 1 wt.% TiO₂ concentration; (c) 3 wt.% TiO₂ concentration; (d) 5 wt.% TiO₂ concentration.

filtration efficiency in removing the dye from the feed solution was calculated using Eq. (2):

$$R(\%) = \left[1 - \frac{C_p}{C_0} \right] \times 100 \quad (2)$$

Where C_p is the dye concentration in the permeate and C_0 is the initial concentration of the dye in the feed.

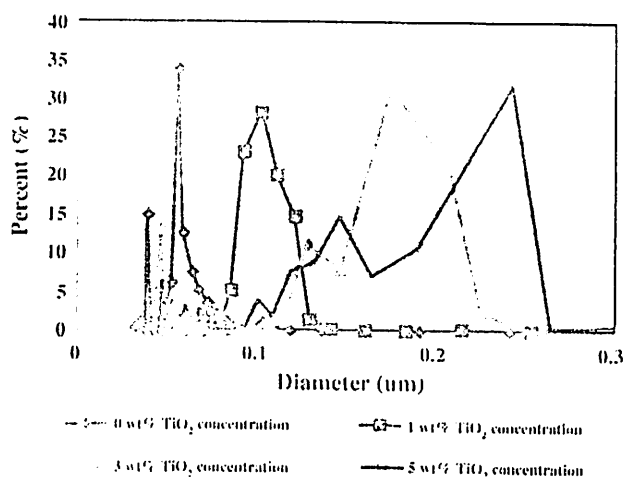


Fig. 5. Pore size distribution of 18 wt.% PVDF ultrafiltration membrane at different TiO₂ concentrations.

2.6. Experimental design -- response surface methodology (RSM)

RSM is a collection of mathematical and statistical technique that can be used to study the effect of several factors at different levels and their influence on each other. The objective of RSM is to determine the optimum set of operational variables of the process [15,16,20]. Besides that, it also helps us to obtain the surface contour that provides a good way for visualizing the factor interaction. RSM basically consist of 3 major steps, which are experimental design, model analysis and condition optimization. Experimental designs such as CCD are useful for RSM because they do not require an excessive number of experimental runs to estimate the main effects and interactions between the variables and able to develop higher polynomial response model with less number of factor n. The total

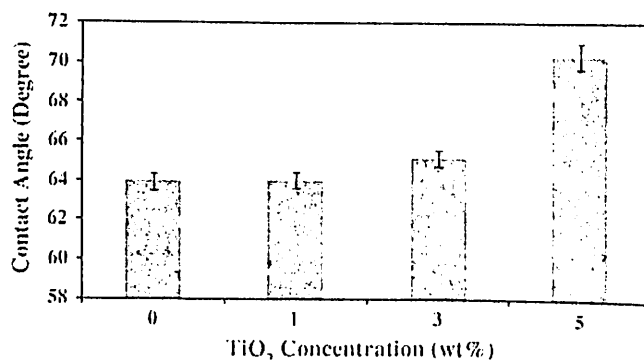


Fig. 6. Contact angle of 18 wt.% PVDF ultrafiltration membrane at different TiO₂ concentrations.

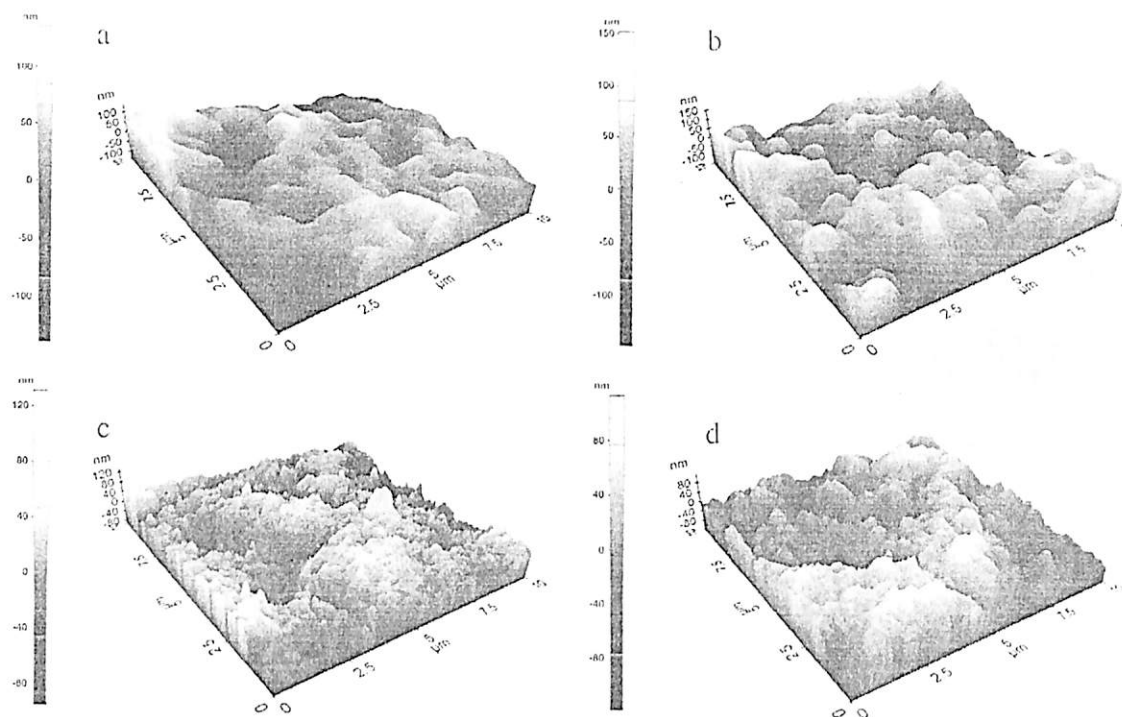


Fig. 7. AFM images of 18 wt.% of PVDF ultrafiltration membrane surface at casting thickness of 400 μm for (a) neat; (b) 1 wt.% TiO_2 concentration; (c) 3 wt.% TiO_2 concentration; and (d) 5 wt.% TiO_2 concentration.

number of experiments to be performed in a 2 level study is generally given as sum of the 2^n factorial runs, $2n$ axial or star runs, and n_c center runs ($2^n + 2n + n_c$), where n is the number of independent process variables [15].

In this study, response surface methodology of UF membrane modification by adding different concentrations of TiO_2 nanoparticles was carried out using three independent process variables, namely: polymer concentration (12–18 wt.%) [21,22], membrane casting thickness (200–400 μm) [23,24], and TiO_2 concentration (1–5 wt.%) [25,26]. The RSM designed in this study was based on CCD in which the factorial portion was a full factorial design (FFD) with all combinations of the three factors at two level where the factor levels are coded to the usual low (-1) and high ($+1$) values, the axial or star points for which all but two factors were set at level 0 and the one factor was set at the outer value corresponding to an alpha value of 1.5. The center points (coded level 0), which were the midpoints between the high and low levels, were repeated six times, to provide an

estimate of experimental error variance. The design involved 20 runs and the response variables measured were the flux coefficient, J ($\text{L}/\text{m}^2\cdot\text{h}$) and the rejection coefficient, y (%).

To simplify the recording of the conditions of an experiment and processing of the experimental data, the factor levels are selected in such a way that the upper level corresponds to $+1$, the lower level to -1 and the basic level to 0. The coded values ± 1.5 give the corresponding values of each factor in proportionality with the unit variation intervals selected for each factor. The operating ranges and the levels of the considered variables are shown in Table 1.

3. Results and discussion

3.1. Response surface and ANOVA analysis

The responses of full factorial CCD were systematically conducted using the Design Expert software (Version 6.0.6, Stat-Ease Inc., MN, USA) to examine the effect and interactions of polymer concentration (A), membrane casting thickness (B) and TiO_2 concentration (C) on membrane permeation flux and rejection ability. The design layout and its responses are summarized in Table 2. The contour plots were fitted to analyze the interaction between independent process factors and the desired responses, based on mathematical analysis of the experimental data. Interactions among membrane fabrication parameters, including polymer concentration, membrane casting thickness and TiO_2 concentration were found and could induce significant effects on membrane performance.

Table 5
Analysis of variance (ANOVA) for membrane rejection ability regression model and model terms.

Response	Model terms	Sum of squares (SS)	Degree of freedom (DF)	Mean square (MS)	F-value	Prob > F	
Membrane rejection, %	Quadratic model	702.20	5	140.44	19.53	<0.0001	Significant
	A	50.98	1	50.98	7.09	0.0186	
	B	231.43	1	231.43	32.18	<0.0001	
	C	166.06	1	166.06	23.09	0.0003	
	B^2	137.76	1	137.76	19.15	0.0006	
	AC	115.98	1	115.98	16.13	0.0013	
Residual		100.69	14	7.19			Not significant
	Lack of fit	75.19	9	8.35	1.64	0.3049	
	Pure error	25.50	5	5.10			
Cor total		802.89	19				

Table 6
Summary of ANOVA and regression analysis for membrane rejection ability.

Response model	R-Squared	Adj R-Squared	Pred R-Squared	Adeq precision
Quadratic model	0.8746	0.8298	0.6684	16.882

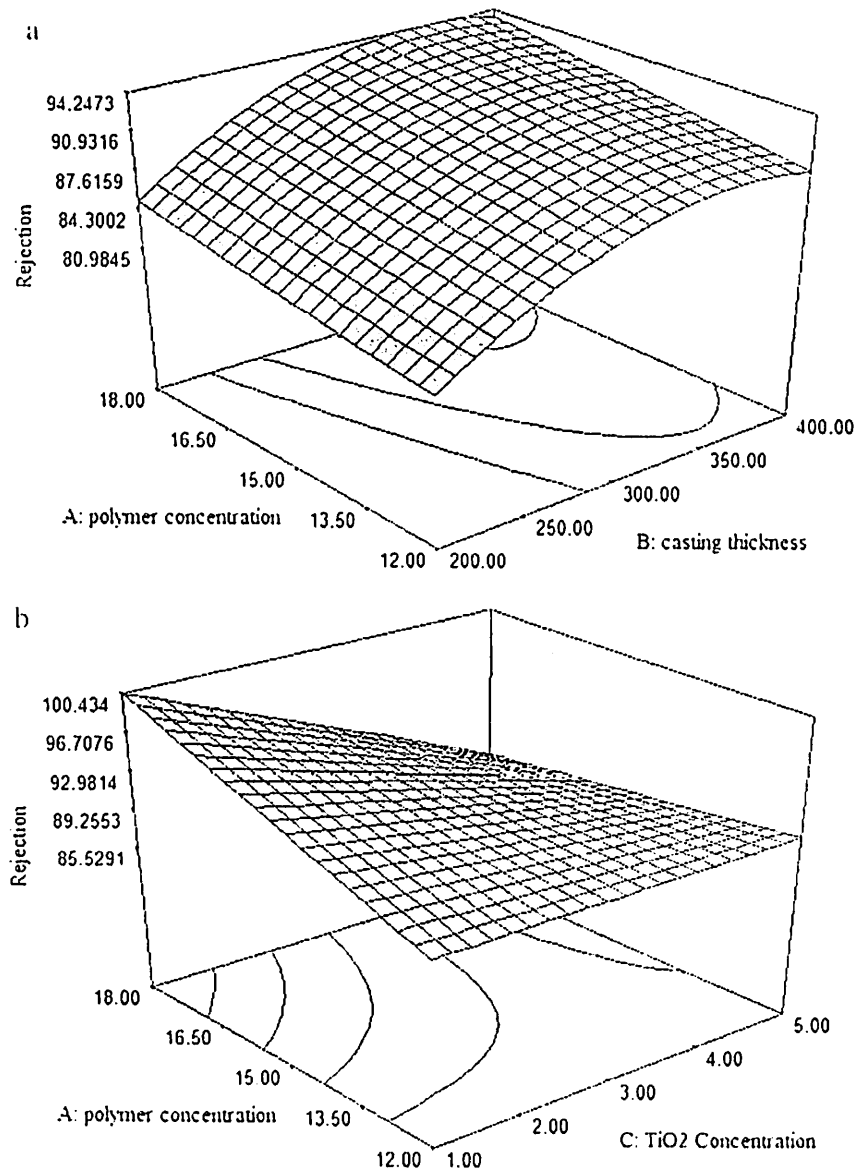


Fig. 8. Response surface plotted on (a) polymer concentration: casting thickness; (b) polymer concentration: TiO₂ concentration for membrane rejection ability.

3.2. Statistical model for membrane permeation flux

Table 3 shows all the suggested parameters (A: Polymer concentration, B: Casting thickness, C: TiO₂ concentration) that have first order effect on membrane permeation flux. Meanwhile, quadratic effect of casting thickness (B^2) and TiO₂ concentration (C^2), as well as interaction effect of polymer concentration and casting thickness (AB) also showed significant model term where $\text{prob} > F$ values were less than 0.05. The analysis of variance (ANOVA) is considered to be essential to test the significance of the model predicted. $p < 0.05$ indicated that the regression models are statistically significant with 95% confidence level in the range studied. The lack of fit model shows that $p > 0.05$ indicating lack of fit is not significant for the developed models with 95% confidence level. The larger the F-value and the smaller the $\text{prob} > F$, the more significant the corresponding factor is. Thus, the significant ranking in this study was C: first order effect of TiO₂ concentration $>$ B: first order effect of casting thickness $>$ A: first order effect of polymer concentration $>$ C^2 : quadratic

effect of TiO₂ concentration $>$ AB: interaction effect of polymer concentration and casting thickness $>$ B^2 : quadratic effect of casting thickness. An interaction effects may arise when the relationship between interacting variables had a simultaneous influence on the response variable. From Table 3, it could be noticed that polymer concentration (A) and casting thickness (B) have a significant interaction on permeation flux. This means that the polymer concentration and casting thickness had simultaneous effects on manipulating the morphology of membrane layer, thus, influencing the permeation flux. On the other hand, the TiO₂ concentration (C) could only give the direct influence on membrane permeation performance.

As shown in Table 4, the empirical model of permeation flux shows good validity and reliability as shown by the value of R-Squared (0.9798), Adj R-Squared (0.9705) and Pred R-Squared (0.9550) which were reasonable close to 1. The Pred R-Squared of 0.9550 is in reasonable agreement with the Adj R-Squared of 0.9705. Adeq precision measures the signal to noise ratio. A ratio greater than 4 is desirable. Table 4 shows an adeq precision ratio of

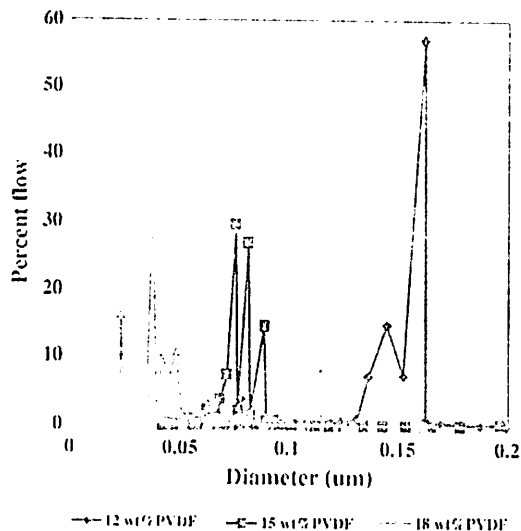


Fig. 9. Pore size distribution of neat PVDF ultrafiltration membrane at different polymer concentrations.

39.972 which indicates an adequate signal and agreed that this model can be used to navigate the design space.

The following model with coded value of the membrane permeate flux (J) was developed.

$$J = 83.34 - 16.53 \cdot A - 22.39 \cdot B + 28.46 \cdot C - 4.19 \cdot B^2 - 5.32 \cdot C^2 - 5.18 \cdot A \cdot B \quad (3)$$

Subjected to: $-\alpha \leq x \leq +\alpha$ where $x = A, B, C$.

In terms of actual factors the empirical model was

$$J = -71.18748 - 0.33157 \cdot A + 0.73396 \cdot B + 22.20525 \cdot C - 4.18599E-004 \cdot B^2 - 1.32928 \cdot C^2 + 0.017258 \cdot A \cdot B \quad (4)$$

Subjected to: $12 \text{ wt.\%} \leq A \leq 18 \text{ wt.\%}$, $200 \mu\text{m} \leq B \leq 400 \mu\text{m}$, $1 \text{ wt.\%} \leq C \leq 5 \text{ wt.\%}$.

This model can be used to predict the membrane permeate flux coefficient within the limits of experimental parameters.

3.2.1. Membrane permeation flux analysis

Fig. 1 shows the predicted membrane permeation flux presented in a three-dimensional response surface plot which can be used to understand the effect of the parameters on the permeation flux. Highly permeable membrane could only be produced at low polymer concentration, high casting thickness (Fig. 1a) and high TiO₂ concentration (Fig. 1b). Polymer concentration has a negative effect on the membrane permeation flux as shown in Fig. 1. This is due to the fact that the viscosity of the polymer solution increased with the increasing of polymer concentration as shown in Fig. 2. The polymer solution viscosity is an important parameter that influences the rheological behavior of the polymer solution which imposed kinetic hindrance for solvent exchange during the membrane formation process. Higher dope viscosity would slow down the mass transfer rate during membrane formation process,

thus prevent the creation of macroporous structure caused by instantaneous demixing [27]. The higher viscosity of the polymer solution will affect the mass transfer of the solvent and non-solvent which resulted in higher resistant of solvent diffusion between the polymer solution and the coagulation bath, thus delays the solvent–polymer demixing. Higher polymer concentration will induce the formation of skin layer before the demixing occurs; as a result flux was expected to decrease. Mulder (1991) explained that the increase in polymer concentration in the membrane casting dope implies a higher volume fraction of polymer, leading to lower porosity and as a result a decrease in flux is observed [28]. On the other hand, Fig. 2 shows that the addition of TiO₂ in casting dope would increase the viscosity of solution which could decrease the permeation flux. However, the higher content of TiO₂ was found to be able to enhance the permeation flux due to its highly hydrophilic properties that will be discussed later.

The significant effect of the membrane casting thickness on the permeation flux can be observed from Fig. 1a. It was unexpected that the permeation flux increased with the increased of membrane casting thickness as additional thickness might exert extra flow resistance. Increasing the membrane casting thickness however leads to membrane structure transition from spongelike to more fingerlike structure as shown in FESEM cross-sectional images in Fig. 3. Increasing in membrane casting thickness resulted in higher fingerlike to spongelike structure ratio. Fingerlike structure would allow less resistance for water flow compared to the spongelike structure, thus higher fingerlike to spongelike structure ratio for thicker membrane leads to higher permeation flux. The same phenomenon was also observed by other researchers, Azari et al. (2010) who found that decreasing the thickness of cast polymer solution in a membrane fabrication process may lead to structure transition from finger to spongelike structure [29]. Vogrin et al. (2002) found out that the cross-sectional morphology of membranes formed from cast thickness of 150 and 300 µm was absent of macrovoid while membranes prepared from cast thickness of 500 µm clearly had macrovoids [24].

Fig. 1b shows that the membrane permeation flux was enhanced with the increased of TiO₂ concentration. This might be due to i) the increasing hydrophilicity by TiO₂ nanoparticles in composite membrane, or ii) the increasing of membrane pore size. The addition of TiO₂ into the polymer matrix demonstrated an obvious change of membrane morphology by changing the rheological behavior of polymer solution. Higher dope viscosity will affect the mass transfer of solvent and non-solvent during the phase inversion process which resulted in higher resistance of solvent and non-solvent diffusion between the polymer solution and the coagulation bath. The thermodynamic behavior of solution was also affected due to the hydrophilic nature of TiO₂. The nonsolvent influx was expected to be increased due to the pulling force of the nanoparticles which enhanced the instantaneous liquid–liquid demixing. On the other hand, solvent molecules can diffuse more readily from the polymer matrix to the coagulation bath due to the decreased interaction between polymer and solvent molecules by the barrier created by nanoparticles [30]. As a result, spinodal demixing is likely to occur which resulted in a highly connected porous structure that provides less resistance to water permeation [31]. However, higher TiO₂ concentration could cause TiO₂ agglomeration as shown in FESEM images (Fig. 4) as a consequence of increasing solution viscosity. TiO₂ agglomeration had created a bigger surface pore size (membrane defect) due to the high surface tension between TiO₂ and PVDF as indicated in Fig. 5.

Theoretically, the surface of TiO₂ nanoparticles consists of a hydroxyl group which could attract water molecules to pass through the membrane thus responsible for hydrophilicity increment. Many studies had been carried out to investigate the effect of TiO₂ concentration on the membrane flux. Bae and Tak (2005) found that TiO₂ composite membrane could be more hydrophilic than neat polymeric membrane due to the higher affinity of TiO₂ towards water [14]. Yuliwati and Ismail (2011), Wu et al. (2008) and Cao et al. (2006)

Table 7
Final thickness of neat PVDF ultrafiltration membrane at different membrane casting thicknesses.

Membrane formulation		Final thickness (µm)
Polymer concentration (wt.%)	Nominal casting thickness (µm)	
18	200	55.67 ± 0.66
18	300	90.13 ± 0.64
18	400	117.6 ± 0.92

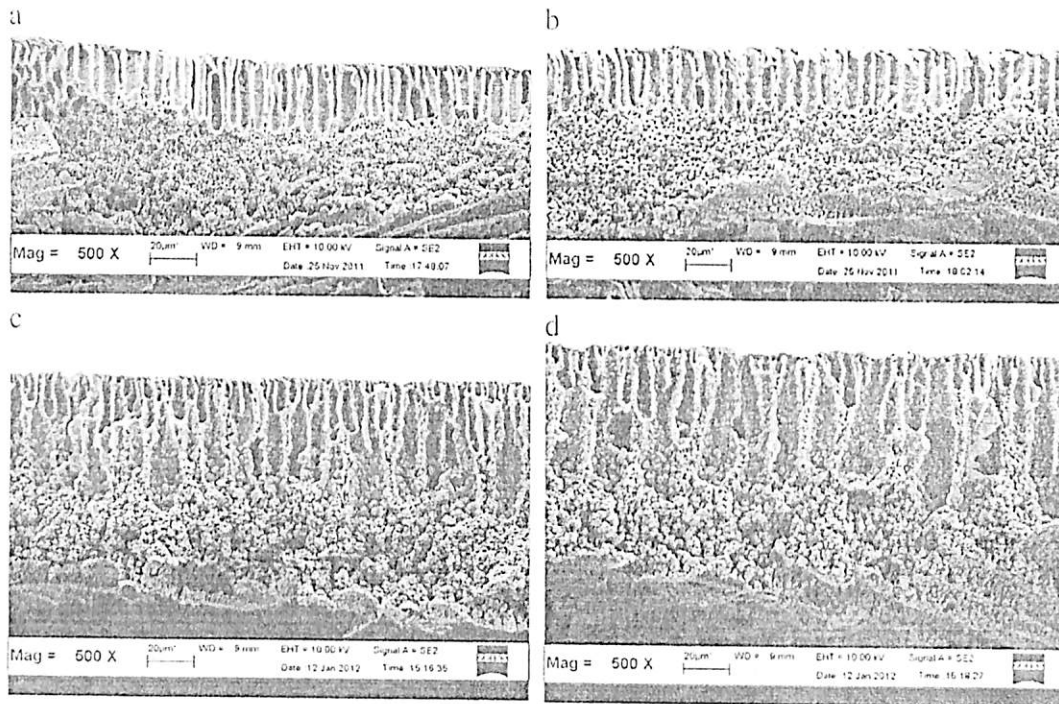


Fig. 10. FESEM images of 18 wt.% of PVDF ultrafiltration membrane cross-sectional at casting thickness of 400 μm for (a) neat; (b) 1 wt.% TiO₂ concentration; (c) 3 wt.% TiO₂ concentration; and (d) 5 wt.% TiO₂ concentration.

had reported that TiO₂ particles which contain hydroxyl group on its surface were responsible for the hydrophilicity increment and fouling mitigation [10,32,33]. Oh et al. (2009) modified PVDF ultrafiltration membrane by dispersing nano sized TiO₂ particles in a PVDF solution. PVDF membrane fouling was reduced by changing the membrane surface from hydrophobic to hydrophilic after TiO₂ addition [34].

Based on these literature findings, it was expected that the membrane with a lower contact angle could be produced at a higher content of hydrophilic TiO₂. However, in our works, the opposite observation as shown in Fig. 6 was found in which the increasing of TiO₂ concentration increased the contact angles correspondingly. It is an unwanted phenomenon as it might impair the membrane permeation flux mainly due to the higher surface tension between the water molecules and the membrane surface. This phenomenon could be attributed to the changes of roughness of membrane 'microstructure' as shown in the AFM images (Fig. 7). The images clearly indicate that the micro-roughness of the membranes surface increased structurally with the increasing of TiO₂ concentration. Increasing membrane roughness has another disadvantage as it could easily trap foulants in the valley which reduces membrane performance and antifouling ability [26].

The effect of microstructure roughness could be explained by Young's equation which relates the surface tension of a drop of water on a solid is given by the relation

$$\gamma_{SL} + \gamma_{LV} \cos \theta = \gamma_{SV} \tag{5}$$

where, γ_{SL} , γ_{LV} , and γ_{SV} are the surface tensions of solid–liquid, liquid–vapor and solid–vapor, respectively. Eq. (5) is suitable for non-porous surface. However, for porous surface, Eq. (5) should be modified to accommodate for the effect of porosity (ϵ) by:

$$\cos \theta = \frac{1}{\gamma_{LV}} (1 - \epsilon) |\gamma_{SV} - \gamma_{SL}| \tag{6}$$

Positive value of $\gamma_{SV} - \gamma_{SL}$ means that the contact angle value is $< 90^\circ$ which indicates that the solid surface is hydrophilic whereas negative value of $\gamma_{SV} - \gamma_{SL}$ means that the contact angle value is

$> 90^\circ$ which means it is a hydrophobic surface. Surface effective porosity is likely to be increased with the increasing of TiO₂ concentration due to air gap trapped within the micro-protruded structure and caused the increase of surface contact angle. Based on the above findings, it could be concluded that the flux increment is more likely caused by the pore enlargement compared to the hydrophilization effect of TiO₂.

3.3. Statistical model for membrane rejection ability

Table 5 shows that the membrane rejection performance was contributed by the first order effects of the membrane fabrication parameters, polymer concentration (A), Casting thickness (B), TiO₂ concentration (C), quadratic effect of casting thickness (B²) and interaction effect between polymer concentration and TiO₂ concentration (AC). These parameters have a significant model term where prob > F values were less than 0.05. The significance of the model was determined by the analysis of variance (ANOVA) which shows that $p < 0.05$ was statistically significant with the 95% confidence level in the range studied. The lack of fit model shows $p > 0.05$ and indicated that there was an adequate goodness-of-fit. The significant ranking in this study was B: first order effect of casting thickness > C: first order effect of TiO₂ concentration > B²: quadratic effect of casting thickness > AC: interaction effect of polymer concentration and TiO₂ concentration > A: first order effect of polymer concentration as shown in Table 5. This empirical model was satisfactory and shows reasonable validity and reliability for membrane rejection prediction, with R-Squared (0.8746) and Adj R-Squared (0.8298), as shown in Table 6. Table 6 shows that the adeq precision ratio of 16.882 indicates an adequate signal and agreed that this model can be used to predict the rejection behavior.

The following model with coded value of the membrane rejection ability (y) was developed.

$$y = 90.96 + 2.02 \cdot A + 4.30 \cdot B - 3.64 \cdot C - 3.65 \cdot B^2 - 3.81 \cdot A \cdot C \tag{7}$$

Subjected to: $-\alpha \leq x \leq +\alpha$ where $x = A, B, C$.

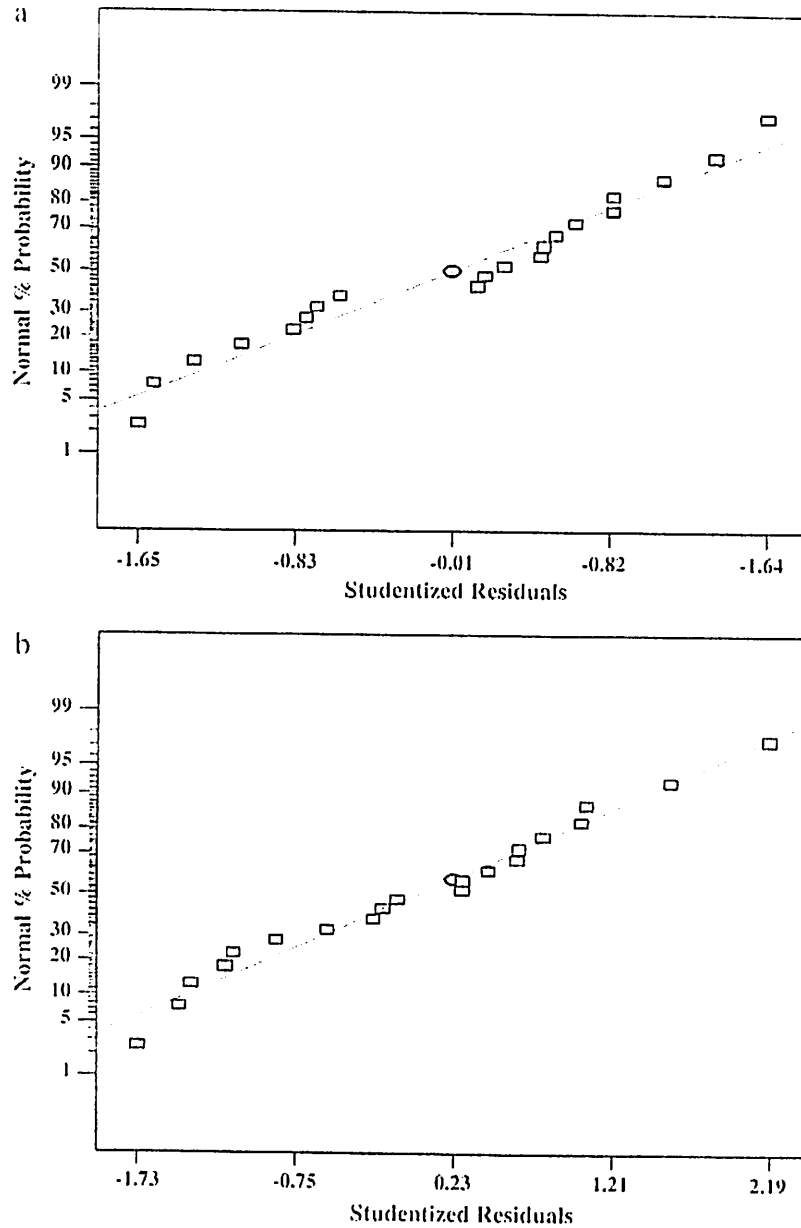


Fig. 11. Plot of normal % probability versus residual for membrane (a) permeation flux; (b) rejection ability.

In term of actual factors the empirical model was

$$y = 11.97219 + 2.57695 \cdot A + 0.26232 \cdot B - 7.69635 \cdot C - 3.65491E-004 \cdot B^2 - 0.63458 \cdot A \cdot C \quad (8)$$

subjected to: 12 wt.% $\leq A \leq$ 18 wt.%, 200 $\mu\text{m} \leq B \leq$ 400 μm , 1 wt.% $\leq C \leq$ 5 wt.%.

This model can be used to predict the membrane rejection ability coefficient within the limits of experimental parameters.

3.3.1. Membrane rejection analysis

Three-dimensional response surface plots were developed to study the parameter interactions. As shown in Fig. 8, higher MB-SDS rejection could be achieved by preparing the membrane at high polymer concentration, high casting thickness (Fig. 8a) and low TiO_2 concentration (Fig. 8b).

Polymer concentration has a positive effect on the membrane rejection ability. A linear increase of rejection ability with polymer

concentration was observed in Fig. 8, which indicated that the rejection ability of MEUF process is under the polymer concentration controlled region. As shown in Fig. 9, the increased of polymer concentration resulted in the decreased of mean pore size; which could effectively block the passage of micelle, consequently better rejection could be achieved. This phenomenon is in accordance with the increasing membrane density and decreasing void fraction with an increase of the polymer concentration in the casting dope [22]. See-Toh et al. (2007) found a similar phenomenon that a decrease in polymer concentration was found to give a higher molecular weight cut-off (MWCO) [23].

Fig. 8a shows the interactive effect of the polymer concentration and membrane casting thickness on membrane rejection. The rejection ability is higher for the thicker cast membrane. Increasing in membrane casting thickness had led to thicker final thickness of the produced membrane as shown in Table 7 which consists of more adsorption site for the free dye, thus enhanced the rejection ability of the produced membrane. Fig. 8b shows that under low polymer

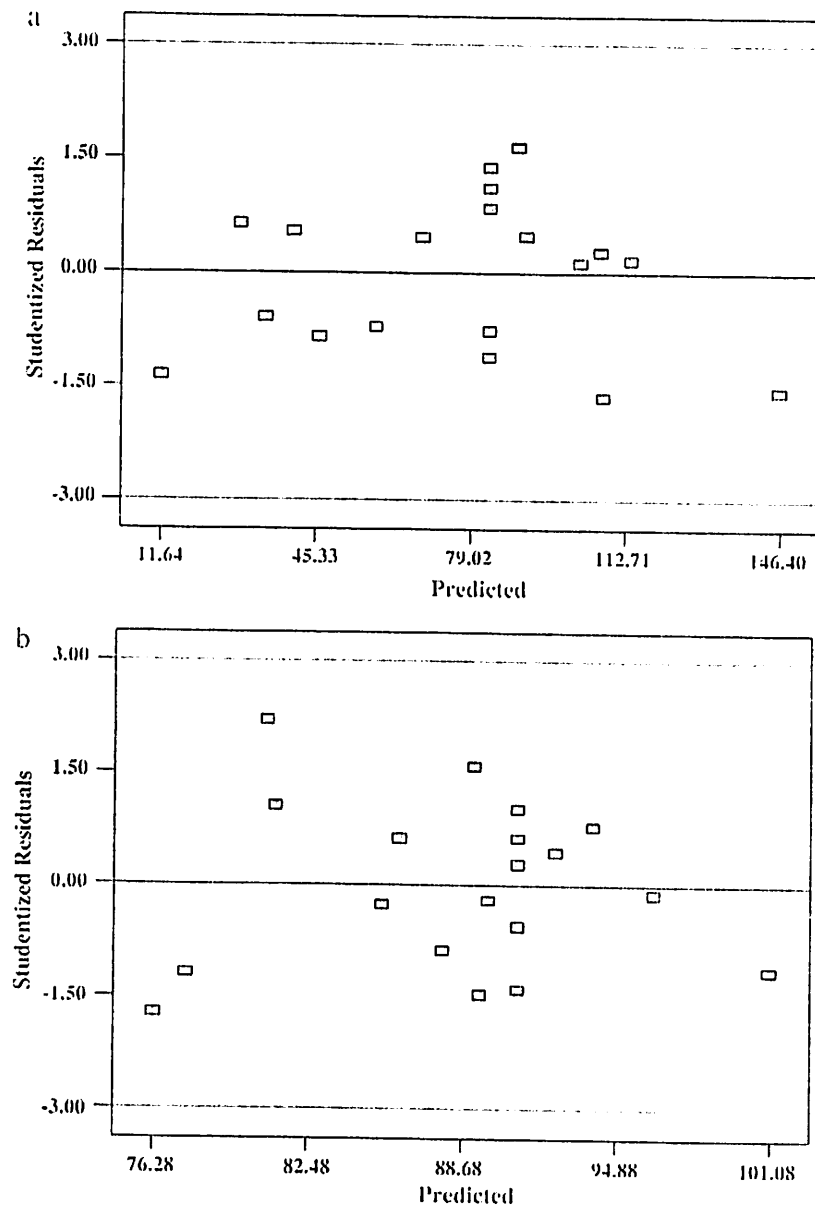


Fig. 12. Plot of studentized residual versus predicted for membrane (a) permeation flux; (b) rejection ability.

concentration (12 wt.%), the effect of TiO_2 concentration seems to give a minor effect on membrane rejection ability. However, at higher polymer concentration, TiO_2 concentration showed negative effect on membrane rejection ability. This apparent change of response surface plane as shown in Fig. 8b could be observed through the interaction coefficient term (AC) between polymer concentration (A) and TiO_2 concentration (C). This phenomenon is due to the rheology behavior of the polymer dopes as shown previously in Fig. 2. The viscosity of the solutions with higher polymer concentration could be further increased by adding TiO_2 into the casting solution. TiO_2 dispersibility was greatly reduced in such a high viscous dope solution which causes the membrane defect due to TiO_2 clustering. Membrane with 1 wt.% TiO_2 concentration exhibits better dye removal compared to the other membrane. It is most probably due to better dispersibility of the TiO_2 . Beyond 3 wt.% of TiO_2 concentration, it could be clearly seen on the surface that TiO_2 agglomeration starts to occur which not only reduced the adsorption site of the membrane but also caused

membrane defect as shown in the FESEM images in Fig. 4. This can be directly observed from the FESEM cross-sectional images (as shown in Fig. 10) that at higher TiO_2 concentration, the diameter of the fingerlike structure was relatively larger which resulted in poor dye retention. Furthermore it could be clearly seen that TiO_2 agglomeration occurred at sponge-like structure layer which resulted in the lower accessibility of the dye onto the polymeric matrix.

3.4. Verification of regression model on diagnostic plot

Plot of the normal % probability versus residual is shown in Fig. 11. The normal probability plot of the residuals is an important diagnostic tool that used to determine the residual analysis of response surface design. It is used to detect and to ensure that the errors are normally distributed (as the residuals fall near to a straight line) and is independent of each other [15], and thus, support adequacy of the least-square fit. Fig. 11 shows that there is no obvious indication of non-

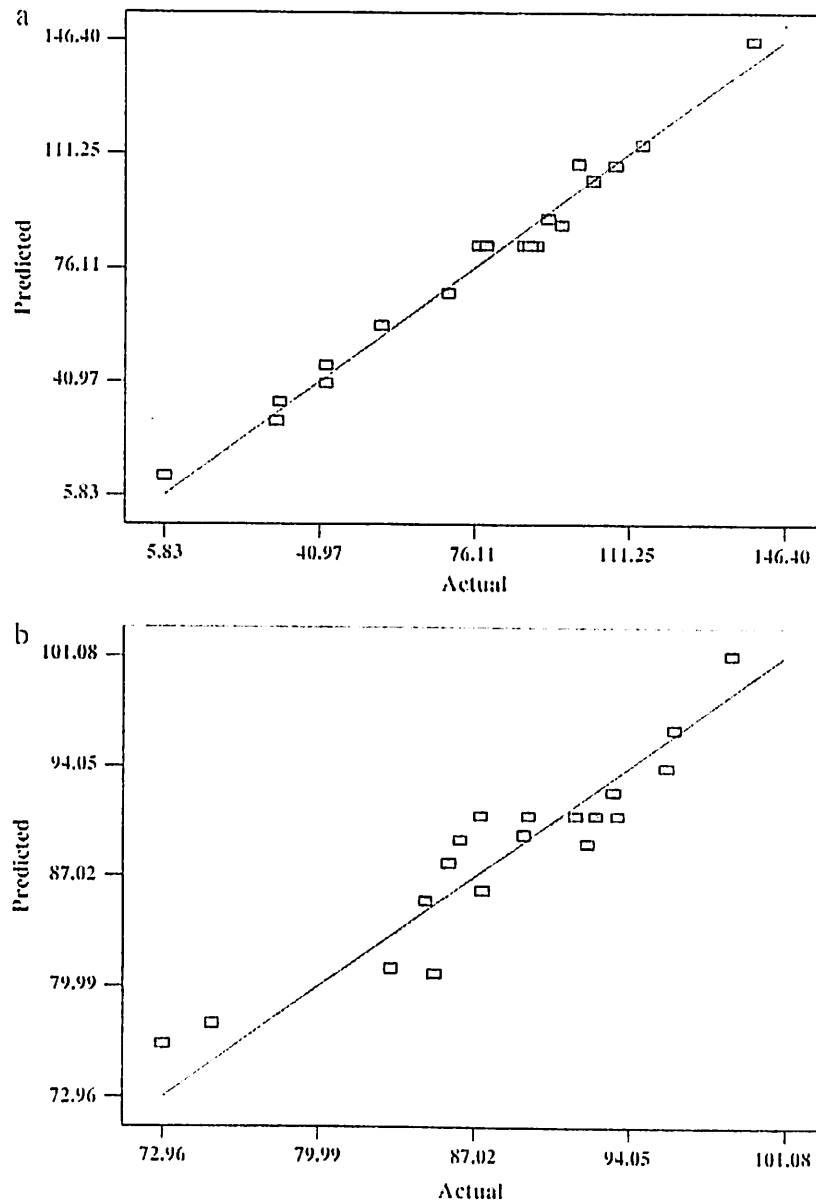


Fig. 14. Plot of predicted versus actual for membrane (a) permeation flux; (b) rejection ability.

optimum membrane performance could be prepared by optimizing the membrane dope formulation and preparation conditions. Polymer concentration, membrane casting thickness and TiO_2 concentration were identified as dominant membrane fabrication parameters in controlling membrane physical and chemical properties, and thus influenced the membrane performance. TiO_2 concentration was found to be the major parameter in affecting the membrane permeation flux followed by membrane casting thickness and polymer concentration due to its effect on membrane morphology. On the other hand, main parameters of membrane casting thickness and TiO_2 concentration had the strongest influence on membrane rejection ability due to its enhanced site for separation and pore size. The optimum membrane fabrication parameters could be prepared at 18 wt.% of polymer concentration, 400 μm of casting thickness and 1.62 wt.% of TiO_2 concentration to achieve high membrane permeate flux and rejection ability. The corresponding experimental value of the permeate flux and rejection ability under the optimum condition of the variables was determined as $53.28 \pm 2.75 \text{ L/h.m}^2$ and $99.02 \pm 0.55\%$. It was found to be in good agreement and very close to the optimized value predicted from CCD, that

were 57.68 L/h.m^2 and 98.77%, showing that the validity of the empirical models was confirmed.

Acknowledgment

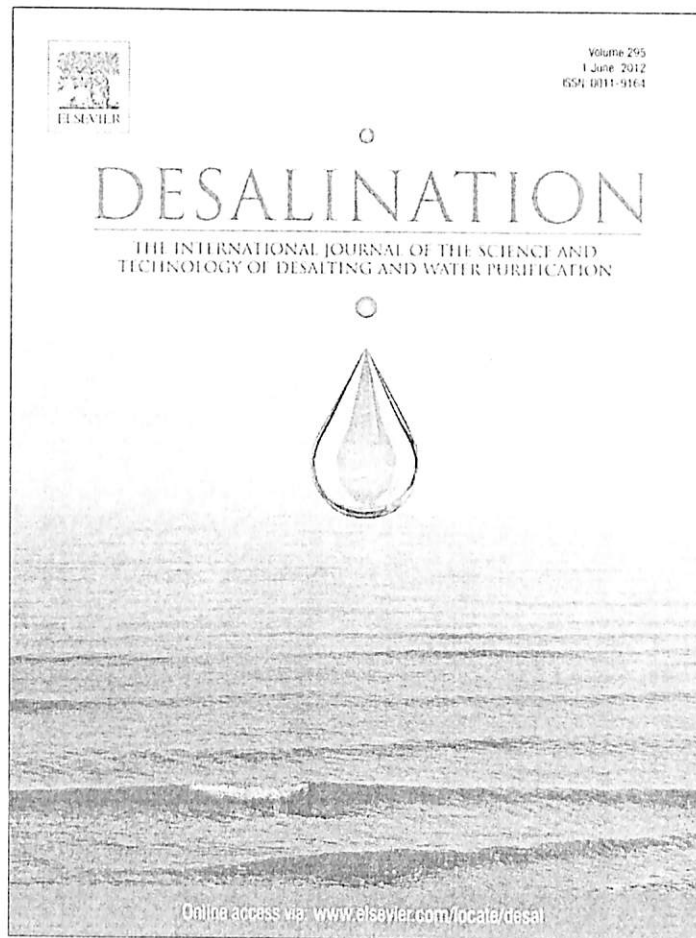
The authors wish to thank the financial support granted by Universiti Sains Malaysia (RU Grant) (1001/PJKIMIA/811172), Malaysia Toray Science Foundation (MISF) Science and Technology Research Grant (304/PJKIMIA/G050179/M126), USM Membrane Science and Technology Cluster and the Ministry of Higher Education (MyMaster).

References

- [1] M. Bielska, J. Szymanowski, Removal of methylene blue from waste water using micellar enhanced ultrafiltration, *Water Res.* 40 (2006) 1027–1033.
- [2] S. Wang, Z.H. Zhu, A. Coomes, F. Haghsereshi, G.Q. Lu, The physical and surface chemical characteristics of activated carbons and the adsorption of methylene blue from wastewater, *J. Colloid Interface Sci.* 284 (2005) 440–446.
- [3] V. Gotob, A. Vinder, M. Simonic, Efficiency of the coagulation/flocculation method for the treatment of dye bath effluents, *Dyes Pigm.* 67 (2005) 93–97.

- [4] S. Seshadri, P.L. Bishop, A.M. Agha, Anaerobic/aerobic treatment of selected azo dyes in waste water, *Waste Manag.* 15 (1994) 127–137.
- [5] B. Sarkar, S. DasGupta, S. De, Application of external electric field to enhance the permeate flux during micellar enhanced ultrafiltration, *Sep. Purif. Technol.* 66 (2009) 263–272.
- [6] I. Xiarchos, A. Jaworska, G. Zakrzewska-Trznadel, Response surface methodology for the modelling of copper removal from aqueous solutions using micellar-enhanced ultrafiltration, *J. Membr. Sci.* 321 (2008) 222–231.
- [7] I. Koyuncu, D. Topacik, E. Yuksek, Reuse of reactive dyehouse wastewater by nanofiltration: process water quality and economical implications, *Sep. Purif. Technol.* 36 (2004) 77–85.
- [8] J.G. Choi, T.H. Bae, J.H. Kim, T.M. Tak, A.A. Randall, The behavior of membrane fouling initiation on the crossflow membrane bioreactor system, *J. Membr. Sci.* 203 (2002) 103–113.
- [9] A. Rahimpour, S.S. Madaeni, A.H. Taheri, Y. Mansourpanah, Coupling TiO₂ nanoparticles with UV irradiation for modification of polyethersulfone ultrafiltration membranes, *J. Membr. Sci.* 313 (2008) 158–169.
- [10] X. Cao, J. Ma, X. Shi, Z. Ren, Effect of TiO₂ nanoparticle size on the performance of PVDF membrane, *Appl. Surf. Sci.* 253 (2006) 2003–2010.
- [11] Y. Wei, H.-Q. Chu, B.-Z. Dong, X. Li, S.-J. Xia, Z.-M. Qiang, Effect of TiO₂ nanowire addition on PVDF ultrafiltration membrane performance, *Desalination* 272 (2011) 90–97.
- [12] M.-L. Luo, J.-Q. Zhao, W. Tang, C.-S. Pu, Hydrophilic modification of poly(ether sulfone) ultrafiltration membrane surface by self-assembly of TiO₂ nanoparticles, *Appl. Surf. Sci.* 249 (2005) 76–84.
- [13] S.S. Madaeni, N. Ghaemi, Characterization of self-cleaning RO membranes coated with TiO₂ particles under UV irradiation, *J. Membr. Sci.* 303 (2007) 221–233.
- [14] T.-H. Bae, T.-M. Tak, Effect of TiO₂ nanoparticles on fouling mitigation of ultrafiltration membranes for activated sludge filtration, *J. Membr. Sci.* 249 (2005) 1–8.
- [15] K.P. Singh, S. Gupta, A.K. Singh, S. Sinha, Optimizing adsorption of crystal violet dye from water by magnetic nanocomposite using response surface modeling approach, *J. Hazard. Mater.* 186 (2011) 1462–1473.
- [16] F. Rigas, *Statistical Design of Experiments and Optimization of Industrial Processes*, NTUA Press, Athens, 1986 (in Greek).
- [17] M. Khayet, M.N.A. Seman, N. Hilal, Response surface modeling and optimization of composite nanofiltration modified membranes, *J. Membr. Sci.* 349 (2010) 113–122.
- [18] A.L. Ahmad, S.C. Low, S.R.A. Shukor, A. Ismail, Optimization of membrane performance by thermal-mechanical stretching process using responses surface methodology (RSM), *Sep. Purif. Technol.* 66 (2009) 177–186.
- [19] A.J. Ismail, P.Y. Lai, Development of defect-free asymmetric polysulfone membranes for gas separation using response surface methodology, *Sep. Purif. Technol.* 40 (2004) 191–207.
- [20] D.C. Montgomery, *Response Surface Methods and Other Approaches to Process Optimization Design and Analysis of Experiments*, 5th edition, John Wiley & Sons, Inc., 2001, p. 427.
- [21] D.B. Mosqueda-Jimenez, R.M. Narbaiz, T. Matsuura, G. Chowdhury, C. Pleizier, J.P. Santerre, Influence of processing conditions on the properties of ultrafiltration membranes, *J. Membr. Sci.* 231 (2004) 209–224.
- [22] G. Bakeri, A.F. Ismail, M. Shariaty-Niassar, T. Matsuura, Effect of polymer concentration on the structure and performance of polyetherimide hollow fiber membranes, *J. Membr. Sci.* 363 (2010) 103–111.
- [23] Y.H. See-Toh, F.C. Ferreira, A.G. Livingston, The influence of membrane formation parameters on the functional performance of organic solvent nanofiltration membranes, *J. Membr. Sci.* 209 (2007) 236–250.
- [24] N. Vogrin, C. Stropnik, V. Musil, M. Brumen, The wet phase separation: the effect of cast solution thickness on the appearance of macrovoids in the membrane forming ternary cellulose acetate/acetone/water system, *J. Membr. Sci.* 207 (2002) 139–141.
- [25] R.A. Danoufar, S.-J. You, H.-H. Chou, Study the self cleaning, antibacterial and photocatalytic properties of TiO₂ entrapped PVDF membranes, *J. Hazard. Mater.* 172 (2009) 1321–1328.
- [26] A. Razmjou, J. Mansouri, V. Chen, The effects of mechanical and chemical modification of TiO₂ nanoparticles on the surface chemistry, structure and fouling performance of PES ultrafiltration membranes, *J. Membr. Sci.* 378 (2011) 73–84.
- [27] L.-F. Han, Z.-L. Xu, L.-Y. Yu, Y.-M. Wei, Y. Cao, Performance of PVDF/multi-nanoparticles composite hollow fibre ultrafiltration membranes, *Iran. Polym. J.* 19 (2010) 553–565.
- [28] M. Mulder, *Basic Principle of Membrane Technology*, Kluwer Academic Publishers, Dordrecht, The Netherlands, 1991.
- [29] S. Azari, M. Karimi, M.H. Kish, Structural properties of the poly(acrylonitrile) membrane prepared with different cast thicknesses, *Ind. Eng. Chem. Res.* 49 (2010) 2442–2448.
- [30] I.C. Kim, K.H. Lee, T.M. Tak, Preparation and characterization of integrally skinned uncharged polyetherimide asymmetric nanofiltration membrane, *J. Membr. Sci.* 183 (2001) 235–247.
- [31] P.v.d. Witte, P.J. Dijkstra, J.W.A.v.d. Berg, J. Feijen, Review: phase separation processes in polymer solution in relation to membrane formation, *J. Membr. Sci.* 117 (1996) 1–31.
- [32] E. Yulwati, A.F. Ismail, Effect of additives concentration on the surface properties and performance of PVDF ultrafiltration membranes for refinery produced wastewater treatment, *Desalination* 273 (2011) 226–234.
- [33] G. Wu, S. Gan, L. Cui, Y. Xu, Preparation and characterization of PES/TiO₂ composite membranes, *Appl. Surf. Sci.* 254 (2008) 7080–7086.
- [34] S.J. Oh, N. Kim, Y.T. Lee, Preparation and characterization of PVDF/TiO₂ organic-inorganic composite membranes for fouling resistance improvement, *J. Membr. Sci.* 345 (2009) 13–20.

Provided for non-commercial research and education use.
Not for reproduction, distribution or commercial use.

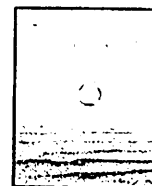


This article appeared in a journal published by Elsevier. The attached copy is furnished to the author for internal non-commercial research and education use, including for instruction at the authors institution and sharing with colleagues.

Other uses, including reproduction and distribution, or selling or licensing copies, or posting to personal, institutional or third party websites are prohibited.

In most cases authors are permitted to post their version of the article (e.g. in Word or Tex form) to their personal website or institutional repository. Authors requiring further information regarding Elsevier's archiving and manuscript policies are encouraged to visit:

<http://www.elsevier.com/copyright>



Preparation and characterization of PVDF/TiO₂ mixed matrix membrane via in situ colloidal precipitation method

Y.H. Teow, A.L. Ahmad, J.K. Lim, B.S. Ooi*

School of Chemical Engineering, Engineering Campus, Universiti Sains Malaysia, Seri Ampangan, 14300 Nibong Tebal, Penang, Malaysia

ARTICLE INFO

Article history:

Received 18 January 2012

Received in revised form 23 March 2012

Accepted 24 March 2012

Available online 26 April 2012

Keywords:

Mixed matrix membrane

Fouling resistance

TiO₂ dispersion

Colloidal precipitation method

Phase inversion

Particle size distribution

ABSTRACT

In this study, titanium dioxide (TiO₂) nanoparticles (NPs) were incorporated into polyvinylidene fluoride (PVDF) membrane to produce a mixed matrix membrane via phase inversion and colloidal precipitation method. In order to avoid agglomeration and to maintain the stability of NPs in the coagulation bath, NPs were dispersed in the bath via sonication and peptization. The membrane surface morphology and distribution pattern of NPs on the membrane surface were observed by field emission scanning electron microscopy. It was found that the NP size and distribution of NPs on the membrane surface were affected to a very great extent by the type of solvent used in the dope formulation and concentration of TiO₂ in the coagulation bath. Membrane prepared using N-methyl-2-pyrrolidone (NMP) as solvent has smaller surface particles and narrower particle size distribution compared to N-N-dimethylacetamide (DMAc) and N,N-dimethyl formamide (DMF) due to the hydrophobic/hydrophilic interactions between NPs and polymer solution. However, the pore size of membrane prepared using NMP was relatively big, thus resulted in poorer humic acid (HA) rejection. PVDF/TiO₂ mixed matrix membrane using DMAc as solvent with 0.01 g/L of TiO₂ in the coagulation bath exhibited extraordinary permeability (43.21 L/m² h) with superior retention properties (98.28%) of humic acid.

© 2012 Elsevier B.V. All rights reserved.

1. Introduction

Recently, nano-sized colloidal particles have extended their advance applications into membrane technologies by improving their synergistic effects on water and wastewater treatment [1]. The unique large surface-to-volume ratio and strong reactivity properties of NP make it an ideal candidate to be incorporated into polymeric matrix for highly specific applications [2,3]. Beneficial effects of NP-based membranes on the mitigation of membrane fouling have been reported recently [4–6]. Among different metal oxide NPs, TiO₂ which serves as a good candidate as hydrophilic filler has attracted great research interests in improving the membrane permeability and fouling-resistance [5,7]. Kwak et al. claimed that the deposition of TiO₂ NPs into hand-cast polyamide composite membrane had made an obvious difference in both hydrophilicity and flux [8].

Many technical innovations in mixed matrix membrane production have been carried out to incorporate TiO₂ into the membrane polymeric matrix. Among others are photocatalytic reactor combined cross flow filtration, membrane submerged within the slurry reactor and TiO₂ coated or entrapped membrane [9–11]. However, the high surface energy of TiO₂ NPs often results in agglomeration; leading to low functional surface area, which is a conspicuous drawback

for application. Besides, the addition of TiO₂ NPs in most of the case will alter the physical properties of the neat membranes. Therefore, for feasible application, it is crucial to obtain ultrafine and stable nanodispersions for production of thin mixed matrix membrane films with low surface roughness and high surface area of TiO₂ NPs [12,13].

The preparation of size-controlled, monodispersed NPs is of primary importance to these exciting applications. Three methods commonly employed by researchers to immobilize TiO₂ NPs on flat polymeric ultrafiltration membrane (UF) are: i) deposition of TiO₂ NPs on the membrane surface by direct filtration of NP aqueous suspension [9,11,14]; ii) entrapment of TiO₂ NPs in a polymer matrix of membrane by adding NPs into the casting solution [6–8,10,15]; and iii) fabrication of TiO₂/polymer mixed matrix membrane via electrostatic self-assembly between TiO₂ nanocomposites and anionic polymers [16]. However, there are a few drawbacks in these methods as the physically and electrostatically embedded TiO₂ could be poorly distributed in the membrane matrix due to the poor mixing or shearing of the polymer solution as well as low stability of the colloid.

Recent works on improving dispersion of TiO₂ in the membrane matrix reported include surface modification of TiO₂ or modification of the polymer itself. TiO₂ modification was performed using coupling agent and other steric repulsive polymeric materials such as aminopropyltriethoxysilane [17] and γ -aminopropyltriethoxysilane [18]. Polymer modification was achieved via electrostatic self-assembly between TiO₂ NPs and the modified functional groups on the polymer such as sulfonic acid [16]; diethanolamine [19]; and 4-vinylpyridine-co-acrylamide [20]. However, incorporation of these extra components

* Corresponding author. Tel.: +60 4 5996418.

E-mail address: chobs@eng.usm.my (B.S. Ooi).

might change the morphology of the membrane as well as hinder the photocatalytic property of TiO₂.

In the present work, mixed-matrix polyvinylidene fluoride (PVDF/TiO₂) membrane prepared via colloidal precipitation method was explored. Through this method, the pore forming and TiO₂ embedding processes could be carried out in the coagulation bath simultaneously. It was hypothesized that through the in situ colloidal precipitation method, not only the dispersion of finer TiO₂ NPs on the membrane surface could be improved; the membrane morphological changes could also be minimized optimizing membrane performance.

2. Experiment

2.1. Materials

Ultrafiltration flat sheet membranes were fabricated from different casting solutions of polyvinylidene fluoride, PVDF (Solvay Pharmaceuticals, Inc., USA). The casting solutions were prepared by dissolving PVDF in either N-methyl-2-pyrrolidone, NMP (Merck, Germany) (purity (GC) ≥99.5%), N,N-dimethyl formamide, DMF (Merck KGA, Germany) (purity (GC) ≥99.8%) or N,N-dimethylacetamide, DMAc (Merck, Germany) (Assay (GC, area %) ≥99%). These solvents were employed without further purification. A commercial form of inorganic photocatalytic titanium dioxide, TiO₂ (particle size of 20 nm) nanopowder purchased from TitanPE Technologies, Inc., China (trade name: PC-20) that contains about 85% anatase and 15% rutile was used as received.

Synthetic humic acid (HA) with molecular weight mainly ranging from 20,000 to 50,000 g/mol was obtained from Sigma-Aldrich and used without further purification. Sodium hydroxide, NaOH was used to improve the dissolution of HA in water. At pH = 10, 20 mg HA powder was added and dissolved in 1 L of 0.1 mol/L NaOH (Sigma Aldrich, USA) under vigorous stirring.

2.2. Preparation of stable TiO₂ suspension

Chemical and mechanical methods were carried out to enhance the TiO₂ colloidal stability in the coagulation bath. These methods are described as below.

2.2.1. Chemical method

Firstly, to increase the stability of the TiO₂ particles in distilled water, the chemical modification of the original TiO₂ nanopowder was carried out by adjusting the pH value of the TiO₂ suspension. Hydrochloric acid solution (HCl) was added drop-wise and mechanically stirred until it reaches equilibrium of pH 4.0 to achieve electrostatic stability (zeta potential > +30 mV). The pH value of the TiO₂ suspensions was measured using a pH meter (Eutech Instruments).

2.2.2. Mechanical method

To further break down the TiO₂ cluster, TiO₂ solution was subjected to 15 min ultrasonic irradiation using Telsonic ultrasonic horn (SG-24-500P, Telsonic Ultrasonics). The frequency of the ultrasound was kept constant at 18.4 kHz.

2.3. Membrane formation and in situ particle embedment

The membrane casting solutions were prepared by dissolving pre-dried PVDF (24 hour oven drying at 70 °C) using the polymer solvents; NMP, DMF and DMAc in a 200 mL beaker. Composition of the PVDF/solvent solutions was kept constant at 18:82 in weight percentage.

In order to obtain complete dissolution of the polymer solution, the mixture was subjected to an initial constant stirring of 250 rpm at 65 °C for 4 h to form a homogenous solution. The homogenous membrane polymer solution was then left overnight with stirring

at 40 °C. Air bubbles were removed by standing the solution overnight. Solvent loss by evaporation was negligible due to the high boiling points of NMP (202–204 °C), DMAc (164–166 °C) and DMF (153 °C).

The polymer solution was cast using a thin film applicator (Elcometer 4340, Elcometer (Asia) Pte. Ltd.) on a flat glass plate wrapped with non-woven polyester fabric (Holleytex 3329, Ahlstrom) to form a solution layer at a nominal thickness of 200 μm. The polyester fabric acts as support, providing mechanical strength to the membrane for pressure resistant. The nascent membrane on the glass plate was then solidified by immediate immersion into a coagulation bath at room temperature (26 °C) to avoid excessive surface evaporation. The immersion was left for a day to ensure complete solidification and removal of residual solvent from the membranes. The fabricated membrane was then recovered from the coagulation bath after detaching it from the glass plate and subsequently rinsed with and soaked in a bath of fresh distilled water. Drying was sequentially done after dipping the membrane in ethanol to avoid microbial growth.

In order to introduce TiO₂ particles on the membrane surface, PVDF solution layers were immersed into the coagulation bath with TiO₂ colloidal suspension. The concentration of TiO₂ dosed into the distilled water was varied for 0.001 g/L, 0.01 g/L and 0.1 g/L. The preparation conditions of the membranes were summarized in Table 1.

2.4. Membrane characterization

2.4.1. SEM analysis

Top surface morphology of the PVDF/TiO₂ mixed matrix membranes was observed using a Field Emission Scanning Electron Microscope (FESEM) (SUPRA 35 VP, Carl Zeiss Inc.). For FESEM observation, the membrane samples were cut into appropriate size and mounted on the sample holders. K 550 sputter coater was used to coat the outer surface of the membrane sample with a thin layer of gold under vacuum to provide electrical conductivity. After gold/palladium sputtering, the samples were examined under the electron microscope at potentials of 10.0 kV.

2.4.2. Pore size distribution

Pore size of the membranes was determined using gas flow/liquid displacement method via Capillary Flow Porometer Porolux 1000 (CNC Instruments). Membrane samples with a diameter of 10 mm were characterized using the "dry up-wet up" method. In this method, gas flow was measured as a function of transmembrane pressure, through wetted membrane with 1,1,2,3,3,3-hexafluoropropene and the dried membrane. The pore size distribution was estimated using PMI software.

Table 1
Membrane dope and coagulation bath formulation.

Membrane number	PVDF weight ratio (%)	Solvent weight ratio (%)	Solvents	TiO ₂ concentration (g/L)
M1 (a)	18	82	NMP	0.000
M1 (b)	18	82	NMP	0.001
M1 (c)	18	82	NMP	0.010
M1 (d)	18	82	NMP	0.100
M2 (a)	18	82	DMAc	0.000
M2 (b)	18	82	DMAc	0.001
M2 (c)	18	82	DMAc	0.010
M2 (d)	18	82	DMAc	0.100
M3 (a)	18	82	DMF	0.000
M3 (b)	18	82	DMF	0.001
M3 (c)	18	82	DMF	0.010
M3 (d)	18	82	DMF	0.100

2.4.3. Identification of crystalline phase

X-ray diffraction (XRD) technique was used to identify the crystalline phases of PVDF on the membrane surface. Modified surfaces of the membrane were subjected to X-ray radiation and the diffraction data were collected on a BRUKER AXS D8 ADVANCE diffractometer (Bruker AXS, GmbH). The system is equipped with a Cu X-ray tube and a LynxEye detector operated at 60 kV and 80 mA, and the configuration was calibrated using a lanthanum boride (LaB6) powder standard (ICDD PDF#34-0427). Scanning was performed from 10° to 80° (2 θ -angle), with a step width of 0.02° and a sampling time of 0.3 s per step.

2.4.4. Surface tension (wettability) measurement

The membrane wettability is characterized by static contact angle of the membrane samples, which was measured based on sessile drop technique using a DropMeter A-100 contact angle system (Rame-Hart Instrument Co., U.S.A.). The membrane sample was stuck onto a glass slide using double-sided tape to ensure its top surface was upward and flat. A droplet (~13 μ L) of deionized water was dropped onto the dry membrane surface using a microsyringe at room temperature (21 \pm 1 °C). Immediately, a microscope with long working distance 6.5 \times objectives was used to capture micrographs at high frequency (100 Pcs/s). The reported contact angles were average values from the measurements taken at 10 different locations on the membrane surface, as a measure to minimize random error.

2.4.5. Streaming potential

The surface properties of the membranes were examined using streaming potential device. The streaming potential was evaluated using a device constructed from two Plexiglas chambers with Ag/Ag/Cl electrodes inserted at each end. Data were obtained using 10 mM NaCl at pH 7.0, with the fluid flow across the membrane surface. The apparent zeta potential (ξ) was evaluated from the slope using the Helmholtz–Smoluchowski equation [21–23]

$$\xi = \left(\frac{\eta \Lambda_0}{\epsilon_0 \epsilon_r} \right) \frac{dE_z}{d\Delta P} \quad (1)$$

where Λ_0 is the solution conductivity, η is the absolute viscosity of medium, ϵ_0 is the permittivity of vacuum, and ϵ_r is the dielectric constant of the medium.

As streaming potential is linearly dependent on the applied pressure differential, it allows apparent zeta potential to be evaluated directly from Eq. (1). Several studies have shown that Eq. (1) provides useful information on the charge characteristics of membranes even though the Helmholtz–Smoluchowski equation neglects the effects

of surface conductance and overlapping double layers [22,23]. All results in this study were reported in terms of apparent zeta potential data as calculated from Eq. (1).

2.5. Permeation flux and rejection of humic acid measurements

A laboratory bench scale cross-flow recirculation unit was used to study permeation flux and rejection of the mixed matrix membrane using 20 mg/L of humic acid (HA) as model solution at ambient temperature (25 °C). The schematic diagram of permeation unit is shown in Fig. 1. The produced flat sheet membrane was cut and housed in the stainless steel circular membrane test cell with a diameter of 5.1 cm (effective membrane filtration area of 20.43 cm²) and sealed with a rubber O-ring. Synthetic HA solution was charged into a 5 L feed tank and re-circulated at a constant cross-flow rate of 0.04 L/min using the peristaltic pump (Hydra-Cell, Wanner International). Filtration pressure was controlled by a needle valve to 0.5 bar. Absorbance of the collected permeates was measured using UV spectrophotometer (UV mini-1240, Shimadzu).

Pure water flux was determined by direct measurement of the permeate volume over the time,

$$F = \frac{V}{At} \quad (2)$$

where F is the pure water flux (L/m² h), V is the permeate volume (L), A is the membrane surface area (m²), and t is the time (h).

Experimental rejection of solute (R) was calculated from the feed solution (HA solution) and permeate solution using the following equation:

$$R(\%) = \left(1 - \frac{C_p}{C_f} \right) \times 100\% \quad (3)$$

where R is the rejection ultrafiltration process (%), C_p is the concentration of the permeate solution and C_f is the concentration of the feed solution.

3. Results and discussions

3.1. Morphologies of PVDF/TiO₂ mixed matrix membrane

Fig. 2 shows the SEM top surface images of PVDF/TiO₂ mixed matrix membranes for membranes prepared using different types of solvents and immersed in colloidal suspension containing 0.001 g/L, 0.01 g/L and 0.1 g/L of TiO₂. As could be seen from Fig. 3 with 5.00 k \times

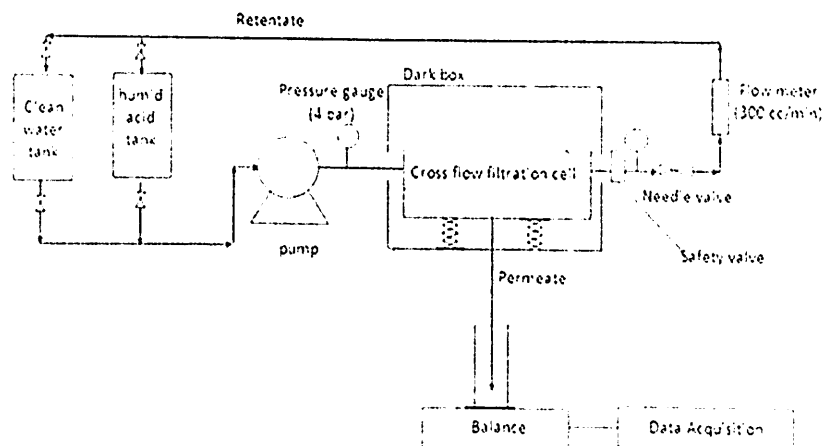


Fig. 1. Schematic of cross-flow recirculation membrane filtration setup.

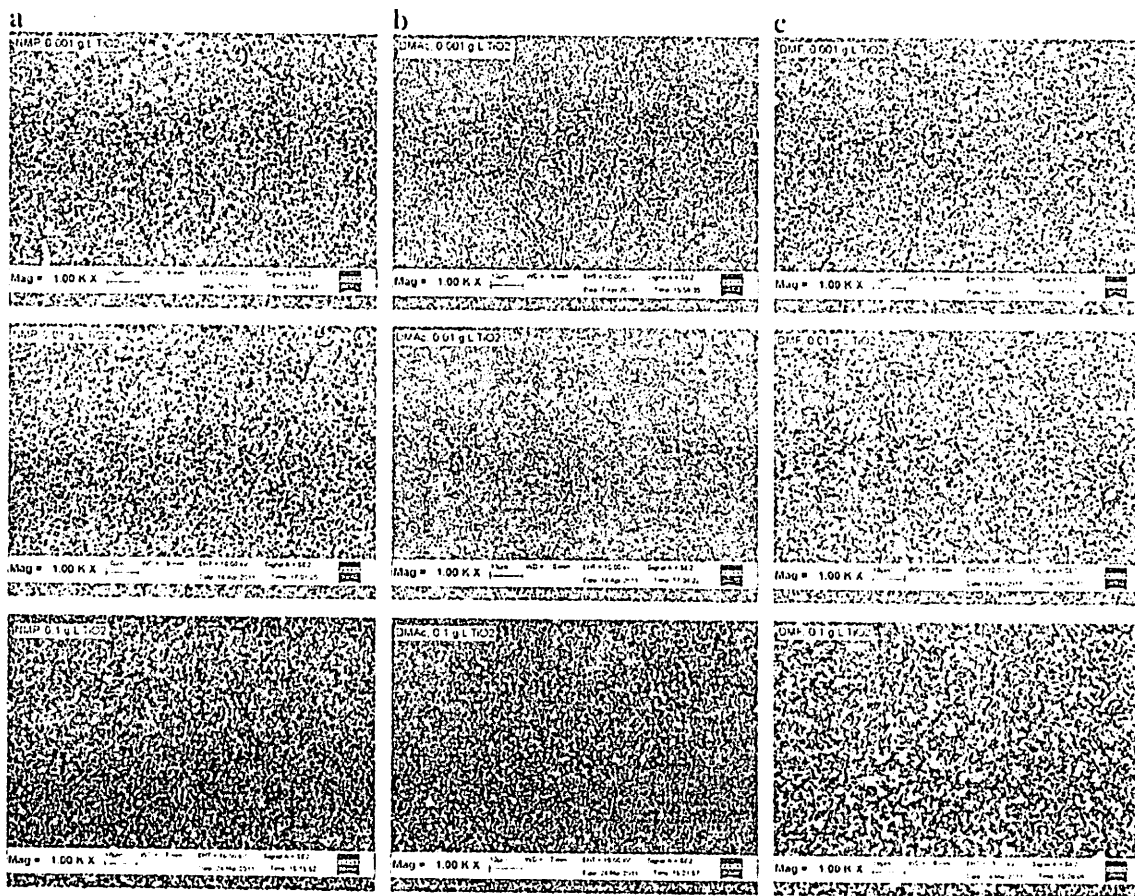


Fig. 2. FESEM micrographs reveal the detail of the topography structure of PVDF membrane fabricated with different solvents and different TiO_2 concentrations at 1.00 k \times : (a) NMP (b) DMAc (c) DMF

of magnification, cellular pore structure appeared on the surface of PVDF membrane using DMF as solvent while for membranes with NMP and DMAc as solvents, membranes with more connected pores were observed. The experimental results indicated that choice of solvent did contribute to structural change of the membrane morphology [24–26].

The morphological changes of membrane prepared using different solvent systems could be related to the solubility parameters of solvent in water. Rate of solvent–nonsolvent (water) inter-diffusion depends on value of solubility parameters of the solvent and non-solvent. The solubility parameter difference $\Delta\delta_{S-NS}$ between solvent system of the casting solution and non-solvent system of the coagulation bath can be calculated using the following equation:

$$\Delta\delta_{S-NS} = \sqrt{(\delta_{d,S} - \delta_{d,NS})^2 + (\delta_{p,S} - \delta_{p,NS})^2 + (\delta_{h,S} - \delta_{h,NS})^2} \quad (4)$$

where δ_p is Hansen polarity parameter ($\text{Cal}^{1/2} \text{cm}^{-3/2}$), δ_d is Hansen dispersion parameter and δ_h is Hansen hydrogen parameter. It has been known that lower value of this parameter corresponds to a higher affinity of the liquids; hence promotes higher solvent outflux and non-solvent influx, and a better miscibility [27]. Solubility parameters of water with the organic solvent increased in the following order: DMF (31.14) < DMAc (32.44) < NMP (35.38) which dictates that miscibility of water–solvent decreased in reverse trend: DMF > DMAc > NMP. Improved miscibility of DMF with water momentarily increased the

polymer concentration at the interface due to the higher solvent outflux. As a result, membrane with tighter pore size could be produced.

As shown in Figs. 2 and 3, with the increasing TiO_2 concentration, the amount of TiO_2 particles deposited on the surface was increased and exists as different sizes of snowflake. This is the result of TiO_2 particle agglomeration at higher TiO_2 concentration. The increasing number of TiO_2 particles on membrane surface will likely provide additional hydrophilicity strength to the membrane, possibly increasing the permeate water flux and its antifouling properties. However, higher TiO_2 concentration might induce the aggregation of TiO_2 particles thus blocking the pores of membranes.

Sizes of NPs distributed on the PVDF/ TiO_2 mixed matrix membrane surface were measured from the FESEM images using ImageJ 1.43 u software at 10.00 k \times magnification, and the results are presented in Fig. 4. Fig. 4 shows that different solvents (used in polymer solution) did play an important role in changing the particle size distribution on the membrane surface. Membranes using NMP (M1) as solvent produced smaller surface particles compared to the systems using DMAc (M2) and DMF (M3) as solvents. This phenomenon is probably due to the higher surface tension between DMF and TiO_2 compared to NMP- TiO_2 which promotes particle aggregation during the phase inversion. The surface tensions between the solvents and NPs are actually following the trend of the solubility parameter. The higher the solubility parameter of solvent–water means the least hydrophilicity of the solvent. As a result, the relatively hydrophobic solvent would induce colloidal instability when it was brought into contact with the hydrophilic TiO_2 NPs. Consequently, the relatively hydrophobic DMF has the tendency to form larger TiO_2 aggregates.

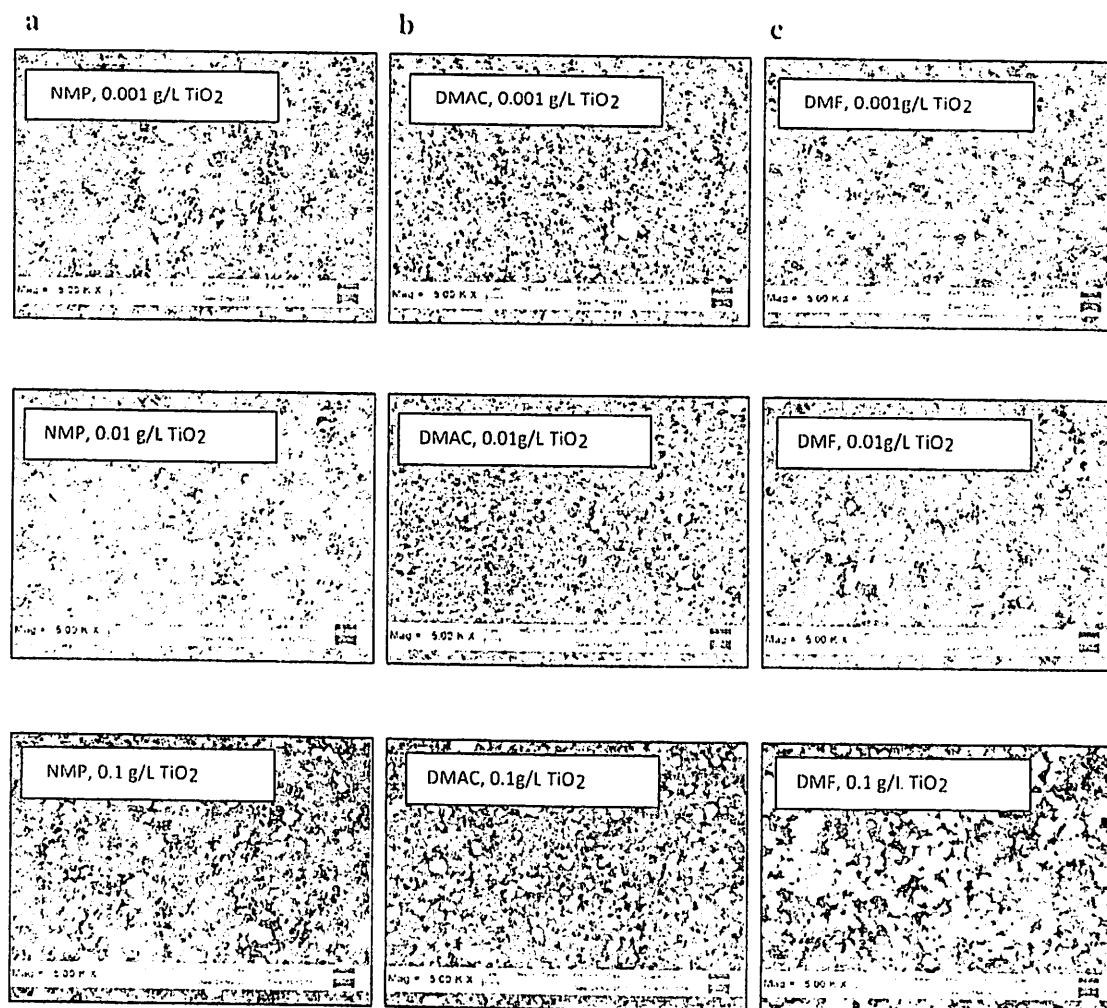


Fig. 3. FESEM micrographs reveal the detail of the topography structure of PVDF membrane fabricated with different solvents and different TiO_2 concentrations at 5.00 kV. (a) NMP (b) DMAC (c) DMF.

Besides, Mackay et al. [28] found that dispersion of NPs into a polymeric liquid is thermodynamically stable for systems where the radius of gyration (R_g) of the linear polymer is greater than the radius of the NPs. In this case, different solvents will most likely affect the R_g value of the polymer solution. The solvent that contributes to greater R_g in polymer solution is suggested to have smaller TiO_2 particle size distribution on membrane surface with relatively stable TiO_2 NPs dispersion. The relations between the root-mean square radius of gyration of the chain in the three solvents and the molecular weight obtained by Ali and Raina [29] using the theory of Inagaki et al. [30], were $\langle S^2 \rangle = 2.82 \times 10^{-1} M_w^{0.45}$, $2.95 \times 10^{-1} M_w^{0.55}$, and $8.13 \times 10^{-2} M_w^{0.51}$ for NMP, DMAC and DMF respectively. It can be concluded that the polymer chains are more extended in DMAC than in DMF and NMP. So, it is not surprising to observe that DMF gave a relatively poor particle size distribution as the PVDF has the smallest gyration radius when it was exposed to DMF environment.

We tried to relate the size of the particle to its colloid stability in the solution bath during phase inversion. As commonly known, repulsive potential V_R of the TiO_2 NPs is a complex function of $V_R = 2 \pi \epsilon a \zeta^2 \exp(-\kappa D)$ where a is the particle radius, ϵ is the solvent dielectric constant, κ is a function of the ionic composition and ζ is the zeta potential. The dielectric constant of NMP, DMAC and DMF are 32.20, 37.78 and 36.71 respectively. Based on the value of ϵ , TiO_2 suspension should be relatively stable for DMF system as the diffusion of DMF with higher dielectric constant should provide relatively higher repulsive

force within the particles. However, a reverse trend was observed whereby M3 (DMF system) showing the worst clustering phenomenon.

From the results obtained from solubility parameters, hydrophilic interaction gyration radius as well as colloidal stability, it can be concluded that the effect of solvent on particle size distribution is to a greater extent affected by the hydrophobic/hydrophilic interaction rather than the electrostatic interaction between the NPs and polymer solution. This phenomenon could lead to a better understanding on how to prepare well distributed NPs in the polymer matrix.

3.2. Pore size distribution

Selection of solvent is crucial not only for its particle size distribution but it is one of the important parameter that affects the pore size distributions of the membranes. As shown in Fig. 5, membrane prepared using NMP as solvent has a relatively larger pore size and a wider pore size distribution compared to membrane using DMAC and DMF as solvents. The maximum diameter of pore, $d_{p,max}$ for membrane prepared using NMP as solvent was around 0.100 μm , while for membrane prepared using DMAC and DMF as solvents was around 0.075 μm and 0.050 μm , respectively.

Membrane pore size distribution would be changed upon incorporation of TiO_2 NPs depending on the type of solvent used. For NMP, the addition of TiO_2 did increase the maximum pore size but its effect on pore size distributions was not significant. On the other

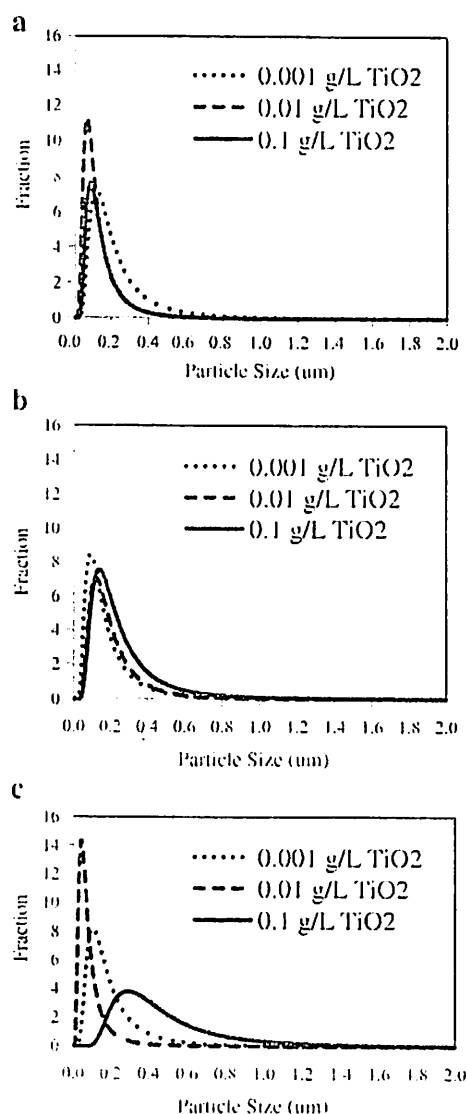


Fig. 4. Effect of solvent type on TiO_2 particle size distribution (a) NMP (b) DMAc (c) DMF.

hand, for membranes prepared using DMAc and DMF as solvents even pore size distribution was improved by adding 0.1 g/L and 0.01 g/L of TiO_2 but became poorer at lowest TiO_2 loading (0.001 g/L). It can be concluded that membranes prepared using high affinity solvent such as NMP and DMAc have a tendency to reduce its pore size by adding NPs. These results were similar with what was observed by Damodar et al. who found that the number of small pore size increases with increasing TiO_2 content [31]. This is probably due to the increase of stress between polymer and TiO_2 NPs as a result organic shrinkage occurred during the precipitation process of wet-casting polymeric membranes. Another plausible reason is because of pore blocking due to the precipitation of NPs on the pore wall which further reduced the pore size.

3.3. Polymorph analysis

XRD diffraction patterns of TiO_2 NPs, PVDF membrane and PVDF/ TiO_2 mixed matrix membrane are shown in Fig. 6. It can be seen that the XRD pattern of PVDF/ TiO_2 mixed matrix membrane had four crystalline characteristic peaks at 2θ of 18.570° , 20.395° , 25.405° and 38.712° that was analogous with the predominant characteristic peaks of PVDF membrane and TiO_2 crystal powder, respectively. Due

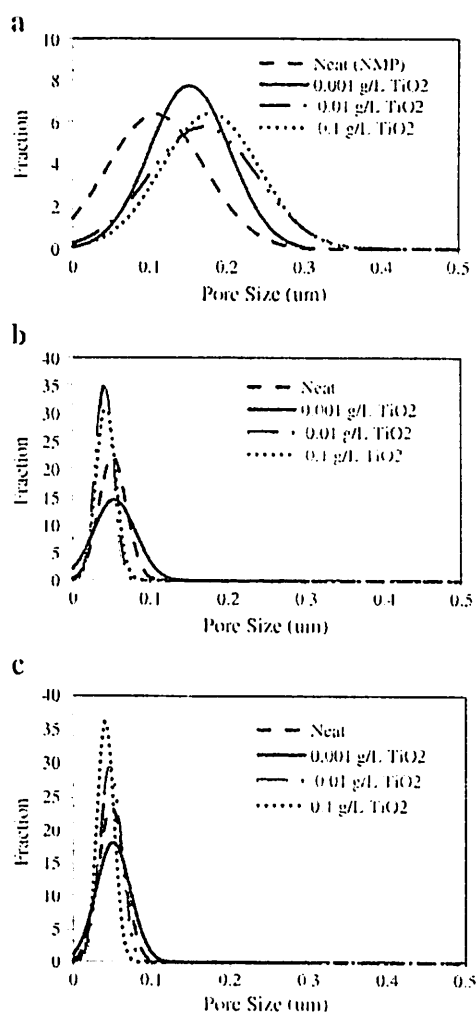


Fig. 5. Pore size distribution of the PVDF/ TiO_2 mixed matrix membrane and neat membrane (a) NMP (b) DMAc (c) DMF.

to the low concentration of TiO_2 NPs in PVDF/ TiO_2 mixed matrix membrane, only characteristic peaks could be seen in XRD patterns. However, their locations were slightly shifted, when compared with the pattern of TiO_2 NPs at 2θ of 25.209° and 37.722° respectively. The shift of characteristic peaks indicated that there are interactions between polymer and TiO_2 which influenced the PVDF crystal structure (transition of phase) in the mixed matrix membrane.

The direct evidence of polymorph change of the PVDF membrane can also be seen in Fig. 6. The neat PVDF membrane exhibited peaks at 2θ of 18.69° and 20.11° ; characteristic of α -polymorph [32], which was close to the literature data of 18.5° and 20.2° from Wang et al. [33]. There was a significant change of polymorph after the inclusion of PC-20 in the neat PVDF membrane. The α -polymorph of the PVDF membrane increased with the addition of TiO_2 . This phenomenon was expected as hydrophilic nature of TiO_2 NPs would enhance the α -polymorph which promises excellent hydrophilic characteristic of the composite membrane.

3.4. Permeation flux and rejection of membranes

The effect of solvent and TiO_2 concentration on mixed matrix membrane contact angle, permeability and rejection of HA was investigated through cross-flow membrane filtration experiments and the membrane performances were summarized in Table 2. All the presented

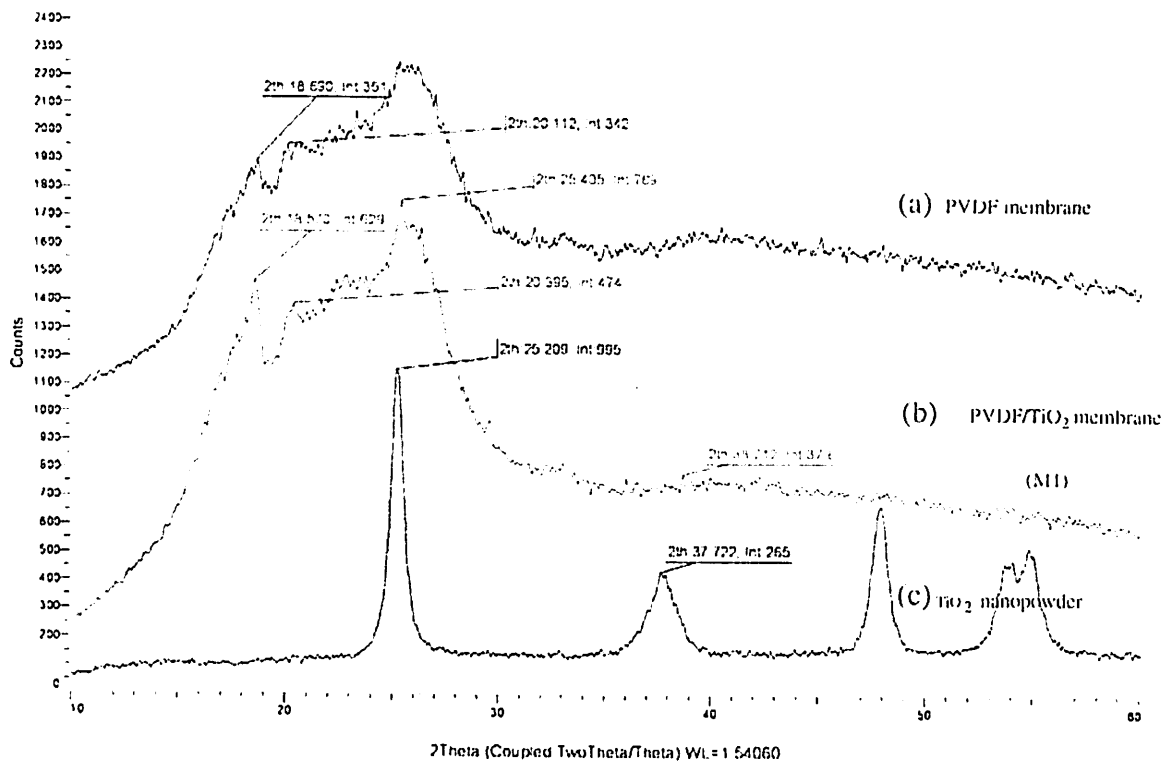


Fig. 6. X-ray diffraction diffractogram of (a) PVDF membrane (b) PVDF/TiO₂ mixed matrix membrane module M1 (c) TiO₂ nanopowder.

membrane permeability and rejection of HA results corresponded to the average of three replications with the membrane tested randomly chosen from different independent sheets. The effect of membrane hydrophilization on PVDF/TiO₂ mixed matrix membranes could be evaluated by the performance of HA solution flux (F).

Comparing the HA permeation of neat PVDF membrane using NMP, DMAc and DMF as solvents, which were labeled as M1 (a), M2 (a) and M3 (a) respectively, the flux for the neat membrane using NMP as solvent is 5 times higher than that for DMAc and DMF. This is mainly due to the fact that membranes prepared using NMP as solvent have larger pores (as shown in Fig. 5).

As shown in Table 2, the PVDF/TiO₂ mixed matrix membrane in average has higher flux in comparison to the neat membrane, even though there was not much change in terms of contact angle attributed to the increase in hydrophilicity of the membrane due to TiO₂ NPs and narrowing of pores occurred for DMAc and DMF. Theoretically, contact

angle measurement is mainly affected by membrane surface hydrophobicity, roughness, porosity, pore size, and pore size distribution. Rana and Matsuura [34] reported that the contact angle value of membrane with higher roughness is higher compared to the other membrane of lower surface roughness, even though both membranes are having similar hydrophilicity. Therefore, it was hypothesized that the slight increases of contact angle in Table 2 are mainly due to the higher surface roughness created with the increasing of TiO₂ concentration, whereby the water droplet is not directly in contact with the membrane surface as TiO₂ NPs will build a barrier between them, which then impaired the membrane surface wettability. Although TiO₂ NPs that are deposited on the membrane surface show the increasing trend of the contact angle of the membrane, it does not mean that TiO₂ has reduced the membrane hydrophilicity. In fact, the increasing α -polymorph of PVDF membrane with the addition of TiO₂ in Fig. 6 as in Section 3.3 proved that the hydrophilicity of PVDF membrane has been improved remarkably with the introduction of TiO₂ NPs on membrane surface via in situ colloidal precipitation method. These results are in consistent with other research findings [16,35,36] which observed that the modified membrane with the addition of TiO₂ showed higher flux for sludge filtration compared to neat polymeric membrane. Nonetheless, the larger effective surface area caused by the roughness could greatly improve the flux of membrane.

Table 2 shows that 0.01 g/l. of TiO₂ contributes to the most excellent result in increasing membrane permeability as it exhibited the highest membrane permeability for all types of solvents used. The observed flux increase (improved hydrophilicity) upon integration of TiO₂ NPs can be explained as such. During the exchange of TiO₂ NPs onto the membrane surface, the PVDF membrane was exposed in the low pH HCl, in which the acid has caused partial hydrolysis of the membrane surface to increase its hydrophilicity, and hence increased the permeate water flux [37]. However, at higher concentration of TiO₂ (0.1 g/L), the membrane permeability was largely declined. This phenomenon may be due to the higher agglomeration tendency for

Table 2
The effect of TiO₂ concentration and types of solvents on contact angle, permeate flux and rejection.

Solvents	Membrane number	TiO ₂ concentration (g/L)	Contact angle (°)	Permeate flux (L/m ² h)	Rejection (%)
NMP	M1 (a)	0.000	68.54 ± 0.61	142.12	91.57
	M1 (b)	0.001	70.25 ± 0.89	171.09	92.13
	M1 (c)	0.010	69.32 ± 0.50	209.79	94.70
	M1 (d)	0.100	73.05 ± 0.89	138.76	96.94
DMAc	M2 (a)	0.000	67.56 ± 0.92	37.70	98.08
	M2 (b)	0.001	67.01 ± 0.87	43.15	98.28
	M2 (c)	0.010	68.24 ± 0.81	43.21	98.28
	M2 (d)	0.100	70.68 ± 0.86	39.70	98.06
DMF	M3 (a)	0.000	67.46 ± 1.27	33.13	97.81
	M3 (b)	0.001	66.81 ± 1.19	34.02	97.88
	M3 (c)	0.010	70.32 ± 1.35	37.26	98.58
	M3 (d)	0.100	71.53 ± 1.05	33.19	97.25

TiO₂ particle in water suspension which blocks the membrane pores during immersion precipitation.

Besides the flux performance, removal efficiency of HA was found to be affected by the presence of TiO₂ on the membrane surface for membrane using NMP and DMF as solvents. Membrane using DMAc (M2) was found to have the greatest ability to remove HA (>98%), followed by DMF (M3) and NMP (M1). The differences in solute rejection of each membrane are mainly contributed by the steric hindrance of the membranes due to the pore size. Membrane M1 with bigger pore size has the poorest HA rejection compared to M2 and M3 membranes. However, with the addition of TiO₂, the rejection performance of M1 was improved from 90% to 97% even through the pore size was increased. This phenomenon indicated that HA might form macromolecule (aggregate) at the surface with the hydrodynamic size bigger than 0.2 μm. Pore opening will allow more passage of pure water, which therefore improved the HA rejection. However, the overall rejection of M1 membrane is still low compared to M2 and M3 membranes mainly due to the leakage of smaller HA molecules.

Additionally, variation in membrane properties such as surface charge by TiO₂ NPs might affect the physico-chemical interactions of membrane and its solution [38]. The apparent zeta potential of the neat membrane and PVDF/TiO₂ mixed-matrix membrane prepared using DMAc as solvent at 0.001 g/L, 0.01 g/L and 0.1 g/L concentrations were -8.505, -10.43, -10.22 and -10.44 mV respectively. The increasing net negative charge on the PVDF/TiO₂ mixed-matrix membranes compared to neat membrane could be attributed to the presence of TiO₂ NPs. Both HA and TiO₂ particles on membrane surface which possess negatively charged surface will then create a strong electrostatic repulsion between HA and surface of TiO₂. Therefore, in addition to hydrophilic characters, increasing of membrane surface negative charge with the introduction of TiO₂ NPs was expected to provide additional advantage in lowering fouling propensity.

In overall, the membrane performance in terms of HA removal could be improved by embedding the TiO₂ NPs into the PVDF membrane matrix. The addition of TiO₂ could enhance the permeation flux at different degrees depending on the type of solvent used. The flux enhancement effect is following the order of NMP > DMAc > DMF. Besides, it is worthwhile to note that the addition of 0.01 g/L of TiO₂ could enhance both the rejection and flux of the membrane. Membrane prepared using DMAc as solvent coagulated in 0.01 g/L of TiO₂ suspension was found to be the best membrane in terms of HA rejection and water flux.

4. Conclusion

Stable TiO₂ colloids in coagulation bath were successfully embedded to the membrane surface through phase inversion and colloidal precipitation method. It was found that the membrane prepared using NMP and DMAc as solvents has better particle size distribution compared to DMF. The particle size distribution is mainly contributed by the hydrophobic interaction between the NPs and the polymer solution. However, membrane prepared using NMP has relatively bigger pore size which resulted in poorer HA removal compared to DMAc and DMF. Nonetheless, using the in situ colloidal precipitation method, the changes of the physical structure of PVDF/TiO₂ mixed matrix membranes could be minimized.

Permeation tests with HA solution proved that permeability and rejection of the mixed matrix membrane were significantly improved due to its enhanced roughness as well as hydrophilicity. By adding 0.01 g/L of TiO₂ NPs into coagulation bath, the optimum membrane performance was obtained together with the dramatic increase of the permeate flux without compensating its HA rejection. Membrane prepared using 0.01 g/L of TiO₂ and DMAc as solvent is the best membrane which give 43.21 L/m² h of flux and rejection as high as 98.28% of HA.

Although membrane prepared using DMAc as solvent presents a good result on particle size distribution with flux enhancement, further research on long hour HA filtration test has to be carried out in the future to test on the chemical stability of TiO₂ dispersed in PVDF matrix and its antifouling properties.

Acknowledgments

The authors wish to thank the sponsors of this project for their financial supports, namely Universiti Sains Malaysia (USM) Research University Grant (1001/PJKIMIA/811172), Malaysia Toray Science Foundation (MISF) Science and Technology Research Grant (304/PJKIMIA/6050179/M126) and USM Membrane Science and Technology Cluster.

References

- [1] J. Kim, B. Brüggem, The use of nanoparticles in polymeric and ceramic membrane structures: review of manufacturing procedures and performance improvement for water treatment, *Environ. Pollut.* 158 (2010) 2335–2349.
- [2] P. He, A.C. Zhou, Nanometer composite technology and application in polymer modification, *Acromolecule Aviso.* 2 (2001) 74–82.
- [3] Z.P. Fang, Y.Z. Xu, C.W. Xu, Modification mechanisms of nanoparticles on polymers, *J. Mater. Sci. Eng.* 21 (2) (2003) 279–282.
- [4] AWWA Membrane Technology Research Committee, Recent advances and research need in membrane fouling, *J. AWWA.* 97 (8) (2005) 78–89.
- [5] J.B. Li, J.W. Zhu, M.S. Zheng, Morphologies and properties of poly(phthalazine ether sulfone ketone) matrix ultrafiltration membranes with entrapped TiO₂ nanoparticles, *J. Appl. Polym. Sci.* 103 (6) (2007) 3623–3629.
- [6] J.F. Li, Z.L. Xu, H. Yang, L.Y. Yu, M. Liu, Effect of TiO₂ nanoparticles on the surface morphology and performance of microporous PES membrane, *Appl. Surf. Sci.* 255 (2009) 4725–4732.
- [7] S.H. Kim, S.Y. Kwak, B.H. Sohn, T.H. Park, Design of TiO₂ nanoparticle self-assembled aromatic polyamide thin-film composite (TFC) membrane as an approach to solve biofouling problem, *J. Membr. Sci.* 211 (2003) 157–165.
- [8] S.Y. Kwak, S.H. Kim, S.S. Kim, Hybrid organic-inorganic reverse osmosis (RO) membrane for bactericidal anti-fouling. 1. Preparation and characterization of TiO₂ nanoparticle self-assembled aromatic polyamide thin-film-composite (TFC) membrane, *Environ. Sci. Technol.* 35 (2001) 2388–2394.
- [9] I. Erdei, N. Arerachakul, S. Vigneswaran, A combined photocatalytic slurry reactor-immersed membrane module system for advanced wastewater treatment, *Sep. Purif. Technol.* 62 (2008) 382–388.
- [10] R. Molinari, F. Pirillo, V. Loddo, L. Palmisano, Photocatalytic degradation of dyes by using a membrane reactor, *Chem. Eng. Process.* 43 (2004) 1103–1114.
- [11] W. Xi, S. Geissen, Separation of titanium dioxide from photocatalytically treated water by cross-flow microfiltration, *Water Res.* 35 (5) (2001) 1256–1262.
- [12] K. Ebert, D. Fritsch, C. Kull, C. Tjahjawiguna, Influence of inorganic fillers on the compaction behaviour of porous polymer based membranes, *J. Membr. Sci.* 233 (2004) 71–78.
- [13] X.H. Cao, J. Ma, X.H. Shi, Z.J. Ren, Effect of TiO₂ nanoparticle size on the performance of PVDF membrane, *Appl. Surf. Sci.* 253 (2006) 2003–2010.
- [14] D.P. Ho, S. Vigneswaran, H.H. Ngo, Integration of photocatalysis and microfiltration in removing effluent organic matter from treated sewage effluent, *Sep. Sci. Technol.* 45 (2010) 155–162.
- [15] M.A. Artale, V. Augugliaro, F. Drioli, G. Colemme, C. Grande, V. Loddo, R. Molinari, L. Palmisano, M. Schiavello, Preparation and characterization of membranes with entrapped TiO₂ and preliminary photocatalytic tests, *Ann. Chim.* 91 (2001) 127–136.
- [16] T.Y. Bae, I.C. Kim, T.M. Tak, Preparation and characterization of fouling-resistant TiO₂ self-assembled nanocomposite membranes, *J. Membr. Sci.* 275 (1–2) (2006) 1–5.
- [17] A. Razmjou, J. Mansouri, V. Chen, The effect of mechanical and chemical modification of TiO₂ nanoparticles on the surface chemistry, structure and fouling performance of PES ultrafiltration membranes, *J. Membr. Sci.* 378 (1–2) (2011) 73–84.
- [18] G.P. Wu, S.Y. Gan, L.Z. Cui, Y.Y. Xu, Preparation and characterization of PES/TiO₂ composite membranes, *Appl. Surf. Sci.* 254 (21) (2008) 7080–7086.
- [19] Y. Mansourpanah, S.S. Madaeni, A. Rahimpour, Formation of appropriate sites on nanofiltration membrane surface for binding TiO₂ photo-catalyst: performance, characterization and fouling resistant capability, *J. Membr. Sci.* 330 (1–2) (2009) 297–305.
- [20] Amr A. Essawy, A. El-Hag Ali, M.S.A. Abdel-Mottaleb, Application of novel copolymer-TiO₂ membranes for some textile dyes adsorptive removal from aqueous solution and photocatalytic decolorization, *J. Hazard. Mater.* 157 (2–3) (2008) 547–552.
- [21] D.B. Burns, A.L. Zdyney, Effect of solution pH on protein transport through ultrafiltration membranes, *Biotechnol. Bioeng.* 64 (1) (1999) 27–37.
- [22] M. Nyström, M. Lindström, E. Matthiasson, Streaming potential as a tool in the characterization of ultrafiltration membranes, *Colloid Surf.* 36 (3) (1989) 297–312.
- [23] M. Nyström, A. Pihlajamäki, N. Ehsani, Characterization of ultrafiltration membranes by simultaneous streaming potential and flux measurements, *J. Membr. Sci.* 87 (3) (1994) 245–256.

- [24] J. Kamo, T. Hirai, K. Kamada, Solvent-induced morphological change of microporous hollow fiber membranes, *J. Membr. Sci.* 70 (2–3) (1992) 217–224.
- [25] R. Guan, H. Dai, C.H. Li, J.H. Liu, J. Xu, Effect of casting solvent on the morphology and performance of sulfonated polyethersulfone membranes, *J. Membr. Sci.* 277 (1–2) (2006) 148–156.
- [26] T. Sener, E. Okumus, T. Gurkan, L. Yilmaz, The effect of different solvents on the performance of zeolite-filled composite pervaporation membranes, *Desalination* 261 (1–2) (2010) 181–185.
- [27] P. Vandezande, X. Li, L.E.M. Gevers, I.F.J. Vankelecom, High throughput study of phase inversion parameters for polyimide-based SRNF membranes, *J. Membr. Sci.* 330 (1–2) (2009) 307–318.
- [28] M.E. Mackay, A. Tuteja, P.M. Duxbury, C.J. Hawker, B.V. Horn, Z. Guan, G. Chen, R.S. Krishnan, General strategies for nanoparticle dispersion, *Science* 311 (2006) 1740–1743.
- [29] S. Ali, A.K. Rama, Dilute solution behaviour of poly(vinylidene fluoride), Intrinsic viscosity and light scattering studies, *Die Makromol. Chem.* 179 (12) (1978) 2925–2930.
- [30] H. Inagaki, H. Suzuki, M. Fujii, T. Matsuo, Note on experimental tests of theories for the excluded volume effect in polymer coils, *J. Phys. Chem.* 70 (1966) 1718–1726.
- [31] R.A. Damodar, S.J. You, H.H. Chou, Study the self cleaning, antibacterial and photocatalytic properties of TiO₂ entrapped PVDF membranes, *J. Hazard. Mater.* 172 (2009) 1321–1328.
- [32] Y. Takahashi, H. Tadokoro, Monomer sequence distributions in four-component polyesters as determined by carbon-13 and hydrogen-1 NMR, *Macromolecules* 13 (1980) 1317.
- [33] W. Wang, S. Zhang, L. Srisombat, T.R. Lee, R.C. Advincula, Gold-nanoparticle- and gold-nanoshell-induced polymorphism in poly(vinylidene fluoride), *Macromol. Mater. Eng.* 296 (2011) 178–184.
- [34] D. Rana, T. Matsuura, Surface modifications for antifouling membranes, *Chem. Rev.* 110 (2010) 2448–2471.
- [35] T.H. Bae, T.M. Tak, Preparation of TiO₂ self-assembled polymeric nanocomposite membranes and examination of their fouling mitigation effects in a membrane bioreactor system, *J. Membr. Sci.* 266 (2005) 1–5.
- [36] L.Y. Yu, H.M. Shen, Z.L. Xu, PVDF-TiO₂ composite hollow fiber ultrafiltration membranes prepared by TiO₂ sol-gel method and blending method, *J. Appl. Polym. Sci.* 113 (2009) 1763–1772.
- [37] A. Kulkarni, D. Mukherjee, V.N. Gill, Flux enhancement by hydrophilization of thin film composite reverse osmosis membranes, *J. Membr. Sci.* 114 (1996) 39–50.
- [38] N. Lee, G. Amy, J. Crouse, H. Buisson, Identification and understanding of fouling in low-pressure membrane (MF/UF) filtration by natural organic matter (NOM), *Water Res.* 38 (2004) 4511–4523.

Studies on the Surface Properties of Mixed-Matrix Membrane and Its Antifouling Properties for Humic Acid Removal

Y. H. Teow, A. L. Ahmad, J. K. Lim, B.S. Ooi

School of Chemical Engineering, Engineering Campus, Universiti Sains Malaysia, Seri Ampangan, 14300 Nibong Tebal, Penang, Malaysia

Correspondence to: B.S. Ooi (E-mail: chobs@eng.usm.my)

ABSTRACT: A major factor limiting the use of ultrafiltration (UF) membrane in water treatment process is the membrane fouling by natural organic matter such as humic acid (HA). In this work, neat PVDF and PVDF/TiO₂ mixed-matrix membranes were prepared and compared in terms of their antifouling properties. Two commercial types of TiO₂ namely PC-20 and P25 were embedded to prepare the mixed matrix membranes via *in situ* colloidal precipitation method. The contact angles for the mixed-matrix membranes were slightly reduced while the zeta potential was increased (more negatively charged) compared with the neat membrane. Filtration of HA with the presence of Ca²⁺ demonstrated that mixed-matrix membrane could significantly mitigate the fouling tendency compared with the neat membrane with flux ratio (J/J_0) of 0.65, 0.70, and 0.82 for neat PVDF membrane, PVDF/TiO₂ mixed-matrix membrane embedded with P25 and PC-20, respectively. PC-20 with higher anatase polymorphs exhibited better antifouling properties due to its hydrophilicity nature. © 2012 Wiley Periodicals, Inc. *J. Appl. Polym. Sci.* 000: 000–000, 2012

KEYWORDS: membranes; nanoparticles; nanowires and nanocrystals; particle size distribution; phase separation

Received 4 January 2012; accepted 18 August 2012; published online

DOI: 10.1002/app.38494

INTRODUCTION

Polyvinylidene fluoride (PVDF) is one of the most extensively applied membrane materials in the industry. However, PVDF UF membrane with its relatively hydrophobic nature limits its application in water separation process as they exhibit lower permeation flux due to the high surface tension between water and the membrane surface and more susceptible to fouling. Fouling caused by natural organic matter (NOM) is a major obstacle for efficient use of ultrafiltration (UF) membranes in the water purification process. Fouling could greatly reduce the permeate flux and increasing the operational pressure, which leads to a higher operational cost, and a short membrane lifespan. Several studies had demonstrated that humic acid (HA), which is an important forebonding of trihalomethane and haloacetic acids, has a major influence on membrane fouling in the application for water treatment.^{1,2} HA exists ubiquitously in the aquatic environment which primarily results from the microbiological degradation of surrounding vegetation and animal decay that enter surface water through rain water run-off from the surrounding land.³ Humic acid are thought to be the complex aromatic macromolecules owing to the presence of both aromatic and aliphatic substances with three main functional groups: carboxylic acids (COOH), phenolic alcohols (OH), and methoxy carbonyls (C=O).⁴

The effects of solution chemistry that plays an important role on HA fouling were broadly investigated in several membrane processes.^{5–7} The charge and configurations of HA macromolecules is extensively affected by its solution chemistry, which could alter the structure and hydraulic resistance of the foulant deposit layer. Wang et al., Hong et al. studied the effect of solution chemistry on membrane fouling in the treatment of water solutions containing HA. The results showed that the CaCl₂ or MgCl₂ salts could readily form complexes with the functional groups of humic macromolecules, increase the electrostatic shielding among the charged HA molecules and change the charge of both humic substances and membrane surface thus caused more severe fouling.^{3,5,8}

A variation in membrane properties such as pore size, surface charge and hydrophilicity might affect the physico-chemical interactions of membrane and its solution.⁹ In the previous study, Kabsch-Korbutowicz et al. investigated the deterioration of permeate flux during the UF of HA and found that hydrophobic UF membranes were more susceptible to HA fouling than hydrophilic UF membranes.⁷ This finding was in line with the work of Lee et al.¹⁰ who found that the hydrophilic regenerated cellulose membranes has superior antifouling property compared to the hydrophobic polyethersulfone membranes.

Recently, the combination of TiO₂ nanoparticles (NPs) with membrane filtration has been widely reported for its antifouling properties.^{11,12} In addition to hydrophilic characters, membranes which possessed a negative charge on the top selective layer were also found extra useful in lowering fouling propensity.¹³ Kwak et al. reported that the deposition of TiO₂ NPs into hand-cast polyamide composite membrane had made an obvious difference in both hydrophilicity and flux.¹⁴ Among the technical innovations used to incorporate TiO₂ NPs into the membrane polymeric matrix, addition of TiO₂ NPs during coagulation precipitation is considered as one of the most convenient methods to create the impact on membrane hydrophilicity.

Because of the complex chemical and physical interactions (fouling) in the UF process for water solutions containing HA, a more systematic investigation of these interacting aspects is needed. The main objective of this article is to evaluate the effects of membrane surface chemistry on membrane fouling via NPs modification.

EXPERIMENT

Materials

PVDF (Solvay Pharmaceuticals) ultrafiltration membranes were prepared by casting the PVDF in *N-N*-dimethylacetamide, DMAc (Merck, Germany) (Assay (GC, area %) \geq 99%) solution at 200 μ m thickness. Two different types of commercial titanium dioxide, TiO₂ nanopowder were purchased from TitanPE Technologies, China (trade name: PC-20; particle size of 20 nm) and Sigma-Aldrich, St. Louis, MO (trade name: P25; particle size \sim 21 nm). As reported by the manufacturer, PC-20 contains about 85% anatase and 15% rutile, while P25 contains about 75% anatase and 25% rutile. They were used as received.

Synthetic HA obtained from Sigma-Aldrich was used as the organic foulant during the experiment without further purification. Sodium hydroxide, NaOH solution was used to improve the dissolution of HA in water. Feed solutions were prepared by dissolving a preweighed 10 mg of HA powder in 5 L of distilled water. The solution pH was adjusted to pH 7 by addition of small quantities of 0.1M NaOH. To study the effect of HA fouling, the analytical grade inorganic salt (CaCl₂) was used to adjust the total ionic strength of the HA feed solution.

Preparation of Stable TiO₂ Suspension

Chemical and mechanical treatments were carried out to enhance the TiO₂ colloidal stability in the coagulation bath as described below.

Chemical Method. First, in order to increase the stability of the TiO₂ particles in distilled water, the chemical modification of the original TiO₂ nanopowder was carried by adjusting the pH value of the TiO₂ suspension. Hydrochloride acid solution (HCl) was added drop-wise and mechanically stirred until it reaches equilibrium of pH 4.0 to achieve electrostatic stability (zeta potential $>$ +30 mV). The pH value of the TiO₂ suspensions was measured using a pH meter (Eutech Instruments).

Mechanical Method. The TiO₂ cluster was further broken down by subjecting the TiO₂ solution to 15 min ultrasonic

irradiation using Telsonic ultrasonic horn (SG-24-500P, Telsonic Ultrasonics). The frequency of the ultrasound was kept constant at 18.4 kHz.

Membrane Formation and *In Situ* Particle Embedment

The membrane casting solutions were prepared by dissolving predried PVDF (24 h oven dried at 70°C) using DMAc in a 200-mL beaker. Composition of the PVDF/solvent solutions was kept constant at 18:82 in weight percentage.

To obtain complete dissolution and optimal dispersion of the polymer solution, the mixture was subjected to an initial constant stirring of 250 rpm at 65°C for 4 h to form a homogenous solution. The homogenous membrane polymer solution was then left overnight under stirring at 40°C and then kept in a centrifuge tube. The trapped air bubbles were removed by standing the solution overnight. Solvent loss by evaporation was negligible due to the high boiling point of DMAc at 164–166°C.

The polymer solution was cast using a thin film applicator (Elcometer 4340, Elcometer (Asia) Pte) on a flat glass plate wrapped with nonwoven polyester fabric (Holleytex 3329, Ahlstrom) to form a film at nominal thickness of 200 μ m. The polyester fabric acts as membrane support layer, providing mechanical strength to the membrane for pressure resistant. Thereafter, the nascent membrane on the glass plate was solidified by immersion into a precipitation water (distilled water) bath immediately to avoid excessive surface evaporation. The immersion was left for a day to ensure complete solidification and removal of residual solvent from the membranes. The resulting fabricated membrane was recovered from the coagulation bath after detaching from the glass plate and subsequently rinsed with and soaked in a bath of fresh distilled water. Drying was sequentially done after dipping the membrane in ethanol to avoid microbial growth.

To introduce TiO₂ particles on the membrane surface, the casted nascent PVDF membrane on the glass plate was immersed into 0.001 g/L TiO₂ colloidal suspension as prepared by using the method stated in Section 2.2. Since the membrane surface solidification and particle embedment occur simultaneously, this particle incorporation method is an *in situ* approach to embed particles onto the membrane surface.

Membrane Characterization

SEM Analysis. Top surfaces morphology of the PVDF/TiO₂ mixed matrix membranes was observed using a Field Emission Scanning Electron Microscope (FESEM) (SUPRA 35 VP, Carl Zeiss). For FESEM observation, the membrane samples were cut into appropriate size and mounted on the sample holders. K 550 sputter coater was used to coat the outer surface of the membrane sample with a thin layer of gold under vacuum to provide electrical conductivity. After gold/palladium sputtering, the samples were examined under the electron microscope at potentials of 10.0 kV. Using the same sample in SEM, the surface composition analysis including quality of dispersion and existence of TiO₂ particles on the membrane surface were carried out using energy dispersive X-ray (EDX) (EDAX).

Pore Size Distribution. Pore size of the membranes was determined using gas flow/liquid displacement method via Capillary

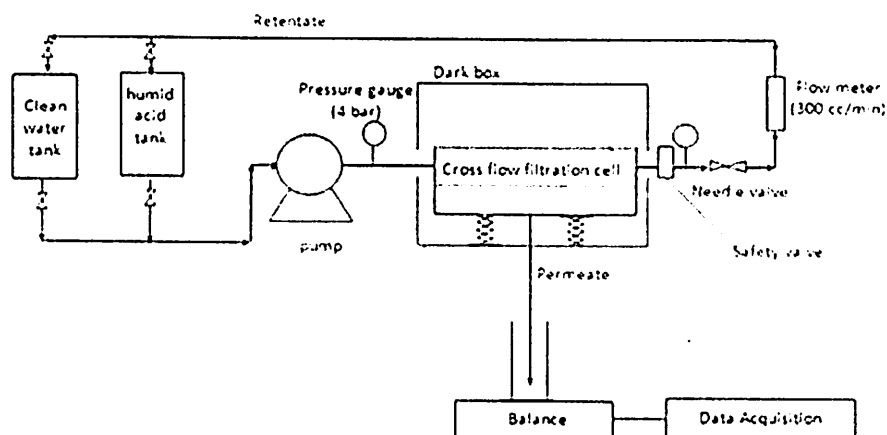


Figure 1. Schematic diagram of cross-flow recirculation membrane filtration rig.

Flow Porometer Porolux 1000 (Benelux Scientific, Germany). Membrane samples with diameter of 10 mm were characterized using the "dry up-wet up" method. In this method, gas flow was measured as a function of transmembrane pressure, initially through wetting of membrane with 1,1,2,3,3,3-hexafluoropropane followed by dry flow of gas through the membrane. The pore size distribution was estimated using PMI software.

TGA. The thermal stability and degradation of PVDF/TiO₂ mixed matrix membranes was examined by Thermal Gravitational Analysis (Perkin Elmer, USA) performed by a means of TGA 7 Thermogravimetric Analyzer. Aluminum open pans were used as sample holders. A membrane sample was placed on a pan by means of a plastic syringe in order to keep the sample mass and shape as uniform as possible. The sample mass weighing approximately 5–7 mg was used. Degradation temperatures were determined by heating the membrane sample using pure oxygen under ambient pressure at a heating rate of 20°C/min for the temperature range of 30–850°C and observing regions of significant weight loss. The TiO₂ concentration on membrane surface was estimated from the residual weight.

Surface Tension (Wettability) Measurement. The membrane wettability is characterized by static contact angle method based on sessile drop technique using a DropMeter A-100 contact angle system (Rame-Hart Instrument). The membrane sample was stuck onto a glass slide using double-sided tape to ensure its top surface was upward and flat. A droplet (~13 µL) of deionized water was dropped onto the dry membrane surface using a microsyringe at room temperature (21 ± 1°C). Immediately, a microscope with long working distance 6.5 × objectives was used to capture micrographs at high frequency (100 Pcs/s). The reported contact angles were average values from the measurements taken at 10 different locations on the membrane surface, as a measure to minimize random error.

Streaming Potential. The surface properties of the membranes were examined using streaming potential device. The streaming potential was evaluated using a device constructed from two

Plexiglas chambers with Ag/Ag/Cl electrodes inserted at each end. Data were obtained using 10 mM NaCl at pH 7.0, with the fluid flow across the membrane surface. The apparent zeta potential (ζ) was evaluated from the slope using the Helmholtz-Smoluchowski equation

$$\zeta = \left(\frac{\eta \Lambda_0}{\epsilon_0 \epsilon_r} \right) \frac{dE_z}{d\Delta P} \quad (1)$$

where Λ_0 is the solution conductivity, η is the absolute viscosity of medium, ϵ_0 is the permittivity of vacuum, and ϵ_r is the dielectric constant of the medium.

As streaming potential is linearly dependent on the applied pressure differential, it allows apparent zeta potential to be evaluated directly from eq. (1). Several studies have shown that eq. (1) provides useful information on the charge characteristics of membranes even though the Helmholtz-Smoluchowski equation neglects the effects of surface conductance and overlapping double layers. All results in this study were reported in terms of apparent zeta potential data as calculated from eq. (1).

Crossflow Filtration

Figure 1 displays the schematic diagram of the experimental set up for crossflow filtration. The rig mainly consist of a membrane cross-flow filtration cell, feed reservoir (HA tank and clean water tank), peristaltic pump, flow meter for measuring flow rate, balance for measuring filtrate flow with data acquisition system, pressure gauge to show the equilibrium pressure and to evaluate the membrane performance under different pressure. All produced flat sheet membranes were cut into the disc shape and laid on top of the membrane holder in a designed stainless steel circular membrane test cell with a diameter of 5.1 cm (effective membrane filtration area of 20.43 cm² excluding the area cover by the O-ring) and tightened by a rubber O-ring.

Before the experiment was carried out, the membrane was compressed using distilled water at constant pressure of 1.0 bar for 1 h and left for a day. During the experiment, the synthetic HA solution was charged into a 3 L feed tank and recirculated at a

constant cross-flow rate per unit projection membrane area of 0.04 L/min using the peristaltic pump (Hydra-Cell, Wanner International). Filtration pressure was generated using a peristaltic pump and controlled by a needle valve at 0.5 bar while the permeate side was opened to the atmosphere. The retentate was returned to the feed tank (HA tank) to minimize the changes of feed concentration. Fresh feed solution was added every 2 h in order to maintain constant concentration. Permeate flux was measured every 1 min by weight differences obtained online from the analytical balance.

RESULTS AND DISCUSSIONS

Morphologies of PVDF/TiO₂ Mixed Matrix Membrane

Figure 2 shows the SEM top surface images of PVDF/TiO₂ mixed matrix membranes for membranes prepared using DMAc as solvent immersed into different type of commercial TiO₂ colloidal suspension containing 0.001 g/L TiO₂ NPs. It can be seen from Figure 2 that connected pore structure appeared on the surface of PVDF membrane using DMAc as solvent and the type of commercial TiO₂ nanopowder used does not contribute to the structural change of membrane morphology due to its similar kinetic and thermodynamic environment during phase inversion.

In this colloidal precipitation method, TiO₂ nanoparticles were introduced into the whole membrane matrix during solvent exchange process as reported in our previous works.¹⁵ This can be proven by the cross-sectional SEM images as well as the EDX line mapping in Figure 3. As apparent from the figure, the titanium line scanning of both mixed matrix membrane shows a uniform and similar distribution pattern which had proven the embedment of TiO₂ NPs in the membrane matrix, indicating that the polymer is homogeneously embedded with the TiO₂ NPs. However, the titanium signal recorded for membrane prepared by 0.001 g/L PC-20 was much more uniform compared to 0.001 g/L P25. Therefore, it can be ruled out that this was caused by higher degree of aggregation of PC-20 during the *in situ* precipitation process, produces membrane with poorer particle size distribution.

Sizes of NPs distributed on the PVDF/TiO₂ mixed matrix membrane surface were measured from the FESEM images using ImageJ 1.43 u software at 10.00 k \times magnification, and the results are presented in Figure 4. Figure 4 shows that different type of commercial TiO₂ nanopowder did play an important role in changing the particle size distribution on the membrane surface. Membranes using P25 as colloidal suspension produced smaller surface particles compared with the systems using PC-20. This phenomenon is probably due to the higher agglomeration tendency of PC-20 compared to P25 which promote particle aggregation during the phase inversion. The increasing deposition of TiO₂ particles on membrane surface will likely provide additional hydrophilicity strength to the membrane, possibly increasing the permeate water flux and its antifouling properties.

Pore Size Distribution

Pore size distributions of the neat and PVDF/TiO₂ mixed-matrix membrane were shown in Figure 5. As can be seen from Figure 5, all the membranes prepared had quite similar pore

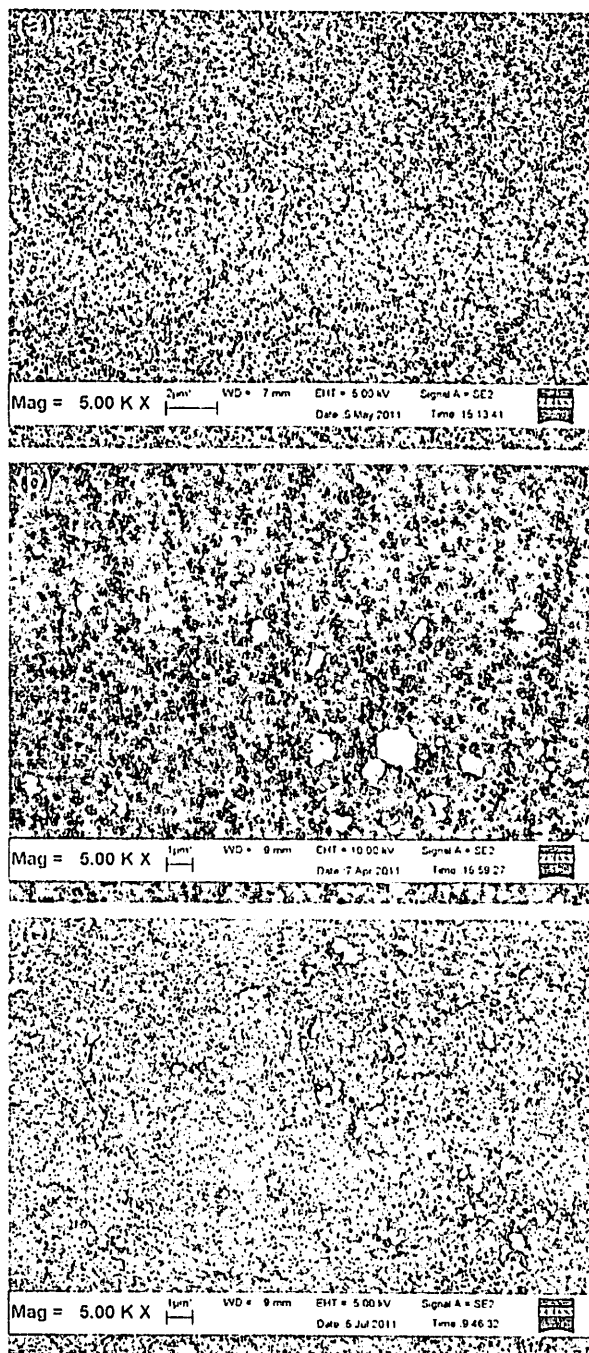


Figure 2. FESEM micrographs reveal detail of topography structure of PVDF/TiO₂ mixed matrix membrane (a) neat (b) 0.001 g/L PC-20 (c) 0.001 g/L P25.

size distribution. The maximum number of pore, $r_{p,max}$ for the neat and mixed-matrix membrane is around 0.05 μm whereas the pore size distribution was slightly wider for mixed-matrix membrane prepared via *in situ* colloidal precipitation method. By adding TiO₂ NPs into the membrane polymeric matrix, it induced the bigger pores; this is probably due to the seeding

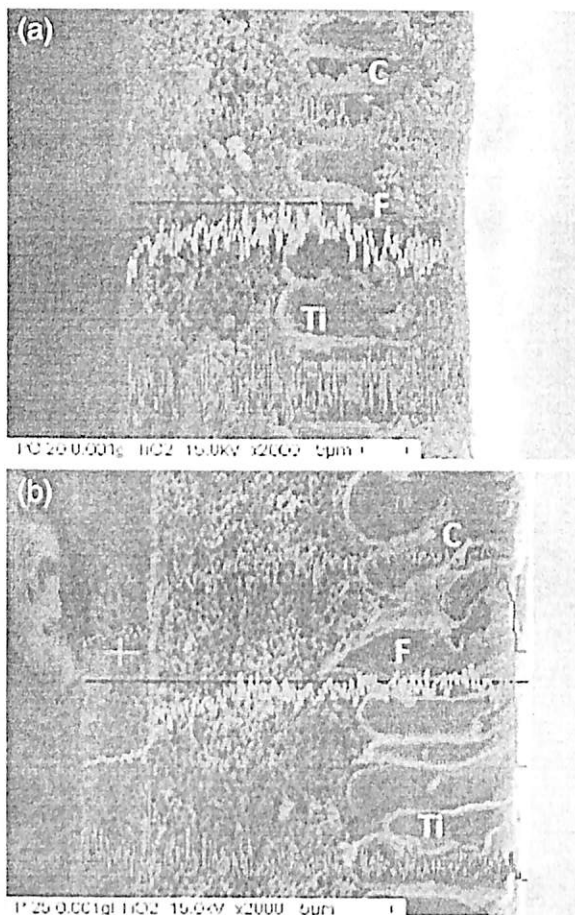


Figure 3. The TiO₂ distribution pattern on PVDF/TiO₂ mixed matrix membrane immersed in (a) 0.001 g/L PC-20 (b) 0.001 g/L P25. [Color figure can be viewed in the online issue, which is available at wileyonlinelibrary.com.]

effect of fine NPs which induced the early vitrification of the polymer. As a result bigger pores were produced. However, the increase of membrane pore size of was not significant indicating that colloidal precipitation method is an ideal method to prepare membrane with minimum changes to its physical properties.

TgA

The TGA analysis of PVDF/TiO₂ mixed matrix membrane with TiO₂ concentration of 0.001 g/L before and after undergoes 6 h of pure water flux filtration process was reported in Figure 6. Neat PVDF membrane is almost fully decomposed when the samples heated up to 850°C in oxygen atmosphere. Thus, titanium was the main component of the residual of PVDF/TiO₂ mixed matrix membranes. According to the TGA results in Figure 6, after thermal decomposition at 850°C, the residual weight percent of titanium particles in membrane prepared before and after 6 h of membrane filtration process for both 0.001 g/L of P25 and PC 20 TiO₂ were almost the same ranging from 3 to 4 wt %. These results indicated that the high stability of TiO₂ NPs on PVDF matrix was obtained due to the hydrogen

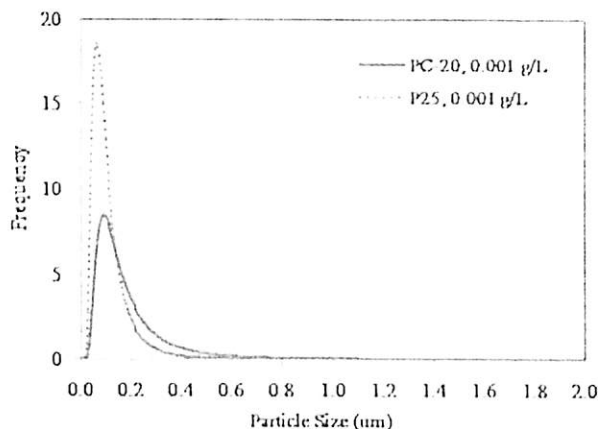


Figure 4. TiO₂ particle size distribution on the PVDF/TiO₂ mixed matrix membrane. [Color figure can be viewed in the online issue, which is available at wileyonlinelibrary.com.]

bonding between fluoride of PVDF and the partially hydroxylised TiO₂ surface.¹⁵

Contact Angle

Surface tensions of membranes were determined by contact angle measurement. Hydrophilicity is the commonly used term in measuring water-solid surface interaction as a result of surface tension equilibrium (Young's Equation). The lower the contact angle, the more hydrophilic membrane will be. Contact angle is governed by the chemical composition as well as geometric structures of the surfaces. It was reported that water contact angle playing an important role in changing the permeation flux and fouling behavior of the membrane.^{16,17}

The contact angles of the neat PVDF membrane and PVDF/TiO₂ mixed-matrix membrane prepared by PC-20 and P25 are shown in Figure 7. As depicted in Figure 7, the contact angle for PVDF membrane was reduced slightly with the incorporation of TiO₂ NPs via *in situ* colloidal precipitation method. This was mainly due to the TiO₂ NPs that were deposited on the PVDF/TiO₂ mixed-matrix membrane consisted of hydroxyl group which increased the membrane hydrophilicity.¹⁸ This phenomenon had also been reported by many researchers, such

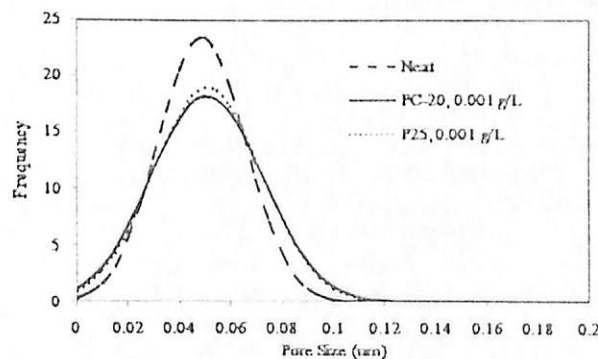


Figure 5. Pore size distribution of the PVDF/TiO₂ mixed-matrix membrane and neat membrane.

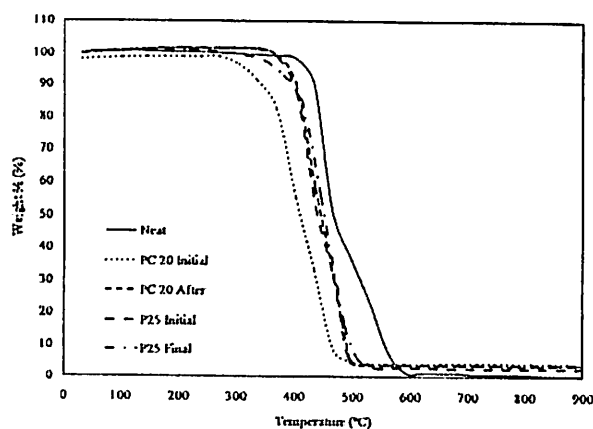


Figure 6. TGA thermograms of neat and PVDF/TiO₂ mixed matrix membrane before and after 6 h of membrane filtration process.

as Bae & Tak (2005) and Rahimpour et al. (2008) who found that the membrane surface contact angle decreased with the increased of entrapped TiO₂ concentration.^{19,20}

In our study, less reduction of contact angle for PVDF/TiO₂ mixed-matrix membrane prepared by P25 compared with PC-20 has been observed, shows that PC-20 is relatively more hydrophilic than P25. Therefore, it was postulated that the hydrophilicity of PC-20 embedment could be relatively more significant compared with P25. This is most likely due to the different degree of crystallinity for each commercial TiO₂ nanopowders. The TiO₂ with anatase crystal structure has been reported by many researchers to have good characteristic in hydrophilicity.

Streaming Potential

Figure 8 shows the zeta potentials of the neat membrane and PVDF/TiO₂ mixed-matrix membrane prepared at pH 7.0 and

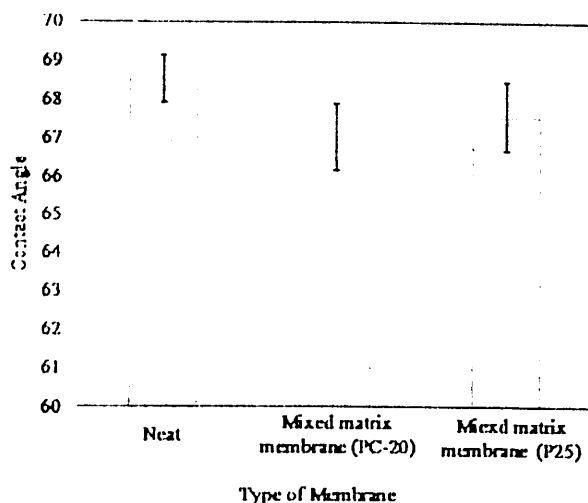
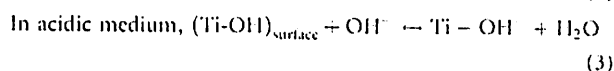
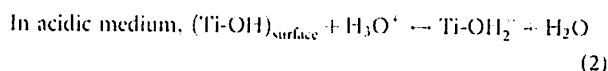


Figure 7. Contact angle of neat PVDF membrane and PVDF/TiO₂ mixed-matrix membranes. [Color figure can be viewed in the online issue, which is available at [wileyonlinelibrary.com](http://www.intelibrary.com).]

under the environment of 10 mM NaCl. The neat membrane and PVDF/TiO₂ mixed-matrix membranes obviously showed different electrokinetic properties at the same pH value. Although both membranes were negatively charged under 10⁻² M NaCl solution environment, the zeta potential of the PVDF/TiO₂ mixed-matrix membrane was having higher value. The apparent zeta potential of the neat membrane and PVDF/TiO₂ mixed-matrix membrane prepared with PC-20 and P25 at concentration of 0.001 g/L were -8.505, -10.43, and -10.30 mV respectively. The negative charge of the neat membrane is due to the presence of dipolar polarization (orientation polarization) effect inherent by PVDF polar molecules on the base polymer and the preferential adsorption of negative chloride ions from the solution.²¹

Generally, the amphoteric behavior of mineral oxides is due to protonation and deprotonation of hydroxyl groups on the material surface.²² The adsorption model of H₂O-TiO₂ in a stream atmosphere has been ascribed by Marrison (1980) who showed that the inequivalent adsorption of H⁺ and OH⁻ on the TiO₂ could takes place with OH⁻ being adsorbed by the titanium cation and H⁺ is adsorbed by the oxygen anion.^{12,23} The adsorption of H⁺ and OH⁻ on the TiO₂ surface might not be equivalent and depends on the pH of the solution,¹² in which the surface net charge density and the surface potential of the membrane could be changed accordingly:



Equation (2) leads to a net positive charge on the surface of TiO₂ NPs due to the adsorbed OH⁻ reacting with the H⁺ in the solution; while eq. (3) leads to the net negative charge of TiO₂ NPs due to the adsorbed H⁺ reacting with the OH⁻ in the solution. The IEP of the TiO₂ NPs was reported to be ~pH

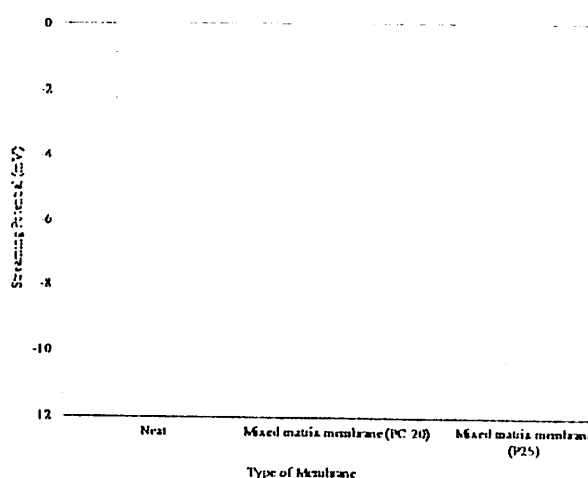


Figure 8. Effect of TiO₂ embedment on streaming potential with 1 mM CaCl₂ solution at pH 7.0. [Color figure can be viewed in the online issue, which is available at [wileyonlinelibrary.com](http://www.intelibrary.com).]

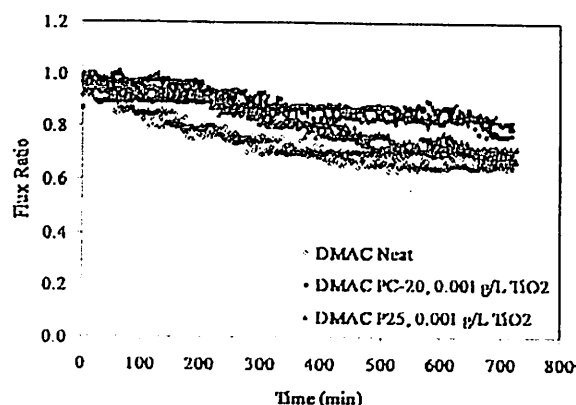


Figure 9. Effect of embedded TiO_2 on membrane fouling process. Operation conditions during the experiment: $[\text{HA}] = 2 \text{ mg/L}$; $[\text{Ca}^{2+}] = 1 \text{ mM}$ (as CaCl_2); pH 7.0; temperature = $25 \pm 1^\circ\text{C}$; crossflow velocity = 4.0 L/h , operating pressure = 0.5 bar .

6.3,²⁴ so for NaCl solution at pH 7.0, which is greater than the IEP, the membrane would be negatively charged. The absolute value of the zeta potential for PVDF/ TiO_2 mixed-matrix membranes is almost constant for both PC-20 and P25/ TiO_2 NPs. This is because, with the same concentration of TiO_2 , the presence of counter-ions or charge density in the diffuse layer is almost the same, and thus results in similar value of streaming potential.

Streaming potential could provide useful information on HA fouling mechanism on membrane surface. Negatively charged TiO_2 particles on membrane surface demonstrate a strong ability to repel HA from its aqueous solution. At pH 7, both HA and TiO_2 particles possess negatively charged surface which creates a strong electrostatic repulsion between HA and surface of TiO_2 . Therefore, no significant absorption of HA on membrane surface was observed. The experimental results of HA absorption by Li et al. agrees with our postulation. According to Li et al., it was clear that the coverage of HA on the TiO_2 catalyst surface is obviously pH-dependent as the TiO_2 particles demonstrated a strong ability to adsorb HA on TiO_2 particles a low pH condition (pH < 3), but at pH 7 onwards, the absorption of HA become very difficult.¹² Therefore, increasing of membrane surface negative charge with the introduction of TiO_2 NPs is able to withstand fouling caused by adsorption.

Effects of TiO_2 Embedment on Membrane Fouling

The common salts, which can be easily found in a variety of wastewaters, including monovalent ions (Na^+ , Cl^-), divalent hardness cations (Ca^{2+} , Mg^{2+}), and divalent anions (SO_4^{2-}).⁸ As reported by Wang et al., in the treatment of water solution containing HA, HA macromolecules was more readily form complexes with monovalent ions and change both humic substances and membrane surface charge which cause more severe fouling.⁸ On the other hand, Srisurichan et al. claimed that at low pH, the dissociation of HA is lower and the available carboxyl functional groups for Ca^{2+} are limited; thus, the complexation decreases. Their results show that the amount of coagulate was highest at pH 7 and decreased with decreasing pH.²⁵ This work

was further proved by Hong and Elimelech⁵ which showed the similar trend. In this work, we carried out the fouling test based on 1 mM CaCl_2 salt and solution pH of 7.

The performance of PVDF/ TiO_2 mixed-matrix membrane on the HA fouling behavior are presented in Figure 9. The initial water fluxes for neat PVDF membrane, PVDF/ TiO_2 mixed-matrix membrane embedded with PC-20 and P25 are 51.55, 53.03, and $53.32 \text{ L/m}^2 \text{ h}$ respectively showing that the mixed matrix membrane are relatively more hydrophilic. The observed flux increased upon integration of TiO_2 NPs can be explained by two possible reasons. During the exchange of TiO_2 NPs into the membrane surface, the PVDF membrane is exposed in the low pH HCl, in which the acid has been found to cause partial hydrolysis on the membrane surface and increase hydrophilicity, and hence increased the permeate water flux.²⁶ The other explanation may involve the water uptake characteristics of TiO_2 particles,²⁷ which are considered to be further contributions to the increase of permeate water flux.

Referring to Figure 9, for PVDF/ TiO_2 mixed-matrix membrane with PC-20, the permeate flux was observed to be greater than PVDF/ TiO_2 mixed-matrix membrane with P25, suggesting that PC-20 is more hydrophilic (higher anatase content) and had therefore promises a better HA fouling mitigation effect. This finding was in line with the work of Cao et al.²⁸ who claimed that, compared with the rutile TiO_2 NPs (average diameter $\sim 30 \text{ nm}$), anatase TiO_2 NPs with a smaller diameter ($\sim 10 \text{ nm}$) are reported to have a better antifouling effect on the membrane prepared.

In addition to hydrophilic characters, PVDF/ TiO_2 mixed-matrix membranes which possessed more negative charge on the top selective layer were also contribute in lowering fouling propensity. With the embedment of TiO_2 NPs into PVDF membrane polymeric matrix, it increased the zeta potential of the membrane surface. Sufficient electrostatic repulsion appears between highly charged PVDF/ TiO_2 mixed-matrix membranes and HA aggregates alleviated the fouling phenomenon.

The fouling behavior is expressed in term of flux reduction based on flux ratio changes over time. One can see that with the presence of CaCl_2 salt in HA solution, neat PVDF membrane caused more severe fouling than PVDF/ TiO_2 mixed-matrix membranes. Membrane fouling could be influenced by hydrodynamic conditions, such as permeation drag and back transport, and chemical interaction between foulants and membranes.²⁹ In order to relate the hydrophilicity with antifouling properties, the membranes were tested under similar hydrodynamic conditions and most important close to similar membrane physical properties. The later property could not be achieved by employing the conventional NPs embedment method but it could be achieved via our proposed surface coagulation method.

The result in Figure 9 clearly reveal the considerable flux decline, with a J/J_0 of 0.65, 0.70, and 0.82 for neat PVDF membrane, PVDF/ TiO_2 mixed-matrix membrane embedded with PC-20 and P25, respectively after 12 h of operation (the end of each curve). These results suggest that the

incorporation of TiO₂ into PVDF membrane had successfully reduced the fouling propensity of the membrane towards HA. The dark brown deposit layer could be obviously observed on the neat membrane surface but to a less extent on the mixed matrix membrane.

The severe fouling of neat PVDF membrane by HA macromolecules occurs because the organic substances are transported to the membrane and accumulated near the membrane surface, which causes an increase in hydraulic resistance.^{5,6,30,31} Since HA contains negatively charged carboxyl groups, divalent cations such as, Ca²⁺ acts like a binding agent between the membrane surface and the negatively charged carboxyl groups of the HA.³² As a result, the electrical repulsion between the membrane surface and the HA molecules was weakened^{5,33} and adsorption occurred.

On the other hand, HA macromolecules appear to be less adsorbed onto the PVDF/TiO₂ mixed-matrix membrane as indicated by the less fouling phenomenon. This finding indicates that the hydrophilicity of PVDF membrane has been improved remarkably with the introduction of TiO₂ NPs on membrane surface via *in situ* colloidal precipitation method. The more hydrophilic of PVDF/TiO₂ mixed-matrix membrane than that the neat PVDF membrane is due to the higher affinity of TiO₂ towards water. Therefore, hydrophobic adsorption between HA macromolecules and PVDF/TiO₂ mixed-matrix membrane was reduced. Water molecules were attracted into the membrane matrix, forming a shielding layer to prevent fouling. These results are in consistent with other researcher findings^{19,34,35,36} who observed that the modified membrane with addition of TiO₂ showed higher flux for sludge filtration than neat polymeric membrane.

CONCLUSIONS

The effect of TiO₂ embedment into PVDF membrane polymeric matrix has been investigated for HA fouling phenomenon. The contact angle for PVDF membrane was slightly reduced and the surface zeta potential was increased with the incorporation of TiO₂ NPs. The results demonstrated that the PVDF/TiO₂ mixed-matrix membrane could be less prone to HA deposition as it exhibited a higher degree of hydrophilicity compared with neat PVDF membrane with the flux ratio for neat PVDF membrane, PVDF/TiO₂ mixed-matrix membrane embedded with PC-20 and P25 are 0.65, 0.70, and 0.82, respectively. PC-20 showed better antifouling properties compared to P25 due to its higher anatase polymorph. These properties render the membrane and HA with sufficient electrostatic repulsion and therefore enhanced the fouling mitigation. The effect of TiO₂ NPs on membrane antifouling could be realized only if the membranes were compared with the same basis (hydrodynamic and physical properties) which can be realized using the proposed colloidal precipitation method.

ACKNOWLEDGMENTS

The authors wish to thank the sponsors of this project for their financial supports, namely Universiti Sains Malaysia (USM) Research University Grant (1001/PJKIMIA/811172), Malaysia

Toray Science Foundation (MTSF) Science and Technology Research Grant (304/PJKIMIA/6050179/M126), MOSTI e-Sciencefund (305/PJKIMIA/6013604) and USM Membrane Cluster.

REFERENCES

- Kimura, K.; Hane, Y.; Watanabe, Y.; Amy, G.; Ohkuma, N. *Water Res.* 2004, 38 (14–15), 3431.
- Yamamura, H.; Chae, S.; Kimura, K.; Watanabe, Y. *Water Res.* 2007, 41, 3812.
- Nyström, M.; Rouhomäki, K.; Kaipia, L. *Desalination* 1996, 106, 79.
- Wei, Y.; Zydney, A. L. *J. Membr. Sci.* 1999, 157, 1.
- Hong, S. K.; Elimelech, M. *J. Membr. Sci.* 1997, 132, 159.
- Braghetta, A.; DiGiano, F. A.; Ball, W. P. *J. Environ. Eng. ASCE* 1998, 124, 1087.
- Kabsch-Korbutowicz, M.; Majewska-Nowak, K.; Winnicki, T. *Desalination* 1999, 126, 179.
- Wang, Z.; Zhao, Y.; Wang, J.; Wang, S. *Desalination* 2005, 178, 171.
- Lee, N.; Amy, G.; Crouse, J.; Buisson, H. *Water Res.* 2004, 38, 4511.
- Lee, E. K.; Chen, V.; Fane, A. G. *Desalination* 2008, 218, 257.
- Li, J. B.; Zhu, J. W.; Zheng, M. S. *J. Appl. Polym. Sci.* 2007, 103, 3623.
- Li, X. Z.; Fan, C. M.; Sun, Y. P. *Chemosphere* 2002, 48, 453.
- Cho, J. W.; Amy, G.; Pellegrino, J. *J. Membr. Sci.* 2000, 164, 89.
- Kvak, S. Y.; Kim, S. H.; Kim, S. S. *Environ. Sci. Technol.* 2001, 35, 2388.
- Teow, Y. H.; Ahmad, A. L.; Lim, J. K.; Ooi, B. S. *Desalination* 2012, 295, 61.
- Gau, H.; Herminghaus, S.; Lenz, P.; Lipowsky, R. *Science* 1999, 283, 46.
- Li, M.; Zhai, J.; Liu, H.; Song, Y.; Jiang, L.; Zhu, D. *J. Phys. Chem. B* 2003, 107, 9954.
- Yuliwati, Y.; Ismail, A. F. *Desalination* 2010, 273, 226.
- Bac, T. H.; Tak, T. M. *J. Membr. Sci.* 2005, 266, 1.
- Rahimpour, A.; Madaeni, S. S.; Taheri, A. H.; Mansourpanah, Y. *J. Membr. Sci.* 2008, 313, 158.
- Burns, D. B.; Zydney, A. L. *J. Membr. Sci.* 2000, 172(1–2), 39.
- Regazzoni, A. E.; Blesa, M. A.; Maroto, A. J. G. *J. Colloid Interf. Sci.* 1983, 91, 560.
- Marrison, S. R. In *Electrochemistry at Semiconductor and Oxidation Metal Electrodes*; Plenum Press, New York, 1980.
- O'Shea, K. E.; Cardona, C. *J. Photoch. Photobio. A* 1995, 91, 67.
- Srisurichan, S.; Jiratananon, R.; Jane, A. G. *Desalination* 2005, 174, 63.



26. Kulkarni, A.; Mukherjee, D.; Gill, W. N. *J. Membr. Sci.* 1996, 114, 39.
27. Khare, S. Presented at International Conference on Polymer Characteristics (POLYCHAR-8). University of North Texas, Denton, TX. 2000, 11-14.
28. Cao, X.; Ma, J.; Shi, X.; Ren, Z. *Appl. Surf. Sci.* 2006, 253, 2003.
29. Maximous, N.; Nakhla, G.; Wan, W. *J. Membr. Sci.* 2009, 339 (1-2), 93.
30. Wei, W.; Zydney, A. L. *Environ. Sci. Technol.* 2000, 34, 5043.
31. Cho, J. W.; Amy, G.; Pellegrino, J. *Water Res.* 1999, 33, 2517.
32. Jucker, C.; Clark, M. M. *J. Membr. Sci.* 1994, 97, 37.
33. Schäfer, A. I. Natural Organics Removal Using Membranes, PhD Thesis, University of New South Wales, 1999.
34. Bae, T. H.; Kim, I. C.; Tak, T. M. *J. Membr. Sci.* 2006, 275, 1.
35. Kim, S. H.; Kwak, S. Y.; Sohn, B. H.; Park, T. H. *J. Membr. Sci.* 2003, 211, 157.
36. Li, Y. Y.; Shen, H. M.; Xu, Z. L. *J. Appl. Polym. Sci.* 2009, 113, 1763.

Mixed-Matrix Membrane for Humic Acid Removal: Influence of Different Types of TiO₂ on Membrane Morphology and Performance

Y. H. Teow, B. S. Ooi, A. L. Ahmad, and J. K. Lim

Abstract—Different types of titanium dioxide (TiO₂) nanoparticles (NPs) (PC-20, P25 and X500), with various particle sizes in coagulation bath were incorporated as a nanofiller into membrane matrix. The NPs were added to the polyvinylidene fluoride (PVDF) ultrafiltration (UF) membranes via phase inversion and colloidal precipitation method. A series of test, such as surface field emission scanning electron microscopy (FESEM) images, energy-dispersive X-ray spectroscopy (EDX) mapping and pore size measurement were performed to characterize the modified mixed-matrix membranes. FESEM was applied to observe the distribution pattern of TiO₂ NPs in the membrane matrix and its distribution was examined using (EDX). The size and distribution of TiO₂ NPs on the membrane surface was affected to a very great extent by the size of TiO₂ prepared in the coagulation bath. Conversely, the presence of TiO₂ on membrane surface does not provide any significant changes on the membrane pore size distribution, suggesting that in situ precipitation method is suitable to prepare mixed-matrix membrane without scarifying the membrane rejection ability. The performance of the UF membranes fabricated from the nano-sized TiO₂ particles were evaluated by measuring the membrane permeates flux and humic acid (HA) rejection. The experiment demonstrated that the flux improvements of the membranes were improved due to the pore enlargement (defect) as well as increasing membrane hydrophilicity. The flux of the mixed-matrix membrane prepared by adding X500 nanofiller was the greatest (44.06 L/m²·h), which was determine as the optimum TiO₂ type without scarified the membrane rejection (98.44%) compared to PC-20 and P25. This is due to the relatively small size of X500 which provides better dispersibility in the membrane matrix whereby flux was enhanced due to improve of hydrophilicity without the expense of poor humic acid rejection.

Index Terms—Hydrophilicity, colloidal precipitation method, mixed-matrix membrane, ultrafiltration

1. INTRODUCTION

Attributed to its unique large surface-to-volume ratio and strong reactivity properties, nano-sized colloidal particles have extended their advance applications into membrane technologies for two major purposes. One of the purposes is to produce membrane with desirable structure due to the

particles interaction with polymer chains and/or solvent during membrane preparation [1]. The other aim is to improve the synergetic effects on water and wastewater treatment due to improved hydrophilic properties [2], [3]. These structural modifications have been proven and reported by many researcher such as Li *et al.* (2007), Kim *et al.* (2003), Kim and Bruggen (2010) and Razjou *et al.* (2011) that favor a higher selectivity and permeability in water separation and satisfactory performance in ultrafiltration (UF) and nanofiltration (NF) membranes [4]-[7].

Among metal oxide nanoparticles (NPs), titanium dioxide (TiO₂) with photocatalytic and desirable hydrophilic properties emerges as a highly promising candidate to be incorporated into polymeric matrix [8], [9]. In recent years, TiO₂ nano-inorganic mixed matrix membranes have attracted great research interests to provide a solution to the trade-off problem faced by the polymeric membranes in water separation [10]-[12] and to improve the membrane performance by increasing hydrophilicity [4], [5], [13], [14]. Two common technical innovations in mixed matrix membranes production have been carried out: assembling NPs on the surface of the porous membranes [5], [13], [15], [16] or blending NPs into the polymeric casting solution [5], [16]-[19]. However, the high surface energy of TiO₂ NPs added in the casting solution often results in poor NPs distribution in the membrane matrix through entrapment of TiO₂ NPs in a polymer matrix of membrane. The poor distribution is due to the poor mixing or shearing of the polymer solution as well as low stability of the colloid; leading to low functional surface area, which is a conspicuous drawback for application. Therefore, for feasible application, the preparation of size-controlled, monodispersed NPs is of primary importance.

In the present work, mixed-matrix polyvinylidene fluoride (PVDF/TiO₂) membrane was prepared via in situ colloidal precipitation method. Mechanical and chemical approaches were applied for TiO₂ modification to increase homogeneity in dispersion, reduce agglomeration, improve stability of TiO₂ NPs and enhance the nanofiller-polymer interaction. The aim of the current work is to investigate the effect of sizes and types of TiO₂ NPs on the membrane hydrophilicity enhancement and structure of the TiO₂ embedded PVDF UF membrane prepared by in situ colloidal precipitation method. Three different sizes (from 8 nm to 21 nm) and types (PC-20, P25 and X500) of TiO₂ NPs were used. The influence of dispersing TiO₂ NPs on membrane properties was examined based on surface morphology, membrane permeability and humic acid (HA) rejection.

Manuscript received September 14, 2012; revised November 22, 2012. This work was supported in part by the Universiti Sains Malaysia (USM) Research University Grant (1001/PJK/MIA/811172), MOSTI eScience-Fund (305/PJK/MIA/6013604) and USM Membrane Science and Technology Cluster.

The authors are with the School of Chemical Engineering, Universiti Sains Malaysia, Penang, Malaysia (e-mail: yentham@hotmail.com, chobso@eng.usm.my, chlanf@eng.usm.my, chjtkang@eng.usm.my).

II. MATERIALS AND METHODS

A. Materials

Polyvinylidene fluoride (PVDF) (FA6010.1001, Solvay Plastics, Inc., USA) ultrafiltration flat sheet membranes were fabricated by casting the PVDF in *N,N*-dimethylacetamide, DMAc (Merck, Germany) (Assay (GC, area %) \geq 99%) solution at 200 μm thickness. Three different types of commercial titanium dioxide, TiO_2 nanopowder were purchased from TitanPE Technologies, Inc., China (trade name: PC-20 and X500) and Sigma-Aldrich, St. Louis, MO, USA (trade name: P25). The characteristics of these nanoparticles (NPs) are presented in Table I. Synthetic HA with molecular weight mainly ranging from 20,000 to 50,000 was obtained from Sigma-Aldrich and used as the organic foulant during the experiment without further purification. Sodium hydroxide, NaOH solution was used to improve the dissolution of HA in water. For permeation test, feed solutions were prepared by dissolving a pre-weighed 20 mg of HA powder in 1L of distilled water under vigorous stirring and the solution pH was adjusted to pH 10 by addition of a small quantity of 0.1 M NaOH.

TABLE I. CHARACTERISTICS OF THE USED TiO_2 NANOPOWDER

TiO_2 Samples	Crystalline phase	Average crystalline size (nm)	Average size in suspension (nm)
PC-20	75% Anatase	20	461.3
	25% Rutile		
P25	80% Anatase	21	200
	20% Rutile		
X500	Anatase	< 8	38

B. Preparation of Stable TiO_2 Suspension

Chemical and mechanical methods were carried out to enhance the TiO_2 colloidal stability in the coagulation bath as described below.

Chemical method. Firstly, in order to increase the stability of the TiO_2 NPs in distilled water, the chemical modification of the original TiO_2 nanopowder was carried out by adjusting the pH value of the TiO_2 suspension. Hydrochloride acid solution (HCl) was added drop-wise and mechanically stirred until it reaches an equilibrium of pH 4.0 to achieve electrostatic stability (zeta potential $> +30\text{mV}$). The pH value of the TiO_2 suspensions was measured using a pH meter (Eutech Instruments).

Mechanical method. The TiO_2 cluster was further broken down by subjecting the TiO_2 solution to 15 min ultrasonic irradiation using Telsonic ultrasonic horn (SG-24-500P, Telsonic Ultrasonics). Frequency of the ultrasound was kept constant at 18.4 kHz.

C. Membrane Formation and in Situ Particle Embedment

The membrane casting solutions were prepared by dissolving pre-dried PVDF (24 h of oven drying at 70 °C) using the polymer solvents; DMAc in a 200 mL beaker. Composition of the PVDF/DMAc was kept constant at 18:82 in weight percentage.

In order to obtain complete dissolution and optimal dispersion of the polymer solution, the mixture was subjected to an initial constant stirring of 250 rpm at 65 °C for 4 hours to form a homogenous solution. The homogenous membrane

polymer solution was then left overnight under stirring at 40 °C. The trapped air bubbles were removed by standing the solution overnight. Solvent loss by evaporation was negligible due to the high boiling point of DMAc (163-166 °C).

The polymer solution was cast using a thin film applicator (Elcometer 4340, Elcometer (Asia) Pte. Ltd.) on a flat glass plate wrapped with non-woven polyester fabric (Holleytex 3329, Ahlstrom) to form a solution layer at nominal thickness of 200 μm . The polyester fabric acts as membrane support layer, providing mechanical strength to the membrane for pressure resistance. The nascent membrane on the glass plate was then solidified by immediate immersion into a coagulation bath at room temperature (26 °C) to avoid excessive surface evaporation. The immersion was left for a day to ensure complete solidification and removal of residual solvent from the membranes. The fabricated membrane was then recovered from the coagulation bath after detaching it from the glass plate and subsequently rinsed with and soaked in a bath of fresh distilled water. Drying was sequentially done after dipping the membrane in ethanol to avoid microbial growth.

In order to introduce TiO_2 NPs onto the membrane surface, PVDF solution layers were immersed into the coagulation bath with 0.1 g/L of TiO_2 colloidal suspension as prepared by using the method stated in Section II B. Since the membrane surface solidification and NPs embedment occur simultaneously, this NPs incorporation method is an *in situ* approach to embed NPs onto the membrane surface.

D. Membrane Characterization

In order to probe the top surfaces morphology and examine the composition of the PVDF/ TiO_2 mixed-matrix membranes, field emission scanning electron microscope (FESEM) and energy dispersive X-ray (EDX) were performed using a SUPRA 35 VP, Carl Zeiss Inc. The membrane samples were cut into an appropriate size and mounted on the sample holders. K 550 sputter coater was used to coat the outer surface of the membrane sample with a thin layer of gold under vacuum to provide electrical conductivity. After gold sputtering, the samples were examined under the electron microscope at a 10.0 kV potentials.

The membranes pore size was determined using gas flow/liquid displacement method via Capillary Flow Porometer Porolux 1000 (Benelux Scientific, Germany). Membrane samples with a 10mm diameter were characterized using the "dry up-wet up" method. In this method, gas flow was measured as a function of transmembrane pressure, initially through wetting of membrane with 1, 1, 2, 3, 3-hexafluoropropene followed by dry flow of gas through the membrane. The pore size distribution was estimated using PMI software (Benelux Scientific, Germany).

E. Permeation Flux and Rejection of Membranes

A laboratory bench scale cross-flow recirculation unit was used to study permeation flux and rejection of the mixed-matrix membrane using 20 mg/L HA as model solution at ambient temperature (25 °C). The produced flat sheet membrane was cut into the disc shape and laid on top of

the membrane holder in a designed stainless steel circular membrane test cell with a diameter of 5.1 cm (effective membrane filtration area of 20.43 cm²) and sealed with a rubber O-ring. Synthetic HA solution was charged into a 5L feed tank and re-circulated at a constant cross-flow rate of 0.04 L/min using the peristaltic pump (Hydra-Cell, Wanner International). Filtration pressure was controlled by a needle valve to 0.5 bar. Absorbance of the collected permeates was measured using UV spectrophotometer (UV mini-1240, Shimadzu) at wavelength of 254 nm.

Pure water flux was determined by direct measurement of the permeate volume over time,

$$F = \frac{V}{At} \quad (1)$$

where F is the pure water flux (L/m²·h), V is the permeate volume (L), A is the membrane effective surface area (m²), and t is the permeation time (h).

Experimental rejection of solute (R) was calculated from the feed solution (HA solution) and permeate solution using the following equation:

$$R(\%) = \left(1 - \frac{C_p}{C_f}\right) \times 100\% \quad (2)$$

where R is the rejection ultrafiltration process (%), C_p is the concentration of the permeate solution and C_f is the concentration of the feed solution.

III. RESULTS AND DISCUSSIONS

A. Morphologies of PVDF/TiO₂ Mixed-Matrix Membrane

Fig. 1(a) shows the SEM top surface images of PVDF/TiO₂ mixed-matrix membranes immersed in colloidal suspension of different TiO₂ type at concentration of 0.1 g/L. As could be seen from the Fig. 1(a) with 5,00 k \times of magnification, connected pores appeared on the surface of all PVDF membrane using DMAc as solvent.

The presence of TiO₂ Nps in the membrane structure was further confirmed by energy-dispersive X-ray spectrometer (EDX) mapping. Sizes of TiO₂ NPs distributed on the PVDF/TiO₂ mixed-matrix membrane were observed and the results are presented in Fig. 1(b). It could be clearly seen that membrane using X500 (which is the smallest size TiO₂) as hydrophilic filler was able to disperse uniformly into the membrane matrix compared to the membrane prepared by PC-20 and P25. The lesser degree of TiO₂ clustering for membrane prepared using X500 is probably due to the higher thermodynamic stability of X500 in coagulation bath system when it was brought into contact with the solvent and polymer which agrees well with the theory proposed by Mackay et al. [20]. Mackay et al. found that the dispersion of NPs into a polymeric liquid is thermodynamically stable for systems where the radius of gyration (R_g) of the linear polymer is greater than the radius of the NPs (R_p) [20]. In this case, different TiO₂ most likely affect the thermodynamic stability of the system. The relation between the root-mean

square radius of gyration of the chain in DMAc and the molecular weight obtained by Ali and Raina [21] using the theory of Inagaki et al. [22], was $\sqrt{S^2} = 2.95 \times 10^{-4} M_w^{0.57}$. R_g/R_p ratio for PC-20, P25 and X500 are 1:14, 1:6 and 1:1 respectively. X500 which contributes to greater R_g/R_p ratio compared to PC-20 and P25 has better thermodynamic stability. This result is consistent with Bagchi [23] who found that when particles exhibit robust stabilization, such as repelling each other sterically and providing thermodynamic stability, the particles do not cluster. So, it is not surprising to observe that PC-20 and P25 with much bigger average particle sizes (5-12 times bigger than X500) in water suspension induced an aggregate of TiO₂ particles adsorbing or embedding on the surface of PVDF/TiO₂ mixed-matrix membranes during the phase inversion. For mixed-matrix membranes prepared from PC-20 and P25, the tendency to promote the particle clustering gave a relative poor particle size distribution whereby the TiO₂ particles deposited on the surface exist in different sizes of snowflakes. TiO₂ cluster blocked the pores therefore decreasing the microporosity of the PVDF membranes. In general, the type of TiO₂ has a profound effect on the distributions of TiO₂ but it has very slight effect on the membrane structure.

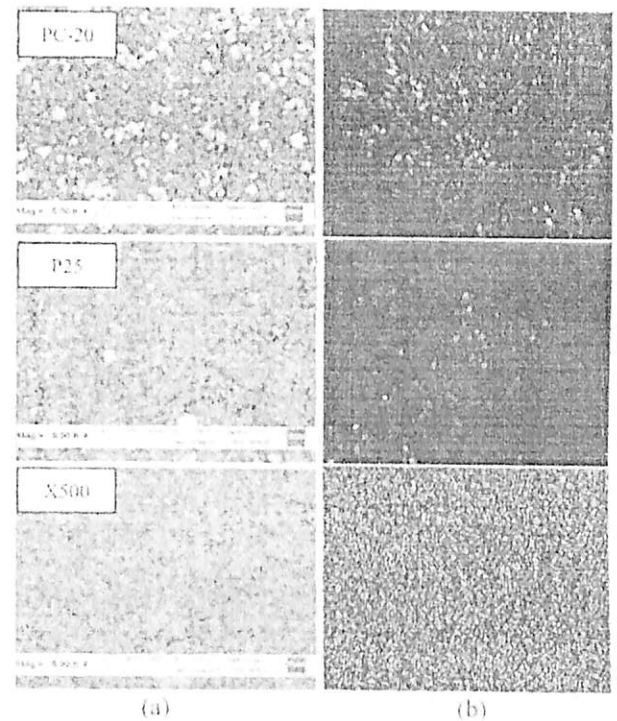


Fig. 1. The surface (a) FFESEM micrographs and (b) EDX mapping of PVDF/TiO₂ mixed-matrix membrane

B. Pore Size Distribution

Pore size distributions of the neat and PVDF/TiO₂ mixed-matrix membrane were shown in Fig. 2. As can be seen from Fig. 2, all the membranes prepared had quite similar pore size distributions. The maximum diameter of pore, $d_{p,max}$ for the neat membrane was around 0.05 μ m while for membrane prepared using PC-20, P25 and X500 were around 0.042 μ m, 0.061 μ m and 0.028 μ m, respectively.

Result showed that the addition of P25 into the membrane polymeric matrix enlarged the pores slightly. The pore

enlargement is probably due to increase of the stress between polymer and TiO_2 Nps, resulted from the organic shrinkage that occurred during the precipitation process of wet-casting polymeric membranes. On the other hand, for membranes prepared using PC-20 and X500 as hydrophilic filler, it has a tendency to reduce its pore size. For X500, due to its smaller NPs size, it provides the seeding effect which induced the early vitrification of the polymer [24]. Followed by solidification, smaller pore size on the surface was observed. Nonetheless, it could not be denied that pore narrowing of mixed-matrix membrane prepared by X500 occurred too. Due to the relatively small particle size of X500, pore blocking is likely to happen. On the other hand, membrane prepared by PC-20 shows stringer evidence of pore blocking due to the precipitation of NPs on the pore wall which further reduced the pore size. These results were similar with what was observed by Damodar *et al.* who found that the number of small-sized pores increase with increasing TiO_2 content [25].

In overall, the changes of membrane pore size were not significant as compared to its particle size distribution using colloidal precipitation method. This indicated that colloidal precipitation method is an ideal method to prepare membrane with minimum changes to its physical properties.

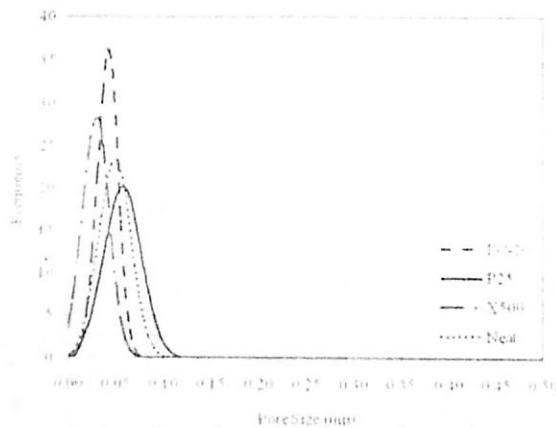


Fig. 2. Pore size distribution of the PVDF/ TiO_2 mixed matrix membrane and neat membrane

C. Permeation Flux and Rejection of Membranes

The effect of different types of TiO_2 on mixed-matrix membrane permeability flux and rejection of HA were investigated through cross-flow membrane filtration experiments. The membrane performances were summarized in Table 2. All the presented membrane permeability and rejection of HA results were obtained using the average of three replications with the membrane tested which was randomly chosen from different independent sheets.

The effect of membrane morphology and hydrophilization on PVDF/ TiO_2 mixed-matrix membranes can be evaluated by the performance of HA solution flux (F). Comparing HA permeation of the neat PVDF membrane and the PVDF/ TiO_2 mixed-matrix membrane using PC-20, P25 and X500 as hydrophilic filler, which were labeled as M1, M2, M3 and M4 respectively, the PVDF/ TiO_2 mixed-matrix membrane always have higher fluxes in comparison with the neat membrane. This result coincides with experimental results by

Luo *et al.*, (2005) which demonstrated that the flux and retention of the TiO_2 composite membrane increased greatly from $70.2 \text{ L/m}^2 \text{ h}$ to $102.9 \text{ L/m}^2 \text{ h}$ and from 21.9% to 34.5% respectively as compared to the neat UF poly(ether sulfone), PES membrane for polyethylene glycol-5000 separation [12]. Additionally, according to Bae *et al.* (2006), it was clear that the initial sharp drop of flux observed for PES polymeric membrane during MBR sludge filtration was alleviated by TiO_2 immobilization whereby the TiO_2 nanocomposite membrane maintained a higher stabilized relative flux (36% of the initial flux) than that of the PES membrane (20% of the initial flux) [26].

It was proposed that the enhanced permeability of mixed-matrix membranes was due to the increasing porosity of the membrane that was resulted from the reduced polymer chain packing by the nanofillers [27],[28]. Table 2 demonstrated that X500 with the best particle distribution contribute to the most excellent result in increasing membrane permeability compared to the other membrane. The flux increased dramatically from $34.97 \text{ L/m}^2 \text{ h}$ to $45.36 \text{ L/m}^2 \text{ h}$ with improved HA rejection. These improvements are due to the pore narrowing as well as improved hydrophilicity of the membrane as suggested previously. A homogeneous particle dispersion offers a larger surface area of NPs which leads to adsorption of more water molecules that are located on the surface of the membrane [29]. On the other hand, the permeability of PC-20 and P25 membranes increased with the compensation of decreasing rejection capability. This phenomenon can be explained by considering the aggregation of PC-20 and P25 in water suspension which blocks the membrane pores. However, this phenomenon deviates from work reported by Shawky *et al.* (2011) in which the incorporation of multi-wall carbon nanotube (MWCNT) into the 10% aromatic polyamide (PA) nanocomposite membrane had increased the HA removal by 54 to 90% with a small sacrifice in the permeate flux, mainly due to the structural compactness of the composite membranes resulted from the strong interaction between MWCNTs and PA matrix which suggests a network structure [30]. The poor thermodynamic stability between the NPs and the polymer enabled the removal of NPs from the surface and resulted in the defect of the membrane structure. This result was proven by the increased flux but reduced rejection capability phenomenon. Additionally, the membrane permeability for the membrane using PC-20 and P25 was slightly decreased compared to the membrane using X500. This phenomenon can be explained by the high aggregation tendency of PC-20 and P25 which reduces the effective surface of NPs and therefore, declines the hydroxyl groups on the surface of mixed-matrix membranes. These results are in good agreement with previous reported works [26],[31].

The observed flux increase (improved hydrophilicity) upon integration of TiO_2 NPs can be explained as such; the PVDF/ TiO_2 mixed-matrix membrane is more hydrophilic than the neat PVDF membrane due to the higher affinity of TiO_2 towards water had reduced the hydrophobic adsorption between HA particle and PVDF/ TiO_2 mixed-matrix membrane. Therefore, water molecules are attracted into the membrane matrix and promoted to pass through the membrane, thus enhancing the membrane flux. These results

flux and rejection (36% for sulfone). It is clear that the flux of neat polymeric membrane is elevated by the composite membrane (36% to 45.36% of the neat polymeric membrane).

Table 2 shows the distribution of TiO₂ NPs on membrane surface. The results of rejection of HA by membrane of P25 and X500 are consistent with those by other researchers [32]-[34] who found that the modified membrane with addition of TiO₂ showed higher flux for sludge filtration than neat polymeric membrane. As a result, fouling-resistant property can also be improved by this method as the hydrophilic membrane will be covered with a layer of water.

TABLE II THE EFFECT OF TiO₂ TYPE ON PERMEATE FLUX AND HUMIC ACID REJECTION

Membrane samples	Membrane number	Permeate flux (L/m ² h)	Rejection (%)
Neat	M1	34.97±2.25	98.20±0.13
PC-20	M2	39.70±4.74	98.06±0.55
P25	M3	38.81±0.58	97.77±0.43
X500	M4	45.36±1.47	98.67±0.14

IV. CONCLUSION

Stable TiO₂ colloids in coagulation bath were successfully embedded to the membrane matrix through phase inversion and colloidal precipitation method. It was found that the membrane prepared with DMAc as solvent and immersed in coagulation bath with 0.1 g/L X500 has relatively well distributed, regular and smaller TiO₂ NPs on membrane surface. The particle size distribution is mainly contributed by the colloidal stability of X500 in the polymer matrix. Membrane prepared using PC-20 and P25 have slightly bigger particle size which provides poor binding force to the membrane matrix.

The PVDF-TiO₂ mixed-matrix membranes had similar structure to the neat PVDF membrane. However, permeation tests with HA solution proved that permeability of the mixed-matrix membrane was significantly improved due to its bigger pore size (defect) as well as enhanced hydrophilicity. By adding 0.1 g/L X500 into the coagulation bath, the membrane performance (flux and rejection) improved dramatically which could be attributed to the narrow pore size and increased hydrophilicity of the membrane. Membrane prepared using X500 is the best membrane which gives 45.36 L/m²·hr of flux and rejection as high as 98.67% of HA. However, for membranes prepared using PC-20 and P25, the poor HA rejection was compensated by the flux increment due to the nonuniformity of the particle distribution which created defects on the membrane surface.

Although, the membrane prepared using X500 as hydrophilic filler presented a good result on particle size distribution with flux enhancement, further research on long hours HA filtration test has to be carried out in the future to test on the chemical stability of TiO₂ dispersed in PVDF matrix and its antifouling (self-cleaning) properties under UV light irradiation.

ACKNOWLEDGMENT

The authors wish to thank the sponsors of this project for their financial supports, namely Universiti Sains Malaysia (USM) Research University Grant (1001/PJKIMIA/811172), MOSTI Science Fund (305/PJKIMIA/6013604), USM Fellowship and USM Membrane Science and Technology Cluster.

REFERENCES

- [1] V. Vatanpour, S. S. Madaeni, A. R. Khataee, F. Salehi, S. Zinadini, and H. A. Mofakher, "TiO₂ embedded mixed matrix PES nanocomposite membranes: Influence of different sizes and types of nanoparticles on antifouling and performance," *Desalination*, vol. 292, pp. 19-29, April 2012.
- [2] P. He and A. C. Zhao, "Nanometer composite technology and application in polymer modification," *Macromolecular Theory*, vol. 2, pp. 74-82, 2001.
- [3] Z. P. Lang, Y. Z. Xu, and C. W. Xu, "Modification mechanisms of nanoparticles on polymers," *J. Mater. Sci. Eng.*, vol. 31, no. 3, pp. 279-282, 2003.
- [4] J. B. Li, J. W. Zhu, and M. S. Zheng, "Morphologies and properties of poly (phthalazone ether sulfone ketone) matrix ultrafiltration membranes with entrapped TiO₂ nanoparticles," *J. Appl. Polym. Sci.*, vol. 103, no. 6, pp. 3623-3629, March 2007.
- [5] S. H. Kim, S. Y. Kwak, B. H. Sohn, and I. H. Park, "Design of TiO₂ nanoparticle self-assembled aromatic polyamide thin-film-composite (TFAC) membrane as a approach to solve fouling problem," *J. Membr. Sci.*, vol. 211, no. 1, pp. 137-165, January 2003.
- [6] J. Kim and B. V. D. Bruggen, "The use of nanoparticles in polymeric and ceramic membrane structures: Review of manufacturing procedures and performance improvement for water treatment," *Environ. Pollut.*, vol. 138, no. 7, pp. 2338-2349, July 2010.
- [7] A. Razoufi, J. Mamiouni, and V. Chen, "The effects of mechanical and chemical modification of TiO₂ nanoparticles on the surface chemistry, structure and fouling performance of PS ultrafiltration membranes," *J. Membr. Sci.*, vol. 378, no. 1-2, pp. 73-84, Aug 2011.
- [8] Y. C. Lee, Y. P. Hong, H. Y. Lee, H. Lim, Y. J. Jung, K. H. Ho, H. S. Jung, and K. S. Hong, "Photocatalysis and hydrophilicity of deposited TiO₂ thin films," *J. Colloid Interface Sci.*, vol. 267, no. 1, pp. 127-133, November 2003.
- [9] F. Peng, J. Lu, H. Guo, Y. Wang, J. Guo, and Z. Jiang, "Hybrid organic-inorganic membrane: Solving the trade-off between permeability and selectivity," *Chem. Mater.*, vol. 17, no. 26, pp. 6790-6796, November 2005.
- [10] H. Gong, M. Radosz, B. F. Towler, and Y. Shen, "Polymer-inorganic nanocomposite membranes for gas separation," *Sep. Purif. Technol.*, vol. 55, no. 3, pp. 291-291, July 2007.
- [11] T. S. Chang, L. Y. Jiang, Y. Li, and S. Kulprathiporn, "Mixed matrix membranes (MMMs) comprising organic polymers with dispersed inorganic fillers for gas separation," *Prog. Polym. Sci.*, vol. 32, no. 4, pp. 483-507, April 2007.
- [12] M. L. Luo, J. Q. Zhao, W. Tang, and C. S. Pei, "Hydrophilic modification of poly (ether sulfone) ultrafiltration membrane surface by self-assembly of TiO₂ nanoparticles," *Appl. Surf. Sci.*, vol. 249, no. 1-4, pp. 78-84, 2005.
- [13] Y. C. Lee, J. Ma, K. Shi, and Z. Ren, "Effect of TiO₂ nanoparticle size on the performance of PVDF membrane," *Appl. Surf. Sci.*, vol. 253, no. 4, pp. 2603-2610, December 2009.
- [14] S. Madaeni, S. Zinadini, and V. Vatanpour, "A new approach to improve antifouling property of PVDF membrane using in situ polymerization of PAA functionalized TiO₂ nanoparticles," *J. Membr. Sci.*, vol. 380, no. 1-2, pp. 155-162, September 2011.
- [15] S. Y. Kwak and S. H. Kim, "Hybrid organic-inorganic reverse osmosis (RO) membrane for bacterial antifouling: I. Preparation and characterization of TiO₂ nanoparticle self-assembled aromatic polyamide thin-film composite (TFAC) membrane," *Environ. Sci. Technol.*, vol. 35, no. 11, pp. 2385-2394, June 2001.
- [16] J. B. Li, Z. F. Xu, H. Yang, J. Y. Yu, and M. Lu, "Effect of TiO₂ nanoparticles on the surface morphology and performance of microporous PES membrane," *Appl. Surf. Sci.*, vol. 255, no. 9, pp. 4725-4732, February 2009.
- [17] M. A. Attale, V. Augugliaro, F. Drioli, G. Gobranzi, C. Grande, A. Loddo, R. Molinari, E. Palmisano, and M. Schiavella, "Preparation and characterization of membranes with entrapped TiO₂ and preliminary photocatalytic tests," *Ann. Chim.*, vol. 91, no. 3-4, pp. 127-136, 2001.
- [18] R. Molinari, E. Pirillo, V. Loddo, and E. Palmisano, "Photocatalytic degradation of dyes by using a membrane reactor," *Chem. Eng. Process.*, vol. 43, no. 9, pp. 1103-1114, September 2004.
- [19] R. A. De nodat, S. J. Youn, and H. H. Chou, "Study the self-cleaning, antibacterial and photocatalytic properties of TiO₂ entrapped PVDF membranes," *J. Hazard. Mater.*, vol. 172, no. 2-3, pp. 1321-1328, August 2009.
- [20] M. E. Mackay, A. Untch, P. M. Duxbury, C. C. Howler, B. V. Horn, Z. Guan, G. Chen, and R. S. Krishnan, "General strategies for nanoparticle dispersion," *Science*, vol. 311, no. 5763, pp. 1740-1743, March 2006.

- [21] S. Ali and A. K. Raina, "Dilute solution behavior of poly (vinylidene fluoride). Intrinsic viscosity and light scattering studies," *Die Makromolekulare Chemie*, vol. 179, no. 12, pp. 2925-2930, December 1978.
- [22] H. Inagaki, H. Suzuki, M. Fujii, and T. Matsuo, "Note on experimental tests of theories for the excluded volume effect in polymer coils," *J. Phys. Chem.* vol. 70, no. 6, pp. 1718-1726, June 1966.
- [23] P. Bagchi, "Theory of stabilization of spherical colloidal particles by nonionic polymers," *J. Colloid Interface Sci.* vol. 47, no. 1, pp. 86-99, April 1974.
- [24] Y. H. Teow, A. L. Ahmad, J. K. Lim, and B. S. Ooi, "Studies on the surface properties of mixed matrix membrane and its antifouling properties for humic acid removal," *J. Appl. Polym. Sci.*
- [25] R. A. Damodar, S. J. You, and H. H. Chou, "Study the self cleaning, antibacterial and photocatalytic properties of TiO₂ entrapped PVDF membranes," *J. Hazard Mater.* vol. 172, no. 2-3, pp. 1321-1328, December 2009.
- [26] T. H. Bae, I. C. Kim, and T. M. Tak, "Preparation and characterization of fouling resistant TiO₂ self-assembled nanocomposite membranes," *J. Membr. Sci.* vol. 275, no. 1-2, pp. 1-5, April 2006.
- [27] T. C. Merkel, B. D. Freeman, R. J. Spontak, Z. He, I. Pinnau, P. Meakin, and A. J. Hill, "Sorption, transport, and structural evidence for enhanced free volume in poly (4-methyl-2-pentyne)/fumed silica nanocomposite membranes," *Chem. Mater.* vol. 15, no. 1, pp. 109-123, 2003.
- [28] T. C. Merkel, B. D. Freeman, R. J. Spontak, Z. He, I. Pinnau, P. Meakin, and A. J. Hill, "Ultraporous, reverse-selective nanocomposite membranes," *Science*, vol. 296, no. 55-67, pp. 519-522, April 2002.
- [29] T. Kallio, S. Alajoki, V. Pore, M. Ritala, J. Laine, M. Leskeli, and P. Stenius, "Antifouling properties of TiO₂: Photocatalytic decomposition and adhesion of fatty and rosin acids, sterols and lipophilic wood extractives," *Colloids Surf. A Physicochem. Eng. Aspects*, vol. 291, no. 1-3, pp. 162-179, December 2006.
- [30] A. Rahimpour, S. S. Madaeni, A. H. Taheri, and Y. Mansourpanah, "Coupling TiO₂ nanoparticles with UV irradiation for modification of polyethersulfone ultrafiltration membranes," *J. Membr. Sci.* vol. 313, no. 1-2, pp. 158-169, April 2008.
- [31] Y. Yang, H. Zhang, P. Wang, Q. Zheng, and J. Li, "The influence of nano-sized TiO₂ fillers on the morphologies and properties of PSf UF membrane," *J. Membr. Sci.* vol. 288, no. 1-2, pp. 231-238, February 2007.
- [32] T. H. Bae and T. M. Tak, "Preparation of TiO₂ self-assembled polymeric nanocomposite membranes and examination of their fouling mitigation effects in a membrane bioreactor system," *J. Membr. Sci.* vol. 266, pp. 1-5, October 2005.
- [33] Y. Y. Li, H. M. Shen, and Z. L. Xu, "PVDF-TiO₂ composite hollow fiber ultrafiltration membranes prepared by TiO₂ sol-gel method and blending method," *J. Appl. Polym. Sci.* vol. 113, no. 3, pp. 1763-1772, December 2008.
- [34] H. A. Shawky, S. R. Chae, S. Lim, and M. R. Wiesner, "Synthesis and characterization of carbon nanotube/polymer nanocomposite membrane for water treatment," *Desalination*, vol. 272, no. 1-3, pp. 46-50, May 2011.



Y. H. Teow is currently a Ph. D scholar of School of Chemical Engineering, Engineering Campus, Universiti Sains Malaysia (USM), Penang, Malaysia. She obtained her Bachelor of Engineering (Hons) Chemical Engineering from Universiti Tunku Abdul Rahman (UTAR), Kuala Lumpur, Malaysia in 2010. She has authored three publications in *Desalination*, *Journal of Applied Polymer Science* and *Global Journal of Physical Chemistry*. Her research activities is principally dedicated in the fields of membrane technology in water purification, ultrafiltration mixed matrix membrane and the combination of water pollution problem and nanotechnology.

Surface chemistry and dispersion property of titanium dioxide nanoparticles in water suspension

Y. H. Teow^{*}, A. L. Ahmad, B. S. Ooi

*School of Chemical Engineering, Engineering Campus, Universiti Sains Malaysia,
Seri Ampangan, 14300 Nibong Tebal, Penang, Malaysia*

**Author for correspondence: Y. H. Teow, email: yeithaan@hotmail.com*

Received 8 Feb 2012; Accepted 1 May 2012; Available Online 8 May 2012

Abstract

Titanium dioxide (TiO₂) nanoparticles (NPs) have attracted great research interests in improving the membrane permeability, fouling-resistance and self-cleaning properties. For application feasibility, the TiO₂ NPs should exist in preferable small aggregate size and should be uniformly dispersed in the polymer film as mixed matrix membrane. The aim of this study is to investigate the effect of pH and ultrasonic irradiation time on the surface chemistry and the dispersibility of TiO₂ NPs. The results showed that for pH < 4.0, a stable PC-20 TiO₂ NPs suspension could be produced with zeta potential > 30 mV, while for P25 TiO₂ NPs, better dispersibility with broader pH range (< pH 5.0) can be observed. Besides, ultrasonic irradiation time is found to contribute its effect on size distribution of TiO₂ NPs in water suspension. The mean size of TiO₂ NPs in water suspension decreased for longer ultrasonic irradiation time.

Keywords: Ultrasonication; Zeta potential; TiO₂ nanoparticles; Water suspension

1. Introduction

With the rapid population and improper industrialization practices over the last two decades, it leads to the detrimental surface and underground water pollution. This phenomenon has raised concerns in the public for stringent environmental legislation and alternative technology in water treatment to increase both drinking water quantity and quality.

Membrane technology has become a dignified separation technology as a valuable means of solute filtering. The use of membrane as advanced water treatment process has raised greatest attention for environmental remediation in producing high quality water with small footprint. However, membrane fouling appears to be the main obstacle in water treatment process by membrane separation [1-3]. It is mainly caused by irreversible deposition of solute in the feed water on the hydrophobic membrane surface or into the membrane pores, which will result in water flux loss and solute selectivity change with time.

A number of approaches to alleviate the membrane fouling and increase the membrane performance have therefore been investigated. These methods include pretreatment of feed solution (flocculation and coagulation), periodic cleaning (physically, biologically or chemically) and hydrophilic modification of membrane surface. Although pretreatment of feed solution by chemical additives and chemical cleaning are effective in lessening the membrane fouling, high chemical usage will impose another environmental pollution. Therefore, increasing in membrane hydrophilicity appears to be a good way for membrane fouling mitigation [4].

Due to its stability, commercial availability, high affinity to water and outstanding photocatalytic activity that can decompose organic foulants on membrane, TiO₂ NPs

appear to be an appealing additive in surface modification of membranes and have been received most attention by numerous researchers in recent years [5-7]. For application feasibility, it is crucial to obtain ultrafine and stable nanodispersions that will produce thin nanocomposite membrane films with low surface roughness and high surface area of TiO₂ NPs [8,9].

To reduce the surface roughness of the fabricated membrane films, the primary size of TiO₂ NPs should be less than 20 nm. Although the primary size of most commercial NPs is quite small (5-50 nm), the high surface energy of TiO₂ NPs causes them to agglomerate in the synthesis and post-synthesis processes [10]. This leads to materials with primary particles in the nanometer range, but with variable and complex networks, shapes, and morphologies, all of which impact the particle size distribution [11].

Ultrasonication is a common method which is used to break up agglomerated TiO₂ NPs. An energy transfer device, an ultrasonic probe, is employed to oscillate the TiO₂ liquid suspension, causing nucleation and solvent bubbles. Bubbles initiating and collapsing on the solid surface can be very effective in fracturing the TiO₂ aggregates. During ultrasonication, effective fracturing on TiO₂ aggregates occurs due to the mechanical attrition [10,12]. It initiates at surface flaws and imperfections. With prolong ultrasonication, large TiO₂ aggregates are broken down into smaller aggregates until there are no more defects to initiate the breakage. Further energy input results no significant attrition. The breakage of TiO₂ agglomerates by ultrasonic irradiation is controlled predominantly by specific energy input (power, time and dispersion volume) [13].

In order to form stable dispersions, it is not enough to break NPs apart. Stabilization of colloidal dispersions of TiO₂ nanopowders by electrostatic interactions generates charges on

the surface of TiO₂ NPs, which acts as a barrier resulting from repulsive force, prevents two particles from adhering to each other forming assemblies. Therefore, stable TiO₂ suspension could be realised only when the TiO₂ particles have sufficiently high repulsion charge to permit any newly formed particles to be reagglomerated. A common way to evaluate the stability of colloidal dispersions is by determining the magnitude of zeta potential. Zeta potential is function of the surface charge of the particles. In dispersions, where value of the zeta potential is close to zero (isoelectric point), particles tend to agglomerate. At higher negative or positive zeta potential (more than 30 mV or less than -30 mV), particles in dispersions tend to repel each other to prevent agglomeration [14]. TiO₂ powders obtained from different manufacturers have dissimilar surface chemistry and as a result exhibit isoelectric points at different pH values [11].

As long-term stability of TiO₂ nanodispersions is important for producing high quality nanocomposite membrane, breakage of the TiO₂ NPs has become a critical issue. The objective of the present investigation is to study the breakage of commercial TiO₂ NPs in water dispersions by means of ultrasonic irradiation maintaining the stability of the NPs based on solution pH.

2. Experimental

2.1. Materials

Two different commercial forms of inorganic photocatalytic titanium dioxide (TiO₂) nanopowder purchased from TitanPE Technologies, Inc., Shanghai, China (trade name: PC-20) and Sigma-Aldrich, St. Louis, MO, USA (trade name: P25) were used as received. As reported by the manufacturer, the primary particle size of PC-20 TiO₂ NPs was 20 nm, while P25 TiO₂ NPs was ~21 nm, respectively.

2.2. Preparation of TiO₂ colloid suspension

Powdered TiO₂ with different weights was dispersed in 100 mL of distilled water for preparing different concentrations of TiO₂ suspensions, 0.1 g/L and 0.05 g/L. The pH of TiO₂ suspensions was then adjusted to values between 2.0-9.0 with hydrochloric acid or sodium hydroxide to obtain suitable zeta potential values in achieving electrostatic stability. Hydrochloric acid or sodium hydroxide was added drop-wise to the TiO₂ suspensions and it was mechanically stirred until it reached equilibrium with a specific pH value. The pH value of the TiO₂ suspensions was measured by using the pH meter (Eutech Instruments Pte. Ltd., Ayer Rajah Crescent, Singapore).

The ultrasonication was conducted using a Telsonic ultrasonic horn SG-24-500P (Telsonic Ultrasonics, Inc., Michigan, USA). The frequency of the ultrasound was kept constant at 18.4 kHz. The efficiency of ultrasonication in TiO₂ dispersion was evaluated by changing the sonication irradiation time. The dispersibility (changes in zeta potential) and TiO₂ particles size distribution under various pHs and ultrasonic irradiation times were determined by using Malvern Zetasizer Nano ZS90 (Malvern Instruments Ltd., U.K.) on the basis of dynamic light scattering theory and cumulant method.

2.3. Characterization of TiO₂ nanoparticles

2.3.1. X-Ray Diffraction (XRD)

X-ray diffraction (XRD) technique was used to identify the crystal structure of TiO₂ NPs, which determines the property and functionality of the TiO₂. XRD analysis was performed on TiO₂ nanopowder samples by subjecting it to X-ray radiation and the diffraction data were collected on a BRUKER AXS D8 ADVANCE diffractometer (Bruker AXS, GmbH). The system is equipped with a Cu X-ray tube (18 kW Cu K α radiation; λ = 0.15418 nm) and a LynxEye detector operated in the theta-theta geometry at 60 kV and 80 mA, and the configuration was calibrated using a lanthanum boride (LaB6) powder standard (ICDD PDF#34-0427). Scanning was performed from 10° to 90° (2 θ -angle), with a step width of 0.02° and a sampling time of 0.3 s per step.

2.3.2. Transmission Electron Microscopy (TEM)

The microstructure of TiO₂ NPs was analyzed by a JEOL transmission electron microscope (TEM, JEOL JEM-200CX) at 120 kV. For the TEM observation, TiO₂ colloidal suspensions (0.1 g/L) were dropped on a carbon-coated grid and then dried at room temperature.

3. Results and Discussion

3.1. Crystal structure and particle size of commercial TiO₂ nanoparticles

The crystal structures of both the commercial TiO₂ NPs (2 θ) were examined by using the X-ray diffraction (XRD) analysis and the spectra were illustrated in Figure 1. θ is the diffraction angle, measured with respect to the incident beam, while 2θ is constant-wavelength diffractometer. It is commonly known that TiO₂ particle has three different crystal forms, anatase, rutile and brookite [7]. In the anatase structure, the oxygen forms a cubic closest packing, and the titanium atoms lie in octahedral voids, while in the rutile form, the oxygen are arranged approximately in a hexagonal closest packing, and the titanium atoms occupy a row pattern. The anatase has been reported by many researchers to be the most photoactive and stable NPs for widespread applications, having good characteristics in bacteria killing, and hydrophilicity whereas the rutile is comparatively photocatalytically inactive or much less active, although it shows strong photoactivity selectivity towards some cases. Therefore, anatase is suitable for membrane modification [15]. Figure 1 shows that the characteristic peaks of PC-20 TiO₂ nanopowder was located at 2 θ of 25.319° which is close to the literature reported data 25.24° of anatase and a small rutile peak at 2 θ of 27.460°, consists of 85% anatase and 15% rutile. It can be identified that the PC-20 TiO₂ nanopowder is mainly composed of anatase, which promises excellent photocatalytic properties, hydrophilicity and anti-fouling characteristics. As for the diffraction pattern of P25 TiO₂ nanopowder, which is a mixture of 75% anatase and 25% rutile, the 2 θ of eminent peaks are 25.230° for anatase and 27.376° for rutile.

Transmission electron microscopy (TEM) was employed to determine the primary particle size of PC-20 and P25 under high magnification (22k \times). The micrographs are shown in Figure 2 (a) and (b) respectively. All these nanopowders were received in the dry form, and all contained large agglomerated particles. As shown in Figure 2, TEM

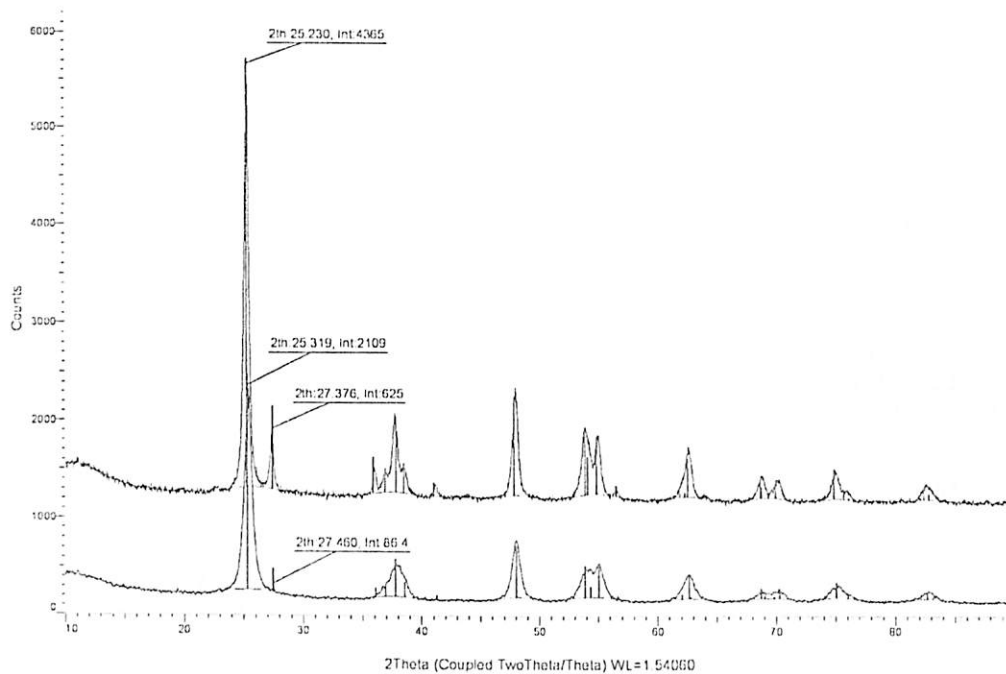
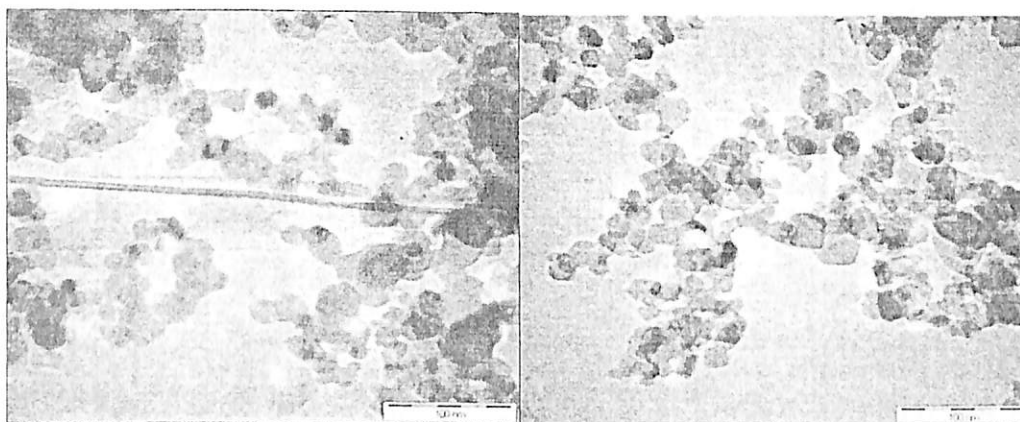


Figure 1. XRD spectrum of the commercial TiO_2 nanopowder (a) P25 TiO_2 nanopowder from Sigma-Aldrich (b) PC-20 TiO_2 nanopowder from TiPE.



(a)

(b)

Figure 2. Morphology of commercial TiO_2 nanopowder (a) PC-20 (b) P25 under 22 k \times of high magnification.

images of both anatase NPs demonstrated almost spherical shape which can be seen in the form of black spots and they are extensively agglomerated with particle size from 75-200 nm and 50-150 nm, respectively. The discrepancy between the particle sizes determined by TEM ascribes to the agglomeration tendency of TiO_2 NPs. With the smaller particle size distribution, P25 could disperse more effectively by the ultrasonic irradiation than the PC-20. The agglomeration of TiO_2 particles is mainly contributed by the drying procedure during the preparation of TEM samples [15].

3.2. Effect of pH on colloid stability of the TiO_2 nanopowders

The optimal dispersing conditions for TiO_2 nanopowder and its long term stability was evaluated based on zeta potential. The zeta potential measurements (by means of the electrophoretic mobility) were performed on Malvern Zetasizer Nano ZS90 equipment. High absolute values of zeta potentials are necessary to achieve electro-statically stabilized TiO_2 NPs in water suspension. In general, the criterion for suspension stability is thought to be $|\zeta| > 30$ mV [11]. A suspension is stable when the zeta potential value is less than -30 mV or greater than +30 mV, particles in dispersions tend to repel each other and hence no agglomeration occurs.

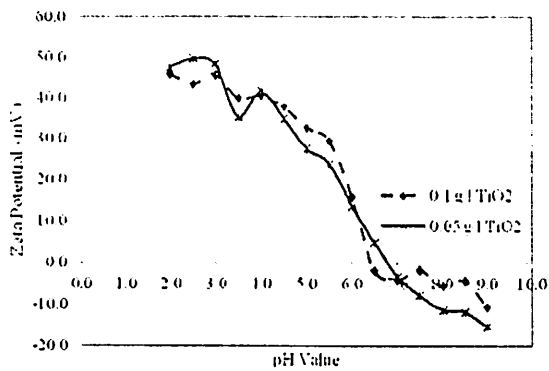


Figure 3. Zeta potential titration of P25 TiO₂ suspension with different concentrations at different solution pHs.

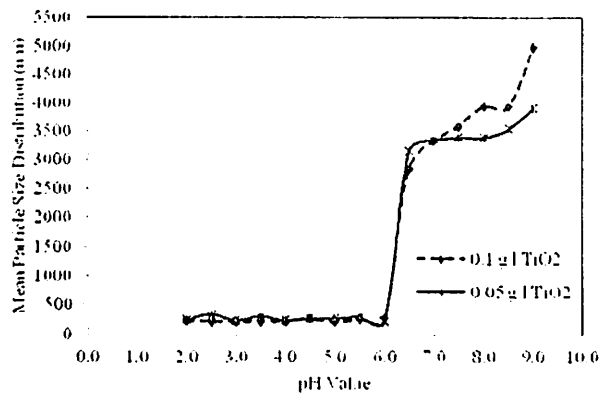


Figure 5. Mean particle size distribution versus pH for different concentrations of P25 TiO₂ NPs.

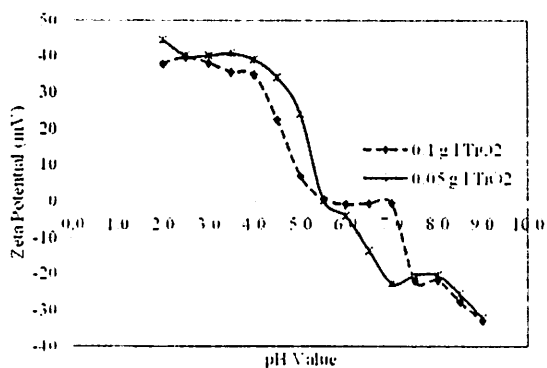


Figure 4. Zeta potential titration of PC-20 TiO₂ suspension with different concentrations at different solution pHs.

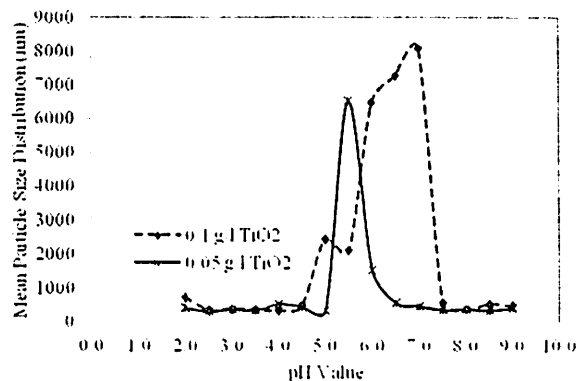


Figure 6. Mean particle size distribution versus pH for different concentrations of PC-20 TiO₂ NPs.

Figures 3-6 present the pH effect of different commercial TiO₂ nanopowders on the stability of the suspensions within the range of pH 2.0-9.0. Figure 3 and Figure 4 show the zeta potential while Figure 5 and Figure 6 show the mean particle size distribution of the colloids under different pH values and different concentrations (0.1 g/L TiO₂ and 0.05 g/L TiO₂). The pH was adjusted with hydrochloric acid immediately after 15 minutes of ultrasonic irradiation to the suspension. The isoelectric point (IEP) is a point (pH value) where the plot passes through zero zeta potential. At this IEP, the colloidal system is least stable. Referring to Figure 3 and Figure 4, the IEP for P25 TiO₂ takes place at neutral pH region while for PC-20 TiO₂ it is at acidic pH region. The higher zeta potential of P25 compared to PC-20 shows that P25 could readily form stable colloidal system within the pH range. For P25 TiO₂ with concentration of 0.05 g/L and 0.1 g/L, high enough zeta potential values were obtained in the broader pH region (as shown in Figure 3) and they are considered stable at pH value lower than 5.0 with comparable mean particle size (as shown in Figure 5). On the contrary, PC-20 NPs demonstrate its stability in suspension at pH value lower than 4.0. For PC-20 TiO₂, higher pH (> pH 6.5) could produce small size of TiO₂ particles as well, however, low in zeta potential value does not endorse its stability in water suspension. Nevertheless, the PC-20 nanopowder suspension flocculates very rapidly which is shown in Figure 6 to have

larger mean particle size distributions, and indicates a strong agglomeration of the NPs.

3.3. Effect of ultrasonic irradiation on TiO₂ dispersion

The effect of ultrasonic irradiation time on the TiO₂ colloids stability were evaluated using Telsonic ultrasonic probe (frequency 18.4 kHz). The results were shown in terms of zeta potential and mean particle size in Figure 7 and 8, respectively.

Initially, the attractive forces among the TiO₂ NPs were stronger than repulsive forces; therefore the TiO₂ NPs in water suspensions tends to agglomerate and the size of agglomerates was extensively large. The ultrasonication caused the breakage of the agglomerates, but shortly after the end of the ultrasonication, the particles reagglomerated back. Breakage of the powder was evident only when the suspensions were adjusted to pH 4.0 immediately after cessation of ultrasonication to permit any newly formed particles to be stably dispersed. The suspension stability for both samples in water suspension along ultrasonic irradiation time was evaluated based on the zeta potential as shown in Figure 7. A noticeable observation is that the zeta potential magnitude for both commercial TiO₂ NPs are higher than +30 mV even under 15 minutes of ultrasonic irradiation indicating the stability of TiO₂ in water suspension. With larger zeta potential presented by P25 TiO₂ NPs, it has higher tendency in repelling each other and there will be less or no tendency for

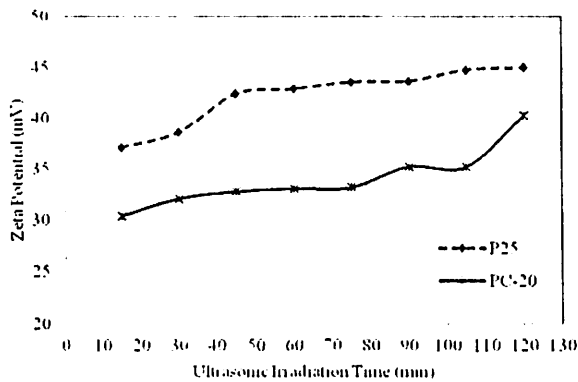


Figure 7. Change in TiO_2 suspension zeta potential with ultrasonic irradiation time.

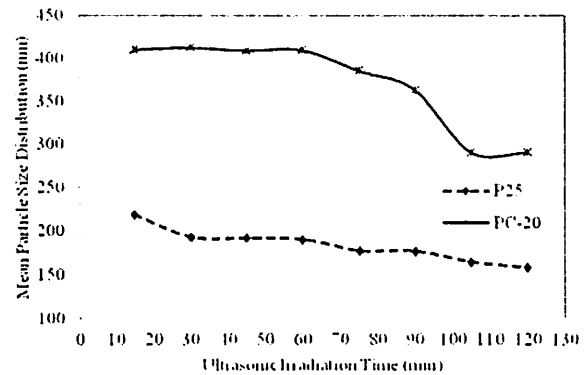


Figure 8. Change in size of agglomerates/aggregates with ultrasonic irradiation time.

the TiO_2 NPs to approach and come together. For both commercial TiO_2 NPs, the zeta potential was increased slowly over a comparatively long ultrasonic irradiation time.

Characterization of the mean particle size distribution was performed by Dynamic Light Scattering (DLS). DLS measures the Brownian motion of the particles and relates it to the particle size. The ultrasonication caused the breakage of the agglomerates into smaller particle size with the increase of ultrasonication period. Referring to Figure 8, for PC-20, no significant change in particle size was observed for ultrasonic irradiation time up to 60 min, suggesting that the attractive forces between primary PC-20 TiO_2 NPs are stronger. From 60 min ultrasonic irradiation time onwards, the mean dispersed particle size of PC-20 TiO_2 aggregates in suspension decreased as irradiation time increased and then reached the smallest value (290.5 nm) at 105 minutes of ultrasonic irradiation time. Following that, the particle size remains constant as it is the minimum particle size for PC-20 TiO_2 NPs that can be reduced by using ultrasonication. On the other hand, the mean dispersed particle size was less than 200 nm and remained almost constant when P25 TiO_2 nanopowder was sonicated for 30 min. The particle size of PC-20 TiO_2 dispersed by ultrasonic irradiation was more widely distributed as compared to that of P25 TiO_2 , indicating that the P25 TiO_2 NPs is more responsive towards ultrasonic irradiation in producing smaller TiO_2 NPs.

While both TiO_2 nanopowder was reported by the manufacturer to have very small particle size which is 20 nm and ~21 nm for PC-20 and P25, respectively, it was very difficult to break into its preliminary particle size using ultrasonication. None of them was successfully broken into their primary particle size within 2 hours of irradiation time.

The degree of cluster breaking highly depends on the inter-particle interaction force. A small adjustment in the manufacturing process will result in extensive changes in particle properties and its size distribution. However, once agglomeration occurs in the synthesis process, it is very difficult to break the particle apart into their primary particle size.

Additionally, dark sediment was eminent at the bottom of the ultrasonicated dispersions, which is attributed to the erosion of the ultrasonic probe, which agrees well with the observation obtained by Mandzy et al. [11]. Long period of ultrasonic irradiation time does not give a promising result in

further reducing the particle size of TiO_2 to higher extent, but resulted in contamination of the samples.

4. Conclusions

Fracture mechanism was observed in the ultrasonication of commercial TiO_2 nanopowders. However, there was no evidence that prolonged ultrasonic irradiation could further break the commercial TiO_2 nanopowders into their primary particle size. During the ultrasonic breakage, electrostatic stabilization of TiO_2 dispersions prevented newly formed particles from reagglomeration by adjusting the pH. Conditions have been optimized to produce stable commercial TiO_2 NPs in water suspensions. P25 TiO_2 nanopowder was suspended with smaller TiO_2 NP size and high zeta potential value in broader pH range (< pH 5.0) compared to PC-20 TiO_2 nanopowder (< pH 4.0). This observation indicates that P25 TiO_2 nanopowder resulted in better dispersion in water suspension. Almost immediate agglomeration of mechanically broken particles was observed when pH value is higher than 5.0 and 4.0 for P25 TiO_2 NPs and PC-20 TiO_2 NPs, respectively. In this study, the effect of ultrasonic irradiation time on the TiO_2 NPs dispersibility has also been clarified. The results showed that 15 minutes is the best ultrasonic irradiation time to obtain well-dispersed TiO_2 suspensions for both commercial TiO_2 nanopowders. Further increase in ultrasonic irradiation time does not give much effect in reducing the mean particle size of TiO_2 NPs.

Acknowledgement

The authors wish to thank the sponsors of this project for their financial supports, namely Universiti Sains Malaysia (USM) Research University Grant (1001/PJKIMIA/811172), Malaysia Toray Science Foundation (MTSF) Science and Technology Research Grant (304/PJKIMIA/6050179/M126) and USM Membrane Science and Technology Cluster.

References

1. A. Akthakul, R. F. Salinaro, A. M. Mayes, *Macromolecules* 37 (2004) 7663.
2. D. Chen, L. K. Weavers, H. W. Walker, *Water Res.* 40 (2006) 840.

3. J. H. Li, Y. Y. Xu, L. P. Zhu, J. H. Wang, C. H. Du, *J. Membr. Sci.* 326 (2009) 659.
4. A. Rahimpour, S. S. Madaeni, A. H. Taheri, Y. Mansourpanah, *J. Membr. Sci.* 313 (2008) 158.
5. A. Fujishima, T. N. Rao, D. A. Tryk, *J. Photochem. Photobiol. C: Photochem. Rev.* 1 (2000) 1.
6. C. C. Li, S. J. Chang, M. Y. Tai, *J. Am. Ceram. Soc.* 93 (2010) 4008.
7. A. Mills, S. L. Hunte, *J. Photochem. Photobiol. A: Chem.* 1 (1997) 108.
8. X. H. Cao, J. Ma, X. H. Shi, *Z. J. Ren. Appl. Surf. Sci.* 253 (2006) 2003.
9. K. Ebert, D. Fritsch, C. Koll, C. Tjahjaviguna, *J. Membr. Sci.* 233 (2004) 71.
10. B. Park, D. Smith, S. Thoma, *Particle Technol.* 76 (1993) 125.
11. N. Mandzy, E. Grulke, T. Druffel, *Powder Technol.* 160 (2005) 121.
12. K. Kusters, S. Pratsinis, S. Thoma, *Powder Technol.* 80 (1994) 253.
13. M. Pohl, H. Schubert, *International Congress for Particle Technology Partec, Nuremberg, Germany (March 2004)* pp. 16-18.
14. www.malvern.co.uk (lecture Dispersion Stability and Zeta Potential).
15. S. H. Kim, S. Y. Kwak, B. H. Sohn, T. H. Park, *J. Membr. Sci.* 211 (2003) 157.

Cite this article as:

Y. H. Teow *et al*: Surface chemistry and dispersion property of titanium dioxide nanoparticles in water suspension. *Global J. Environ. Sci. Technol.* 2012, 2: 16

Preparation of titanium dioxide embedded ultrafiltration membrane: Properties and fouling evaluation

H. P. Ngang^{*}, A. L. Ahmad, B. S. Ooi

*School of Chemical Engineering, Engineering Campus, Universiti Sains Malaysia,
Seri Ampangan 14300, Nibong Tebal, Pulau Pinang, Malaysia*

**Author for correspondence: H. P. Ngang, email: hueypping0404@gmail.com
Received 6 Feb 2012; Accepted 10 Mar 2012; Available Online 10 Mar 2012*

Abstract

In this study, the polyvinylidene fluoride (PVDF)-Titanium dioxide (TiO₂) mixed-matrix membranes were prepared via phase inversion technique. The properties of PVDF-TiO₂ mixed-matrix membranes were characterized based on contact angle and field emission scanning electron microscope (FESEM). The hydrophilicity of the mixed-matrix membrane was greatly enhanced which is a desired property of membrane for water purification. However, at higher content of TiO₂, membrane wettability might be impaired due to the roughness created by the agglomeration of TiO₂ on the surface. The methylene blue removal by mixed-matrix membrane in the absence of sodium dodecyl sulfate (SDS) surfactant is poor due to separation by adsorption mechanism only. However, with the presence of 20 mM surfactant in feed solution dye removal efficiency was increased dramatically. Membrane with 1 wt% TiO₂ exhibited maximum dye removal. Optimum TiO₂ concentration was found around 3 wt%, concentration higher than 3 wt% will result in TiO₂ agglomeration which is not a desired phenomenon because of pore blocking, membrane defect and reduced catalytic surface area.

Keywords: Polyvinylidene fluoride; Titanium dioxide; Mixed-matrix membranes; Methylene blue; Sodium dodecylsulfate

1. Introduction

Dye containing waste stream had caused a series of environmental problems. Among various types of dye, methylene blue (MB) was used in paint production, textile finishing, and as a sensitizer in photo-oxidation of organic pollutants [1]. Various methods are available for the removal of coloured dyes from wastewater, eg. adsorption [2], flocculation/coagulation method [3], biological methods such as biodegradation [4], and membrane separation [5], but each method has their own disadvantages. Activated carbon is always being considered for dye adsorption but is expensive adsorbent due to its high cost of manufacturing and regeneration. The operating cost for flocculation is high and the rejection of dye is poor. Membrane based separation processes have emerged as an attractive alternative to the conventional processes in the various industrial applications due to their unique separation capability, easy to scale-up possibilities and low energy consumption [6]. The nanofiltration (NF) and reverse osmosis (RO) are now recognized as the most suitable techniques for the removal of several toxic dyes. However, its major disadvantages are due to its dense membrane structure, high energy consuming process and higher operating pressure is required to obtain desired performance. Furthermore, decline in permeate flux due to adsorption of organic compound caused serious issues related to membrane fouling [5].

To overcome these drawbacks, ultrafiltration (UF) appears to be more attractive method for wastewater treatment because it offers high fluxes at relatively low pressures [7]. One of the possible methods to remove organic dyes from wastewater is micellar enhanced ultrafiltration (MEUF) [8].

Many studies have shown that MEUF is suitable method for the removal of organic pollutant [8, 9]. MEUF involves the addition of surfactant to wastewater in order to remove organic pollutants effectively and economically. The surface activity of surfactants are derived from their amphiphilic structure that possesses both hydrophilic and hydrophobic parts in one molecule [10]. Surfactant monomer will assemble to form micelles when the surfactants are added into the methylene blue feed solution at levels equals to or higher than their critical micelle concentrations (CMCs). The CMCs of SDS is 8 mM in distilled water.

Micellar enhanced ultrafiltration is a promising method used in wastewater treatment process. However, one of the main barriers to greater use of membrane technology is membrane fouling. Membrane fouling can be reduced by addition of hydrophilic materials to the membrane casting solution [11]. On the other hand, the preparation of novel organic-inorganic composite membranes with control properties has been widely used in recent years. A more recent one to improve the membrane antifouling properties is by using TiO₂ nanoparticles (NPs) on membrane structure and surface. TiO₂ particles can degrade organic foulant effectively with radiation of UV light [12]. TiO₂ had received the most attention among different NPs due to its stability, availability, and promise for applications such as painting, catalysis and photocatalysis, battery, cosmetic, etc [13].

In this paper, neat PVDF membrane and PVDF/TiO₂ mixed-matrix membrane with a defined morphology, high permeability, and enhanced hydrophilicity were prepared by phase inversion methods. The effect of TiO₂ concentration on the rheology, morphologies and the performances of PVDF membranes properties were characterized based on membrane

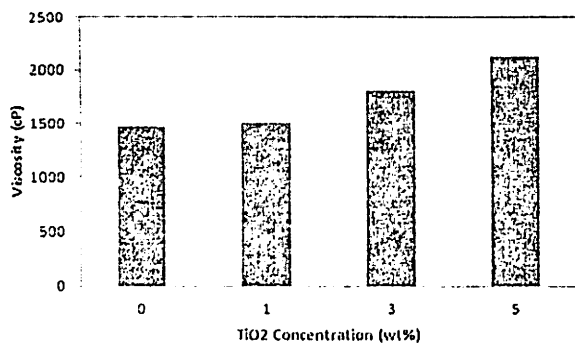


Figure 1. Viscosity of neat PVDF and PVDF/TiO₂ mixed-matrix ultrafiltration membrane dopes.

dope viscosity, membrane contact angle and field emission scanning electron microscope (FESEM) respectively. The neat and mixed-matrix membranes were also compared in terms of the effectiveness of MEUF separation behavior for methylene blue with and without SDS surfactants.

2. Experimental

2.1. Materials

Polyvinylidene fluoride (Solef® PVDF) was supplied by Solvay Solexis, France. N-methyl-2-pyrrolidone (NMP), sodium dodecyl sulfate (SDS) and methylene blue (MB) were purchased from Merck, Germany. Anatase TiO₂, PC-20 (20 nm) was purchased from TitanPE Technologies, Inc., Shanghai. PVDF and TiO₂ nanoparticles were dried in an oven at 70°C for overnight prior to use, while other organic chemicals were obtained in reagent grade purities and used as received. Distilled water was used for all the experiments.

2.2. Experimental procedures

The predetermined amount of TiO₂ was dispersed in n-methylpyrrolidone under sonication for 15 minutes. 15 wt% of PVDF powder was dissolved into the TiO₂ solution and stirred at 60-70°C for 4 hours to ensure a complete dissolution of the polymers. The solution was left for overnight stirring at 40°C. The final solution was then undergoing further sonication for 30 minutes and let to cool down to room temperature. The solution was cast on the tightly woven polyester using Automatic film applicator (Elcometer 4340, E.U.) at nominal thickness of 200 μm. It was immediately immersed into the water bath of distilled water and let the phase inversion occur for 24 hours to remove the residual solvent. PVDF membrane was kept in distilled water prior to use.

The viscosity of membrane dope was measured by a Model DV-III Programmable Rheometer (Brookfield, USA) at 27 ± 2°C to evaluate the rheology effect of polymer solution brought by different concentrations of TiO₂ nanoparticles added. The speed was fixed at 10 rpm and the samples were measured after shearing for 30 seconds.

The UF experiments were performed in a dead-end stirred cell (Amicon 8200, Millipore Co., USA) with a capacity of 200 ml, where the disc membrane has a diameter of 60 mm with a geometric area of 28.27 cm² (excluding the area cover by the O-ring). The applied pressure of the filtration system was controlled by N₂ gas cylinder. The stirring speed was

maintained at 200 rpm using the controllable magnetic stirrer (Heidoph MR3000D, Germany). PVDF membrane was first compacted with distilled water at 2.5 bar until constant pure water flux is achieved to minimize compaction effects. The cell was then emptied and refilled with methylene blue feed solution immediately; and the pressure was lowered to operating pressure, 1.5 bar. The flux and filtration efficiency were measured after a total of 10 ml of permeate were collected.

The pure water flux (J) was calculated as follows:

$$J = \frac{V}{A\Delta t} \quad (1)$$

where V is the volume of permeated water, A (m²) is the membrane area, and Δt (h) is ultrafiltration operation time. The concentration of methylene blue with and without surfactant was measured with a Visible Spectrophotometer (Thermo Spectronic Model Genesys 20, USA) at the maximum absorbance at 662 and 665 nm accordingly. The filtration efficiency in removing the dye from the feed solution was calculated as follows:

$$R(\%) = \left[1 - \frac{C_p}{C_0}\right] \times 100 \quad (2)$$

where C_p is the dye concentration in the permeate and C_0 is the initial concentration of the dye in the feed.

The hydrophilicity change caused by the addition of nanoparticles on membrane top surface was characterized using water contact angle instrument (Rame-Hart Model 300 Advanced Goniometer) based on sessile drop methods. All membranes film were cut into square coupons and mounted onto glass slides. Water drops were controlled at constant volume using the motor-driven syringe. The acquired images were analyzed using DROPimage software to obtain the measurement of contact angles. To minimize experimental error, the contact angle measurement were repeated 5 times for each sample and then averaged.

The top surface morphologies of the fabricated PVDF membranes were observed under Field Emission Scanning Electron Microscope (FESEM CARL ZEISS SUPRA 35VP, Germany). Image magnifications were 20,000x for surface views at 5 kV. All membrane samples were dried at room temperature and coated with a thin layer of gold before observation.

3. Results and Discussion

3.1. Effect of TiO₂ concentration on viscosity of membrane dopes

The neat PVDF membrane dope was a yellow transparent viscous solution while the others were white viscous solutions due to the presence of TiO₂ nanoparticles in the preparation process. Membrane dopes with TiO₂ nanoparticles were obviously more viscous than the neat membrane dope. The addition of the TiO₂ nanoparticles could significantly increase the viscosity of the membranes dopes as shown in Figure 1. The membrane dopes viscosity influences the rheological property between the solvent and non-solvent during the membrane formation process, and imposed kinetic effect for the membrane formation. Membrane morphology is

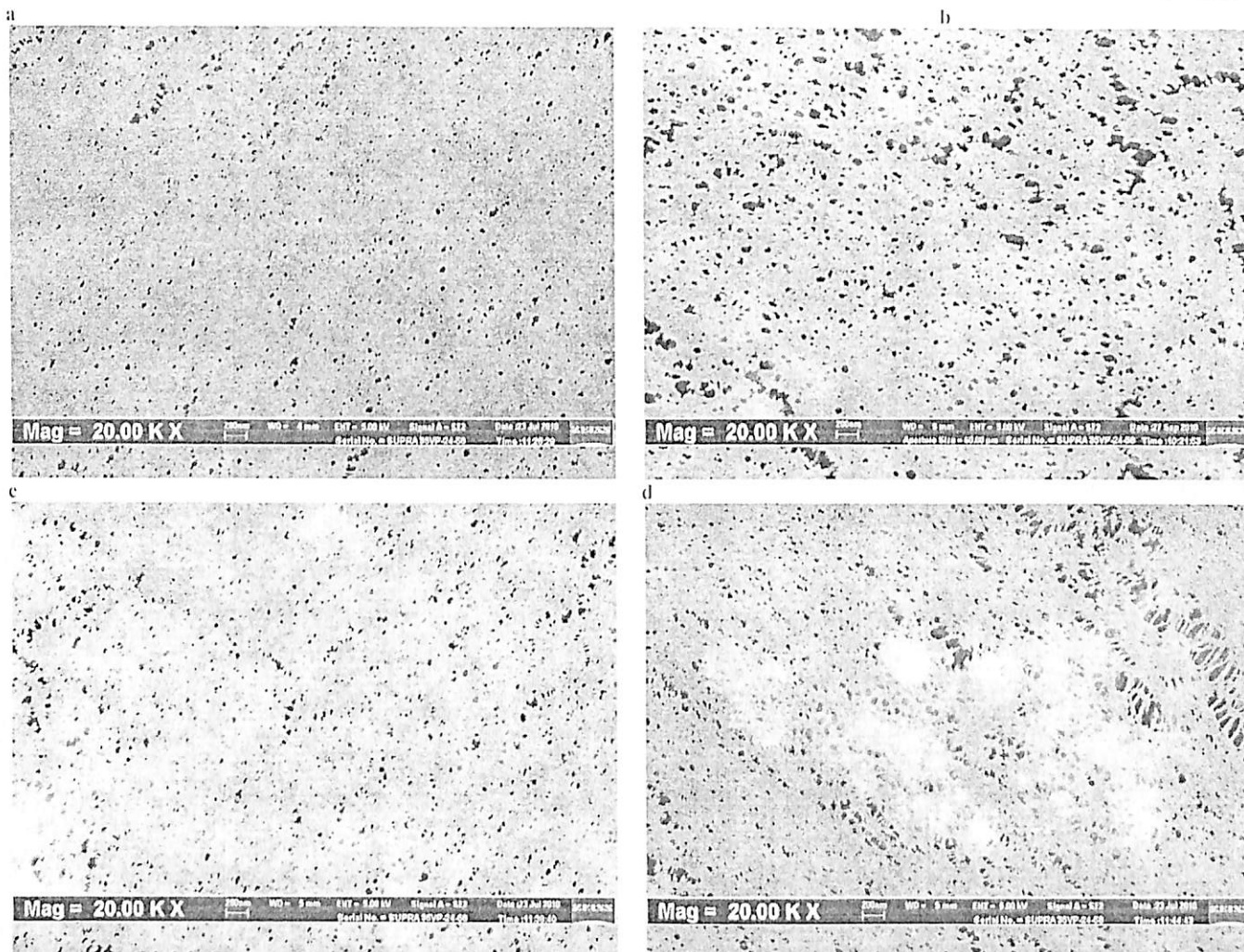


Figure 2. SEM images of mixed-matrix ultrafiltration membrane surface (a) Neat, (b) 1 wt% TiO_2 concentration, (c) 3 wt% TiO_2 concentration, (d) 5 wt% TiO_2 concentration.

influenced by dopes viscosity, higher dopes viscosity would prevent the creation of macroporous structure caused by instantaneous demixing. However, higher dopes viscosity would be a barrier for membrane formation which produced less interconnected sponge structure as will be discussed in the following paragraph.

3.2. Effect of TiO_2 concentration on membrane morphology

Figure 2 shows the surface images of membrane prepared from PVDF/NMP systems with different concentrations of TiO_2 nanoparticles. The addition of TiO_2 nanoparticles into the polymer matrix demonstrated an obvious change of membrane morphology. As discussed in section 3.1, the loaded amounts are able to change rheological behavior of membrane dopes. Higher dope viscosity will affect the mass transfer of solvent and non-solvent which resulted in higher resistance of diffusion between the membrane dope and the coagulation bath. On the other hand, due to the hydrophilic nature of TiO_2 , the thermodynamic behavior of membrane dope is also affected. The penetration velocity of water into nascent membrane increased with increasing TiO_2 loading during the phase inversion method. The nonsolvent influx is expected to be increased due to the

pulling force of the nanoparticles which enhanced the instantaneous liquid-liquid demixing. Solvent molecules can diffuse more readily from the polymer matrix to the coagulation bath due to the decreased interaction between polymer and solvent molecules by barrier created by nanoparticles [14]. As a result, spinodal demixing is likely to occur which result in a highly connected porous structure. However, beyond 3 wt% of TiO_2 concentration, it was clearly seen on the surface whereby TiO_2 agglomeration starts to occur. Agglomeration of TiO_2 is an unwanted phenomenon as it might block the pores of membrane and cause membrane defect. At the same time, it reduced the surface area of the nanoparticles and consequently reduced its photocatalytic properties.

3.3. Effect of TiO_2 dosage on membrane surface wettability

The membranes were characterized in term of surface wettability. Membrane surface wettability is one of the important membrane properties which could affect the flux and fouling behavior of the mixed-matrix membrane. Since TiO_2 nanoparticles were responsible for the hydrophilicity increment and fouling mitigation due to TiO_2 itself contained hydroxyl group [15], addition of TiO_2 is expected to reduce its

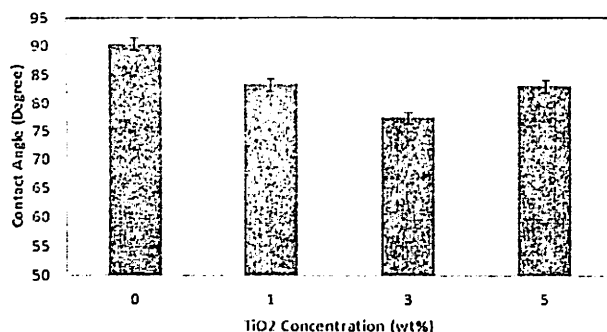


Figure 3. Contact angles of membranes with different TiO₂ concentration.

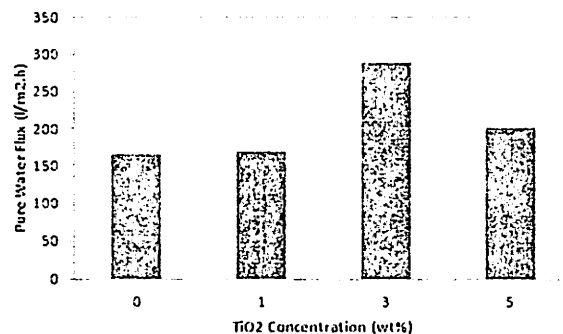


Figure 4. Effect of TiO₂ concentration on membranes pure water flux.

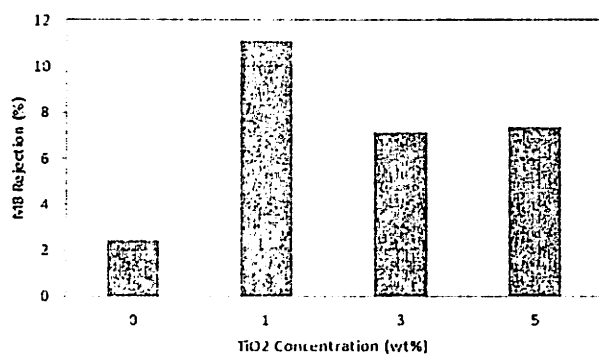


Figure 5. Extent of dye removal with different TiO₂ concentration mixed-matrix membranes.

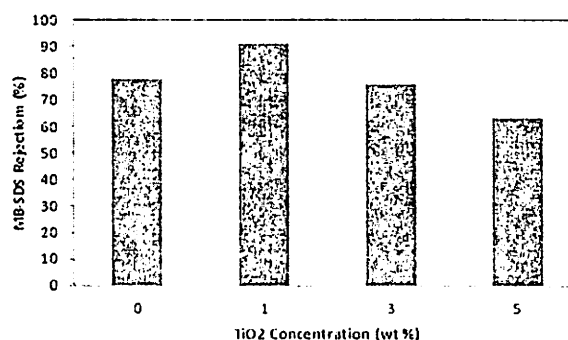


Figure 6. Extent of SDS enhanced dye removal with different TiO₂ concentration mixed-matrix membranes.

contact angle. On the other hand, PVDF membrane is commonly known by its hydrophobic nature. The results of contact angle shown in Figure 3 could verify this phenomenon. When the TiO₂ concentration is increased from 1 to 5 wt%, it was found that contact angle of the membrane decreased significantly from 90° to 75°. Water contact angle values decreased with the increasing concentration of TiO₂ nanoparticles indicated that TiO₂ does contribute in increasing the membrane hydrophilicity. However further increasing of TiO₂ concentration above 3 wt% will cause increase in contact angle mainly due to the increasing surface roughness of agglomerated TiO₂ nanoparticle as shown in section 3.2 SEM picture (Figure 2) as well as increasing pore size. Bae and Tak [16] also observed the same phenomenon in their research that entrapment of TiO₂ nanoparticles in membranes can increase the hydrophilicity of their surface in their research. TiO₂ nanoparticles which contain hydroxyl groups on the membrane surface are responsible for the increase of hydrophilicity [17].

3.4. Membrane performance

3.4.1. Pure water flux

Pure water flux experiment is an important parameter to evaluate the performance of membrane. It was carried out to investigate the influence of TiO₂ concentration on membrane permeability. Figure 4 shows that the pure water flux was enhanced with the increase of TiO₂ concentration with a peak value at 3 wt%. TiO₂ incorporated membranes show higher flux due to the increasing hydrophilicity of mixed-matrix membrane as discussed in section 3.3. TiO₂ mixed-matrix

membrane can be more hydrophilic than neat polymeric membrane due to higher affinity of TiO₂ to water [16]. The hydroxyl group could attract water molecules to pass through the membrane. Besides, bigger and interconnected pore structure of mixed-matrix membrane provides less resistance to water permeation. However, at 5 wt% TiO₂ concentration, a significant decrease of pure water flux was observed. This observation is due to the agglomeration of TiO₂ as shown in the SEM images in Figure 2 which block the pores of the membrane, and subsequently provide higher resistance for water permeation. Soroko and Livingston [18] in their research also find that with the presence of 10 wt% TiO₂ in the polyimide matrix, results in lower flux.

3.4.2. Membrane rejection

The influence of TiO₂ concentrations on membrane rejection was studied. Figure 5 and Figure 6 showed the results of the ultrafiltration of methylene blue (MB) solution without and with the presence of SDS using the neat and mixed-matrix membranes. The retention of MB molecules is negligible (less than 12%) in absence of surfactant. The minor retention could be attributed to the adsorption phenomenon of dye which takes place at the surface and in the pores of membrane. Since the MB molecules are much smaller than membranes pore size, no steric hindrance is expected. Moreover, the net negatively charged surface of PVDF could provide a superior adsorption site for the positively charged methylene blue. Membrane with 1 wt% TiO₂ exhibits maximum dye removal most probably due to the extra site of 1 wt% TiO₂ membrane for adsorption (better rejection). Due to

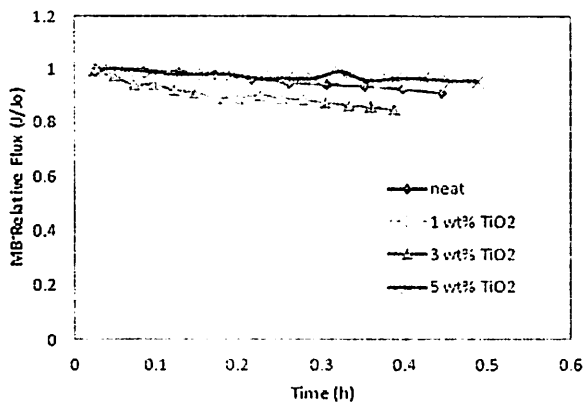


Figure 7. Membrane permeate flux without SDS at different TiO₂ concentration mixed-matrix membranes.

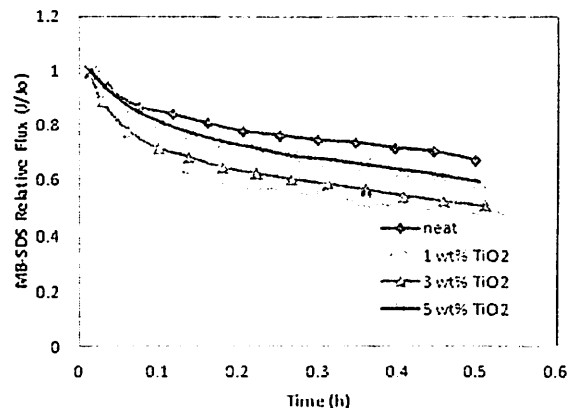


Figure 8. Membrane permeate flux with SDS enhanced at different TiO₂ concentration mixed-matrix membranes.

the hydrophilicity of TiO₂ particles on the membrane surface, the interaction between the MB and the membrane surface will be slightly decreased. TiO₂ will increase the surface porosity however beyond 5 wt% the surface pore will reduce due to the particle agglomeration that cause membrane defect.

On the other hand, with the presence of 20 mM surfactant in feed solution, dye removal was enhanced dramatically. These surfactant molecules form micelles, that can solubilise the MB and are rejected during ultrafiltration process by the prepared membranes. The added surfactant molecules with higher concentration than the critical micelle concentration (CMC) will form micelles which will be retained on the surface of the membranes. The results showed that the electrostatic interaction between MB and surfactants plays an important role in the MB removal.

3.4.3. Membrane antifouling performance with dye solution as model

The influence of TiO₂ concentrations on membrane fouling was studied. Figure 7 and Figure 8 showed the relative permeate flux results of the ultrafiltration of dye solution without and with the present of SDS using the neat and mixed-matrix membrane. The relative permeate flux of MB molecules without surfactant showed in Figure 7 remains constant with time since MB molecules are much smaller than membranes pore size and no steric hindrance is expected.

On the other hand, a relative permeate flux decline is observed with the presence of 20 mM surfactant in feed solution as shown in Figure 8. Lower flux is observed during MB rejection with surfactant than MB itself since bigger micelles block the membrane pores and form a cake layer that delay the filtration process or cause the expected membrane fouling. Membrane with 1 wt % TiO₂ showed highest relative permeates flux decline as shown in Figure 8. Besides, membrane with 1 wt% TiO₂ showed highest MB-SDS removal as discussed in section 3.4.2 due to higher surfactant concentration near the membrane surface that form a cake layer. During ultrafiltration, the higher surfactant concentration near the membrane compared to bulk surfactant concentration [8] causes the flux decline. Nevertheless, beyond 3 wt% TiO₂ concentration, the membrane surface pore will reduce or defect due to the particle agglomeration as discussed in section 3.2. These phenomena are observed from

Figure 6 and Figure 8 that beyond 3 wt%TiO₂ showed lower relative permeate flux decline and decrease in MB-SDS removal efficiency.

4. Conclusions

Mixed-matrix membranes had been prepared by dosing different amounts of TiO₂ nanoparticles in the polyvinylidene fluoride membrane dope. It was found that membranes prepared under different TiO₂ concentrations have different physical and morphological properties. Addition of TiO₂ could enhance membrane hydrophilicity, however, it produced membrane with bigger pore size due to the seeding effect of nanoparticles. At higher TiO₂ concentration, pore size of membrane could be reduced due to the agglomeration of TiO₂ that blocks the membrane pores and causes membrane defect. Pure water flux could be enhanced with 3 wt% TiO₂ concentrations and beyond which the water permeability was impaired due to the blocking effect. Membrane prepared showed very poor sieving mechanism for methylene blue due to small solute/pore ratio. Methylene blue removal can be enhanced dramatically by adding SDS surfactant to the methylene blue feed solution. Methylene blue affinity towards PVDF membrane is higher than TiO₂ which resulted mixed-matrix membrane to have advantage to reduce the membrane fouling phenomenon. These findings provide some useful information for membrane development as it could mitigate the membrane fouling phenomenon through its hydrophilicity improvement and at the same time it reduced the interaction between the dye and the polymer matrix.

Acknowledgement

The authors wish to thank the financial support granted by Universiti Sains Malaysia (RU Grant) (1001/PJKIMIA/811172), USM Membrane Cluster, Malaysia Toray Science Foundation (MTSF) Science and Technology Research Grant (304/PJKIMIA/6050179/M126) and Ministry of Higher Education (MyMaster).

References

1. M. Bielska, J. Szymanowski, *Water Res.* 40 (2006) 1027.
2. S. Wang, Z.H. Zhu, A. Coomes, F. Haghseresh, G.Q. Lu, *J. Colloid Interface Sci.* 284 (2005) 440.
3. V. Golob, A. Vinder, M. Simonic, *Dyes Pigm.* 67 (2005) 93.
4. S. Seshadri, P.L. Bishop, A.M. Agha, *Waste Manage.* 15 (1994) 127.
5. I. Koyuncu, D. Topacik, E. Yuksel, *Sep. Purif. Technol.* 36 (2004) 77.
6. B. Sarkar, S. DasGupta, S. De, *Sep. Purif. Technol.* 66 (2009) 263.
7. M. Bielska, K. Prochaska, *Dyes Pigm.* 74 (2007) 410.
8. N. Zaghbani, A. Hafiane, M. Dhalibi, *Sep. Purif. Technol.* 55 (2007) 117.
9. J.-H. Huang, C.-F. Zhou, G.-M. Zeng, X. Li, J. Niu, H.-J. Huang, et al., *J. Membr. Sci.* 365 (2010) 138.
10. Z. Aksu, S. Ertugrul, G. Dönmez, *Chem. Eng. J.* 158 (2010) 474.
11. A. Rahimpour, S.S. Madaeni, *J. Membr. Sci.* 305 (2007) 299.
12. A. Rahimpour, S. S. Madaeni, A. H. Taheri, Y. Mansourpanah, *J. Membr. Sci.* 313 (2008) 158.
13. X. Cao, J. Ma, X. Shi, Z. Ren, *Appl. Surf. Sci.* 253 (2006) 2003.
14. I.C. Kim, K.H. Lee, T.M. Tak, *J. Membr. Sci.* 183 (2001) 235.
15. E. Yuliwati, A. F. Ismail, *Desalination* 273 (2011) 226.
16. T.-H. Bae, T.-M. Tak, *J. Membr. Sci.* 249 (2005) 1.
17. G. Wu, S. Gan, L. Cui, Y. Xu, *Appl. Surf. Sci.* 254 (2008) 7080.
18. I. Soroko, A. Livingston, *J. Membr. Sci.* 343 (2009) 189.

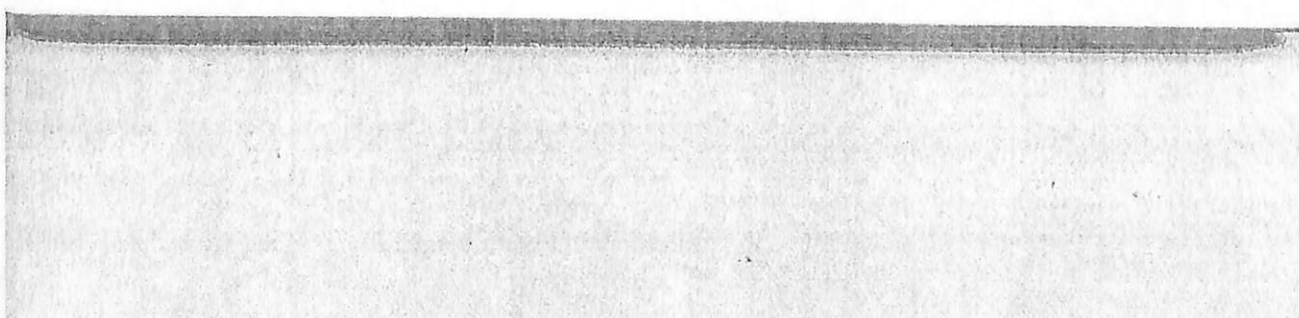
Cite this article as:

H. P. Ngang *et al.*: Preparation of titanium dioxide embedded ultrafiltration membrane: Properties and fouling evaluation. *Global J. Environ. Sci. Technol.* 2012, 2: 13

R E G I O N A L
SYMPOSIUM AND WORKSHOP
Membrane Science and Technology 2011

23 -26 August 2011

Nanyang Executive Centre
Nanyang Technological University



Performance analysis of TiO₂ embedded polyvinylidene fluoride membrane:
A study based on micellar enhanced ultrafiltration for dye removal

H.P. Ngang^a, A.L. Ahmad^a, B.S. Ooi^{a*}

^aSchool of Chemical Engineering, Engineering Campus, Universiti Sains Malaysia, Seri Ampangan 14000,
Nibong Tebal, Pulau Pinang, Malaysia

*: chobs@eng.usm.my

Membrane technology plays an important role as advanced water treatment process due to its low operational cost, and the capability of generating permeate of acceptable quality. However, membrane fouling is one of the main barriers for its applicability. Fouling can be reduced by pretreatment of feed solution, changing operating conditions or reengineered the surface properties of conventional membrane so that it is more fouling resistance or could perform self-cleaning.

In this study, polyvinylidene fluoride (PVDF) ultrafiltration (UF) membranes were prepared by phase inversion method with direct embedding of 1% to 5% TiO₂ nanoparticles into PVDF-DMAC solution. The addition of TiO₂ nanoparticles in the polymer matrix is expected to increase the membrane hydrophilicity and compaction strength. Nonetheless, the poor inorganic-organic interface as well as the TiO₂ clustering problem posed a serious morphology control difficulties. The changes of the membrane morphology as a result of TiO₂ addition could be reflected through the flux and rejection profile of the membrane. Contact angle and field emission scanning electron microscope (FESEM) are used to characterize the effect of TiO₂ nanoparticles on the membrane morphologies. The performance of composite UF membrane was characterized in terms of separation behaviour for SDS enhanced methylene blue.

It was found that by adding TiO₂ nanoparticles into the membrane matrix could alter the membrane flux and rejection. Optimum TiO₂ dosage was found around 3%, due to both results showing optimum flux and rejection. TiO₂ dosage higher than 3% will result in TiO₂ agglomeration and membrane morphology defect.

The mechanism(s) of flux decline during the UF processes were evaluated based on blocking filtration law in which the specific cake resistances in all filtration system were examined and compared.

Q: SDS -

R E G I O N A L
SYMPOSIUM AND WORKSHOP
Membrane Science and Technology 2011

23 -26 August 2011

Nanyang Executive Centre
Nanyang Technological University



Preparation and Characterization of TiO₂ Nanocomposite Membrane via Surface Exchange Method

Y.H. Teow, A.L. Ahmad and B.S. Ooi

^{*}School of Chemical Engineering, Engineering Campus
 Universiti Sains Malaysia, Seri Ampangan, 14300 Nibong Tebal, Penang, Malaysia

*: choobs@eng.usm.my

The use of membrane as advanced water treatment process exhibit high susceptibility toward fouling effect on membrane surface or into the membrane pores. Therefore, membrane fouling has become a major obstacle in order to achieve a high permeate flux over a prolonged period of membrane separation process. In this study, titanium dioxide nanoparticles (TiO₂) were incorporated into polyvinylidene fluoride (PVDF) membrane to produce a nanocomposite membrane via surface exchange method. The corresponding membrane polymer solution was prepared by dissolving 18% weight ratio of PVDF into 82% weight ratio of N,N-dimethyl formamide (DMF), which act as polymer solvent. In order to avoid agglomeration and maintain the stability of TiO₂ nanoparticles in the coagulation bath for membrane immersion, modification on TiO₂ nanoparticles is done via mechanical and chemical modification. TiO₂ nanoparticles in distilled water was sonicate for 15 minutes and then followed by adjusting the pH value of the TiO₂ solution to pH 4.0. Under this circumstance, a zeta potential ~30 mV is achieved in producing a reasonably stable dispersion of TiO₂ nanoparticles in water suspension. The distribution pattern of TiO₂ nanoparticles on the membrane surface was observed by energy-dispersive X-ray spectroscopy (EDX) mapping manner. The effect of the presence of TiO₂ nanoparticles on membrane pore size was studied using the capillary flow porometer. The membrane surface morphology and the wettability of nanocomposite membrane were characterized based on field emission scanning electron microscopy (FESEM) and contact angle goniometer respectively. The results showed that the presence of TiO₂ on membrane surface does not has significant effect on membrane pore size distribution, suggesting that surface exchange method is a suitable method used to prepare nanocomposite membrane without sacrifice of membrane rejection to enhance membrane functionality. On the other hand, the membrane wettability is slightly impaired by incorporating TiO₂ nanoparticles incorporation due to the surface roughness created by the TiO₂ nanoparticles.

- Using computer-aided
- pore size distribution
- why there is some drop at of initial rejection
- The value of Rejection (>95%)
- hydrophobicity - flux not an indicator

Surface Chemistry and Dispersion Property of Titanium Dioxide Nanoparticles in Water Suspension

Y.H. Teow^{a*}, A.L. Ahmad, and B.S. Ooi^a

School of Chemical Engineering, Engineering Campus
Universiti of Sains Malaysia, Seri Ampangan, 14300 Nibong Tebal, Penang, Malaysia.

*E-mail: yeithaan@hotmail.com

Keywords: Ultrasonication; Zeta Potential; TiO₂ Nanoparticles; Water Suspension.

Abstract

Increasing regulations and the need for a reliable potable drinking water supply have propelled the development of modern water treatment process. However, the use of membrane as advanced water treatment process has raised greatest attention for environmental remediation in producing high quality water with small footprint. Although membrane technology has become a dignified separation technology as a valuable means of solute filtering, solute that deposited on the membrane surface or into the membrane pores will consequence in membrane deterioration. To increase the membrane performance, membranes is then being cleaned physically, biologically or chemically. Among these fouling control strategies, chemical cleaning is the most effectual. However, high chemical usage in chemical cleaning will impose another additional environmental pollution. Therefore, in order to enhance the functionality of membrane against the fouling, titanium dioxide nanoparticles (TiO₂) are incorporated in the membrane filtration process. For application feasibility, the TiO₂ nanoparticles should exists in preferable small aggregate size and uniformly dispersed in the polymer film as mixed matrix membrane. The aim of this study is to investigate the effect of pH and ultrasonic irradiation time on the surface chemistry and the dispersibility of TiO₂ nanoparticles. Ultrasonication of TiO₂ nanoparticles in colloidal system is used for the breakage of TiO₂ nanoparticles agglomerates. On the other hand, reagglomeration of the suspension could be prevented by electrostatic stabilization through increasing the particles zeta potential. The results showed that for pH lower than 4.0, a stable PC-20 TiO₂ nanoparticles suspension could be produced with recorded zeta potential value more than 30 mV. While for P25 TiO₂ nanoparticles, it shows better dispersibility with broader pH range (< pH 5.0). Besides, ultrasonic irradiation time is found to contribute its effect on size distribution of TiO₂ nanoparticles in water suspension. The mean size of TiO₂ nanoparticles in water suspension decreased for longer ultrasonic irradiation time. However, after a rapid initial size reduction, continue ultrasonication lead to insignificant TiO₂ nanoparticles size reduction. It was found that pH and time of ultrasonication could play a very important role to produce suspension with good TiO₂ nanoparticles dispersion.

1. Introduction

With the rapid population and improper industrialization practices over the last two decades, it leads to the detrimental surface and underground water pollution. This phenomenon has raised concerns in the public for stringent environmental legislation and alternative technology in water treatment to increase both drinking water quantity and quality.

Membrane technology has become a dignified separation technology as a valuable means of solute filtering. The use of membrane as advanced water treatment process has raised greatest attention for environmental remediation in producing high quality water with small footprint. However, membrane fouling appears to be the main obstacles in water treatment process by membrane separation [Akthakul *et al.*, 2004; Chen *et al.*, 2006; Li *et al.*, 2009]. It is mainly caused by irreversible deposition of solute in the feed water on the hydrophobic membrane surface or into the membrane pores, which will consequence in water flux loss and solute selectivity change with time.

A number of approaches are available to alleviate the membrane fouling and increase the membrane performance have therefore been investigated. These methods include pretreatment of feed solution (flocculation and coagulation), periodic cleaning (physically, biologically or chemically) and hydrophilic modification of membrane surface. Although pretreatment of feed solution by chemical additives and chemical cleaning are effectual in lessening the membrane fouling, high chemical usage will impose another environmental pollution. Therefore, increasene in membrane hydrophilicity appears to be a good way for membrane fouling mitigation [Rahimpour *et al.*, 2008].

Due to its stability, commercial availability, high affinity to water and outstanding photocatalytic activity that can decompose organic foulants on membrane, titanium dioxide nanoparticles (TiO₂) appears to be an appealing additive in surface modification of membranes and has been received most attention by numerous researchers in recent years [Fujishima *et al.*, 2000; Li *et al.*, 2010; Mills and Hunte, 1997]. For application feasibility, it is crucial to obtain ultrafine and stable nanodispersions that will produce thin nanocomposite membrane films with low surface roughness and high surface area of TiO₂ nanoparticles [Cao *et al.*, 2006; Ebert *et al.*, 2004].

To reduce the surface roughness of the fabricated membrane films, the primary size of TiO₂ nanoparticles should be less than 20 nm. Although the primary size of most commercial nanoparticles is quite small (5-50 nm), the high surface energy of TiO₂ nanoparticles causes them to agglomerate in the synthesis and post-synthesis processes [Park *et al.*, 1993]. This leads to materials with primary particles in the nanometer range, but with variable and complex networks, shapes, and morphologies, all which impact the particle size distribution [Mandzy *et al.*, 2005].

Ultrasonication is a common method which is used to break up agglomerated TiO₂ nanoparticles. An energy transfer device, an ultrasonic probe, is employed to oscillate the TiO₂ liquid suspension, causing nucleation and solvent bubbles. Bubbles initiating and collapsing on the solid surface can be very effective in fracturing the TiO₂ aggregates. During ultrasonication, effectual fracturing on TiO₂ aggregates occurs due to the mechanical attrition [Kusters *et al.*, 1994; Park *et al.*, 1993]. It is initiates at surface flaws and imperfections. With prolong ultrasonication, large TiO₂ aggregates are broken down into smaller aggregates until there are no more defects to initiate the breakage. Further energy input results no significant attrition. The breakage of TiO₂ agglomerates by ultrasonic irradiation is controlled predominantly by specific energy input (power, time and dispersion volume) [Pohl and Schubert, 2004].

In order to form stable dispersions, it is not enough to break nanoparticles apart. Stabilization of colloidal dispersions of TiO₂ nanopowders by electrostatic interactions generates charges on the surface of TiO₂ nanoparticles, which acts as a barrier resulting from repulsive force, prevents two particles from adhere to each another, forming assemblies. Therefore, if the TiO₂ particles have sufficiently high repulsion charge, the dispersion will resist flocculation and the colloidal system will be stable. A common way to evaluate the stability of colloidal dispersions is by determining the magnitude of zeta potential. Zeta potential is function of the surface charge of the particles. In dispersions, where value of the zeta potential is close to zero (isoelectric point), particles tend to agglomerate. At higher negative or positive zeta potential (more than 30 mV or less than -30 mV), particles in dispersions tend to repel each other to prevent agglomeration occurs [Malvern Instruments

Ltd., 2011]. Titanium dioxide powders obtained from different manufacturers have dissimilar surface chemistries and as a result exhibit isoelectric points at different pH values [Mandzy *et al.*, 2005].

As long-term stability of TiO₂ nanodispersions is important for producing high quality nanocomposite membrane, breakage of the TiO₂ nanoparticles is become a critical issue. The objective of the present investigation is to study the breakage of commercial TiO₂ nanoparticles in water dispersions by mean of ultrasonic irradiation timemaintaining the stability of the nanoparticles based on solution pH.

2. Experimental

Two different types of nano titanium dioxide (TiO₂) photocatalytic powder were purchased from TitanPE Technologies, Inc., Shanghai, China (trade name: PC-20) and Sigma-Aldrich, St. Louis, MO, USA (trade name: P25). As reported by the manufacturer, the primary particle size of PC-20 TiO₂ nanoparticles was 20 nm, while P25 TiO₂ nanoparticles was ~21 nm respectively. Powdered TiO₂ with different weight was dispersed in 100 mL of distilled water in preparing different concentration of TiO₂ suspensions, 0.1 g/l and 0.05 g/l. The pH of TiO₂ suspensions was then adjusted to values between 2.0-9.0 with hydrochloric acid (HCl) or sodium hydroxide (NaOH) to obtain suitable zeta potential values in achieving electrostatic stability. Hydrochloric acid or sodium hydroxide was added drop-wise to the TiO₂ suspensions and it was mechanically stirred until it reached equilibrium with a specify pH value. The pH value of the TiO₂ suspensions was measured by using the pH meter (Eutech Instruments Pte. Ltd., Ayer Rajah Crescent, Singapore).

The ultrasonication was conducted using a Telsonic ultrasonic horn SG-24-500P (Telsonic Ultrasonics, Inc., Michigan, USA). The frequency of the ultrasound was kept constant at 18.4 kHz. The efficiency of ultrasonic in TiO₂ dispersion was evaluated by changing the sonication irradiation time of TiO₂ nanoparticles in water suspension. The dispersibility (changes in zeta potential) and TiO₂ particles size distribution under various pH and ultrasonic irradiation time were determined by using Malvern Zetasizer Nano ZS90 (Malvern Instruments Ltd., U.K.) on the basis of dynamic light scattering theory and cumulant method.

The crystal structure of TiO₂ nanoparticle was characterized by X-ray diffraction (XRD). XRD analysis was performed on TiO₂ nanopowder samples with a PHI-5400 X-ray diffractometer, operating in the theta-theta geometry using 18 kW Cu K α ($\lambda = 0.15418$ nm) radiation. The microstructure of TiO₂ nanoparticles was analyzed by a JEOL transmission electron microscope (TEM, JEOL JEM-200CX) at 120 kV. For the TEM observation, TiO₂ colloidal suspensions (0.1 g/l) was dropped on a carbon-coated grid and then dried at room temperature. For comparison purposes, both PC-20 TiO₂ and P25 TiO₂ nanoparticles were analyzed for XRD and TEM.

3. Results and Discussion

Crystal Structure and Particle Size of Commercial TiO₂ Nanoparticles

The crystal structure of both commercial TiO₂ nanoparticles (2 Θ) were examined by using the X-ray diffraction (XRD) analysis and the spectrums were illustrated in Fig. 1. Θ is the diffraction angle, measured with respect to the incident beam, while λ is constant-wavelength diffractometer. It is commonly known that TiO₂ particle has three different crystal forms, anatase, rutile and brookite [Mills and Hunte, 1997]. In the anatase structure, the oxygen form a cubic closest packing, and the titanium atom lie in octahedral voids, while in the rutile form, the oxygen are arranged approximately in a hexagonal closest packing, and the titanium atoms occupy a row pattern. The anatase has been reported by many researchers to be the most photoactive and stable nanoparticles for widespread applications, having good characteristic in bacteria killing, and hydrophilicity; whereas the rutile is comparatively photocatalytically inactive or much less active, although it shows strong photoactivity selectivity toward some cases. Therefore, anatase is suitable for membrane modification [Kim *et al.*, 2003]. Fig. 1 shows that the characteristic peaks of PC-20 TiO₂ nanopowder was located at 2 Θ of 25.319° which is close to the literature reported data 25.24° of anatase and a small rutile peak at 2 Θ of 27.460°. consists of 85% anatase and 15% rutile. It can be identified that the PC-20 TiO₂

nanopowder is majority composed of anatase, which promises excellent photocatalytic properties, hydrophilicity and anti-fouling characters. As for the diffraction pattern of P25 TiO₂ nanopowder, which is a mixture of 75% anatase and 25% rutile, the 2θ of eminent peaks are 25.230° for anatase and 27.376° for rutile.

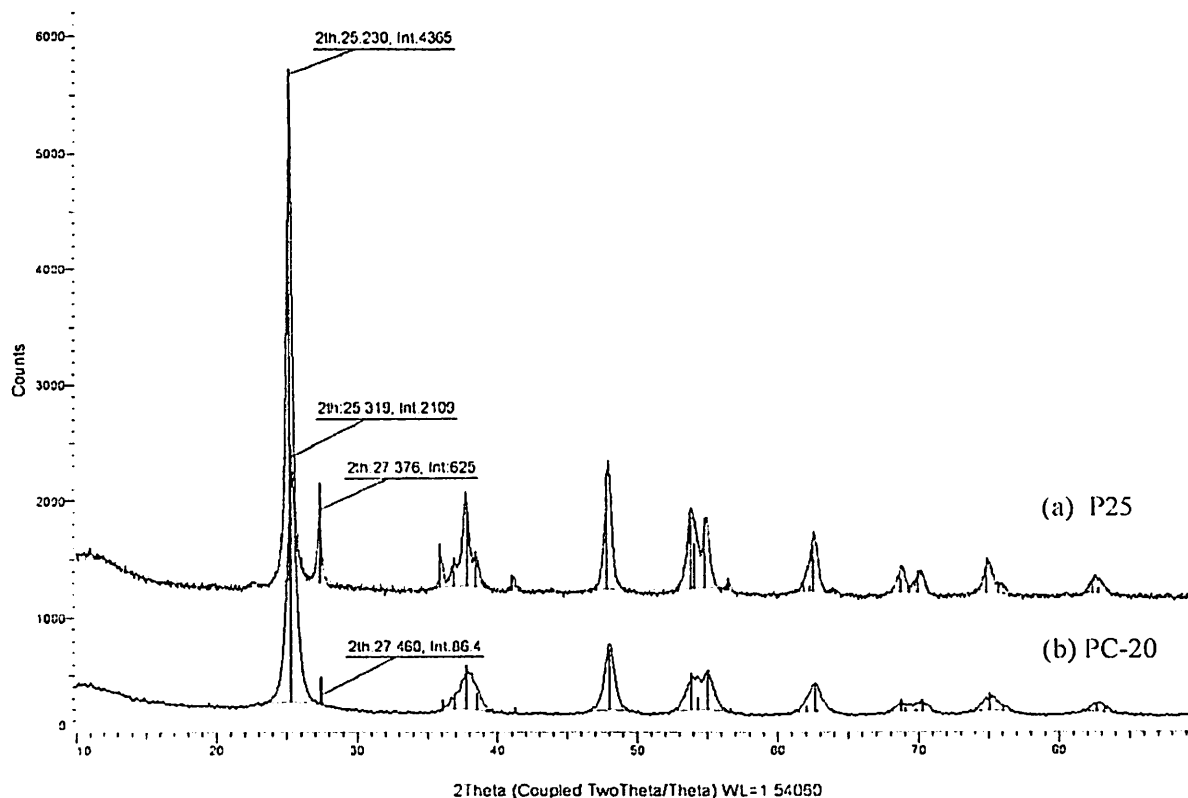


Figure 1: XRD Spectrum of the Commercial TiO₂ Nanopowder (a) P25 TiO₂ Nanopowder from Sigma-Aldrich (b) PC-20 TiO₂ Nanopowder from TiPE

Transmission electron microscopy (TEM) was employed to determine the primary particle size of PC-20 and P25 under high magnification (22k ×). The micrographs were shown in Fig. 2 (a) and (b) respectively. All these nanopowders were received in the dry form, and all contained large agglomerated particles. As shown in Fig. 2, TEM images of both anatase nanoparticles demonstrated almost spherical shape, can be seen in the form of black spots and they are extensively agglomerated with particle size varies from 75-200 nm and 50-150 nm correspondingly. The discrepancy between the particle sizes determined by TEM ascribe to the agglomeration tendency of each TiO₂ nanoparticles. With the smaller particle size distribution, P25 could dispersed more effectively by the ultrasonic irradiation than the PC-20. The agglomeration of TiO₂ particles mainly contribute by the drying procedure during preparation of TEM samples [Kim *et al.*, 2003].

Effect of pH on Colloid Stability of the TiO₂ Nanopowders

The optimal dispersing conditions for TiO₂ nanopowder and its long term stability was evaluated based on zeta potential. The zeta potential measurements (by means of the electrophoretic mobility) were performed on Malvern Zetasizer Nano ZS90 equipment. High absolute values of zeta potentials are necessary to achieve electro-statically stabilized TiO₂ nanoparticles in water suspension. In general, the criterion for suspension stability is thought

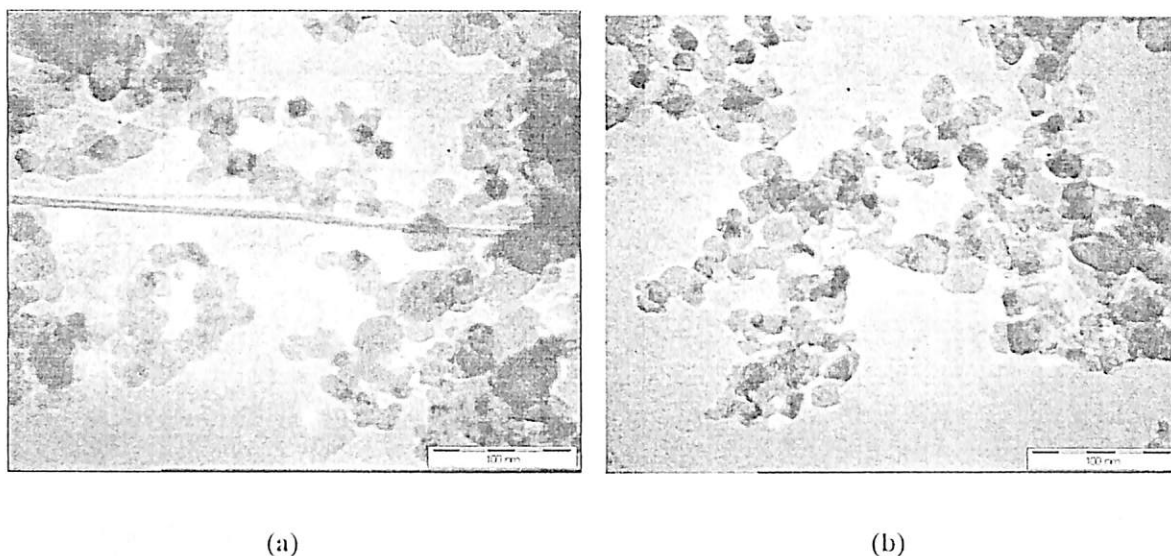


Figure 2: Morphology of Commercial Titanium Dioxide Nanopowder (a) PC-20 (b) P25

to be $|\zeta| > 30$ mV. A suspension is stable when the zeta potential value is less than -30 mV or greater than +30 mV.

Figure. 3 to Figure. 6 present the pH effect of different commercial TiO_2 nanopowder on the stability of the suspensions within the range of pH 2.0-9.0. Figure. 3 and Figure. 4 show the zeta potential while Figure. 5 and Figure. 6 show the mean particle size distribution of the colloids under different pH value and different concentration (0.1 g/l TiO_2 and 0.05 g/l TiO_2). The pH was adjusted with hydrochloric acid (HCl) immediately after 15 minutes of ultrasonic irradiation to the suspension. The isoelectric point (IEP) is a point (pH value) where the plot passes through zero zeta potential. At this IEP, the colloidal system is least stable. Referring to Figure. 3 and Figure. 4, the IEP for P25 TiO_2 takes place at neutral pH region while for PC-20 TiO_2 is at acidic pH region. The higher zeta potential of P25 compared to PC-20 shows that P25 could readily form stable colloids system within the pH range. For P25 TiO_2 with concent-

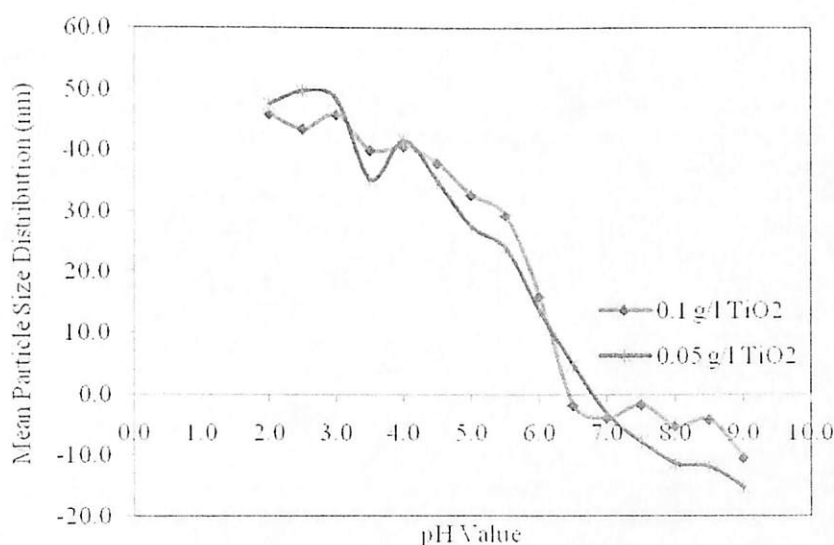


Figure 3: Zeta Potential Titration of P25 TiO_2 Suspension with Different Concentration

ration of 0.05 g/l and 0.1 g/l, high enough zeta potential values were obtained in the broader pH region (as shown in Figure. 3) and they are considered stable at pH value lower than 5.0 with comparable mean particle size (as shown in Figure. 5). On the contrary, PC-20 nanoparticles demonstrate its stability in suspension at pH value lower than 4.0. For PC-20 TiO₂, higher pH (> pH 6.5) could produce small size of TiO₂ particles as well, however, low in zeta potential value does not endorse its stability in water suspension. Nevertheless, the PC-20 nanopowder suspension flocculates very rapidly which is shown in Figure. 6 to have larger mean particle size distributions, should indicate a strong agglomeration of the nanoparticles.

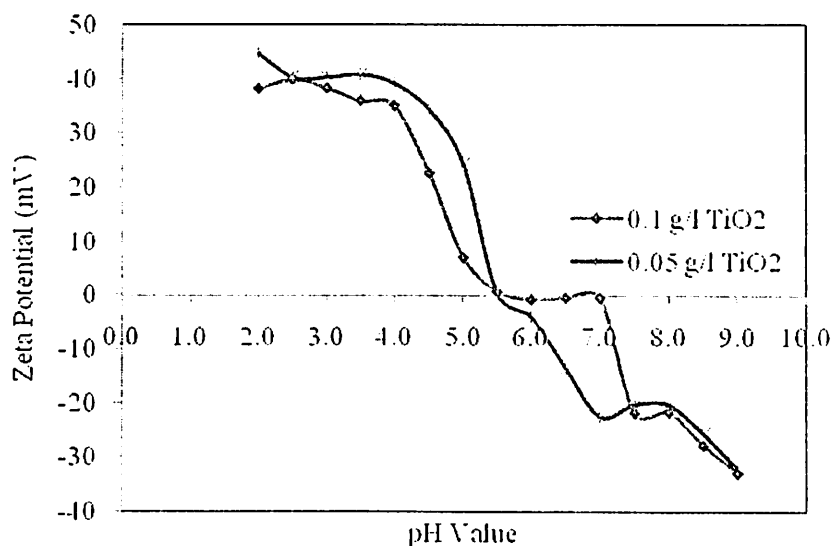


Figure 4: Zeta Potential Titration of PC-20 TiO₂ Suspension with Different Concentration

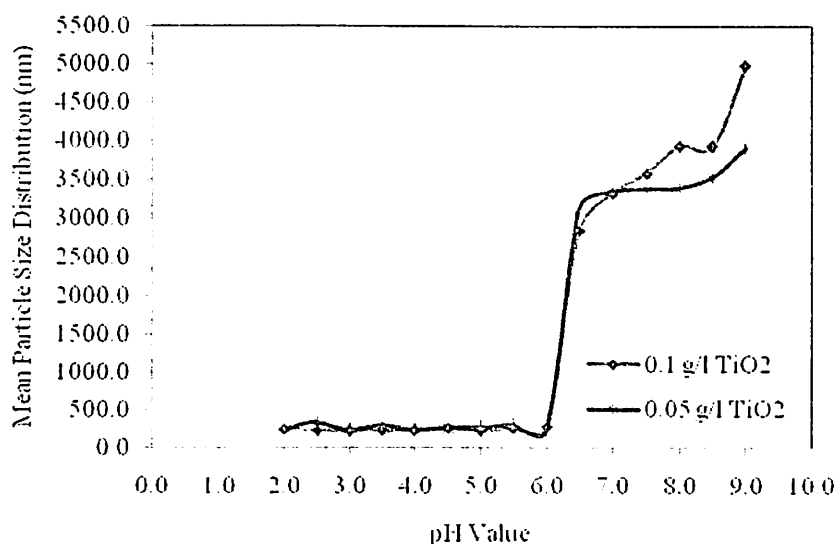


Figure 5: Mean Particle Size Distribution Versus pH for Different Concentration of P25 TiO₂ Nanoparticles

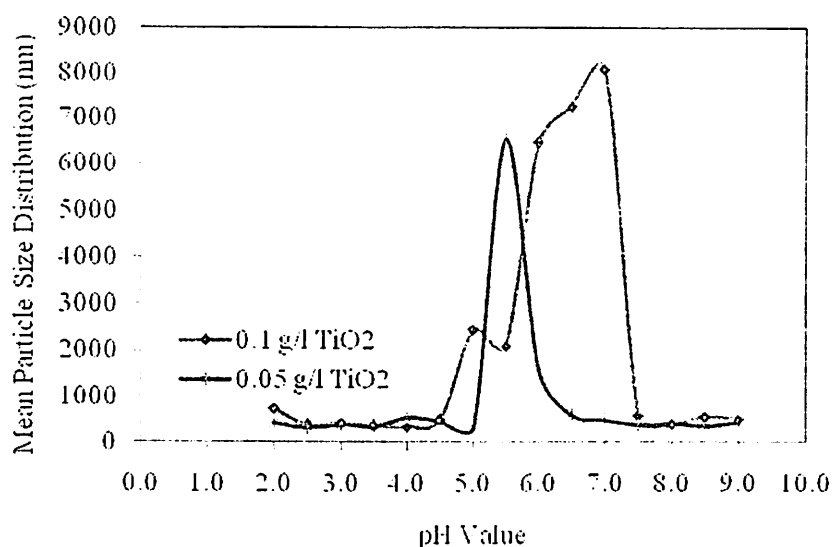


Figure 6: Mean Particle Size Distribution Versus pH for Different Concentration of PC-20 TiO₂ Nanoparticles

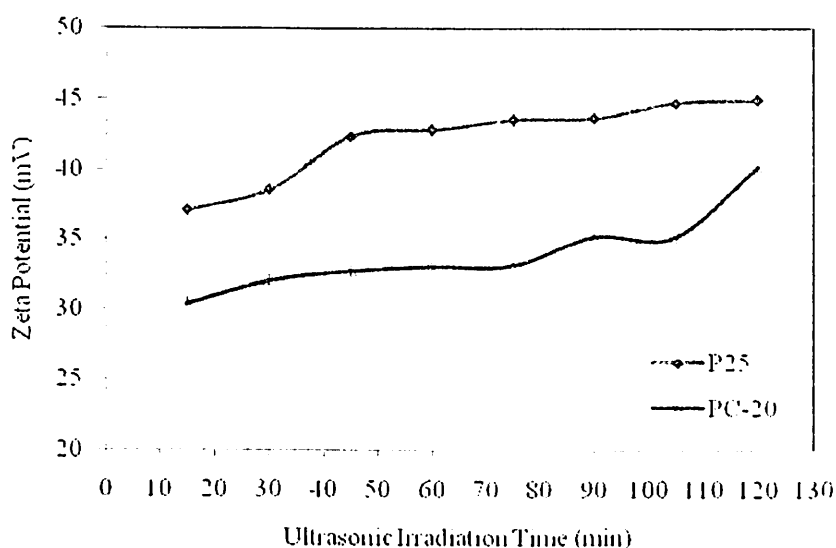


Figure 7: Change in TiO₂ Suspension Zeta Potential with Ultrasonic Irradiation Time

Effect of Ultrasonic Irradiation on TiO₂ Dispersion

The effect of ultrasonic irradiation time on the TiO₂ colloids stability were evaluated using Telsonic ultrasonic probe (frequency 18.4 kHz). The results were shown in terms of zeta potential and mean particle size in Figure. 7 and 8, respectively.

Initially, the attractive forces among the TiO₂ nanoparticles were stronger than repulsive forces; therefore the TiO₂ nanoparticles in water suspensions tends to agglomerate and the size of agglomerates was extensively large. The ultrasonication caused the breakage of the agglomerates, but shortly after the end of the ultrasonication, the particles reagglomerated back. Breakage of the powder was evident only when the suspensions were adjusted to pH 4.0 immediately after cessation of ultrasonication to permit any newly formed particles to be

stably dispersed. The suspension stability for both samples in water suspension along ultrasonic irradiation time was evaluated based on the zeta potential as showed in Figure. 7.

A noticeable observation is that, the zeta potential magnitude for both commercial TiO₂ nanoparticles are higher than +30 mV even under 15 minutes of ultrasonic irradiation, indicated that the stability of TiO₂ in water suspension. With larger zeta potential presented by P25 TiO₂ nanoparticles, it has higher tendency in repelling each another and there will be less or no tendency for the TiO₂ nanoparticles to approach and come together. For both commercial TiO₂ nanoparticles, the zeta potential was increased slowly over a comparatively long range of ultrasonic irradiation time.

Characterization of the mean particle size distribution was performed by Dynamic Light Scattering (DLS). DLS measures the Brownian motion of the particles and relates it to the particle size. The ultrasonication caused the breakage of the agglomerates into smaller particle size with the increasing of ultrasonication period. Referring to Fig. 8, for PC-20, there is no significant change in particle size was observed for ultrasonic irradiation time up to 60 min, suggesting that the attractive forces between primary PC-20 TiO₂ nanoparticles are stronger. From 60 min ultrasonic irradiation time onwards, the mean dispersed particle size of PC-20 TiO₂ aggregates in suspension reduced as irradiation time increased and then reached the smallest value (290.5 nm) at 105 minutes of ultrasonic irradiation time. Following that, the particle size remain constant as it is the minimum particle size for PC-20 TiO₂ nanoparticles can be reduced by using ultrasonication. On the other hand, the mean dispersed particle size was less than 200 nm and remained almost constant when P25 TiO₂ nanopowder was sonicated for 30 min. The particle size of PC-20 TiO₂ dispersed by ultrasonic irradiation was more widely distributed as compared to that of P25 TiO₂, indicates that the P25 TiO₂ nanoparticles is more responsive towards ultrasonic irradiation in producing smaller TiO₂ nanoparticles.

While both TiO₂ nanopowder was reported by the manufacturer to have very small particle size which is 20 nm and ~21 nm for PC-20 and P25 respectively, it was very difficult to break into its preliminary particle size using ultrasonication, none of them was successfully broken into their primary particle size within 2 hours of irradiation time.

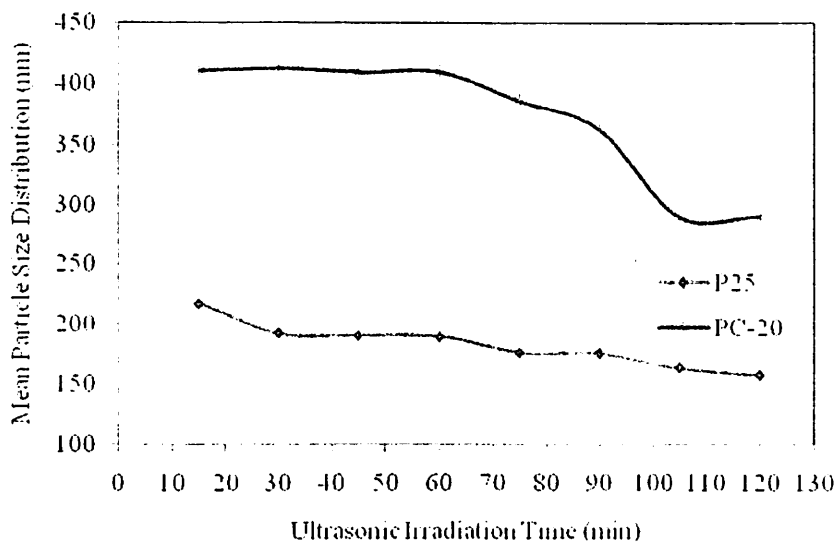


Figure 8: Change in Size of Agglomerates/Aggregates with Ultrasonic Irradiation Time

The degree of cluster breaking is highly depend on the the interaction force of inter-particle. A small adjustment on manufacturing process will results in extensive changes in particle properties and its size distribution. However, once agglomeration occur in the synthesis

process, it is very difficult to break the particle apart into their primary particle size. Additionally, dark sediment was eminent at the bottom of the ultrasonicated dispersions, which is attributed to the erosion of the ultrasonic probe. Long period of ultrasonic irradiation time does not give a promising result in further reducing the particle size of TiO₂ to higher extent, but resulted in contamination of the samples.

4. Conclusion

Fracture mechanism was observed in the ultrasonication of commercial titanium dioxide nanopowders. However, there was no evidence that for prolong ultrasonic irradiation could further break the commercial TiO₂ nanopowders into their primary particle size. During the ultrasonic breakage, electrostatic stabilization of TiO₂ dispersions prevented newly formed particles from reagglomeration by adjusting the pH. Conditions have been optimized to produce stable commercial TiO₂ nanoparticle in water suspensions. P25 TiO₂ nanopowder was able to be suspended and comprises smaller TiO₂ nanoparticle size with high zeta potential value in broader pH range (< pH 5.0) compared with PC-20 TiO₂ nanopowder (< pH 4.0). This observation indicates that P25 TiO₂ nanopowder resulted better dispersion in water suspension. Almost immediate agglomeration of mechanically broken particles was observed when pH value is higher than 5.0 and 4.0 for P25 TiO₂ nanoparticles and PC-20 TiO₂ nanoparticles respectively. In this study, the effect of ultrasonic irradiation time on the TiO₂ nanoparticles dispersibility has also been clarified. The results showed that 15 minutes is the best determined ultrasonic irradiation time to obtain well dispersed TiO₂ suspensions and stable in time for both commercial TiO₂ nanopowders. Further increased in ultrasonic irradiation time does not give much effect in reducing the mean particle size of TiO₂ nanoparticles.

Acknowledgement: The authors wish to thank the financial support granted by Universiti Sains Malaysia (RU Grant) (1001/PJKIMIA/811172) and Malaysia Toray Science Foundation (MTSF) Science and Technology Research Grant 304/PJKIMIA/6050179/M126.

References

- Akthakul, A., Salinaro, R. F. and Mayes A. M. (2004). Antifouling membranes with subnanometer size selectivity. *Macromolecules*. 37, 7663-7668.
- Cao, X. H., Ma, J., Shi, X. H. and Ren, Z. J. (2006). Effect of TiO₂ Nanoparticle size on the Performance of PVDF Membrane. *Appl. Surf. Sci.* 253, 2003-2010.
- Chen, D., Weavers, L. K., and Walker, H. W. (2006). Ultrasonic control of ceramic membrane fouling: effect of particles characteristics. *Water Res.* 40, 840-850.
- Domany, Z., Galambos, I., Vatai, G. & Bekassy Molnar, E. (2002). Humic substances removal from drinking water by membrane filtration. *Desalination*. 145, 333-337.
- Ebert, K., Fritsch, D., Koll, C. and Tjahjaviguna, C. (2004). Influence of Inorganic Fillers on the Compaction Behaviour of Porous Polymer Based Membranes. *J. Membr. Sci.* 233, 71-78.
- Fujishima, A., Rao, T. N. and Tryk, D. A. (2000). Titanium Dioxide Photocatalysis. *J. Photochem. Photobiol. C: Photochem. Rev.* 1, 1-21.
- Kim, S. H., Kwak, S. Y., Sohn, B. H. and Park, T. H. (2003). Design of TiO₂ Nanoparticle Self-Assembled Aromatic Polyamide Thin-Film-Composition (TFC) Membrane as an Approach to Solve Biofouling Problem. *J. Membr. Sci.* 211, 157-165.
- Kusters, K., Pratsinis, S., and Thoma, S. (1994). Energy-Size Reduction Laws for Ultrasonic Fragmentation. *Powder Technology*. 80, 253-263.
- Li, C. C., Chang, S. J. and Tai, M. Y. (2010). Surface Chemistry and Dispersion Property of TiO₂ Nanoparticles. *J. Am. Ceram. Soc.* 93 (12): 4008-4010.
- Li, J. H., Xu, Y. Y., Zhu, L. P., Wang, J. H. and Du, C. H. (2009). Fabrication and Characterization of a Novel TiO₂ Nanoparticle Self-Assembly Membrane with Improved Fouling Resistance. *J. Membr. Sci.* 326, 659-666.
- Mandzy, N., Grulke, E. and Druffel, T. (2005). Breakage of TiO₂ Agglomerates in Electrostatically Stabilized Aqueous Dispersions. *Powder Technology*. 160, 121-126.

- Mills, A., and Hunte, S. L. (1997). An Overview of Semiconductor Photocatalysis. *J. Photochem. Photobiol. A: Chem.* 1, 108.
- Park, B., Smith, D. and Thoma, S. (1993). Determination of Agglomerate Strength Distributions: Part 4. Analysis of Multimodal Particle Size Distributions. *Particle Technology.* 76, 125-133.
- Pohl, M. and Schubert, H. (2004). Dispersion and De-Agglomeration of Nanoparticles in Aqueous Solutions. International Congress for Particle Technology Partec 2004. Nuremberg, Germany, 16-18 March 2004.
- Rahimpour, A., Madaeni, S. S., Taheri, A. H. and Mansourpanah, Y. (2008). Coupling TiO₂ Nanoparticles with UV Irradiation for Modification of Polyethersulfone Ultrafiltration Membrane. *J. Membr. Sci.* 313, 158-169.
- Sato, K., Li, J. G., Kamiya, H., and Ishigaki, T. (2008). Ultrasonic Dispersion of TiO₂ Nanoparticles in Aqueous Suspension. *J. Am. Ceram. Soc.* 91 (8): 2481-2487.
- Sentein, C., Guizard, B., Giraud, S., Ye, C. and Ténégal, F. (2009). Dispersion and Stability of TiO₂ Nanoparticles Synthesized by Laser Pyrolysis in Aqueous Suspensions. *J. Phys: Conf. Ser.* 170, 012013.
- Seung, Y. K., Sung, H. K. and Soon, S. K. (2001). Preparation and Characterization of TiO₂ Nanoparticle Self-Assembled Aromatic Polyamide Thin-Film-Composite (TFC) Membrane. *Environ. Sci. Technol.* 35, 2388-2394.

Preparation of TiO₂ Embedded Ultrafiltration Membrane: Properties and Fouling Evaluation

H.P. Ngang^{*}, A.L. Ahmad, and B.S. Ooi

School of Chemical Engineering, Engineering Campus,
Universiti Sains Malaysia, Seri Ampangan 14300, Nibong Tebal, Pulau Pinang, Malaysia

^{*}E-mail: hueyping0404@gmail.com

Keywords: Micellar Enhanced Ultrafiltration; PVDF; TiO₂; Methylene Blue; Sodium dodecylsulfate.

Abstract

Micellar enhanced ultrafiltration (MEUF) is a separation method which can be used for dye removal. The rejection of a cationic dye, methylene blue by nanocomposite membrane was examined with and without an anionic surfactant, sodium dodecylsulfate (SDS). The dye removal by nanocomposite membrane in the absence of SDS surfactant is poor due to separation by adsorption mechanism only. However, with the presence of 20 mM surfactant in feed solution, dye removal efficiency was increased dramatically. Membrane with 1 wt% TiO₂ exhibited maximum dye removal. The effect of TiO₂ nanoparticles on the physical properties of PVDF membranes were characterized based on contact angle and field emission scanning electron microscope (FESEM). Membrane performances were evaluated for membrane with different TiO₂ concentration in the casting solution. It was found that by adding TiO₂ nanoparticles into the membrane matrix, membrane hydrophilicity could be enhanced which is a desired property of membrane for water purification. However, at higher content of TiO₂, membrane wettability might be impaired due to the roughness created by the agglomeration of TiO₂ on the surface. Besides, addition of TiO₂ could significantly alter the membrane morphology or pores size. By adding TiO₂, interconnected pores were found on the membrane surface. Effect of fouling mitigation increased with nanoparticle dosage, but it reached a limiting content above which fouling mitigation efficiency becomes insignificant. Optimum TiO₂ dosage was found around 3 wt%. Higher dosage will result in TiO₂ agglomeration. This is not a desired phenomenon because it caused membrane pore blocking, membrane defect and reduction of catalytic surface area.

1. Introduction

Dye containing waste stream had caused a series of environmental problems. Among various type of dye, methylene blue (MB) for example has been used in paint production, textile finishing, and as a sensitizer in photo-oxidation of organic pollutants [Bielska and Szymanowski, 2006]. Various methods are available for the removal of colored dyes from wastewater such as adsorption [Wang *et al.*, 2005], flocculation/coagulation method [Golob *et al.*, 2005], biodegradation [Seshadri *et al.*, 2004], and membrane separation [Koyuncu *et al.*, 2004], but each method has their own disadvantages. Activated carbon is always being considered for dye adsorption but it is an expensive adsorbent due to its high cost of manufacturing and regeneration. The operating cost for flocculation is high and the rejection of dye is poor. Membrane based separation processes have emerged as an attractive alternative to the conventional processes in the various industrial applications due to their unique separation capability, easy to scale-up and low energy consumption [Sarkar *et al.*, 2009]. The nanofiltration and reverse osmosis now have been recognized as the most suitable techniques for the removal of several toxic dyes. However, its major disadvantages are due to its dense membrane structure, high energy consuming process and higher operating pressure is required to obtain desired performance. Furthermore, decline in permeate flux due to adsorption of organic compound caused serious issues related to membrane fouling [Koyuncu *et al.*, 2004].

To overcome this drawback, ultrafiltration appears to be more attractive for wastewater treatment because its offer high fluxes at relatively low pressures [Bielska and Prochaska, 2007]. One of the possible methods to remove organic dyes from wastewater is micellar enhanced ultrafiltration (MEUF) [Zaghbani *et al.*, 2007]. Many studies have shown that MEUF is suitable method for the removal of organic pollutant [Huang *et al.*, 2010, Zaghbani *et al.*, 2007]. MEUF involves the addition of surfactant to wastewater in order to remove organic pollutants effectively and economically. The surface activity of surfactants are derived from their amphiphilic structure that posses both hydrophilic and hydrophobic parts in one molecule [Aksu *et al.*, 2010]. Surfactant monomer will assemble to form micelles when the surfactants are added into the methylene blue feed solution at levels equals to or higher than their critical micelle concentrations (CMCs). The CMCs of SDS is 8mM in distilled water.

Micellar enhanced ultrafiltration is a promising method used in waste water treatment process. However, one of the main barriers to greater use of membrane technology is membrane fouling. Membrane fouling is proven can be reduced by addition of hydrophilicity materials to the membrane casting solution [Rahimpour and Madaeni, 2007]. On the other hand, the preparation of novel organic-inorganic composite membranes with control properties has been widely used recently years. A more recent approach to improve the membrane antifouling properties is by using TiO₂ nanoparticles on membrane structure and surface. TiO₂ particles can degrade organic foulant effectively with radiation of UV light [Rahimpour *et al.*, 2008]. TiO₂ had received the most attention among different nanoparticles due to its stability, availability, and promise for applications such as painting, catalysis and photocatalysis. battery, cosmetic, etc [Cao *et al.*, 2006].

In this paper, neat PVDF membrane and PVDF/TiO₂ composite membrane with a defined morphology, high permeability, and enhanced hydrophilicity were prepared by phase inversion methods. The effect of TiO₂ nanoparticles concentration on the rheology, morphologies and the performances of PVDF membranes properties were characterized based on polymer solution viscosity, membrane contact angle and field emission scanning electron microscope (FESEM) respectively. The neat and composite membranes were also compared in terms of the effectiveness of MEUF separation behaviour for methylene blue with and without SDS surfactants.

2. Methodology

Chemicals

Polyvinylidene fluoride (Solef® PVDF) was supplied from Solvay Solexis, France. N-methyl-2-pyrrolidone (NMP), sodium dodecyl sulfate (SDS) and methylene blue were purchased from Merck, Germany. TiO₂ PC-20 (20nm) was purchased from TitanPE Technologies, Inc., Shanghai. Distilled water was used for all experiment.

Membrane Preparation

The predetermined amount of TiO₂ was dispersed in n-methylpyrrolidone under sonication for 15 minutes. 15 wt% of PVDF was then dissolved into the TiO₂ solution and stirred at 60-70°C for 4 hours to ensure a complete dissolution of the polymers. The solution was left to stir overnight at 40°C. The final solution was then subjected to further sonication for 30 minutes and let to cool down to room temperature. The solution was cast on the tightly woven polyester using Automatic film applicator (Elcometer 4340, E.U.) at 200 μm thickness. It was then immediately immersed into the water bath of distilled water and let the phase inversion occur for 24 hours to remove the residual solvent. PVDF membrane was kept in distilled water prior to use.

Polymer Solution Characterization

The viscosity of polymer solution was measured by a Model DV-III Programmable Rheometer (Brookfield, USA) at 25°C to evaluate the rheology effect of polymer solution brought by different dosage of TiO₂ nanoparticles added. The rotation speed was fixed at 10 rpm and the samples were measured after shearing for 30 seconds. The viscosity measurement were repeated for 3 times for each sample and then averaged to minimize the experimental error.

Membrane Characterization

Contact Angle

The hydrophilicity change caused by the addition of nanoparticles on membrane top surface was characterized using water contact angle instrument (Rame-Hart Model 300 Advanced Goniometer) based on sessile drop methods. All membranes film were cut into square coupons and mounted onto glass slides. Water drops were controlled at constant volume using the motor-driven syringe. The acquired images were analyzed using DROPimage software to obtain the measurement of contact angles. To minimize experimental error, the contact angle measurement were repeated 5 times for each sample and then averaged.

Scanning Electron Microscope

The top surface morphologies of the fabricated PVDF membranes were observed under Field Emission Scanning Electron Microscope (FESEM CARL ZEISS SUPRA 35VP, Germany). Image magnifications were 20,000x for surface views at 5kV. All membrane samples were dried at room temperature and coated with a thin layer of gold before observation.

Dead-End Ultrafiltration Experiments

The UF experiments were performed in a dead-end stirred cell (Amicon 8200, Millipore Co., USA) with a capacity of 200ml, where the disc membrane has a diameter of 60mm with a geometric area of 28.27cm² (excluding the area cover by the O-ring). The applied pressure of the filtration system was controlled by N₂ gas cylinder. The stirring speed was maintained at 200rpm using the controllable magnetic stirrer (Heidoph MR3000D, Germany). PVDF membrane was first compacted with distilled water at 2.5 bar until constant pure water flux is achieved to minimize compaction effects. The cell was then emptied and refilled with methylene blue feed solution immediately; and the pressure was lowered to operating pressure of 1.5 bar. The flux and filtration efficiency were measured after a total of 10ml of permeate were collected.

The pure water flux (J) is calculated by Eq.(1):

$$J = \frac{V}{A \Delta t} \quad (1)$$

where V is the volume of permeated water, A (m^2) is the membrane area, and Δt (h) is ultrafiltration operation time. The concentration of methylene blue with and without surfactant was measured with a Visible Spectrophotometer (Thermo Spectronic Model Genesys 20, USA) at the maximum absorbance at 662 and 665nm accordingly. The filtration efficiency in removing the dye from the feed solution was calculated using Eq.(2):

$$R(\%) = \left[1 - \frac{C_p}{C_0}\right] \times 100 \quad (2)$$

where C_p is the dye concentration in the permeate and C_0 is the initial concentration of the dye in the feed.

3. Results and Discussion

Effect of TiO_2 Dosage on Viscosity of Membrane Dopes

The neat PVDF-NMP membrane dope was a yellow transparent viscous solution while the TiO_2 added dopes were white viscous solutions due the presence of TiO_2 nanoparticles. Membrane dopes with TiO_2 nanoparticles were obviously more viscous than the neat membrane dope. As shown in Figure 1, the addition of the TiO_2 nanoparticles could significantly increase the viscosity of the membranes dopes. The membrane dopes viscosity is an important parameter that influence the rheological property of the polymer solution which imposed kinetic effect during the membrane formation process. As a result, membrane morphology is influenced by dopes viscosity. Higher dopes viscosity would prevent the creation of macroporous structure caused by instantaneous demixing, however, higher dopes viscosity would be a barrier for membrane formation which produced less interconnected sponge structure that impaired the water flux which will be discussed next.

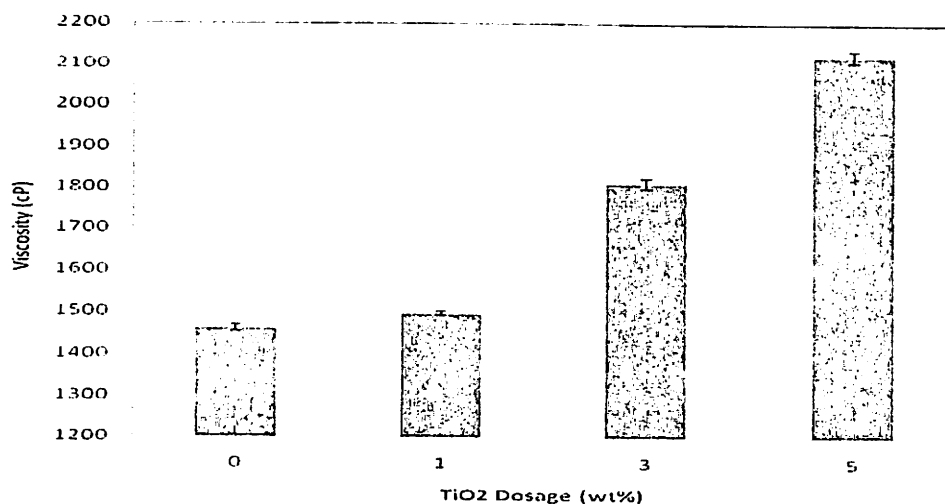


Figure 1: Viscosity of PVDF Nanocomposite Ultrafiltration Membrane Dopes

Effect of TiO_2 Dosage on Membrane Morphology

Figure 2 shows the surface SEM images of membrane prepared from PVDF/NMP systems with different content of TiO_2 nanoparticles. The addition of TiO_2 into the polymer matrix demonstrated an obvious change of membrane morphology. As discussed in section 3.1, the loaded amounts are able to change rheological behaviour of polymer solution. Higher dope viscosity will affect the mass transfer of solvent and non-solvent during the phase inversion process which resulted in higher resistance of solvent diffusion between the polymer solution and the coagulation bath. On the other hand, due to the hydrophilic nature of TiO_2 , the thermodynamic behavior of solution is also affected. The penetration velocity of water into

nascent membrane increased with increasing TiO₂ loading during the phase inversion method. The nonsolvent influx is expected to be increased due to the pulling force of the nanoparticles which enhanced the instantaneous liquid-liquid demixing. Solvent molecules can diffuse more readily from the polymer matrix to the coagulation bath due to the decrease interaction between polymer and solvent molecules by barrier created by nanoparticles [Kim *et al.*, 2001]. As a result, spinodal demixing is likely to occur which resulted in a highly connected porous structure. However, beyond 3 wt% of TiO₂ dosage, it was clearly seen on the surface whereby TiO₂ agglomeration starts to occur. Agglomeration of TiO₂ is an unwanted phenomenon as it might block the pores of membrane and cause membrane defect. At the same time, it reduced the surface area of the nanoparticles and consequently reduced its photocatalytic properties.

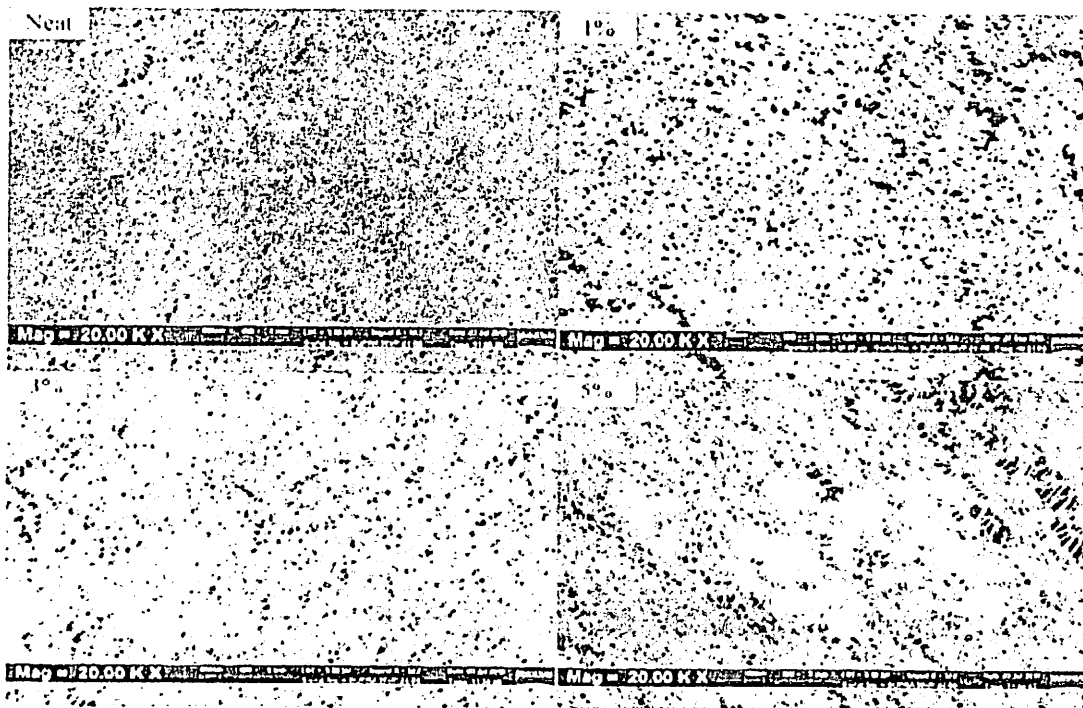


Figure 2: SEM images of PVDF nanocomposite ultrafiltration membrane surface

Effect of TiO₂ Dosage on Membrane Surface Wettability

The membranes were characterized in term of surface wettability. Membrane surface wettability is one of the important membrane properties which could affect the flux and fouling behaviour of the composite membrane. TiO₂ particles which contain hydroxyl group on its surface were responsible for the hydrophilicity increment and fouling mitigation [Yuliwati and Ismail, 2010; Wu *et al.*, 2008]. Therefore, addition of TiO₂ is expected to produce a membrane with reduced contact angle. The results of contact angle shown in Figure 3 could verify this phenomenon. When the TiO₂ dosage is increased from 1 to 5 wt%, it was found that contact angle of the membra . Water contact angle values decreased with the increasing dosage of TiO₂ nanoparticles indicated that TiO₂ do contribute in increasing the membrane hydrophilicity. The same phenomenon also observed by Bae and Tak (2005). However in our study, we found that further increasing of TiO₂ dosage above 3 wt% will cause the increasing of contact angle. It is an unwanted phenomenon as it might impaired the water flux of membrane. This phenomenon is mainly due to the increasing surface roughness of agglomerated TiO₂ nanoparticle as shown in the SEM picture of Figure 2. Young's Equation related the surface tension in such a way:

$$\gamma_{SL} + \gamma_{LV} \cos \theta = \gamma_{SV} \quad (3)$$

Where,

$\gamma_{SL}, \gamma_{LV}, \gamma_{SV}$ are the surface tensions of solid-Liquid, Liquid-vapor and solid-vapor respectively. However, Equation (3) is suitable for non-porous surface. For porous surface, Equation (3) has been modified based on its effective porosity (ϵ) whereby:

$$\cos \theta = \frac{1}{\gamma_{LV}} (1 - \epsilon) [\gamma_{SV} - \gamma_{SL}] \quad (4)$$

Positive value of $\gamma_{SV} - \gamma_{SL}$ means that the solid surface is hydrophilic whereas negative value means hydrophobic surface. For membrane surface with contact angle less than 90° , it is considered a hydrophilic surface. Therefore, at higher surface roughness, surface effective porosity is likely to be increased and caused the increased of surface contact angle.

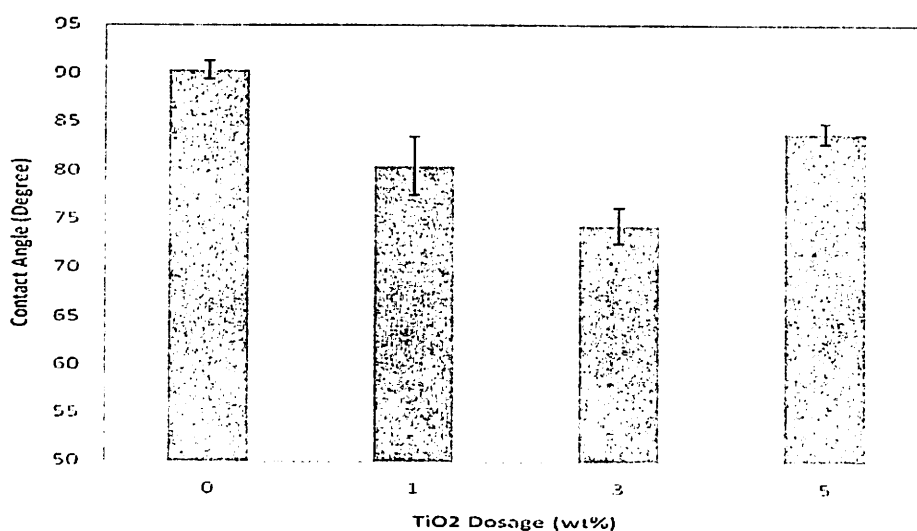


Figure 3: Contact angles of membrane with different TiO₂ dosage

Membrane Performance

Pure Water Flux

Pure water flux experiment is an important parameter to evaluate the performance of membrane. It was carried out to investigate the influence of TiO₂ dosage on permeability. Figure 4 shows that the pure water flux was enhanced with the increased of TiO₂ dosage and achieved its maximum value at 3 wt%. TiO₂ incorporated membranes show higher flux due to the increasing hydrophilicity of composite membrane as discussed in section 3.3. TiO₂ composite membrane could be more hydrophilic than neat polymeric membrane due to the higher affinity of TiO₂ towards water [Bae and Tak, 2005]. The hydroxyl group could attract water molecules to pass through the membrane. Besides, bigger and interconnected pore structure of composite membrane as a result of spinodal decomposition provides less resistance to water permeation. Nonetheless, at 5 wt% of TiO₂ dosage, a significant decreased of pure water flux was observed. This observation is due to the agglomeration of TiO₂ as shown in the SEM images which block the pores of the membrane, and subsequently provide higher resistance for water permeation. This phenomenon is in accordance to what was observed by Soroko and Livingston (2009) in their research who found that with the presence of 10 wt% TiO₂ in the polyimide matrix resulted in lower permeation flux.

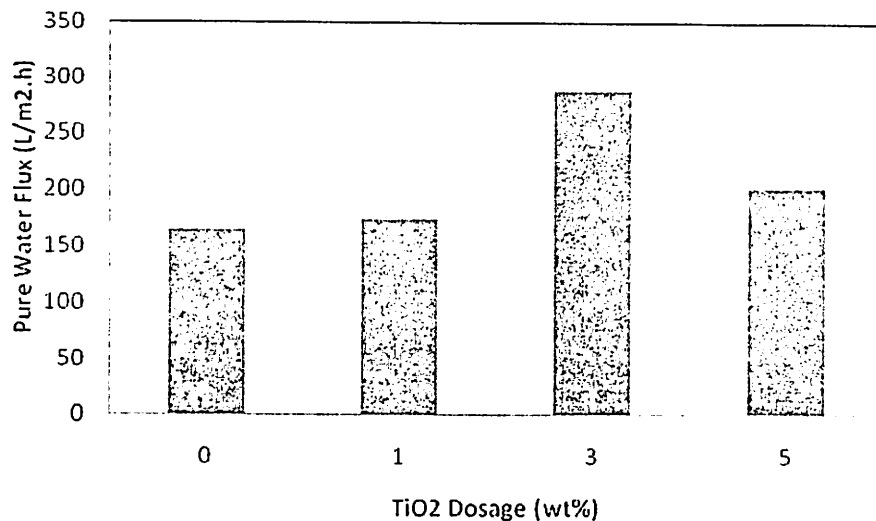


Figure 4: Effect of TiO₂ contents on pure water flux

Membrane Rejection

The study on the effect of TiO₂ concentrations on membrane rejection was also carried out. Figure 5 and Figure 6 show the results of dye removal using the TiO₂ composite membrane without and with the presence of SDS, respectively. The retention of MB molecules was found to be negligible (less than 12%) in the absence of surfactant. The minor retention could be attributed to the adsorption phenomenon of dye which takes place at the surface and in the pores of membrane. Since the MB molecules are much smaller than membranes pore size, no steric hindrance is expected. Moreover, the net negatively charged surface of PVDF could provide a superior adsorption site for the positively charged methylene blue which enhanced the dye removal inspite of the small solute to pore ratio. Membrane with 1 wt% TiO₂ dosage exhibit better dye removal compared to the neat membrane. It is most probably due to the higher surface area of TiO₂ nanoparticles which provide the extra adsorption sites in membrane for adsorption (better rejection). By further adding TiO₂, the overall porosity of the membrane will be reduced due to the particle agglomeration and pore blocking. As a result, a decrease of dye retention was observed.

On the other hand, with the presence of 20 mM surfactant in the feed solution, dye removal was enhanced dramatically. These surfactant molecules could form micelles that solubilised the MB. As a result, a solution with higher solute to pore ratio was created. This facilitates the micellar enhanced ultrafiltration. The added surfactant molecules with higher concentration than the critical micelle concentration (CMC) will form micelles which will be retained on the surface of the TiO₂ composite membrane. The results showed that the electrostatic interaction between MB and surfactants plays an important role in the MB removal.

Membrane Antifouling Performance With Dye Solution as Model

The influence of TiO₂ concentrations on membrane fouling was studied. Figure 7 and Figure 8 showed the relative permeate flux results of the ultrafiltration of dye solution without and in present of SDS using the TiO₂ composite membrane. The relative permeate flux of MB molecules without surfactant showed in Figure 7 remain constant with time due to MB molecules are much smaller than membranes pore size, no steric hindrance is expected.

On the other hand, a relative permeate flux decline is observed with the presence of 20 mM surfactant in feed solution as shown in Figure 8. Membrane with 1wt % TiO₂ showed

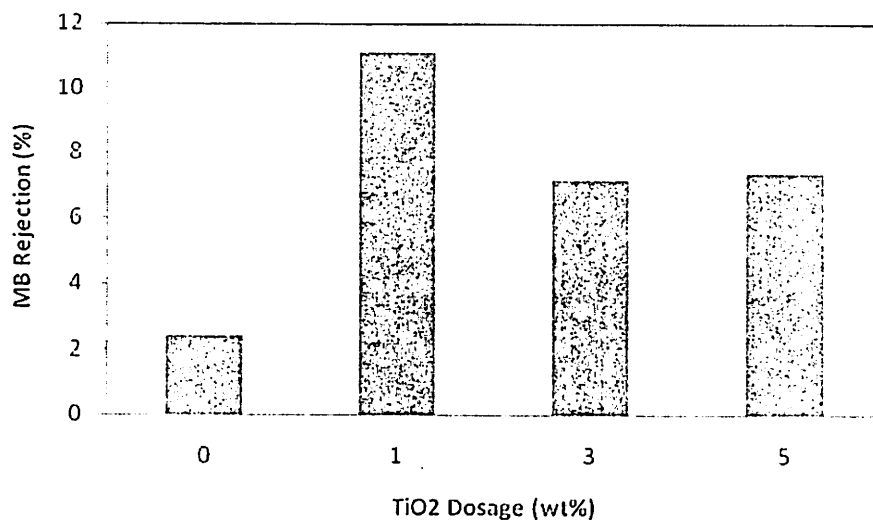


Figure 5: Extent of Dye Removal by Membrane With Different TiO₂ Dosage Composite Membrane

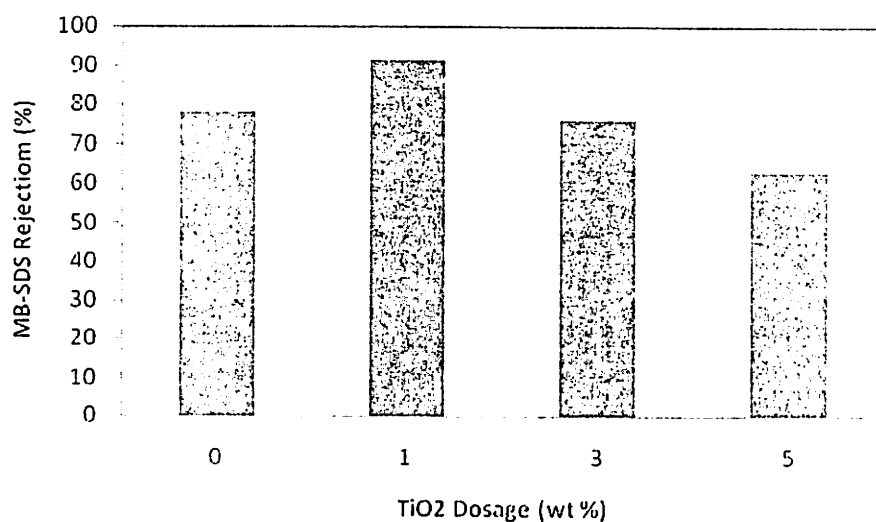


Figure 6: Extent of SDS Enhanced Dye Removal by Membrane With Different TiO₂ Dosage Composite Membrane

highest relative permeates flux declination as shown in Figure 8. The rapid flux declination is most likely due to the build up of cake layer on the membrane surface as the smaller pore size would detain the micelles more effectively. During ultrafiltration, the higher surfactant concentration near the membrane compared to bulk surfactant concentration [Zaghbani *et al.*, 2007] caused the flux decline. Nevertheless, beyond 3 wt% TiO₂ composite membrane onwards, the defect on the membrane surface which resulted in the poorer MB rejection and subsequently slower dye layer buildup. These phenomenons are observed from Figure 6 and Figure 8 that beyond 3 wt%TiO₂ showed lower relative permeate flux declined and decreasing in MB-SDS removal efficiency.

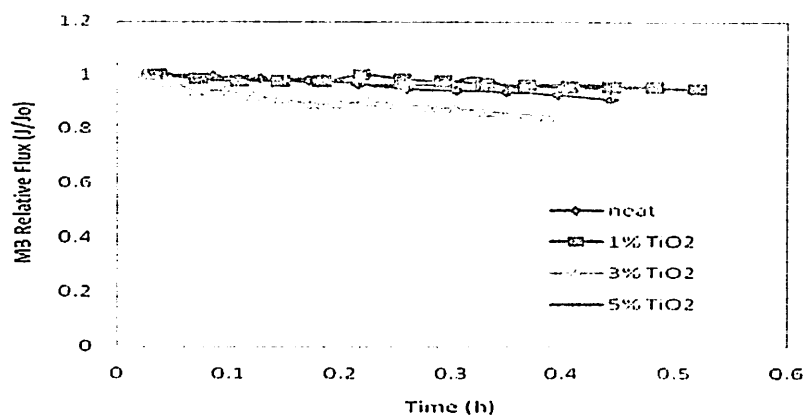


Figure 7: Permeate Flux without SDS by Membrane With Different TiO₂ Dosage Composite Membrane

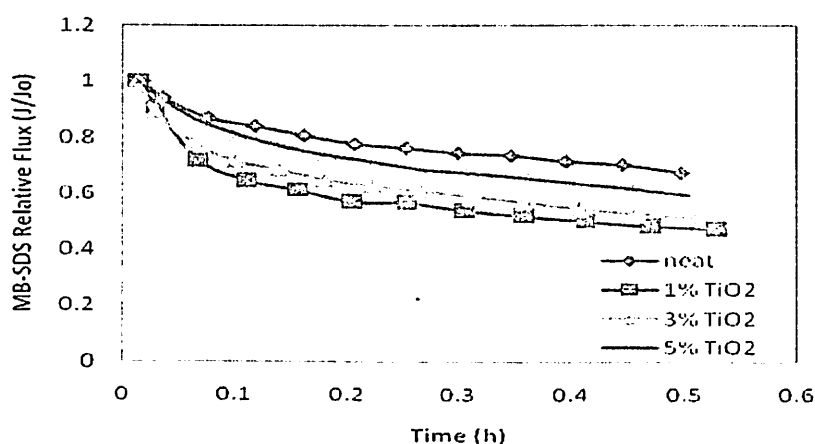


Figure 8: Permeate Flux With SDS by Membrane With Different TiO₂ Dosage Composite Membrane

4. Conclusion

Nanocomposite membranes had been prepared by dosing different amount of TiO₂ nanoparticles in the polyvinylidene fluoride polymer solution. It was found that membranes prepared under different TiO₂ dosage have different physical and morphological properties. Addition of TiO₂ could enhance membrane hydrophilicity, however, it produced membrane with bigger pore size due to the seeding effect of nanoparticles. At higher TiO₂ dosage, pore size of membrane could be reduced due to the agglomeration of TiO₂ that block the membrane pores and cause membrane defect. Pure water flux could be enhanced with 3 wt% TiO₂ dosage and beyond that the water permeability was impaired due to the blocking effect. Membrane prepared showed very poor sieving mechanism for methylene blue due to small solute to pore ratio. Methylene blue removal can be enhanced dramatically by adding SDS surfactant to the methylene blue feed solution. Methylene blue affinity towards PVDF membrane is higher than TiO₂ which has advantage to reduce the membrane fouling phenomenon. The findings provide some useful information for membrane development as it could mitigate the membrane fouling phenomenon through its hydrophilicity improvement and at the same time it reduced the interaction between the dye and the polymer matrix.

Acknowledgement: The authors wish to thank the financial support granted by Universiti Sains Malaysia (RU Grant) (1001/PJKIMIA/811172), Malaysia Toray Science Foundation (MTSF) Science and Technology Research Grant (304/PJKIMIA/6050179/M126) and Ministry of Higher Education (MyMaster).

References

- Aksu, Z., Ertugrul, S., Dönmez, G., 2010. Methylene Blue biosorption by *Rhizopus arrhizus*: Effect of SDS (sodium dodecylsulfate) surfactant on biosorption properties. *Chemical Engineering Journal*. 158, 474–481.
- Bae, T.-H., Tak, T.-M., 2005. Effect of TiO₂ nanoparticles on fouling mitigation of ultrafiltration membranes for activated sludge filtration. *Journal of Membrane Science*. 249, 1-8.
- Bielska, M., Prochaska, K., 2006. Use of ultrafiltration of micellar solutions for dyes separation. *Przemysł Chemiczny*. 85(8-9), 999-1001.
- Bielska, M., Prochaska, K., 2007. Dyes separation by means of cross-flow ultrafiltration of micellar solutions. *Dyes and Pigments*. 74, 410-415.
- Bielska, M., Szymanowski, J., 2006. Removal of methylene blue from waste water using micellar enhanced ultrafiltration. *Water Research*. 40, 1027-1033.
- Cao, X., Ma, J., Shi, X., Ren, Z., 2006. Effect of TiO₂ nanoparticle size on the performance of PVDF membrane. *Applied Surface Science*. 253(4), 2003-2010.
- Golob, V., Vinder, A., Simonic, M., 2005. Efficiency of the coagulation/flocculation method for the treatment of dyebath effluents. *Dyes Pigments*. 67, 93–97.
- Huang, J.-H., Zhou, C.-F., Zeng, G.-M., Li, X., Niu, J., Huang, H.-J., et al., 2010. Micellar-enhanced ultrafiltration of methylene blue from dye wastewater via a polysulfone hollow fiber membrane. *Journal of Membrane Science*. 365(1-2), 138-144.
- Kim, I.C., Lee, K.H., Tak, T.M., 2001. Preparation and characterization of integrally skinned uncharged polyetherimide asymmetric nanofiltration membrane. *Journal of membrane science*. 183, 235-247.
- Koyuncu, I., Topacik, D., Yuksel, E., 2004. Reuse of reactive dyehouse wastewater by nanofiltration: process water quality and economical implications. *Separation Purification Technology*. 36, 77–85.
- Luo, M.-L., Zhao, J.-Q., Tang, W., & Pu, C.-S., 2005. Hydrophilic modification of poly(ether sulfone) ultrafiltration membrane surface by self-assembly of TiO₂ nanoparticles. *Applied Surface Science*. 249, 76-84.
- Rahimpour, A., Madaeni, S.S., 2007. Polyethersulfone (PES)/cellulose acetate phthalate (CAP) blend ultrafiltration membranes: preparation, morphology, performance and anti-fouling properties. *Journal of Membrane Science*. 305, 299–312.
- Rahimpour, A., Madaeni, S. S., Taheri, A. H., & Mansourpanah, Y., 2008. Coupling TiO₂ nanoparticles with UV irradiation for modification of polyethersulfone ultrafiltration membranes. *Journal of Membrane Science*. 313, 158-169.
- Sarkar, B., DasGupta, S., De, S., 2009. Application of external electric field to enhance the permeate flux during micellar enhanced ultrafiltration. *Separation and Purification Technology*. 66, 263–272.
- Seshadri, S., Bishop, P.L., Agha, A.M., 1994. Anaerobic/aerobic treatment of selected azo dyes in waste water. *Waste Manage*. 15, 127–137.
- Soroko, I., Livingston, A., 2009. Impact of TiO₂ nanoparticles on morphology and performance of crosslinked polyimide organic solvent nanofiltration (OSN) membranes. *Journal of Membrane Science*. 343, 189-198.
- Wang, S., Zhu, Z.H., Coomes, A., Haghsersht, F, Lu, G.Q., 2005. The physical and surface chemical characteristics of activated carbons and the adsorption of methylene blue from wastewater. *Journal Colloid Interface Science*. 284, 440–446.
- Wu, G., Gan, S., Cui, L., Xu, Y., 2008. Preparation and characterization of PES/TiO₂ composite membranes. *Applied Surface Science*. 254, 7080-7086.
- Yuliwati, E., Ismail, A. F., 2011. Effect of additives concentration on the surface properties and performance of PVDF ultrafiltration membranes for refinery produced wastewater treatment. *Desalination*. 273(1), 226-234.
- Zaghbani, N., Hafiane, A., Dhabbi, M., 2007. Separation of methylene blue from aqueous solution by micellar enhanced ultrafiltration. *Separation and Purification Technology*. 55(1), 117-124.

Human
Capital
Development

PREPARATION OF MIXED-MATRIX MEMBRANE WITH ANTI-
FOULING AND DEFOLIING PROPERTIES FOR HUMIC ACID
REMOVAL

by

TEOW YIT HUAN

This thesis submitted in fulfillment of the requirements
for the degree of
Doctor of Philosophy

NOVEMBER 2013

ACKNOWLEDGEMENTS

With earnest gratitude and appreciation, I offer my deepest appreciation to my loving parents, Mr. Teow Hock Guan and Madam Ooi Hong Ngor for their unequivocal support throughout my PhD degree for which my mere expression of thanks likewise does not suffice. I would also like to express my special thanks to the one special in my heart, Tay Ching Han, who has endured my varying moods and giving me perpetual supports, as well as stood by me through the good times and bad throughout the length of my study.

My sincere gratitude also goes to my dedicated main supervisor, Dr. Ooi Boon Seng, and both of my co-supervisors, Prof. Abdul Latif Bin Ahmad and Dr. Lim Jit Kang for their prestigious guidance and supervision, invaluable advice, practical view, enormous patience, constant motivation and supports throughout the development of this research. It has been a great adventure and experience that I have gained from their guidance during the undertaking of my PhD degree in Universiti Sains Malaysia.

In particular, I would also like to convey my thankfulness to Dr. Lau Woei Jye and Dr. Low Chong Yu who would have welcomed this academic study and enlightening me the first glance of research when I first became interested in membrane science and technology.

I would also like to express my heart-felt gratitude to all the laboratory technicians and administrative staff of the School of Chemical Engineering for the assistance rendered to me.

On top of that, special thanks to Ee Mee, for her kindness, friendship, unending help and for all the fun we have had in the last three years which making my life blissful and cheerful. Many thanks to Huey Ping, Jing Yao, Swee Pin, Jian Jie and other labmates whom I am not able to address here: thank you for your stimulating discussions, encouragement, support as well as all the sleepless nights we were working together.

Last but not least, I would like to acknowledge Universiti Sains Malaysia for providing me the postgraduate scholarship- Fellowship and financial support under Research University Grant (Project A/C No: 1001/PJKIMIA/811172), MOSTI sciencefund (Project A/C No: 305/PJKIMIA/6013604), and to the USM Membrane Science and Technology Cluster.

Teow Yeit Haan
November 2013

SYNTHESIS AND CHARACTERIZATION OF SELF-CLEANING
PVDF-TiO₂ MIXED-MATRIX MEMBRANE FOR METHYLENE
BLUE REMOVAL

by

NGANG HUEY PING

Thesis submitted in fulfillment of the
requirements for the Degree of
Master of Science

August 2012

ACKNOWLEDGEMENT

First of all, I would like to express my deepest thank to my parents and all my family members for their persevering support and encouragement. They have made me more confident to face the disturbances throughout my entire master degree program.

My sincere thanks to my dedicated supervisors, Dr. Ooi Boon Seng and Prof. Dr. Abdul Latif Ahmad for their excellent supervision and enormous patience throughout my entire master degree program. Furthermore, I would like to thank them for their keen observations regarding my work and providing valuable suggestions about areas that required further study. Thank you very much for the unending help and advices throughout my entire master degree program. I would also like to convey my thankfulness to Dr. Low Siew Chun for her invaluable advice and practical view throughout the development of this research.

Next, I would like to express my thanks to School of Chemical Engineering, USM who gives the great opportunity for me to gain lot of valuable knowledge from this research and thesis. Not forgetting to thank administrative staff of School of Chemical Engineering, Universiti Sains Malaysia especially our respected dean, Professor Dr. Azlina Bt. Harun @ Kamaruddin, deputy dean, office staffs and technicians for giving me full support throughout my research work.

I would like to show my deepest gratitude and thanks to all my beloved friends and colleagues for rendering their help, kindness and moral support towards

me. I might not be able to achieve what I want to be without the support from all of my colleagues.

Last but not least, the financial supports from Universiti Sains Malaysia (Research University Grant) (1001/PJKIMIA/811172), Malaysia Toray Science Foundation (MTSF) Science and Technology Research Grant (304/PJKIMIA/6050179/M126), USM Membrane Cluster and Ministry of Higher Education (MyMaster) are gratefully acknowledged.

2012

UNIVERSITI SAINS MALAYSIA

NURRUL IZZATI BINTI ZAWAWI

NANOCOMPOSITE MEMBRANE TOWARDS HUMIC ACID

ADSORPTION PROPERTIES OF TITANIUM DIOXIDE

**ADSORPTION PROPERTIES OF TITANUM DIOXIDE
NANOCOMPOSITE MEMBRANE TOWARDS HUMIC ACID**

by

NURRUL IZZATI BINTI ZAWAWI

**Thesis submitted in partial fulfillment of the requirements for the
degree of Bachelor of Chemical Engineering**

June 2012

To my beloved abah and ummi

&

family and friends

*For your infinite and unfading love, sacrifice, patience,
encouragement and best wishes*

ACKNOWLEDGEMENT

First and foremost, I would like to express my deepest gratitude to Allah the Almighty for His bless and guidance, I am able to complete this final year project.

First of all, I would like to take this opportunity to express my sincere appreciation to my supervisor, Dr. Ooi Boon Seng for his patience and valuable guidance, advice, kindness and encouragement throughout the study. Through his guidance, I had overcome the barriers and obstacle and learn a lot of improvement from the view of way of solving problems and widen my knowledge. I would like to send my apologies to my supervisor if I had done something wrong or conflict throughout the study.

I also would like to thank Ms. Teow Yiet Haan who always help me and guide me throughout the project. Her kindness is much appreciated by me. My utmost appreciation goes to the staff of School of Chemical Engineering who helped me a lot to achieve the final year project's objectives. I would like to thank all for their time and willingness to guide me and for their encouragement for me to strive for excellence in my project. Also, for all who's has contributed a lot in the process of finishing the project. Their presence really makes this project successful by giving the guidance and helps me with the things I do not know and always kindly share their knowledge.

Lastly, thanks to everyone who has contributed directly or indirectly in completing this task.

Rujukan : USMKP/4252
 Tarikh : 10 Januari 2011
 Kepada : Bendahari

PEJABAT PENGURUSAN & KREATIVITI PENYELIDIKAN (RCMO)
 BAHAGIAN PENYELIDIKAN & INOVASI
 UNIVERSITI SAINS MALAYSIA
 KENYATAAN GAJI STAF SAMBILAN PROJEK/GERAN (SPG)
 [Pelantikan Baru]

MAKLUMAT PERIBADI

1. Nama	: KHOR SIK WEY	6. No. Staf	: USMKP/4252
2. No. Kad Pengenalan	: 910706075710	7. No. Tel (Pejabat)	:
3. Tarikh Lahir	: 6 Julai 1991	8. No. Tel (Bimbit)	: 045981099
4. Taraf Perkahwinan	: BELUM KAHWIN		
5. Jabatan Bertugas	: Ketua Projek : PUSAT PENGAJIAN KEJURUTERAAN KIMA Stat Projek : PUSAT PENGAJIAN KEJURUTERAAN KIMA		

MAKLUMAT GAJI

1. Jawatan & Cred Caji	: Pembantu Penyelidik - SPM (N17)	9. Tarikh Mula Projek/Geran	: 1 Januari 2011
2. Tajuk Projek/Geran	: Study on Simultaneous Phase Inversion and Nanoparticle-Membrane Matrix Binding Process : Dispersy and its Effect on Fouling Degradation	10. Tarikh Tamat Projek/Geran	: 31 Disember 2013
3. No. Akaun Projek/Geran	: 1001/PJKM/V811172	11. Baki geran	:
4. Jenis Projek/Geran	: RUI (Individual)	12. Tarikh Kuatkuasa Lantikan	: 3 Januari 2011
5. Gaji	: RM3281 Sehan	13. Tarikh Tamat Lantikan	: 30 Jun 2011
6. Jenis Gaji	: Harian	14. Nama Bank	: CIMB Bank
7. No. Akaun KWSP	:	15. No. Akaun Bank	: 07280004848520
8. Kadar Caruman KWSP	: 11%		

IMBUHAN TETAP

1. Khidmat Awam	: AMAUN RM 4.6 Sehan	BAYARAN BANTUAN	: AMAUN RM 12 Sehan
-----------------	-------------------------	-----------------	------------------------

CATATAN

Sila abakan surat pemeriksaan doktor, tidak perlu lakukan pemeriksaan kesihatan

PERHATIAN

- Pembayaran Emolomen ini adalah tertakluk kepada status akaun kewangan terkini projek.
 - Kenyataan Gaji (KG) ini adalah betul jika tiada maklumbalas diterima daripada staf dalam tempoh 5 hari dan tarikh KG ini
 - Kemudahan perubahan untuk diri sendiri sahaja (*tanpa perubahan perogikan*)
 - Pelantikan melebihi 3 bulan - Hospital Kerajaan/Pusat Sejahtera (Kampus Induk/Kejuruteraan)/PPT/HUSM
 - Pelantikan kurang 3 bulan - Hospital Kerajaan sahaja
- Untuk makluman pihak tuan/puan, kad rawatan tidak dikeluarkan berkuatkuasa 1 November 2010. Salfinan KG ini akan menggantikan kad rawatan terdahulu.
- Syarat-syarat lain adalah seperti yang termaktub dalam surat tawaran dan Lampran A.

PERAKUAN

Segala maklumat di atas telah diperakukan benar, disemak dan disahkan oleh DR. OOI BOON SENG Ketua Projek/Geran ini pada 5 Januari 2011. Ketua Projek/Geran boleh turut disabtkan di bawah Aka 605 sekiranya terdapat sebarang maklumat yang kurang/tidak tepat.

Tarikh perakuan penerimaan oleh KHOR SIK WEY pada 10 Januari 2011.

(HAZLAN ABDUL HAMID)
 Ketua Penolong Bendahari
 b/p Bendahari

s.k
 Dekan Pengarah
 PUSAT PENGAJIAN KEJURUTERAAN KIMA

 DR. OOI BOON SENG
 Ketua Projek
 PUSAT PENGAJIAN KEJURUTERAAN KIMA

 KHOR SIK WEY
 D/A DR. OOI BOON SENG
 PUSAT PENGAJIAN KEJURUTERAAN KIMA

Rujukan USMKP/4254
Tarikh 6 Januari 2011
Kepada Bendahari

PEJABAT PENGURUSAN & KREATIVITI PENYELIDIKAN (RCMKO)
BAHAGIAN PENYELIDIKAN & INOVASI
UNIVERSITI SAINS MALAYSIA
KENYATAAN GAJI STAF SAMBILAN PROJEK/GERAN (SPG)
[Pelantikan Baru]

MAKLUMAT PERIBADI

1. Nama	NGANG HUEY PING	6. No. Staf	USMKP/4254
2. No. Kad Pengenalan	870404085098	7. No. Tel (Pejabat)	-
3. Tarikh Lahir	4 April 1987	8. No. Tel (Rumah)	0165285776
4. Taraf Perkahwinan	BELUM KAHWIN		
5. Jabatan Destugas	Ketua Projek : PUSAT PENGAJIAN KEJURUTERAAN KIMA Staf Projek : PUSAT PENGAJIAN KEJURUTERAAN KIMA		

MAKLUMAT GAJI

1. Jawatan & Grad Gaji	Pembantu Penyelidik - SPM (N17)	9. Tarikh Mula Projek/Geran	1 Januari 2011
2. Tajuk Projek/Geran	Study on Simultaneous Phase Inversion and Nanoparticle-Membrane Matrix Binding Process : Dispersy and Its Effect on Fouling Degradation	10. Tarikh Tamat Projek/Geran	31 Disember 2013
3. No. Akaun Projek/Geran	1001/PJKK/AV811172	11. Baki geran	-
4. Jenis Projek/Geran	RUI (Individual)	12. Tarikh Kualifikasi Lantikan	3 Januari 2011
5. Gaji	RM 820.38 Sebulan	13. Tarikh Tamat Lantikan	31 Januari 2011
6. Jenis Gaji	Bulanan	14. Nama Bank	Bank Islam Malaysia Berhad
7. No. Akaun KWSP	18733554	15. No. Akaun Bank	08059020123077
8. Kadar Caruman KWSP	11%		

IMBUHAN TETAP

1. Khidmat Awam	AMAUN RM 115 Sebulan	BAYARAN BANTUAN	AMAUN RM 300 Sebulan
-----------------	-------------------------	-----------------	-------------------------

CATATAN

Sila abaikan surat pemeriksaan doktor, tidak perlu lakukan pemeriksaan kesihatan

PERHATIAN

- Pembayaran Emolumen ini adalah tertakluk kepada status akaun kewangan terkini projek.
- Kenyataan Gaji (KG) ini adalah betul jika tiada maklumbalas diterima daripada staf dalam tempoh 5 hari dari tarikh KG ini.
- Kemudahan perubatan untuk diri sendiri sahaja (*tanpa perubatan pergigian*)
 - Pelantikan melebihi 3 bulan - Hospital Kerajaan/Pusat Sejahtera (Kampus Induk/Kejuruteraan)/PPPT/USM
 - Pelantikan kurang 3 bulan - Hospital Kerajaan sahaja

Untuk makluman pihak tuan/puan, kad rawatan tidak dikeluarkan berkuatkuasa 1 November 2010. Salinan KG ini akan menggantikan kad rawatan terdahulu.

- Syarat-syarat lain adalah seperti yang termaklumb dalam surat lawatan dan Lampiran A.

PERAKUAN

Segala maklumat di atas telah diperakukan benar, disemak dan disahkan oleh DR. OOI BOON SENG Ketua Projek/Geran ini pada 6 Januari 2011. Ketua Projek/Geran boleh turut disatitkan di bawah Akta 605 sekiranya terdapat sebarang maklumat yang kurang/tidak tepat

Tarikh perakuan penerimaan oleh NGANG HUEY PING pada 6 Januari 2011.

(HAZLAN ABDUL HAMID)

Ketua Penolong Pendaftar
b/p Pendaftar

s.k
Dekan/Pengarah
PUSAT PENGAJIAN KEJURUTERAAN KIMA

DR. OOI BOON SENG
Ketua Projek
PUSAT PENGAJIAN KEJURUTERAAN KIMA

NGANG HUEY PING
D/A DR. OOI BOON SENG
PUSAT PENGAJIAN KEJURUTERAAN KIMA

Rujukan
Tarikh
Kepada

USMKP/4715
25 Mei 2011
Bendahari

PEJABAT PENKURUSAN & KREATIVITI PENYELIDIKAN (RCMO)
BAHAGIAN PENYELIDIKAN & INOVASI
UNIVERSITI SAINS MALAYSIA
KENYATAAN GAJI STAF SAMBILAN PROJEK/GERAN (SPG)
[Pelantikan Baru]

MAKLUMAT PERIJADI

1. Nama	: NUR SUHALI BT MOHD YATIM	6. No. Staf	: USMKP/4715
2. No. Kad Pengenalan	: 871109075078	7. No. Tel (Pejabat)	: -
3. Tarikh Lahir	: 9 November 1987	8. No. Tel (Bimbe)	: 0134107178
4. Taraf Perkahwinan	: BELUM KAHWIN		
5. Jabatan Bertugas	: Ketua Projek : PUSAT PENGAJIAN KEJURUTERAAN KIMA Staf Projek : PUSAT PENGAJIAN KEJURUTERAAN KIMA		

MAKLUMAT GAJI

1. Jawatan & Creu Gaji	: Pembantu Penyelidik - SPM (N17)	9. Tarikh Mula Projek/Geran	: 1 Januari 2011
2. Tajuk Projek/Geran	: Study on Simultaneous Phase Inversion and Nanoparticle-Membrane Matrix Bndaig Process : Dispersy and its Effect on Fouling Degradation	10. Tarikh Tamat Projek/Geran	: 31 Disember 2013
3. No. Akaun Projek/Geran	: 1001/PJKKMA/011172	11. Baki geran	:
4. Jenis Projek/Geran	: RUI (Individu)	12. Tarikh Kuatkuasa Lantikan	: 1 Jun 2011
5. Gaji	: RM 820.38 Sebulan	13. Tarikh Tamat Lantikan	: 30 Jun 2011
6. Jenis Gaji	: Bulanan	14. Nama Bank	: CIMB Bank
7. No. Ahli KWSP	: 19410351	15. No. Akaun Bank	: 0805002078203
8. Kadar Caruman KWSP	: 11%		

IMBUHAN TETAP

1. Khidmat Awam	: AMAJN RM 115 Sebulan	BAYARAN BANTUAN	: AMAJN RM 300 Sebulan
-----------------	---------------------------	-----------------	---------------------------

CATATAN

Sila abaikan surat pemeriksaan doktor, tidak perlu lakukan pemeriksaan kesihatan

PERHATIAN

- Pembayaran Emolumen ini adalah tertakluk kepada status akaun/ kewangan terkini projek.
- Kenyataan Gaji (KG) ini adalah betul jika tiada maklumbalas diterima daripada staf dalam tempoh 5 hari dari tarikh KG ini.
- Kemudahan perubahan untuk diri sendiri sahaja (*tanpa perubahan pergeseran*)
 - Pelantikan melebihi 3 bulan - Hospital Kerajaan/Pusat Sejahtera (Kampus induk/Kejuruteraan)/PPT/HUSM
 - Pelantikan kurang 3 bulan - Hospital Kerajaan sahaja

Untuk makluman pihak lain/puan, kad rawatan tidak dikeluarkan berkuatkuasa 1 November 2010. Salinan KG ini akan menggantikan kad rawatan terdahulu.
- Syarat-syarat lain adalah seperti yang termaktub dalam surat lawaran dan Lampiran A.

PERAKUAN

Segala maklumat di atas telah diperakui benar, disemak dan disahkan oleh DR. OOI BOON SENG Ketua Projek/Geran ini pada 23 Mei 2011. Ketua Projek/Geran boleh turut disabikan di bawah Akta 605 sekiranya terdapat sebarang maklumat yang kurang/tidak tepat

Tarikh perakuan penerimaan oleh NUR SUHALI BT MOHD YATIM pada 25 Mei 2011.

(HAZLAN ABDUL HAMID)

Ketua Penolong Pendaftar
b/p Pendaftar

s.k.
Dekan/ Pengarah
PUSAT PENGAJIAN KEJURUTERAAN KIMA

DR. OOI BOON SENG
Ketua Projek
PUSAT PENGAJIAN KEJURUTERAAN KIMA

NUR SUHALI BT MOHD YATIM
D/A DR. OOI BOON SENG
PUSAT PENGAJIAN KEJURUTERAAN KIMA

Rujukan : USMKP/4276
 Tarikh : 11 Januari 2011
 Kepada : Bendahan

PEJABAT PENGURUSAN & KREATIFITI PENYELIDIKAN (RCIAK)
 BAHAGIAN PENYELIDIKAN & INOVASI
 UNIVERSITI SAINS MALAYSIA
 KENYATAAN GAJI STAF SAMBILAN PROJEK/GERAN (SPG)
 [Pelantikan Baru]

MAKLUMAT PERIBADI

1. Nama : TEOW YEIT HAWN
 2. No. Kad Pengenalan : 860713205448
 3. Tarikh Lahir : 13 Jun 1985
 4. Taraf Perkahwinan : BELUM KAHWIN
 5. Jabatan Bertugas : Ketua Projek : PUSAT PENGAJIAN KEJURUTERAAN KIMA
 Staf Projek : PUSAT PENGAJIAN KEJURUTERAAN KIMA

6. No. Staf : USMKP/4276
 7. No. Tel (Pejabat) : -
 8. No. Tel (Jimba) : 0164854291

MAKLUMAT GAJI

1. Jawatan & Cred Gaji : Pembantu Penyelidik - SPM (N17)
 2. Tajuk Projek/Geran : Study on Simultaneous Phase Inversion and Nanoparticle-Membrane Matrix Binding Process : Dispersy and Its Effect on Fouling Degradation
 3. No. Akaun Projek/Geran : 1001/PJKM/AB11172
 4. Jenis Projek/Geran : RUI (Individual)
 5. Gaji : RM 820.38 Sebulan
 6. Jenis Gaji : Bulanan
 7. No. Akaun KWSP : 19126364
 8. Kadar Caruman KWSP : 11%

9. Tarikh Mula Projek/Geran : 1 Januari 2011
 10. Tarikh Tamat Projek/Geran : 31 Disember 2013
 11. Baki gajian : -
 12. Tarikh Kuatkuasa Lantikan : 3 Januari 2011
 13. Tarikh Tamat Lantikan : 30 Jun 2011
 14. Nama Bank : CIMB Bank
 15. No. Akaun Bank : 02190007780524

IMBUHAN TETAP

1. Khidmat Awam : AMALIN RM 115 Sebulan
 BAYARAN BANTUAN
 1. Sara Hidup : AMALIN RM 300 Sebulan

CATATAN

Sila abakan sural pemeriksaan doktor, tidak perlu lakukan pemeriksaan kesihatan.

PERHATIAN

- Pembayaran Emolument ini adalah tertakuk kepada status akaun kewangan terkin projek.
- Kenyataan Gaji (KG) ini adalah betul jika tiada maklumbalas diterima daripada staf dalam tempoh 5 hari dari tarikh KG ini.
- Kemudahan perubahan untuk diri sendiri sahaja (*tanpa perubahan perijinan*)
 - Pelantikan melebihi 3 bulan - Hospital Kerajaan/Pusat Sejahtera (Kampus Induk/Kejuruteraan)/PPPT/HUSM
 - Pelantikan kurang 3 bulan - Hospital Kerajaan sahaja

Untuk makluman pihak luar/puan, kad rawatan tidak dikeluarkan berkuatkuasa 1 November 2010. Salinan KG ini akan menggantikan kad rawatan terdahulu.

- Syarat-syarat lain adalah seperti yang termaktub dalam surat tawaran dan Lampiran A.

PERAKUAN

Segala maklumat di atas telah diperakukan benar, disemak dan disahkan oleh DR. OOI BOON SENG Ketua Projek/Geran ini pada 10 Januari 2011. Ketua Projek/Geran boleh turut disabkan di bawah Akta 605 sekiranya terdapat sebarang maklumat yang kurang/tidak tepat.

Tarikh perakuan penerimaan oleh TEOW YEIT HAWN pada 11 Januari 2011.

(HAZLAN ABDUL HAMID)

Ketua Pendaftar
 b/p Pendaftar

s.k. Dekan Pengiran
 PUSAT PENGAJIAN KEJURUTERAAN KIMA
 DR. OOI BOON SENG
 Ketua Projek
 PUSAT PENGAJIAN KEJURUTERAAN KIMA
 TEOW YEIT HAWN
 D/A DR. OOI BOON SENG
 PUSAT PENGAJIAN KEJURUTERAAN KIMA

Rujukan
Tarikh
Kepada

USMKP/6976
20 Mac 2013
Berdahlan

PEJABAT PENGURUSAN & KREATIVITI PENYELIDIKAN (RCMO)
BAHAGIAN PENYELIDIKAN & INOVASI
UNIVERSITI SAINS MALAYSIA
KENYATAAN GAJI STAF SAMBILAN PROJEK/GERAN (SPG)
[Pelantikan Baru]

MAKLUMAT PERIBADI

1. Nama	: WONG HUI YIEN	6. No. Staf	: USMKP/6976
2. No. Kad Pengenalan	: 900610085852	7. No. Tel (Pejabat)	: -
3. Tarikh Lahir	: 16 Jun 1990	8. No. Tel (Banda)	: 0125235645
4. Taraf Perkahwinan	: BELUM KAHWIN		
5. Jabatan Bertugas	: Ketua Projek : PUSAT PENGAJIAN KEJURUTERAAN KIMA Staf Projek : PUSAT PENGAJIAN KEJURUTERAAN KIMA		

MAKLUMAT GAJI

1. Jawatan & Gred Gaji	: Pembantu Penyelidik - SPM (N17)	9. Tarikh Mula Projek/Geran	: 1 Januari 2011
2. Tajuk Projek/Geran	: Study on Simultaneous Phase Inversion and Nanoparticle-Membrane Mixed Bedding Process : Dispersy and Its Effect on Fouling Degradation	10. Tarikh Tamat Projek/Geran	: 31 Disember 2013
3. No. Akaun Projek/Geran	: 1001/PJK/AA/811172	11. Baki geran	: -
4. Jenis Projek/Geran	: RUI (Individu)	12. Tarikh Kualifikasi Lantikan	: 2 Januari 2013
5. Gaji	: RM 620.38 Sebulan	13. Tarikh Tamat Lantikan	: 28 Februari 2013
6. Jenis Gaji	: Bulanan	14. Nama Bank	: Bank Islam Malaysia Berhad
7. No. Ahli KWSP	: 19834420	15. No. Akaun Bank	: 08022020349215
8. Kadar Casuman KWSP	: 11%		

IMBUHAN TETAP

1. Khidmat Awam	: AMAUN RM 115 Sebulan	1. Sara Hidup	: AMAUN RM 300 Sebulan
-----------------	---------------------------	---------------	---------------------------

CATATAN

Sila abaikan surat pemeriksaan doktor, tidak perlu lakukan pemeriksaan kesihatan.

PERHATIAN

- Pembayaran Emolument ini adalah tertakluk kepada status akaun kewangan terkini projek.
- Kenyataan Gaji (KG) ini adalah betul jika iada maklumbalas diterima daripada staf dalam tempoh 5 hari dan tarikh KG ini.
- Kemudahan perubatan untuk diri sendiri sahaja (*tanpa perubatan pergigian*)
 - Pelantikan melebihi 3 bulan - Hospital Kerajaan/Pusat Sejahtera (Kampus Induk/Kejuruteraan)/NPPT/IUSM
 - Pelantikan kurang 3 bulan - Hospital Kerajaan sahaja

Untuk makluman pihak luar/puan, kad rawatan tidak dikeluarkan berkuatkuasa 1 November 2010. Salinan KG ini akan menggantikan kad rawatan terdahulu.
- Syarat-syarat lain adalah seperti yang termaklud dalam surat tawaran dan Lampiran A.

PERAKUAN

Segala maklumat di atas telah diperakukan benar, disemak dan disahkan oleh DR. OOI BOON SENG Ketua Projek/Geran ini pada 2 Januari 2013. Ketua Projek/Geran boleh turut disabitkan di bawah Akta 605 sekiranya terdapat sebarang maklumat yang kurang/tidak tepat

Tarikh perakuan penerimaan oleh WONG HUI YIEN pada 20 Mac 2013.

(PROFESOR Madya DR. LEE KEAT TEONG)

Pengarah
b/p Pendaftaran

s.k
Dekan/Pengarah
PUSAT PENGAJIAN KEJURUTERAAN KIMA

DR. OOI BOON SENG
Ketua Projek
PUSAT PENGAJIAN KEJURUTERAAN KIMA

WONG HUI YIEN
DIA DR. OOI BOON SENG
PUSAT PENGAJIAN KEJURUTERAAN KIMA

Networking
And
Linkages



Home | My Profile | Application | Disbursement | Monitoring | Logout

Project Application Searching

Project Application Searching

(Note: Asterisks (*) may be used as wildcard characters in the search functions. E.g., the search string a*d will find badu*, around and bandstand; both occurrences) Without an Asterisk (*), the system will search for an exact match.)

Project No.

Project Title

Project Leader :

Institution

Project Details

Project No	Project Title	Project Leader	Institution	Status
USM0002692	Synthesis of Polyethersulfone /Zinc oxide Mixed Matrix Hollow Fiber Membrane for Humic Acid Removal	Abdul Latif bin Ahmad	USM	Accepted
03-02-11-SF0041	Simultaneous Saccharification-Fermentation coupled with Pervaporation-Dephlegmation (SSFDP) integrated process for the production of bioethanol	Chin Sim Yee	UMP	Accepted
03-01-05-SF0555	Development and optimization of a novel nano emulsion liquid membrane for cadmium recovery	Abdul Latif bin Ahmad	USM	Accepted
03-01-05-SF0472	Development of monodispersed magnetite nanoparticles enhanced polymeric membrane to remove arsenic from drinking water for the bottom billion	Lim Jit Kang	USM	Accepted
USM0001950	Development of monodispersed magnetite nanoparticles enhanced polymeric membrane to remove arsenic from drinking water for the bottom billion.	Lim Jit Kang	USM	Accepted
03-02-11-SF0165	Evaluation of recycling feasibility and sustainability of physico-chemical integrity of sintered silver nanoparticles removed through biosorption and nanofiltration processes	Rajkumar Durairaj	UTAR	Accepted
03-01-05-SF0563	Development of hollow fiber membrane gas-liquid contactor for CO2 emission reduction	Abdul Latif bin Ahmad	USM	Accepted
03-02-11-SF0183	Evaluation of performance and reusability of recovered sintered silver nanoparticles through biosorption process for the electronics packaging industry	Rajkumar Durairaj	UTAR	Accepted
03-02-11-SF0095	Preparation and Characterization of Biodegradable Cellulosic Fibre Reinforced Polymeric Composites	Chee Swee Yong	UTAR	Accepted
UTAR000017	Evaluation of biosorption processes on the performance of sintered silver nanoparticles for electronic packaging applications	Rajkumar Durairaj	UTAR	Accepted

Abbreviation

- Addr Description:
- ISC Institution Internal Screening Committee
- IC MOSTI Internal Committee
- TFC MOSTI Technical & Financial Committee
- AC MOSTI Approval Committee
- RA Research Agreement

PENFABRIC SDN. BERHAD (14240-M)

- Head Office : Plot 117-119 & 200-202, Prai Free Industrial Zone 1, 13600 Prai, Penang, Malaysia
Tel No. 604 3907000 (General Line)
Fax Nos. 604 3906200 (Group HR/Corporate Affairs), 604 3901705 (Accounts/Finance), 604 2969018 (Sales/Logistics), 604 2954153 (Systems)
- PENFABRIC MILL 1
100-E, Blok C Mk. 12, Phase 3, Bayan Lepas FIZ,
11900 Bayan Lepas, Penang, Malaysia
Tel No. 604 6432611, Fax No. 604 6440114
- PENFABRIC MILL 2
Plot 1 & 2, Prai Wharf Free Industrial Zone,
13600 Prai, Penang, Malaysia
Tel No. 604 3907344, Fax No. 604 3902589
- PENFABRIC MILL 3
150-A, Blok A, Mk. 12, Phase 3, Bayan Lepas FIZ,
11900 Bayan Lepas, Penang, Malaysia
Tel No. 604 6432601, Fax No. 604 6432607
- PENFABRIC MILL 4
Plot 117-119 & 200-102, Prai Free Industrial Zone 1,
13600 Prai, Penang, Malaysia
Tel No. 604 3907000, Fax No. 604 3903380

Auto. Please Reply to Address as Indicated

26th July 2012

Fundamental Science Platform
Research & Innovation Division
University Sains Malaysia
11800 USM, Penang
Malaysia

Attn : Professor Abdul Latif Ahmad

Dear Sir,

Re: Penfabric Mill 4 and Mill 3 Waste Water Improvement Studies on Color

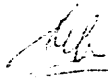
I would like to thank you, Dr. Ooi and Dr. Suzykawati for coming over to Penfabric Mill 4 yesterday to understand and discuss solutions for our effluent color. It was very difficult to get a date suitable for both parties and we are grateful that we could finally make it.

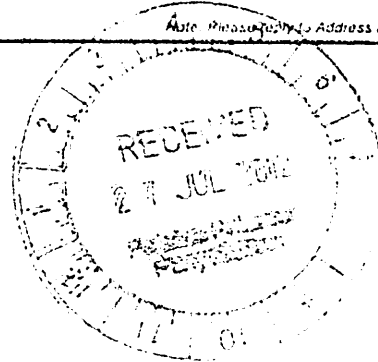
As explained, we would like to use a method which does not cause generation of huge amount of sludges. Thus using coagulants or activated carbon are not favorable as we will have immense problem with handling, drying and storing the sludge, without even mentioning the cost of disposal.

Your membrane system is interesting but please consider also how to deal with the reject (20 - 30% of the waste solution containing high concentration of dyes)

Please advise how we should go about the procedures. Will appreciate very much your prompt feedback.

Thank you.


Ho Sao Boon
General Manager/Director
Penfabric Mill 1, 2, 3 and 4



MINUTES OF MEETING WITH USM RESEARCHERS TO DISCUSS EFFLUENT COLOR PROBLEM OF PENFABRIC MILL 3 AND MILL 4.

Attendants : Prof. Dr. Abdul Latif Ahmad (Research Dean, Research & innovation Division),
 Dr. Ooi Boon Seng (School of Chemical Engineering),
 Dr. Suzylawati Ismail (School of Chemical Engineering),
 Penfabric : Mr. SB Ho (General Manager/Director)
 Mill 3 : Mr. CS Ong
 Mill 4 : M/s. Jaya Paul, Mohd. Zalman, Mohd Faisal, Jenny Ooi

Date & time : 25th July 2012 (Wednesday), 3:00 p.m. – 4:30p.m.

Venue : Technical Meeting room

Recorded by : CS Ong

1. Mr. Jaya Paul welcomed the guests from USM to Penfabric M4. He briefed the guests on company's background and process flow, as well as the products from each mill. Mr. SB Ho further explained on the package yarn dyeing process of Penfabric Mill 3.
2. Both Mill 3 & Mill 4 can comply with all the 31 parameters except for color.
3. For an understanding of the performance, the table below was shown to participants

Parameters	Mill 4		Mill 3		Standard B
	Influent	Effluent	Influent	Effluent	
BOD (mg/L)	600 - 800	< 18	100 - 150	25 - 35	50
COD (mg/L)	1500 - 1600	< 189	500 - 800	150 - 165	250
Suspended Solids (mg/l)	<100	< 13	40 - 60	10 - 20	100
Color (ADMI)	600 - 800	440	400 - 500	280 - 310	200
Flow rates	About 260 m ³ /hour		About 50 m ³ /hour		

Note : Mill 4 concentrated Dye Solution is about 500,000 ADMI

4. Mr. Jaya Paul explained that both M3 and M4 had carried out a series of decolorization tests through consultants and in-house facilities. Some of the tests carried out are coagulation, membrane system, activated carbon and hypochlorite test. Using coagulants or activated carbon is not feasible because of the high sludge generation. There will be immense difficulty to cope with the handling, drying and storage of the sludge (not to mention the high disposal cost).
5. Hypochlorite may be feasible in Mill 3 as tested on the effluent. Testing on conc dye solution in Mill 4 shows poor performance. PAB requested USM to help find a more practical method.

6. Dr. Ooi pointed out that the mixture of waste water containing; over 100 types of dyestuffs of different characteristics and the fluctuation of dyestuffs in production line would cause the decolouration work to be more complicated. Dr. Ooi is also concerned about the amount of surfactant used, as this would impact the organic digestion of bacterias. Mr. Ho informed that the consumption is about 12 tons/month.
7. Mr. Ho enquired about the effectiveness of filtration system in waste water plant of Penfabric M3 & M4. Professor Latif informed that membrane definitely can remove dyes; Penfabric can use ceramic membrane for Ultra-filtration (UF) system as it can withstand high temperatures. He further explained that treating a small and concentrated volume of dye waste water would be more feasible than large volumes of diluted influent. Mr Ho however cautioned that the influent may contain fibres, thereby fouling the membrane.
8. Dr. Ooi suggested drying a small amount of the waste water to get the weight of the dyes and use this to make a correlation with the ADMI figures. Professor Latif suggested to make a balance sheet of the color so as to be sure of the sources of color contaminants. This is important if PAB intends to only treat the dye solution from Pad dry. (Volume about 5000 litres/day)
9. Mr. Jaya Paul asked whether there is a mini decolouration plant in USM campus. Professor Latif explained that there is a pilot plant for waste water of palm oil industry. The pilot plant can work for other industries if they make some modifications. Mr. Jaya Paul enquired about the cost of ceramic membrane. Dr. Ooi said that the ceramic membrane is costly but easier for maintenance. It is suitable for high temperature environment. Dr. Ooi further explained that an Ultra-filtration (UF) and Reverse-osmosis (RO) can recover 70 - 80% of waste water.
10. Prof. Latif suggested that Penfabric write a formal letter to him and he will propose through Usains to issue the MOU & MOA (Memorandum of understanding & Memorandum of agreement) based on the Research Contract to explore and find possible solutions. He will reply to us once we write to him.
11. The meeting adjourned at 5:15pm with thanks to all participants.

External
Research
Grant



Rujukan : HC287
Tarikh : 4 Mei 2012

Dr. Ooi Boon Seng
Pusat Pengajian Kejuruteraan Kimia
Universiti Sains Malaysia
Kampus Kejuruteraan
14300 Nibong Tebal
PULAU PINANG

Universiti Sains Malaysia
Pejabat Pengurusan Dan Kreativiti Penyelidikan
11800 USM, Pulau Pinang
Tel: 04-653 4100
Fax: 04-653 4101
E-mail: ppk@usm.edu.my
www.usm.edu.my

Tuan,

KEPUTUSAN PERMOHONAN SCIENCE FUND 2012

Sukacita dimaklumkan bahawa pihak kami telah mendapat pengesahan bahawa projek tuan seperti berikut telah diluluskan:

Cluster	Project No.	Project Leader	Project Title	Total Grant (RM)
S & T Services	06-01-05-SF0546	Dr. Ooi Boon Seng	"Removal Of Natural Organic Matter (NOM) Using Self-Cleaning Mixed Matrix Membrane"	184,780.00

- Tempoh Projek : 24 bulan (Mac 2012 – Februari 2014)
- Ahli Kumpulan :
i) Profesor Abdul Latif Ahmad (USM)
ii) Dr. Lim Jit Kang (USM)
- No Akaun : 305/PJKIMIA/6013604
- Agihan mengikut tahun seperti yang diluluskan oleh MOSTI adalah seperti berikut

PERKARA	Tahun 1 (2012)
Vot 11000 (Wages and Allowances for Temporary & Contract Personnel)	16,800.00
Vot 21000 (Travel and Transportation)	1,500.00
Vot 24000 (Rental)	240.00
Vot 27000 (Research Materials and Supplies)	22,500.00
Vot 28000 (Minor Modifications and Repairs)	9,000.00
Vot 29000 (Special Services)	6,600.00
Vot 36000 (R&D Equipment and Accessories)	80,000.00
JUMLAH BESAR	136,640.00

MTSF

Malaysia Toray Science Foundation

Penang Office of MTSF
c/o Penfabric Sdn. Berhad,
Block B, Prai Free Industrial Zone 1, 13600 Prai, Penang, Malaysia
Tel (604) 3908157 / 3854151 Fax: (604) 3908260
Email: mtsf@toray.com.my
Website: <http://www.mtsf.org/>

Our Ref : CRO-CA/09.324 (09/G116)

12 October 2009

1. Vice Chancellor
Universiti Sains Malaysia
11800 Minden
Penang
2. Dr. Ooi Boon Seng
School of Chemical Engineering
Universiti Sains Malaysia, Engineering Campus
Seri Ampangan, 14300 Nibong Tebal

Dear Sir/Dr. Ooi Boon Seng

YEAR 2009 MTSF SCIENCE & TECHNOLOGY RESEARCH GRANT

Our heartiest congratulations to your University and Dr. Ooi Boon Seng who has been selected as one of the fourteen recipients of the Year 2009 MTSF Science & Technology Research Grant which carries a grant of RM20,000.00 funded by Toray Science Foundation of Japan.

As recommended by the Selection Committee, this grant of RM20,000.00 is to be used for payment of the following goods/services relating to the research project titled "*Preparing and characterization of a simultaneous pore forming and titanium binding nanocomposite membrane for fouling mitigation*"

Equipment & Consumables : RM20,000.00

The grant will be presented to Dr. Ooi Boon Seng at a ceremony to be held on 15 December 2009 (Tuesday) at 10.00 am at Hotel Nikko, Kuala Lumpur. We will send to you and Dr. Ooi the invitation and other relevant details in due course

It is the Foundation's policy that all research grants for the selected recipients shall be paid to the Universities/Institutions concerned. As the custodian, the Universities/Institutions shall, upon receipt of the grant recipient's written requests, pay from this grant to the grant recipient or directly to the suppliers for equipment/consumables used for the research project. Upon completion of the research, any unused balance of the awarded amount shall have to be refunded to the Foundation

Continued 2/-



Final Statements

User Name: AIN / USMKRCLIVE / PRIMIA		Program Code: Votebook 9100		Current Program : Votebook (Invoer)		
Current Date: 04/07/2014 9:20:46 AM		Version: 15.19, Last Updated at 06/07/2013		DR: 13.00, 9/18/2010 VB: 13.01, 3/14/2011		
Current Language: English / Malay		Language: English		Switch Language: English / Malay		
43	Projek Kumpulan Wang Ulu Panyekahan	1001.223.0.PRIMIA R11172	0.00	0.00	0.00	0.00%
44	Projek Kumpulan Wang Ulu Panyekahan	1001.223.0.PRIMIA R11172	4,427.28	0.00	0.00	4,427.28
45	SubTotal		4,427.28	0.00	0.00	4,427.28
46	Projek Kumpulan Wang Ulu Panyekahan	1001.223.0.PRIMIA R11172	2,375.02	0.00	0.00	-2,375.02
47	Projek Kumpulan Wang Ulu Panyekahan	1001.223.0.PRIMIA R11172	2,500.00	0.00	0.00	2,500.00
48	Projek Kumpulan Wang Ulu Panyekahan	1001.223.0.PRIMIA R11172	469.00	0.00	0.00	469.00
49	Projek Kumpulan Wang Ulu Panyekahan	1001.223.0.PRIMIA R11172	449.14	0.00	0.00	-449.14
50	SubTotal		1,500.00	0.00	0.00	1,500.00
51	Projek Kumpulan Wang Ulu Panyekahan	1001.223.0.PRIMIA R11172	4,195.28	0.00	0.00	3,484.76
52	Projek Kumpulan Wang Ulu Panyekahan	1001.223.0.PRIMIA R11172	10,030.00	0.00	0.00	10,030.00
53	Projek Kumpulan Wang Ulu Panyekahan	1001.223.0.PRIMIA R11172	5,147.08	0.00	0.00	-5,776.68
54	SubTotal		10,836.95	0.00	0.00	9,654.95
55	Projek Kumpulan Wang Ulu Panyekahan	1001.315.0.PRIMIA R11172	13,863.41	0.00	0.00	-13,863.41
56	SubTotal		13,863.41	0.00	0.00	-13,863.41
5666	GrandTotal		1,469.82	0.00	0.00	276.82